Functional hydrophilic polymers for chemoselective coupling

Dissertation zur Erlangung des
naturwissenschaftlichen Doktorgrades
der Julius-Maximilians-Universität Würzburg

vorgelegt von

Diplom-Chemiker
Michael Schmitz

aus Bedburg

Würzburg 2016

Eingereicht bei der Fakultät für Chemie und Pharmazie am

_____

Gutachter der schriftlichen Arbeit

1. Gutachter: _____
2. Gutachter: _____

Prüfer des öffentlichen Promotionskolloquiums

1. Prüfer: _____
2. Prüfer: _____
3. Prüfer: _____

Datum des öffentlichen Promotionskolloquiums

_____

Doktorurkunde ausgehändigt am

_____

„So eine Arbeit wird eigentlich nie fertig, man muss sie für fertig erklären, wenn man nach der Zeit und den Umständen das Möglichste getan hat.“

Johann Wolfgang von Goethe

Die vorliegende Arbeit wurde in der Abteilung für Funktionswerkstoffe der Medizin und Zahnheilkunde, Universität zu Würzburg, Würzburg, Deutschland in der Zeit von Februar 2011 bis April 2016 unter der Leitung von Herrn Prof. Dr. Jürgen Groll angefertigt.

Table of contents

Abbreviations and symbols

Abbreviations

ACN	acetonitrile
AFM	atomic force microscopy
AIBN	azobisisobutyronitrile
aq.	aqueous
ATRP	atom-transfer radical-polymerization
a.u.	arbitrary units
Boc	*tert*-butyloxycarbonyl
ButenOx	2-butenyl-oxazoline
CaH_2	calcium hydride
$CDCl_3$	deuterated chloroform
CD_3CN	deuterated acetonitrile
CDI	1,1-carbonyldiimidazole
CEAC	2-chloroethyl-ammonium chloride
cm	centimeter
CMC	critical micelle concentration
Co	Cobalt
Cr	Chromium
CSIRO	Commonwealth Scientific and Industrial Research
CTA	chain transfer agent
CuAAC	copper catalyzed azide–alkyne cycloaddition
cyclTE	cyclic thioester
cys-POx	cysteine functionalized poly(2-oxazoline)s
d	day
DBU	diazabicycloundecene
DCC	*N,N'*-dicyclohexylcarbodiimide
DCM	dichloromethane
DecenOx	2-decenyl-oxazoline
DLS	dynamic light scattering
DMF	*N,N*-dimethylformamide
DMPA	2,2-dimethoxyphenylacetophenone

DMSO	dimethyl sulfoxide
DMSO-d_6	deuterated dimethyl sulfoxide
DNA	deoxyribonucleic acid
D_2O	deuterium oxide
DP	degree of polymerization
DP_{calc}	calculated degree of polymerization
DP_{exp}	experimental degree of polymerization
ECM	extracellular matrix
EDC	1-ethyl-3-(3-dimethyl-aminopropyl)-1-carbodiimide
et al.	Et alii (and others)
EtN_3	triethylamine
EtOx	2-ethyl-oxazoline
EO	ethylene oxide
eq	equivalent
etc	etcetera
FDA	Food and Drug Administration
fps	frames per second
FT-IR	Fourier transformed infrared
FTz4CA	3-formyl-2,2-dimethylthiazolidine-4-carboxylic acid
g	gram
h	hour
HFIP	1,1,1,3.3,3-hexafluoro-2-propanol
HPLC	high-performance liquid chromatography
HRP	horse radish peroxidase
Hz	hertz
[I]	concentration of the initiator
IL-8	interleukin-8
IME	inverse mini-emulsion
IR	infrared
kDa	kilo Dalton
kg	kilogram
kHz	kilohertz
KOH	potassium hydroxide

kV	kilovolt
L	liter
LCST	lower critical solution temperature
M	Molar
[M]	concentration of the monomer
MALDI ToF MS	matrix-assisted laser desorption/ionization time of flight mass spectroscopy
mbar	millibar
MeOH	methanol
MeOx	2-methyl-2-oxazoline
Me-TOS	methyl tosylate
mg	milligram
MHz	megahertz
min	minute
mL	milliliter
mm	millimeter
mmol	millimol
M_n	number-averaged molar mass
MPAA	4-mercaptophenylacetic acid
MS	mass spectrum
MTT	3-(4,5-dimethylthiazol-2-yl)-2,5-diphenyltetrazolium bromide
M_w	weight-averaged molar mass
MWCO	molecular weight cut-off
m/z	mass-to-charge ratio
NaOH	sodium hydroxide
NCL	native chemical ligation
NCO	isocyanate
NCO-sP(EO-*stat*-PO)	isocyanate functionalized six-arm, star-shaped poly(ethylene oxide-*stat*-propylene oxide)
NHS	*N*-hydroxysuccinimide
Ni	Nickel
nm	nanometer

NMP	nitroxide-mediated polymerization
NMR	nuclear magnetic resonance
NTA	nanoparticle tracking analysis
O_2	oxygen
OEGA	oligo(ethylene glycol) acrylate
OEGMA	oligo(ethylene glycol) methacrylate
PBS	phosphate-buffered saline
P(ButenOx)	poly(2-butenyl-2-oxazoline)
PCL	poly(*ε*-caprolactone)
P(DecenOx)	poly(2-decenyl-2-oxazoline)
PEG	poly(ethylene glycol)
PEO	poly(ethylene oxide)
P(EtOx)	poly(2-ethyl-2-oxazoline)
PFPA	pentafluorophenyl acrylate
PFPMA	pentafluorophenyl methacrylate
PGA	poly(glycolic acid)
pH	negative logarithmic value of the hydrogen ion concentration
PLA	poly(lactic acid)
$P_m^{\cdot}$	newly generated radical polymer chain
P(MeOx)	poly(2-methyl-2-oxazoline)
$P_n^{\cdot}$	propargating radical polymer chain
PNIPAM	poly(*N*-isopropylacrylamide)
P(OEGA)	poly[oligo(ethylene glycol) acrylate]
P(OEGMA)	poly[oligo(ethylene glycol) methacrylate]
PO	propylene oxide
POx	poly(2-oxazoline)
P(PFPA)	poly(pentafluorophenyl acrylate)
ppm	parts per million
PPO	poly(propylene oxide)
PU	poly(urethane)
PVA	poly(vinyl alcohol)
$R^{\cdot}$	intermediate radical

RAFT	reversible addition-fragmentation chain transfer
ROP	ring opening polymerization
RT	room temperature
s	second
SEC	size exclusion chromatography
SEM	scanning electron microscopy
T	temperature
*t*BGE	*tert*-butyl glycidyl ether
T_{CP}	cloud point temperature
TE	Tissue engineering
TFA	trifluoroacetic acid
T_g	glass transition temperature
THF	tetrahydrofuran
THz	thiazolidine
Ti	Titan
T_m	melting temperature
TNBSA	trinitrobenzenesulfonic acid
UCST	upper critical solution temperature
UV	ultraviolet
UV-Vis	ultraviolet and visible
V	volume
W	watt
WST	water soluble tetrazolium
XTT	2,3-bis-(2-methoxy-4-nitro-5-sulfophenyl)-2H-tetrazolium-5-carboxaniline

Symbols

°	degree
°C	degree Celsius
%	percent
wt%	percentage by weight
Đ	dispersity
δ	chemical shift (NMR)
Δ	difference

λ	wavelength
Ø	diameter
µL	microliter
µg	microgram
µmol	micromol
3D	three dimensional
ε-CL	ε-caprolactone

Chapter 1

Scope of the thesis

Biocompatibility of materials is an imperative property for application as implant or in regenerative medicine. Biocompatibility is described as “[…] the ability of a material to perform with an appropriate host response in a specific application.”[1]. In other words, biocompatibility means ”[…] the compatibility between a technical and a biological system.”[2].

The introduction of foreign objects deliberately into the human body cannot be distinguished by the body from objects introduced accidentally. These implants, or in general biomaterials are described as “[…] a substance that has been engineered to take a form which, alone or as part of a complex system, is used to direct, by control of interactions with components of living systems, the course of any therapeutic or diagnostic procedure, in human or veterinary medicine.”[3]. The immune response can lead to the rejection or the inflammation of an implant, where biomolecules such as proteins and cells adsorb onto the surface of the material caused significantly by hydrophobic interactions and less so by electrostatic interactions. To circumvent the rejection of the biomaterial, scientists work to control unspecific protein adsorption onto such surfaces. Therefore the material has to be protected from the immune response, which can be suppressed by a hydrophilization of the materials surface. Hydrophilic polymers like poly(ethylene oxide) (PEO), also known as poly(ethylene glycol) (PEG) (PEG < 20 kDa < PEO), have gained tremendous interest as polymers for medical applications. In combination with its hydrophilic character, the “stealth effect” that PEG/PEO exhibits in the human body and that leads to a protection against protein interaction and to a certain extent also immune recognition increased its importance. Moreover, it can be renally cleared up to molecular weights of 30 kDa.[4] This lead to the abundant use of PEG for functionalization of different materials. However, the simple molecular structure of PEG limits the functionalization opportunities that enable specific interactions with the biological system. To mimic the complexity of the human body, there is great need for a system that boasts chemoselective functionalization, which provides preferential reaction of specific functionality in contrast to all other possible reactions.

Cells are surrounded by the extracellular matrix (ECM) which consists of fibrous materials in combination with different glycosaminoglycans, proteoglycans and adhesion proteins, where complicated interactions between all single components take place. The ability to mimic these surroundings within an artificial ECM or on an

implant surface would contribute to a more authentic setting for cells and would be extremely beneficial, advancing opportunities in tissue engineering and regenerative medicine.

In preliminary studies, fibrous material was functionalized with a six-arm, star-shaped PEG-based prepolymer with terminal reactive isocyanate groups (NCO-sP(EO-*stat*-PO)).[5] On the one hand, the additive caused a beneficial hydrophilization of the fibers surfaces, while enabling further functionalization through provision of an isocyanate group. On the other hand, the functional groups were extremely reactive and not specific or chemoselective. Poly(2-oxazoline)s (POx) or poly(oligo ethylene glycol) acrylates (P(OEGA)) exhibit the "stealth-effect" and biocompatibility[6-7] that PEG possesses, however, the side-chain functionality of the former is advantageous and can be introduced by facile variation of monomers.[8] In addition to hydrophilicity of the biomaterials' surface, in order to mimic the complex environment of the ECM, additional and specific functional groups are crucial for targeted cell adhesion.

Therefore, the **aim of this thesis** was the synthesis of hydrophilic polymers for multiple linkages of biomolecules via chemoselective coupling reactions which can then, amongst other applications such as nanogel preparation be used for the modification of biomaterials surfaces.

Chapter 2 gives a literature background of polymer based biomaterials and highlights certain living polymerization reactions. Moreover, different hydrophilic polymers like POx and P(OEGA) are introduced, including some chemoselective coupling reactions that are extremely interesting to mimic specific interactions inside the human body.

The materials and methods used for experiments are shown in **Chapter 3,** whereby supporting information about the theoretical background of each method and the precise description of each implementation is given.

Chapter 4 covers the synthesis of chemoselective, hydrophilic copolymers. Firstly, an initiator for the cationic living polymerization of poly(2-methyl-2-oxazoline) (PMeOx) was synthesized. The polymers were terminated with different functional groups, setting the foundation for either the Cu-catalyzed azide-alkyne cycloaddition (CuAAC) or specific amine coupling. After the reaction with a thiazolidine building block by thiol–ene chemistry and deprotection, the cysteine amount was quantified

and polymers were tested for their biocompatibility. Moreover, oligo(ethylene glycol) acrylate was copolymerized with pentafluorophenyl acrylate via reversible addition-fragmentation chain transfer (RAFT) polymerization for chemoselecitve functionalization with an amine functionalized thiazolidine or cyclic thioester to prepare polymers for additional “Native Chemical Ligation” (NCL), the chemoselective reaction of a thioester and a cysteine residue.

Subsequent to the polymer functionalization, coupling reactions were performed. Besides the functionalization via CuAAC, POx was further functionalized by employing NCL, whereby the polymer could be coupled to two different model peptides via NCL resulting in multimodal bio-functionalized conjugates. Similarly, NCL was also performed with chemoselectively functionalized P(OEGA).

Separately, the thiol of the cysteine-functionalized POx (cys-POx) was employed for chemical crosslinking, and the preparation of nanogels as drug delivery systems was achieved.

Chapter 5 comprises the experimental section providing in-depth information about each experiment performed throughout this thesis, including all supporting information such as SEC measurements with their associated elugrams.

Parts of this chapter were published in

M. Schmitz[+], M. Kuhlmann[+], O. Reimann, C. P. R. Hackenberger, J. Groll, “Side-Chain Cysteine-Functionalized Poly(2-Oxazoline)s for Multiple Peptide Conjugation by Native Chemical Ligation”, *Biomacromolecules* **2015**, *16*, 1088-1094.

Chapter 2

Theoretical background

2.1 Polymer based biomaterials

Modern everyday life would not be possible without polymers – cars, computers, storage media, sports equipment, dishes, bottles, eye wear, textiles – all these belongings mainly consists of “plastic” which is mostly interchangeable with the word polymer. Many industries, such as packaging, textiles and sports, profit from cheap polymer production. More importantly, polymers are also used to produce for medical devices. The medical industry has a great need for materials that mimic the properties of nature, in order to replace lost of function in the human body.

The human body is a very complex system, whereby different replacement materials are required to obtain the functionality needed for different purposes. Metals and ceramic materials are used because of their good mechanical stability with prevalent use of stainless steels, Ti or Co-Cr-alloys and Ni-Ti-alloys in such applications as in osteosynthesis and dental surgeries, or as joint replacements, and as surgical instruments in the case of metals. Ceramic materials are made out of aluminium and zirconium oxides, or calcium phosphates, and are especially used in dental surgery.[2]

Interest in use of polymeric materials as medical devices began in the 1960s, mainly because of their versatility in shape and surface functionality. The popularity since then has continued to increase as more and more applications have been realized. Moreover, economically polymers are much cheaper compared with metals. Wintermantel *et al.* provided an overview of polymers in the book, “Medizintechnik – Life Science Engineering”[2], detailing the plethora of polymers available for use in medical applications, including both natural and synthetic polymers (**Table 2–1** and **Table 2–2**).

Table 2–1 shows an overview of the most important natural polymers used as biomaterials. The major advantage of natural polymers is their inherent biocompatibility and biofunctionality. This is why they can be used for applications inside the body, such as in the correction of tissue defects (burns victims) or for artificial blood vessels. They are also found as suture, controlled release systems and wound care or additionally besides medical applications in food industry. Though hyaluronic acid, is not mentioned in the book of Wintermantel *et al.*, it is a major component inside the human body (e.g. the extracellular matrix)[9] and now plays an important role as a biomaterial.[10] It is applied in orthopedics for osteoarthritis

treatment, as well as in cosmetic industry, and is used as anti-wrinkle injections just as collagen.

Although natural materials possess inherent biocompatibility and biofunctional adhesion anchors, the disadvantages are batch-to-batch variability – caused by broad molecular weight distributions – and the limited modification options. Furthermore, usage restrictions may arise due to the risk of immunogenicity and disease transfer. For industry, the limited availability of natural sources of collagen and other natural materials leads to high costs which can be an issue.

Table 2–1: *Overview of natural polymers used in medical applications.*

Natural polymer	Medical application	Lit.
collagen	Replacement for: blood vessels, cardiac valves, bones, tendons and ligaments; Implants for: cornea, ureter; correction of tissue defects: burns, bedsores, ulcer; others: dialysis membranes, cosmetic uses	[11]
Chitin and chitosan	Replacement for: blood vessels correction of tissue; defects: burns; others: surgery, wound cover, contact lenses, suture, controlled release systems, dentistry, orthopedics, cosmetics, biotechnology, food industry	[12]
Fibrin	Wound care, fibrin splice	[13]
Hyaluronic acid	Orthopedics (osteoarthritis), wound care, cosmetic uses Hydrogels (still under research): cartilage tissue engineering, cardiac repair, molecule delivery, valvular engineering, control of stem cell behavior, microdevides	[10,14-15]

Table 2–2: *Overview of synthetic polymers used in medical applications.*

synthetic polymer	Medical application	Lit.
Polyethylene (PE)	LDPE, LLDPE as films, containers, tubes; UHMWPE: knee and finger joint implants	2
Polymethyl methacrylate (PMMA)	Dental surgery, intraocular lenses, contact lenses, modified PMMA as bone cement	16-19
Polytetrafluoroethylene (PTFE)	Vascular implants (still under research, controverse results)	20
Polylactide and Polyglykolide (PLA and PGA)	suture, drug delivery systems	21
Polyhydroxyalkanoate (PHA)	Micro capsules for controlled drug delivery systems, suture, wound care, vascular implant	22
Polycaprolactone (PCL)	Sutures, wound dressings, contraceptive devices, dentistry	23-27
Polyanhydride	drug delivery systems	28-30
Poly(ortho ester)	Subcutaneously implantable controlled therapeutic systems	31
Polylactide and Polyglykolide (PLA and PGA)	suture, drug delivery systems	21
Polysiloxane	Blood vessels, urethra, implants: eyes, female breasts, finger, toes, wirists, elbows	32
Polyurethane (PU)	as copolymer for artificial vascular implants	33-34
Polyethylene terephthalate (PET)	artificial vascular implants; replacement for: tendons and ligaments, suture	35-36
Polyamide (PA)	Aromatic PA (Kevlar®) as artificial tendons and ligaments, but degradable (still under research)	37
Polyetheretherketon (PEEK)	Load-bearing implants, composite material (still under research)	38-39
Polysulfon (PSU)	Reusable packaging in complex forms	2
Poly-2-hydroxymethyl methacrylate (PHEMA)	hydrogels: contact lenses, coatings for sutures	40
Polyacetale (Polyoxymethylene, POM)	Automatic dispenser for paper test for blood tubes, extracorporeal clips	41

Table 2–2 summarizes synthetic polymers mentioned in the book by Wintermantel *et al.* and gives an overview of the medical applications of the polymers. A few polymers, namely polyesters such as poly(lactid acid), poly(caprolactone) and polyurethane include degradable groups, hence, they are used as sutures, temporary glues and membranes, or in pharmacy as controlled drug delivery systems as they can be tailored to control their degradation profile. Other polymers like polyvinyl chloride (PVC) and polycarbonate (PC) also have applications as medical devices, but are not used as biomaterials in the human body.[2] Nevertheless they are economically extremely relevant as the costs of syringes, bags, tubes, containers and catheters have been reduced tremendously, because of large-scale production of these polymers.

The hydrophilicity of poly(vinyl alcohol) and poly(ethylene oxide) (PEO, which is also known as poly(ethylene glycol), PEG; PEG < 20 kDa < PEO) is also interesting for biomaterial applications. The human body cannot distinguish foreign objects that have been introduced deliberately or accidentally, therefore, a biomaterial has to be protected from the immune response. This lead to the abundant use of PEG for functionalization of different materials (especially peptides and proteins) – named "PEGylation".[42-46]

Synthetic polymers like PEG can be polymerized in a "living polymerization method" which provides control over the molecular weight distribution of polymers resulting in narrow dispersity's, a key factor in biomedical science. Synthetic materials consequently offer more control over structural properties and have a lower immunogenic risk. They represent a more reliable source of raw material and they are economically advantageous.

2.2 Living polymerizations

The controlled synthesis of designed polymers with regards to their molar masses and molecular distribution as well as their composition, architecture, microstructure, and functionality, is a central area in polymeric chemistry. Szwarc *et al.* established the terminology of “living polymers” in 1956.[47] A general polymerization consists of three steps: initiation, propagation, and termination or transfer. In “living polymerization conditions”, the initiation step is faster than propagation, and the termination or transfer step do not occur. The method makes the synthesis of defined polymers, such as block copolymers with different sequence length possible, because the chain ends stay active and polymerization occurs until complete monomer consumption. Furthermore, the control of molar mass distribution (Poisson distribution) is a main advantage of living polymerizations **(Figure 2–1**).[48] The degree of polymerization (DP) can easily be adjusted by choosing the required ratio of monomer to initiator. These characteristics make the living polymerization technique outstanding in biomaterial application as defined and reproducible polymers are key products in this field.

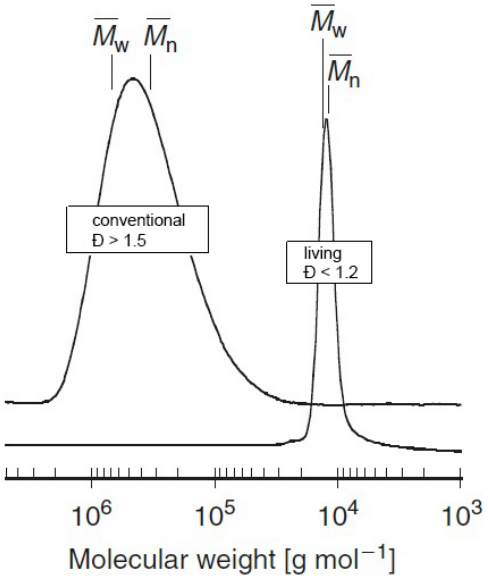

$$Đ = \frac{\overline{M_w}}{\overline{M_n}}$$

with $\overline{M_n} \leq \overline{M_w}$

$$\overline{M_n} = \frac{\sum_i n_i M_i}{\sum_i n_i}$$

$$\overline{M_w} = \frac{\sum_i n_i M_i^2}{\sum_i n_i M_i} = \frac{\sum_i m_i M_i}{\sum_i m_i}$$

with $m = n \cdot M$

Figure 2–1: *Dispersity for a conventional and a living radical polymerization. Modified from Moad et al.[49] (2005), with permission from CSIRO Publishing.*

Figure 2–1 describes the different dispersities for conventional and living radical polymerization of polystyrene. In polymer synthesis, a molar mass distribution arises which can be characterized by the dispersity *Đ*.[50] In conventional polymerization techniques, this value is higher than 1.5 whereas in a living mechanism it is below 1.2. *Đ* is a measure of the polymerization quality and is defined as a ratio between weight-averaged molar mass ($\bar{M}_w$) and number-averaged molar mass ($\bar{M}_n$).[51] A monodisperse sample is obtained if $\bar{M}_w$ equals $\bar{M}_n$ (*Đ* = 1), i.e. all polymer chains in a polymer component have the same length (same DP). This can only be realized in biochemistry for example in peptide or DNA synthesis. In polymer chemistry the distribution of polymer chains is polydisperse and the broadness of the distribution can additionally be described by the polydispersity coefficient (U), which is described as:[51]

$$U = \frac{\overline{M_w}}{\overline{M_n}} - 1$$

In the case of a Poisson distribution a direct dependency of U with the number-averaged degree of polymerization ($\bar{N}_n$) can be calculated:[51]

$$U = \frac{1}{\overline{N_n}}$$

That implies:

$$U = Đ - 1$$

$$Đ = U + 1$$

$$Đ = \frac{1}{\overline{N_n}} + 1$$

With this, the dispersity of a polymeric sample gets smaller, i.e. the sample more defined, with increasing $\bar{N}_n$. With respect to the definition of a narrow distributed polymer of *Đ* = 1.2 this can be reached only for $\bar{N}_n$higher than five.

Different living polymerization techniques exist, depending on the nature of the monomer and will be illustrated in the following. In chapter 2.3.2 the cationic ring-opening polymerization of 2-oxazolines and in chapter 2.4.1 the reversible-deactivation radical polymerization of oligo(ethylene glycol) acrylates are described.

2.3 Poly(2-oxazoline)s

PEG was and is still the “gold standard” for stealth polymers and is routinely used in the clinic. Nevertheless, there is growing evidence that PEGylated proteins can elicit antibody formation against PEG which may limit therapeutic efficacy[52-53], however this is still under discussion[54]. From a more chemical view point, the preparation of PEG is not straightforward as highly reactive oxirane monomers are needed. Lastly, the (bio-)chemical functionalization of PEG is limited to the distal ends of the polymer chain.

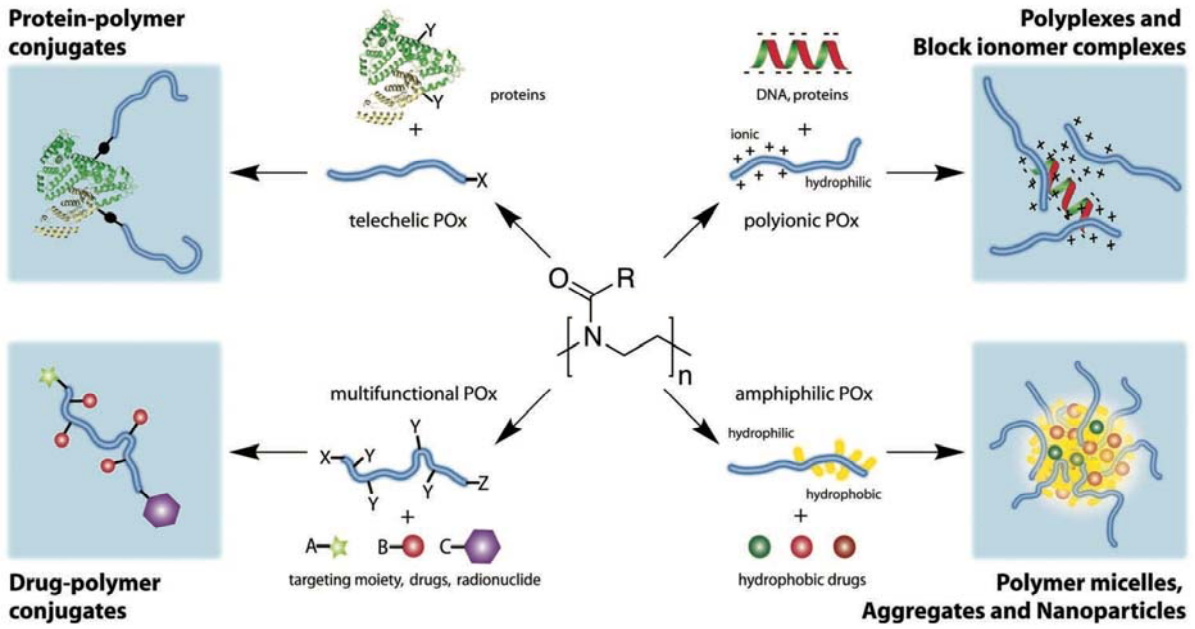

Figure 2–2: *Polymer therapeutics based on poly(2-oxazoline)s. Reprinted with permission from lit.*[8]*. Copyright (2012) John Wiley and Sons.*

Poly(2-oxazoline)s (POx) are an upcoming class of polymers being a potential alternative to PEG.[6,55-56] After the discovery in the 1960s[57-59], POx was completely disregarded as potential candidate for biomaterials in the preceding years in polymer science, although it is very versatile applicable (**Figure 2–2**). POx can be used for protein conjugation[8] in most cases with the hydrophilic poly(2-methyl-2-oxazoline) (P(MeOx)) or poly(2-ethyl-2-oxazoline) (P(EtOx))[60-64] as they showed the same “stealth effect” as PEG[65-66] and are also known to be biocompatible[67-68]. Different

reviews have been published that describe the enormous potential of POx in context of biomedical applications while comparing POx with other water-soluble polymers like PEG.[8,69-70]

The living cationic ring-opening polymerization of 2-substituted 2-oxazolines is an easy and experimentally robust method for synthesis (see Chapter 2.3.2). It offers the advantage of controlled DP with polymer architectures that have low dispersity and broad variability in terms of the chemical functionalization of the polymer side-chains through the use of functional monomers. Most of these monomers used are in the liquid state and are easy manageable during polymerization.

2.3.1 2-Oxazoline

Oxazolines are five-membered heterocycles with three different structural isomers, depending on the position of the double bond within the ring (**Figure 2–3**). 2-oxazolines were mostly examined and applied in polymer chemistry.

The first synthesis of 2-methyl-2-oxazoline (MeOx) was published in 19th century by Gabriel and Eschenbach.[71] In organic synthesis, oxazolines are used as ligands in asymmetric metal catalysis reactions[72], or as protection groups for carbon acids[73]. The most important application today of 2-oxazolines is their use in polymerization.

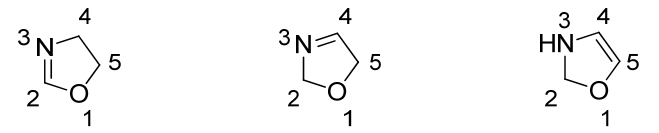

Figure 2–3: *Different structure isomere classes of oxazolines.*

As reviewed by Aoi and Okada in 1996,[74] various monomers are accessible as versatile synthetic routes make the synthesis of defined monomers possible. Only 2-substituted monomers are known for their use in living cationic ring opening polymerization. The substitution in the four and five position leads to chiral 2-oxazolines which are more important for enantioselective catalysis as ligands, and

less important for polymerizations as chain propagation is hindered due to the sterical demand of the substitutes.[75]

2.3.2 Living cationic polymerization of 2-oxazolines

Kagiya *et al.* mentioned the cationic ring opening polymerization of 2-oxazolines first in the 1960s.[57] Many reviews exist describing the living character of the polymerization.[76-77] Different methods are possible for the synthesis of POx. Cationic initiators like Lewis-acids, strong proton acids and their esters (triflate, tosylate), or alkyl halogenides are in use in combination with aprotic dipolar solvents like acetonitrile (ACN) or benzonitrile.

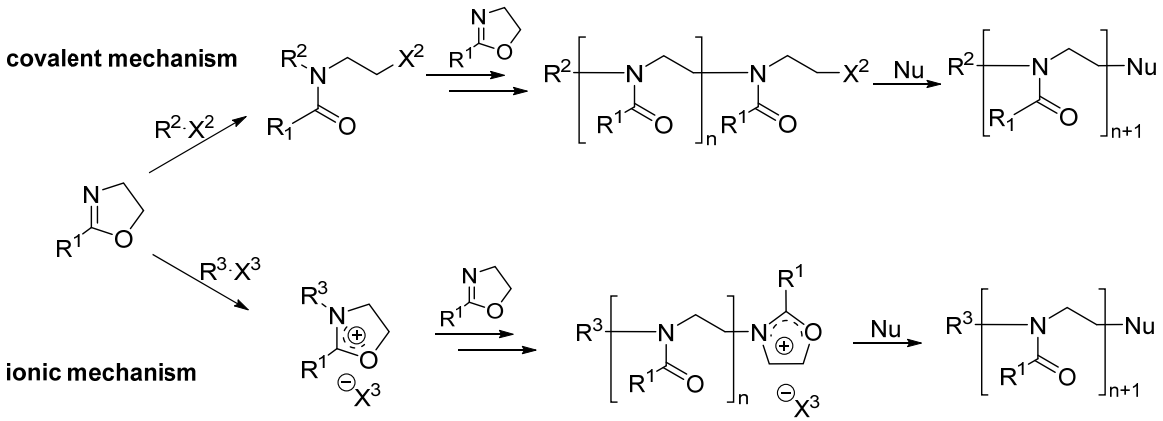

Scheme 2–1: *Different mechanisms of 2-oxazoline polymerization.*

There is a distinction between two different polymerization mechanisms, being the covalent and the ionic mechanism (**Scheme 2–1**). An electrophile attacks the nucleophilic nitrogen of the oxazoline ring. In the covalent mechanism, this attack leads to ring-opening under formation of a linear covalent amide structure, whereas in the ionic mechanism ring opening occurs after attack of a second oxazoline. Following, additional oxazolines can be added as both species are still electrophilic. The mechanism depends on various factors like nucleophilicity of the initiator, of the counterion and of the monomer itself. For example, with the non-nucleophilic *p*-toluenesulfonate (tosylate) as counterion any kind of 2-oxazoline will be

polymerized in the ionic mechanism. Even solvents like ACN influence the mechanism by stabilizing the propagating cation due to its polarity and donor properties. In a few cases, the mechanism of POx polymerization is not “living” as Litt *et al.* found out in the 1970s.[78] Proton transfer of a living polymer chain-end to a monomer unit provoke an enamine group which can attack as a new initiator (**Scheme 2–2**). Although, the described experiments were performed at high temperatures (T > 120°C), with bulk polymerization and very high $[M]_0/[I]_0$ ratios, side-reactions may occur which lead to broader molecular weight distributions. This was also observed by Hoogenboom *et al.* during polymerization of P(EtOx) at very high or too low monomer concentration ($[M]_0$ > 7M, $[M]_0$ < 3M).[79]

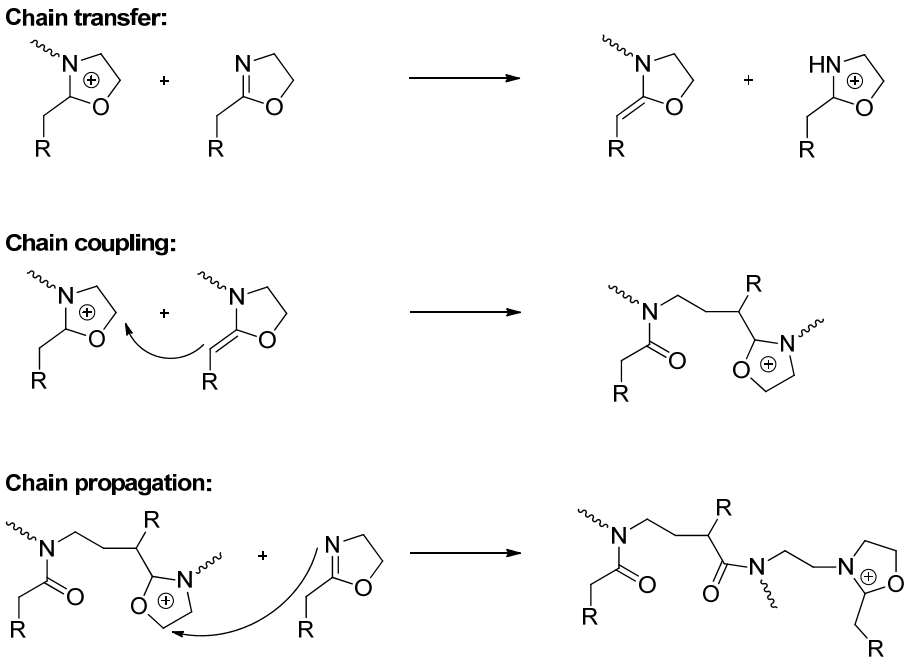

Scheme 2–2: *Suggested mechanism of chain transfer, chain coupling and repolymerization during the cationic ring-opening polymerization of 2-oxazolines. Adapted with permission from litl.[78] Copyright (1975) Taylor & Francis.*

In summary, the cationic polymerization of 2-oxazolines has a living character in most cases, when certain polymerization conditions are taken into account. Based on this living character of the mechanism, it is possible to design different architectures, compositions, or block copolymers as well as side-chain and endfunctionalized POx.

The application possibilities of these polypeptide-like polyamides are enormous. In the last decades, the field of research on POx has expanded to include the biomedical field, due to POx being biocompatible and water-soluble.

2.3.3 Polymer analogue functionalization of POx

Oxazoline monomers with allyl side-chains combine oxazoline-based advantages like biocompatibility with the opportunity of functionalization through thiol–ene reactions. The preparation of homopolymers based on 2-butenyl-2-oxazoline (ButenOx) and copolymers in combination with EtOx were shown to follow a living character polymerization, and thiol–ene modification with six different thiols was performed to yield amphiphilic polymers.[80] ButenOx homopolymers were recently used for the synthesis of DNA–polymer-conjugates by using thiol–ene UV reaction or DCC coupling techniques.[81-82]

The living character of the copolymerization of 2-decenyl-2-oxazoline (DecenOx) in combination with MeOx or EtOx has also been shown.[83] Furthermore, the groups of Hoogenboom and Dargaville used microwave irradiation in the polymerization of POx which is quite often used.[68,84-85]

Size exclusion chromatography (SEC) measurements showed the formation of well-defined polymers with *Đ* around 1.2. This value was exceeded if polymers with higher molecular weights were synthesized (around 200 repetition units) and suggests that chain transfer reactions are occurring. Kinetic studies showed a nearly random distribution of DecenOx with both, MeOx and EtOx, nevertheless MeOx conversion was slightly faster than DecenOx conversion, whereby the latter was slightly faster than EtOx.

Cesana *et al.*[86] followed the approach of synthesizing thiol-functionalized POx, but they prepared a new 2-oxazoline monomer with a protected thiol group before copolymerizing it with EtOx and after deprotection used the thiol for further polymer modification by Michael addition.

POx especially permits chemoselective coupling using NCL which is described in chapter 2.5.4. NCL reactions are widely used in the field of chemical biology to obtain challenging peptides and whole length proteins,[87-88] but they are also used in polymer chemistry for hydrogel crosslinking.[89] Luxenhofer used NCL for the synthesis of

multiple peptide bonds at the polymer side-chain.[90] A new monomer was synthesized which allows azide–alkine chemistry.[91] After the reaction with an azide-functionalized thioester, NCL was successfully performed with the cysteine residue of a pentapeptide, CREKA, which is known to bind to breast cancer tissue. The Jordan group also modified POx with protected aldehyde side-chains for chemoselective ligation with amino-oxy groups after deprotection.[92] They found a quantitative conversion of the side-chain functionalities with *O*-benzylhydroxylamine·HCl.

Azide–alkine chemistry was used for the synthesis of different block copolymers with poly(*N*-isopropylacrylamide) (PNIPAM), PCL or PLA.[93] Kempe *et al.* combined azide–alkine, thiol–ene and Diels-Alder reaction in one multifunctional copoly(2-oxazoline).[94] The polymer bears anthracene- and azide-function at the termini as well as alkene groups in the side-chain for multiple functionalization possibilities (**Figure 2–4**).

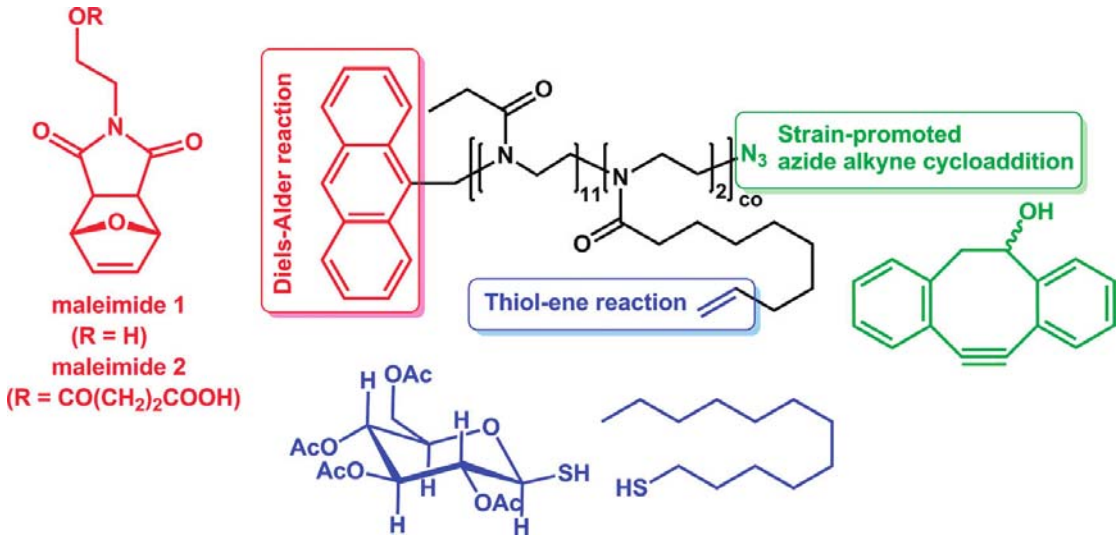

Figure 2–4: *Schematic representation of the polymer scaffold exhibiting different functionalities for the incorporation of various residues by three orthogonal efficient metal-free ("Click") reactions. Reprinted with permission from lit.[94]. Copyright (2011) American Chemical Society.*

POx was also investigated as fibrous material in 2009, where the electrospinning of P(EtOx) was successfully shown.[95] Buruaga *et al*. used water, THF, and DMF as solvents and optimized volume feed rate, applied voltage and concentration for

homogeneous fiber production. Our group in cooperation with Luxenhofer, published the manufacturing of P(EtOx) fibers by melt electrospinning writing. This method allows the 3D stacking of fibrous structures filaments as low as 5 µm in diameter.[96] Recently a company from USA, Huntsville, Alabama, called “Serina Therapeutics” work with POx as drug delivery system, using click chemistry for the conjugation of the polymer with different drugs and are currently in a Phase 1 program in patients suffering from Parkinson’s disease.[97]

2.4 Poly[oligo(ethylene glycol) acrylate]

PEG is still the gold standard for polymers as biomaterials. As this polymer class is quite demanding to produce, as low temperature anionic polymerization of EO is needed, the search for alternative polymer systems are needed. One of these alternatives is the so called poly[oligo(ethylene glycol) (meth)acrylate] (P(OEG(M)A), **Figure 2–5**).

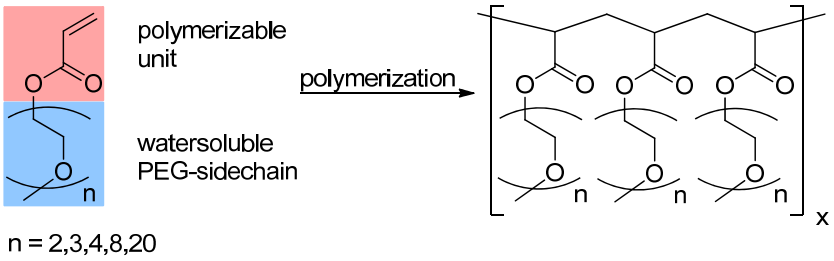

Figure 2–5: *Molecular structure of nonlinear PEG-analogues constructed with oligo(ethylene glycol) acrylate (macro)monomers. Adapted with permission from lit.[7] Copyright (2008) John Wiley and Sons.*

The presence of an acrylate group tailored with different repeat units of ethylene glycol makes a living radical polymerization possible, without losing hydrophilicity or biocompatibility.[98-99] In addition, this polymer class is extremely versatile for biomedical research as the grafted structures exhibit stimuli-responsive properties that are typically not attainable with linear PEG. For instance, these polymers generally display a lower critical solution temperature (LCST) in pure water or in physiological medium. LCST means a phase separation above a certain temperature resulting in the precipitation of the polymer. In an appropriate solvent polymer chains are present as extended coils (the polymer is dissolved). An enhancement of the temperature results in the formation of compact polymer coils provable by light scattering methods whereby interaction between solvent and polymer chains have to be taken into account. This characteristic makes them interesting for biomedical application as “smart” materials similar to PNIPAM.[7,100] Han *et al.* first reported the living anionic polymerization of OEGMA homopolymers in 2003[101], but these polymers were not widely recognized until the work of Lutz was published in 2006[102].

It was demonstrated that the tunability of the cloud point temperature (T_{CP}) can be controlled by copolymerization of ratios of short and long OEGMA monomers using atom transfer radical polymerization. T_{CP} describes the phenomenon of the phase separation of polymers in water or other solvents at a certain temperature. Recently, Vancoillie *et al.* reviewed the thermoresponsive properties of P(OEGA) and its copolymers.[103]

2.4.1 Reversible-deactivation radical polymerization

The conventional process of radical polymerization is a chain reaction type. Initiating radicals add to monomer units that initiate the polymerization. The addition of monomers to the reactive chain-end causes chain propagation. If radicals react by combination or disproportionation, chain termination occurs. In conventional radical polymerization chains are continuously formed, propagate and are terminated by radical–radical reaction. *Đ* is broader than in an ideal living process and results in values of $\bar{M}_w / \bar{M}_n > 1.5$ (**Figure 2–1**).

Different polymerization mechanisms control the value of *Đ* being < 1.2. In these cases, the polymer chains are initiated at the beginning, grow at the same rate and the reactive end groups remain, meaning no termination takes place. In living radical polymerization this implies that the side reaction of radical–radical termination is reduced to zero, which consequently means all chains are not simultaneously active. Irreversible chain termination is suppressed in the method of living polymerization. This is only possible if “reagents are present which react with the propagating radicals by reversible deactivation or reversible chain transfer so that the majority of chains are maintained in a dormant form.”[49] In contrast to the conventional process, the number of active chain ends is lower as a consequence of rapid equilibration between the active and dormant species. In these conditions, all chains have an equal chance for growth, although periodically, the molecular weight increases linearly with conversion and *Đ* can be narrow (< 1.2).

There are different techniques to promote the stabilization of radicals during polymerization. In the early 1980s, the mechanism of “Nitroxide-mediated Polymerization” (NMP) was established and has been exploited in order to synthesize polymers, especially styrene and acrylates, with narrow molecular-weight

distributions.[104-108] In all cases, the polymerization of unsaturated monomers produce radicals, but in the same way stabilizes them in the living mechanism. The use of transition metals like in ATRP or NMP is established, while organic agents in "reversible addition–fragmentation chain-transfer" (RAFT) polymerizations are more preferred in polymer science for biomedical application as these agents are biocompatible in contrast to copper in ATRP. The RAFT technique was also used in the present work and will be annotated in the following.

The use of addition–fragmentation chain transfer agents to control polymerization was first reported in the 1980s. The acronym RAFT was not adopted for use at that time. In 1997, a patent was registered describing the living radical polymerization using thiocarbonylthio RAFT agents.[109] In the same year, conference reports and papers were published describing the process of RAFT.[108,110] In the RAFT process, a free radical polymerization is turned into a living polymerization by simply adding the so called RAFT agent (thio-carbonylthio compounds, **Scheme 2–3**).

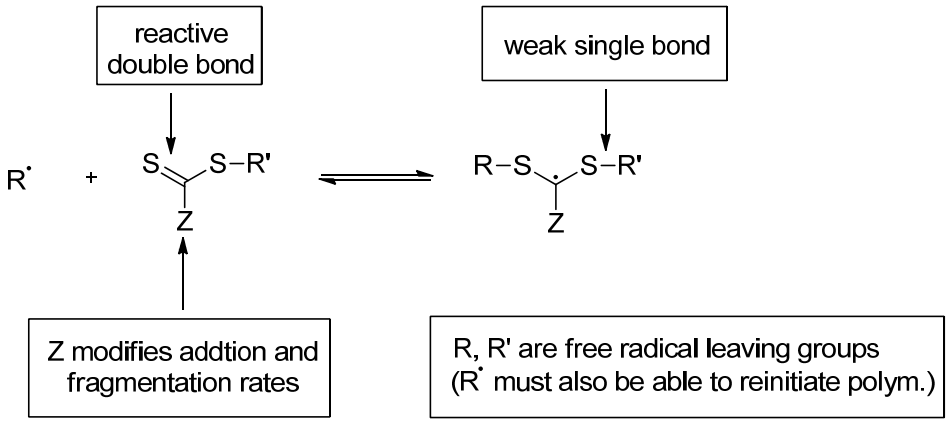

Scheme 2–3: *Structural features of thiocarbonylthio RAFT agent and the intermediate formed on radical addition. Modified from Moad et al.[49] (2005), with permission from CSIRO Publishing.*

A wide range of thiocarbonylthio compounds can be used, whereas the effectiveness of the RAFT agent depends on the monomer being polymerized and depends strongly on the properties of the free-radical leaving group R and the group Z. They can be chosen to activate or deactivate the thiocarbonyl double bond and modify the

stability of the intermediate radicals (**Scheme 2–3**). Moad, Rizzardo and Thang from CSIRO in Australia reviewed the design and synthesis of different RAFT agents.[49,111] The mechanism of a RAFT polymerization is shown in **Scheme 2–4**.

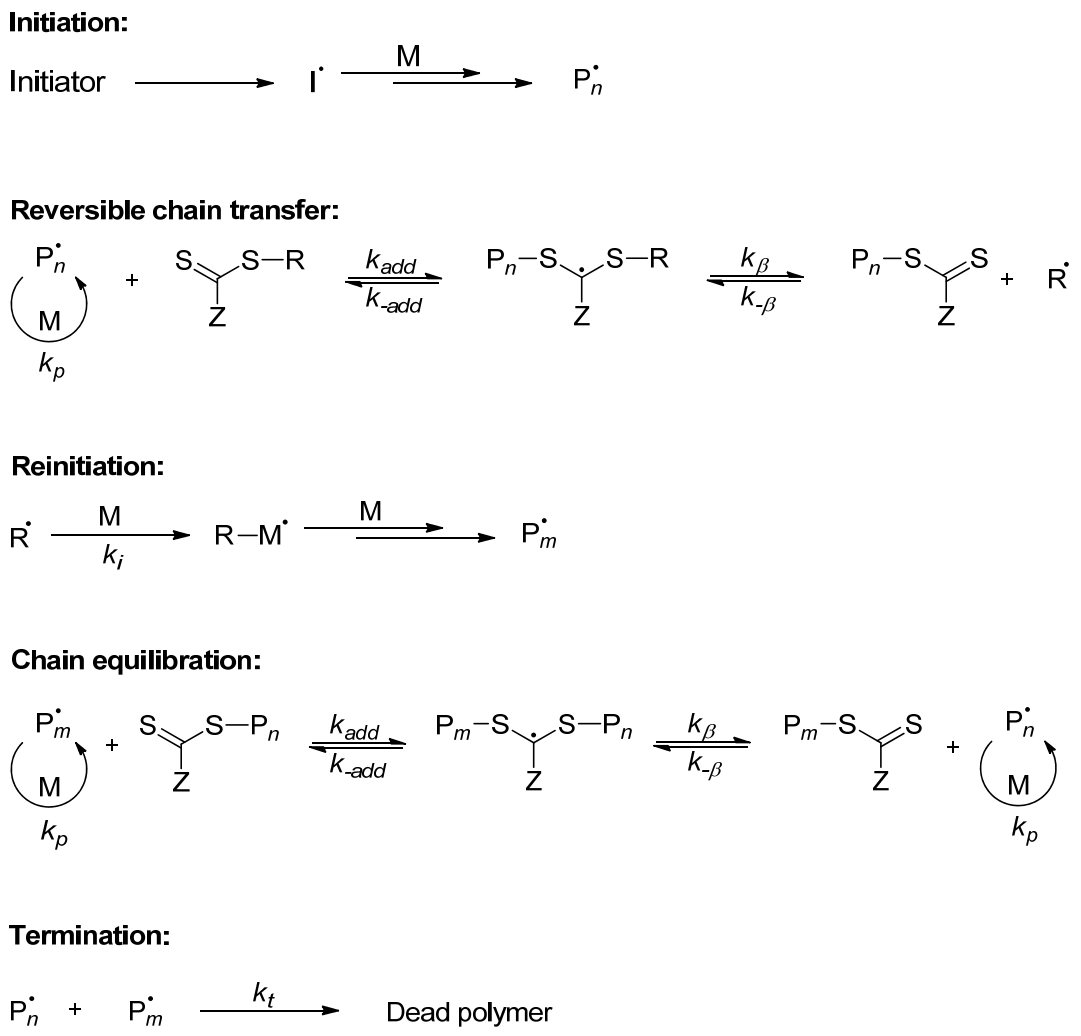

Scheme 2–4: *Mechanism of RAFT polymerization. Modified from Moad et al.[49] (2005), with permission from CSIRO Publishing.*

The most important fact is the stabilization of the developed radical, resulting in a sequence of addition–fragmentation equilibria. The polymerization is started by an initiator, in most cases a radical source like azobisisobutyronitrile (AIBN). The propagating radical polymer chain ($P_n^{\bullet}$) is developed via frequent addition of monomer units.

The addition of the thiocarbonylthio compound leads to a stabilized radical followed by fragmentation of an intermediate radical ($R^{\bullet}$). This radical is able to react with monomers and results in a newly generated radical polymer chain ($P_m^{\bullet}$). A fast equilibrium between active propagating radicals ($P_n^{\bullet}$ and $P_m^{\bullet}$) and a dormant species results in narrow *Đ* as all polymeric chains have the same possibility to grow. In many polymerizations, the polymer chain retains the thiocarbonythio compound as the end group, resulting in stable but active materials, making the synthesis of block copolymers possible.

2.4.2 Functionalization of P(OEGA) and active esters

The copolymerization of OEGA with an active ester component makes the synthesis of hydrophilic and biocompatible polymers, with the ability for post-functionalization, possible. Active esters first successfully fulfilled their function in the area of peptide synthesis in organic chemistry.[112] Numerous active esters have been focused on like activated methyl esters, thiophenylesters or NHS-esters as well as aryl esters with electron withdrawing substituents in the aromatic ring.[113-116] Recently, Das and Theato reviewed the methods of different pendent activated ester moiety in the side-chain of polymers and the "opportunities and challenges for the design of functional macromolecules".[117]

The use of pentafluorophenyl acrylate (PFPA) as active component was a development of the previously used pentachlorophenyl ester that was reactive but the sterical demand of the leaving group hindered the breakthrough in solid-phase peptide synthesis. In the following, fluoro-substituted aromats served as leaving group with much less sterical hindrance.[118]

Beija *et al.* copolymerized PFPA with OEGA or diethylene glycol acrylate by RAFT polymerization.[119] They examined the effect of reaction conditions, such as solvent, for the post-polymerization reaction with furfuryl amine as model amine, where protic and polar solvents gave best results. Afterwards they modified the copolymer with various amines for the preparation of polymer–antibiotics.

Thermoresponsive poly[oligo(ethylene glycol) (meth)acrylamide]s were synthesized from P(PFPA) with different repeating units of the side-chains which serve for PEG

analogous.[99] LCST and an upper critical solution temperature (UCST) behavior were examined in water and alcohols.

Jones *et al.* used P(OEGMA) for the synthesis of tunable thermoresponsive protein–polymer conjugates.[120] They functionalized a reduced peptide consisting of 32 amino acids (Salmon calcitonin) by thiol–ene chemistry with an ATRP-initiator for the radical polymerization of OEGMA. The one-pot protocol yielded well-defined conjugates with tunable T_{CP} ranging from 24°C to 51°C, showing that the polymerization of monomers with different side-chains has a strong influence on T_{CP}.

In combination with active esters, like succinimidyl methacrylate, P(OEGMA) was used for the synthesis of multifunctional, magnetical core–shell particles for the immobilization of trypsin.[121] Kinetic experiments have shown that the specific enzyme activity of particle-bonded trypsin was not lower compared to soluble trypsin. Furthermore, the nanostructures' potential for selective tagging and separation of the exposed surface of endothelial cells could be shown. This characteristic facilitates the isolation and identification of membrane proteins.

OEGA has been frequently used in the synthesis and formation of hydrogels.[122-125] Pentafluorophenyl esters as alternative to succinimidyl esters, were copolymerized with OEG(M)A in order to synthesize reversible and irreversible hydrogels by the reaction of active ester residues with different kinds of crosslinkers.[126] Using cysteamine hydrochloride or cystamine dihydrochloride, redox-sensitive hydrogels could be synthesized. After hydrogel reduction, a permanent crosslinking *via* Michael-type addition is possible, by using diacrylates.

RAFT polymerization of OEGMA in combination with PLA was also used for the preparation of fibrous material.[127] The copolymers served as additives in Polylactide fibers and increased surface hydrophilicity. Other copolymers were compared and it was shown that microphase separation of the incompatible hydrophilic component occurs. After the immobilization of RGD, human mesenchymal progenitor cells showed much better adhesion to the fibers with surface-adhesive heterogeneity compared to fibers with only adhesive or inert surface chemistries.

PFPMA was also used for the preparation of fiber structures and was further functionalized with different saccharides e.g. mannose, which can enhances the cytokine production of macrophages.[128] They showed the successful implementation of a reactive mesh platform for further (bio-)functionalization.

2.5 Chemoselective coupling reactions

Chemoselective coupling reactions are very important in organic synthesis and help to create specific molecular compositions. Transferring this kind of reaction type to polymer science is possible and would allow to specifically introduce desired chemical functions.

Chemoselectivity is the selective reaction of one functional group with another even though other functional groups are present. In other words, chemoselectivity describes the appearance of a preferential reaction in contrast to other possible reactions. This reaction type is of great importance particularly in complex environments like e.g. the extracellular matrix in the human body. In the following, a number of different coupling methods will be described, especially the seemingly powerful click chemistry techniques for chemoselective coupling reactions.

2.5.1 Click chemistry

The term of click chemistry was established by Sharpless *et al.* in 2001[129], describing chemical reactions that have the following characteristics:

- The starting materials and reagents must be readily available
- The reaction must be modular and wide in scope
- The reaction conditions must be simple (insensitive to oxygen and water)
- No solvent or harmless solvent (like water) should be used that should be easily removed
- Only inoffensive byproducts should be generated (removable by nonchromatographic methods)
- The reaction must be stereospecific (but not necessarily enantioselective)
- The product isolation must be simple
- The reaction should give very high yields
- The product should be stable under physiological conditions

These types of reactions are versatile and provide the ability to create many functionalities using simple chemistry. Many different research groups have used various click chemistry reactions with different mechanisms that have fast reaction times and high yields as promising characteristics.

In today's language the use of click chemistry is often mistaken with the Cu(I)-catalyzed azide–alkine reaction (CuAAC, coined by the Sharpless group[130] and Meldal[131]). The reaction conditions conformed quite well to the characteristics of click chemistry except the copper was used as a catalyst which is especially disadvantageous if products should be used furthermore as biomaterial, but this opinion is under discussion.[132-134]

2.5.2 Azide–alkyne chemistry

The mechanism of CuAAC, is shown in **Scheme 2–5**. The mechanism is complex and is not absolutely confirmed to this day. Additional literature describes many different reaction conditions of azide–alkyne chemistry.[135-137]

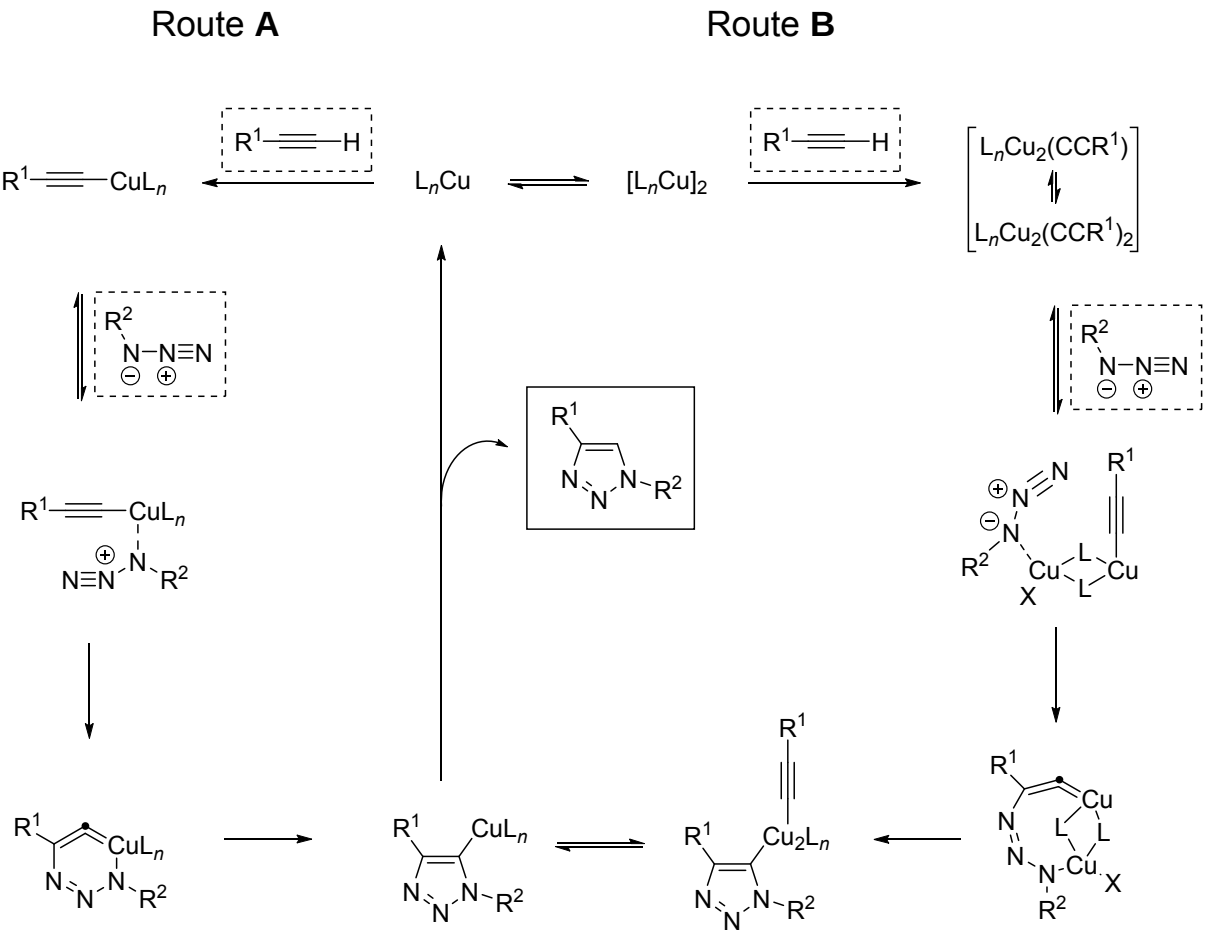

Scheme 2–5: *Suggested mechanism of Cu-catalyzed reaction of an alkine with an azide. Adapted with permission from lit.[138] Copyright (2009) John Wiley and Sons.*

The amount of copper used in such reactions is extremely important with respect to biomedical applications. There are different options available to avoid the use of copper as a catalyst, but these are coupled with other challenges such as ring tension, azides with substituted cyclooctines, activated alkines, or electron-poor alkines.[139-140]

In the following, two further reaction mechanisms will be demonstrated which closely fulfill the characteristics of click chemistry. They can produce high yields while needing no chemical catalysts (except UV-light), with very simple reaction conditions and products that are stable under physiological conditions.

2.5.3 Thiol–ene chemistry

The process of thiol–ene coupling was first used by Goodyear in 1839,[141] and later the mechanism became known as vulcanization. The reaction of thiols to olefins was already observed in 1905 by Posner[142] and found versatile applications ranging from polymer to low molecular chemistry.

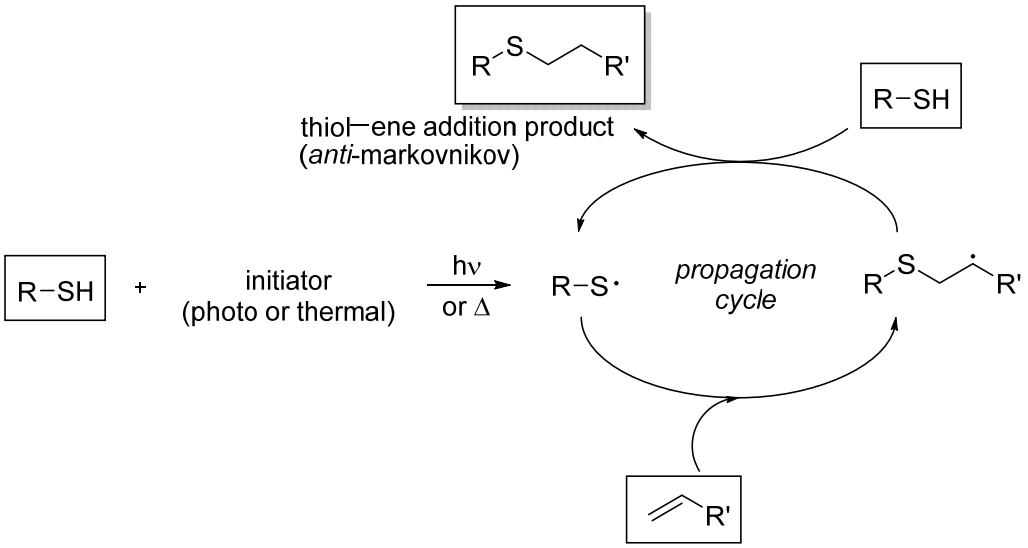

Scheme 2–6: *General radical mechanism of thiol–ene reactions. Adapted with permission from lit.[143] Copyright (2010) John Wiley and Sons.*

Many of the previously mentioned attributes of click chemistry are realized in the reaction of thiols with double bonds which can be proceeded by a radical (thiol–ene reaction)[144] or an anionic chain (thiol-Michael addition)[145]. The radical mechanism for the thiol–ene reaction is shown in **Scheme 2–6**. An initiator creates radicals, transforming the thiol to a thiyl radical which can then react with an olefin. After radical transfer onto the next thiol, the *anti*-markovnikov product (the hydrogen prefers the carbon which contains less hydrogens) is formed, if the stability of the intermediate radical-species is not negatively influenced by the substituents. Hoyle and Bowman demonstrated the robustness of thiol–ene coupling and summarized many results in an excellent review.[146]

2.5.4 Native chemical ligation

The native chemical ligation (NCL) is a highly chemoselective reaction between *C*-terminal thioesters and *N*-terminal cysteine residues. In 1994 the Kent group published the synthesis of proteins by NCL allowing the direct synthesis of native backbone proteins of moderate size.[147] They used NCL for the formation of Interleucin-8 (IL-8) consisting of two different synthetic peptide fragments. In the following years, NCL was used to synthesize multivalent peptides and protein dendrimers[148], or for hydrogel crosslinking[89,149]. In 2006, the kinetically-control convergent chemical synthesis of proteins, and insights into the mechanism and catalysis of NCL reactions were published.[150-151]

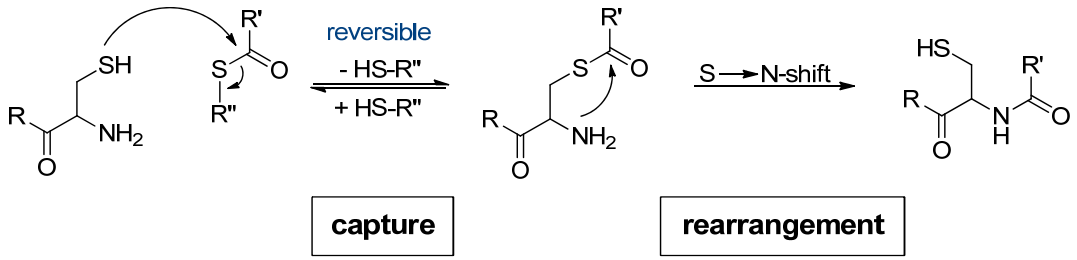

Scheme 2–7: *Schematic overview of native chemical ligation (NCL). Adapted with permission from lit.[152] Copyright (2008) John Wiley and Sons.*

The mechanism for NCL is shown in **Scheme 2–7.** The first step is a nucleophilic attack of the cysteines' thiol to the thioester. This reversible-capture step leads to a thioester linked product followed by rearrangement (S→N acyl shift) to the stable amide- or peptide-bond. Importantly, only *N*-terminal cysteines are able to undergo the S→N shift and consequently no other cysteine compounds can interfere in the reaction.

The most important advantage of the reaction is the chemoselectivity, as well as the recovery of thiol-functionality which can be used for further functionalization[153]. Moreover, the linkage is performed under mild conditions regarding temperature and pressure while the solvent used can be an aqueous solution around neutral pH. The solvent used is significant as thioesters are not stable under basic conditions and on the other hand acids reduce the reactivity of the cys-thiol and the *N*-terminal amines. The reaction times are fast and can be influenced by amino acids localized at the *C*-terminus of the thioester[154], and the type of thioester itself[155].

In contrast to the conventional NCL, the use of a cyclic thioester structure (**Scheme 2–8**) results in the formation of a single conjugate product without the release of soluble thiol-containing molecules as side products which are potentially cytotoxic to certain cell lines.[156] The resulting product has significantly higher biocompatibility in contrast to products formed from conventional NCL. Furthermore, two thiol groups are left after the NCL with the cyclic thioester, which can be used for further functionalization like oxidation in order to design new hydrogels for drug delivery systems.

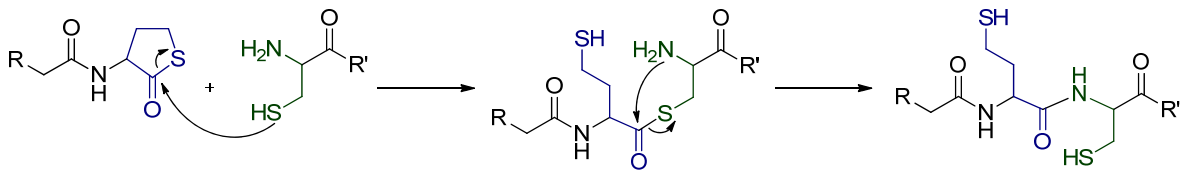

Scheme 2–8: *Native chemical ligation with cyclic thioester structure for NCL without the formation of cytotoxic side products.*

2.6 Drug delivery with hydrogels and nanogels

Ringsdorf proposed polymeric materials for drug delivery in 1975 and created an extensive research in polymeric based drug delivery systems.[157] It was described that hydrogels are extremely interesting in the field of pharmaceutical application, besides biomedical engineering because they combine interesting characteristics like good mechanical properties, high water content, and biocompatibility.[158] Furthermore, the tunability of the chemical and three-dimensional physical structure makes them remarkable as biomaterials and extremely interesting for nanotechnology in cancer therapy[159].

Farrugia *et al.* synthesized copolymers with DecenOx and MeOx and exploited the preparation of cytocompatible hydrogels.[160] The same system was used for the fabrication of POx-based polymer capsules using CuAAC and thiol–ene chemistry for crosslinking.[161]

Copolymers of EtOx and DecenOx were also used for nanoparticle approaches.[162] Chujo *et al.* functionalized POx with maleimide- and furan-residues in order to use a Diels-Alder reaction for reversible gel formation.[163] Crosslinking was performed at temperatures above 80°C and stabile hydrogels were formed. The degree of swelling could be adjusted by the amount of functional groups available for crosslinking.

The Schubert group used amine-functionalized POx for the synthesis of hydrogel structures which could be applied for genetic material binding and release in diagnostics or pathogen detection.[164] They observed a lower critical solution temperature (LCST) behavior of the polymers with the LCST behavior being dependant on the amount of amine-functionalized monomer in the polymer composition. The formed hydrogels had a bead-like microstructure which was characterized by SEM imaging.

McAllister *et al.*[165] showed the importance of polymeric nanogels produced via inverse micro-emulsion polymerization as potential gene and antisense delivery agents. Inverse micro- or mini-emulsion (IME) is one possibility to prepare nanogels. A mini-emulsion consists of an aqueous dispersion of surfactant-stabilized oil droplets within a size range of 50 – 500 nm and is prepared by shearing a system containing oil, water, a surfactant and a strong hydrophobe.[166] In an IME, a water

phase is swirled in an oil phase, stabilized by surfactants and these water droplets can be used as mini-reactors.

The use of redox-sensitive material as nanogels is very promising, as different environments in the human body can be utilized for targeted drug delivery.[167] The rapid and reversible thiol–disulfide exchange is fundamental in the biological functions of living cells.

Water-soluble polymers with thiol- or cysteine-functionality make the preparation of redox-sensitive hydrogels possible. These crosslinked networks are qualified for biotherapeutics and low molecular weight drug delivery when the crosslinking base of disulfide-bridges. These gels are able to release the cargo almost quantitatively inside cells, because here a reductive environment prevail which cleaves the redox-sensitive bonds. Saito *et al.*[168] published a review which focused on the understanding where and how the disulfide bond in the bioconjugate is reduced upon contact with biological mileu for designing and interpreting new delivery strategies.

The synthesis of redox-sensitive nanogels consisting of PG[169-170] or PG in combination with NCO-sP(EO-*stat*-PO)[171] was previously shown. Singh *et al.* demonstrated that different oxidation catalysts like alloxan and horse radish peroxidase (HRP) could be used in IME as a replacement for the harsh hydrogen peroxide usually used. They also presented a strategy to control the size of PG nanogels. Early, the thiol-functionalization of POx for the synthesis of switchable hydrogels were completed.[172] Gelation was initiated by the thiol-functionalized component which was sensitive to reduction and oxidation whereby the crosslinking through intermolecular disulfide-bridges could be adjusted.

Chapter 3

Materials and methods

3.1 Atomic force microscopy

Atomic force microscopy (AFM) is a method for surface analysis of various materials. A needle tip mechanically scans the sample's surface, measures the atomic forces and consequently acquires information about the surface chemistry in the nanometer scale range.[173-175]

AFM measurements were used to confirm particle formation of cysteine-functionalized POx (cys-POx) after inverse miniemulsion (IME). Glimmer was used as substrate, whereby the first layer was detached with adhesive tape to generate a clean and smooth surface. Before measurement with a Nanosurf FlexAFM from Nanosurf the nanogel solution was simply dropped onto the surface and the water was evaporated. The cantilever rad a radius of 7 nm, the resolution was 512 points·line^{-1} at a measuring speed of 0.8 s·line^{-1}.

3.2 Dynamic light scattering

The measurement principle of dynamic light scattering (DLS) relies on the Rayleigh scattering, which is described as the omnidirectional scattering of light of small particles.[176-177] When a monochromatic light source (laser) is used, the Brownian motion (movement of particles and molecules in solution) of particles causes a fluctuation of the scattering intensity. The movement speed of the particles in solution is dependent on their size, whereby information about their hydrodynamic radius is acquired with the determined diffusion coefficient.[178]

DLS was used for the measurement of particle sizes by photo correlation spectroscopy using Zeta Potential/Particle Sizer NICOMP^{TM} 380 ZLS from PSS Nicomp Particle Sizing Systems. Measurements were performed at a scattering angle of 90°. The wave length of the laser was 639 nm. For filter-initialization a sample with an intense light scattering was employed whereby the device adjusts the filter position with the biggest aperture, with the most intensive detectable scattering intensity (ND-value 192, position of the filter) of the sample. As intensity setpoint a value was chosen, which was about 15 % above the highest value of scattering but was at most 300 kHz. This value was used as orientation for filter setup. If the range

of dispersion is higher than the intensity setpoint, the filter was closed until the intensity of scattering at the detector conforms with the intensity setpoint.
Disposable glass- or plastic-cuvettes were used for measurement in water. Three cycles of measurements, each with 5 min, were performed, whereby the measured values were averaged over the total measurement time.

3.3 Fourier transformed infrared spectroscopy

Fourier transformed infrared spectroscopy (FTIR spectroscopy) is a method of structural clarification whereby infrared radiation is used for the vibrational excitation of bonds. Infrared active molecules have a permanent or induced dipole moment. The incident radiation induces an excitation of all molecules dependent on the radiation energy or frequency which consequently changes the dipole moment and generates a characteristic signal.
FTIR spectroscopy was used for the analysis of different functionalized polymers. The measurements were performed with a “NICOLET iS10” (Thermo Fischer Scientific; Waltham, Massachusetts, USA) spectrometer by using the software “OMNIC 8.2” (Thermo Fischer Scientific; Waltham, Massachusetts, USA).

3.4 Luminescence measurements

Luminescence measurements were used during the biocompatibility test of different polymers and gave information about the number of cells and cell viability. The measurements were carried out on Elisa Reader Spectrafluor Plus (Tecan, Deutschland, GmbH, Crailsheim).

3.5 Matrix-assisted laser desorption/ionization – Time of flight mass spectrometry measurements

Matrix-assisted laser desorption/ionization – time of flight mass spectrometry (MALDI ToF MS) is an analytical technique for the measurement of molecular masses and therefore can be used for molecular weight analysis of synthetic polymers.[179] The technique relies on the co-crystallization of the analyte and a matrix. After the integration of the analyte in the crystal lattice of the matrix, a laser ablates small pieces of the matrix-analyte sample that is transferred into the mass spectrometer by vacuum and separated by the mass-to-charge (m/z) ratios.[180] If a ToF MS is used, the time of flight gives information about the analytes' composition.

MALDI ToF MS measurements were acquired on a time of flight mass spectrometer (Bruker Daltonics autoflex II), equipped with a SCOUT^{TM} MTP MALDI Ion Source. The standard was prepared by mixing a solution of CsI_3 (10% in ACN) with DCTB solution (2.5% in ACN) in a ratio of V/V = 1/1 and 1 µL was spotted on the aluminium maldi target (Bruker Daltonics MTP 384 massive target T; Part No.: 26755). A polymer solution (10 mg·mL^{-1} in $CHCl_3$/MeOH, V/V, 2/1) and a matrix solution (25 mg·mL^{-1} dithranol in chloroform) were prepared. 2 µL of the polymer solution and 20 µL of the matrix solution were combined and spotted on the maldi target. 200 shots at 20 Hz of a 337 nm nitrogen laser (LTB MNL205 BA352A61, laser power 53%) were applied and the specta were accumulated with a cut off of 450 g·mol^{-1}.

MALDI ToF measurements of the polymer–peptide conjugates(*) were performed on a Microflex LT system from Bruker (Am Studio 2D, 12489 Berlin, Germany) and processed and analyzed by FlexAnalysis 3 MALDI software. 1 µL of a 9:1 mixture of 2,5-dihydroxybenzoic acid and 2-hydroxy-5-methoxybenzoic acid (SDHB) matrix was added to 1 µL water containing 0.1% TFA and 1 µL of sample. Subsequently, the solution was carefully mixed by pipetting and spotted. Analysis was performed in the linear positive ion mode. For each spectrum 10,000 consecutive laser shots were accumulated (20 shots·s^{-1}).

3.6 Nanoparticle tracking analysis

Nanoparticle tracking analysis (NTA) relies on the same phenomena as DLS, specifically the Brownian motion and light scattering of particles in a solution. Similarly, the user obtains information about the size/hydrodynamic radius distribution of particles in solution with the benefit of real visualization by a high-sensitive camera.[181]

NTA was used for the measurement of particle size-distribution and -concentration whereby the system NanoSight NS500 from Malvern Instruments was used. The wavelength of the laser was 635 nm. The nanogels suspensions were diluted 1000-times with millipore water and were characterized at 23°C. The length of the video was set to be 60 s by a frequency of regeneration of 13.7 fps. The camera level was chosen to show the highest value of particles, whereby the noise was minimized. As detection threshold a value was determined where most of the visible particles were counted by the software but the amount of multiple particle assignment of one scattering center was as little as possible.

3.7 Nuclear magnetic resonance

Nuclear magnet resonance (NMR, ^{1}H-NMR, ^{13}C-NMR, ^{19}F-NMR) was used for structural clarification of molecules and polymers. Additionally, it enables the analysis of polymeric endgroups by which the repetition units of monomers in polymers can be calculated. NMR uses the interaction between the magnetically moment (or vector) of atom cores with an externally applied magnetically field. The applied field causes a splitting of the nuclear levels (spin +1/2 and -1/2). By energy absorption or emission, the spins are allowed to change their levels and consequently a different population of both possible states appears. A deactivation of the outer magnetic field ensures the relaxation of the spins to the equilibrium state and free induction decay is recorded. A NMR spectrum can be obtained with the help of a Fourier transformation.[182]

NMR spectra were recorded on a Bruker Fourier 300 at 300 MHz, Bruker Fourier 400 at 400 MHz, or on a Bruker Fourier 600 at 600 MHz. Deuterated chloroform ($CDCl_3$),

dimethyl sulfoxide (DMSO-d_6), acetonitrile (CD_3CN), and deuterium oxide (D_2O) spectra were recorded with non-deuterated solvent signals as internal reference.

3.8 Raman spectroscopy

Raman spectroscopy makes the measurement of vibration spectra possible and is similar to FTIR spectroscopy; however, the process is different in that Raman spectroscopy deals with scattering processes in contrast to IR spectroscopy where absorption processes occur. Electromagnetic radiation can be scattered by molecules elastically (Rayleigh scattering) or inelastically (Raman radiation). The inelastic scattering provokes a changing of the energy that can be measured. In Raman spectroscopy the periodic change of polarizability is largely responsible for the intensity of Raman signals.[183]

Raman spectroscopy was used for the analysis of cysteine functionalized polymers and more specific for the analysis of thiol or disulfide-bonds in the polymeric molecules. The measurements were performed with a “DXR RAMAN Mcroscope” (Thermo Fisher Scientific; Waltham, Massachusetts, USA) with a special resolution of min 540 nm, a confocal depth resoltution of min 1.7 µm, with a laser class 1 and an excitation laser of 780 nm.

3.9 Scanning electron microscopy

Scanning electron microscopy (SEM) can enable the visualization of surfaces for various materials. In SEM an electron ray (x-ray) screens the surface of a sample whereby electrons interact with the object and a three dimensional image is generated.

SEM images of the nanoparticles were made in the group of Prof. Dr. Frank Würthner in the Institute of Organic Chemistry. The sample was applied to a copper holder and was mounted to a stub shuttle. Prior to examination, the specimen was plunged into slush (mixture of solid/liquid nitrogen) and was rapidly frozen. The sample was transferred into a sealed vacuum transfer device to the precooled stage

of the preparation chamber (Quorum PP2000T) which was mounted on to the SEM and was fractured. Controlled freeze-drying of the fractured surface was performed for 2 min at a temperature of −85°C and at a pressure of $p \approx 10^{-6}$ mbar. The specimen was cooled to -150°C again and transferred into a SEM sample chamber maintained at about -150 °C. Images of the sample were taken using a Zeiss Ultra *plus* field emission scanning electron microscope operated at 2 kV with an aperture size set to 30 µm to avoid excessive charging and radiation damage of the areas imaged.

3.10 Size exclusion chromatography

In size exclusion chromatography (SEC) a polymer solution is applied to a column which is filled with a porous material (in most cases crosslinked polystyrene). The polymer is eluted with a solvent whereby the separation of the molecules is dependent on the size. Each molecule has a hydrodynamic volume that is dependent on the molecular weight and governs the permeation of the polymer-molecules into the pores of the static phase. Big molecules are not able to invade the pores, as much as small molecules, and are eluted first. Particles with the smallest hydrodynamic volume remain the longest in the pores and are eluted at the end. The eluted solution can be analyzed by different detectors like refractive index- or viscometer-detectors and provide information about M_n, M_w and *Đ.* SEC is not an absolute method as a calibration curve is needed that incorporates standards with extremely narrow molecular weight distributions, to obtain a relationship between molecular weight (M) and elution volume (V_e).

$$log\ M = a - b \cdot V_e$$

SEC elugrams were recorded on two different systems, depending on which solvent was used. Using **DMF** (including 1 $g \cdot L^{-1}$ of LiBr) as solvent with a flow rate of 1.0 $mL \cdot min^{-1}$ and a high-pressure liquid chromatography pump (Agilent), refractive index detector (Agilent) and PSS SDVlinear M column (length = 300 mm, width = 8 mm, particle size = 5µm). For calibration poly(ethylene oxide) standards (PSS) were used. **Water** as solvent was added by 0.1M $NaNO_3$ and 0.02% NaN_3. A flow rate of 0.7 $mL \cdot min^{-1}$ was adjusted. The system consists of a Viscotek SECmax

(in-line degasser, 2-piston-pump and autosampler), column oven at 35°C, refractive index detector (Viscotek), viscosity detector (Viscotek 270 detector), and Viscotek A-Columns for aqueous GPC/SEC (Length = 300 mm, width = 8 mm, porous poly hydroxymethacrylate polymer, particle size = 13 um). For calibration poly(ethylene oxide) standards (Malvern) were used.

3.11 UV-LEDs

UV-LEDs were used for the thiol–ene chemistry of allyl-functionalized POx and were obtained by Polymerschmiede (Aachen, Germany) having 4 UV-LED cubes with 11 W (each) and a wavelength of 365 nm.

3.12 UV-Vis absorption measurements

UV-Vis adsorption measurements were used for the TNBSA assay and were performed on a Genesys 10S Bio Spectrophotometer at room temperature using a wavelength of 335 nm.

Parts of this chapter were published in

M. Schmitz[+], M. Kuhlmann[+], O. Reimann, C. P. R. Hackenberger, J. Groll, “Side-Chain Cysteine-Functionalized Poly(2-Oxazoline)s for Multiple Peptide Conjugation by Native Chemical Ligation”, *Biomacromolecules* **2015**, *16*, 1088-1094.

(*) This work was performed in cooperation with the group of Christian P. R. Hackenberger at Department Chemical Biology II, Leibniz-Institut für Molekulare Pharmakologie (FMO) in Berlin and Humboldt Universität zu Berlin, Department Chemie, Berlin. Oliver Reimann at the aforementioned institute performed the peptide synthesis, NCL experiments as well as MALDI ToF and HPLC measurements.

Chapter 4

Results and discussion

4.1 Synthesis of functional polymers

The use of clickable P(MeOx) as biomaterial, makes the formation of reactive substances possible. They would be able to react with numerous components, if they bear the correct opposite functionality (azide or alkyne) in their molecular structure. All polymerizations were performed in dry argon atmosphere independent of which monomers or initiators were used. MeOx and acetonitrile were stirred over CaH_2 overnight and were freshly distilled before use.

4.1.1 Propargyl tosylate for azide–alkine chemistry

In order to functionalize POx at the termini, two different procedures are possible to use: Firstly, the possibility to introduce functionality with the initiator to the *α*-terminus of a polymer. Alternatively, the polymerization may be terminated, by an appropriate reagent, (e.g. NaN_3, chapter 4.1.4) at the *ω*-terminus.

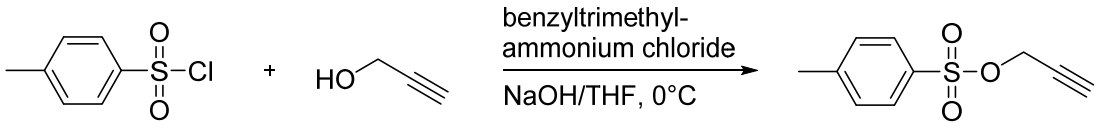

Scheme 4–1: *Schematic overview of the synthesis of propargyl tosylate.*

The use of functional initiators is established in literature, for example using alkyne endgroups for further azide–alkyne chemistry.[184] Propargyl tosylate was synthesized using a biphasic solvent system of NaOH (aq., 2.5 M) and THF at 0°C. Typically, tosylation of acohols is performed with excess of tosyl chloride, but in this case chromatographic purification is needed to provide clean products. Using a small excess of propargyl alcohol makes an aqueous workup possible in order to remove redundant propargyl alcohol. The product could be isolated in good yields of about 91%.

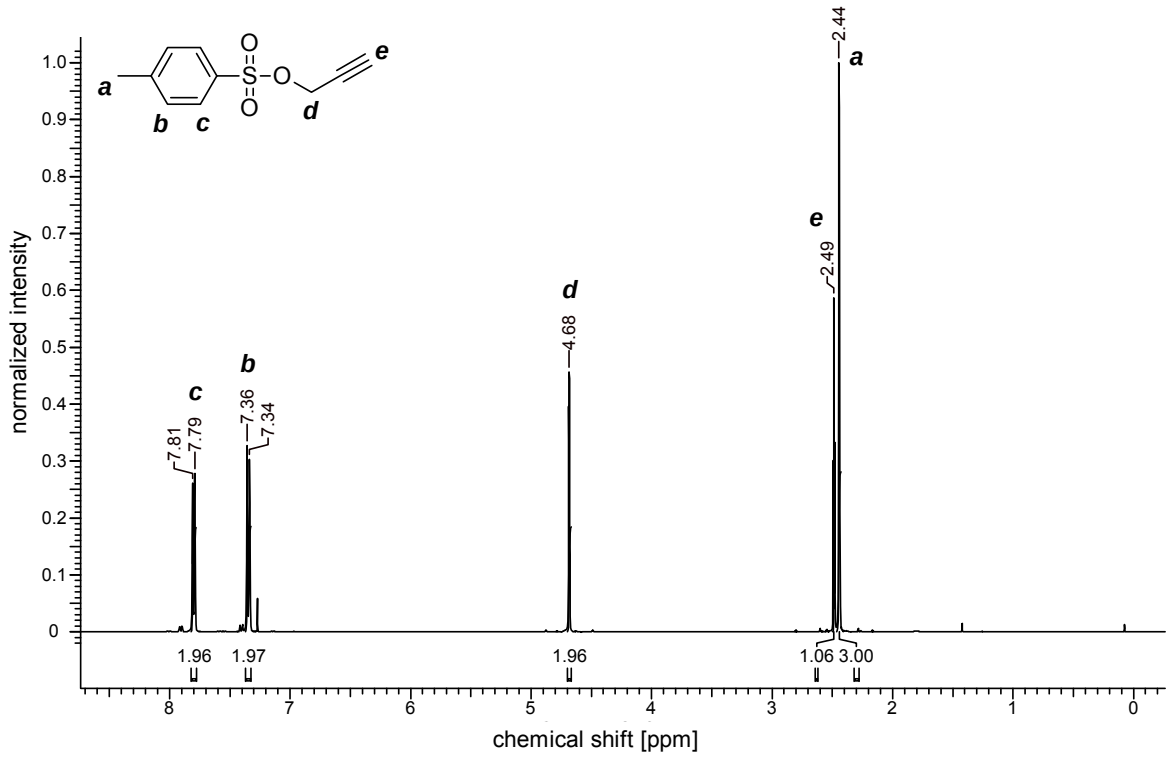

Figure 4–1: *^{1}H-NMR spectrum of alkyne-tosylate in $CDCl_3$ after purification.*

The ^{1}H-NMR spectrum of the synthesized initiator is shown in **Figure 4–1** and all signals can be assigned to the corresponding protons. The signal at δ = 2.44 ppm can be assigned to the protons of the methyl group of the toluene component. Next to this signal, the proton of the alkyne group is visible at δ = 2.49 ppm. At δ = 4.68 ppm, the signal of the methylene group next to the triple bond is visible. Signals at δ = 7.34 – 7.36 ppm and 7.79 – 7.81 ppm can be assigned to the aromatic unit.

4.1.2 Alkyne-functionalized P(MeOx) for azide–alkine chemistry

In order to functionalize P(MeOx) with an alkyne at the α-terminus, a cationic ring opening polymerization of MeOx was initiated by propargyl tosylate based on known literature.[185] The initiator was dried over CaH_2 and was distilled before use. Initiator, solvent and monomer were assembled in the glovebox, and the polymerization was

carried out in a flask at 70°C for 24 h in dry argon atmosphere. In chapter 2.3.2, the mechanism of the polymerization was described in detail.

Figure 4–2 shows a ^{1}H-NMR-section of alkyne functionalized P(MeOx) (in deuterated acetonitrile). The signal at δ = 4.17 – 4.09 ppm can be assigned to the methylene group of the initiator which serves as internal reference in order to calculate DP. The molar ratio of initiator to monomer was 1:50, which can also be determined from the ^{1}H-NMR spectrum as 51–52 repeating units are shown. It is important to mention that this value is dependent on the deuterated solvent used during NMR measurement. In deuterated chloroform or water, the end-functionality is often not visible (especially after dialysis), thus deuterated acetonitrile is the best solvent for ^{1}H-NMR analytics of P(MeOx).

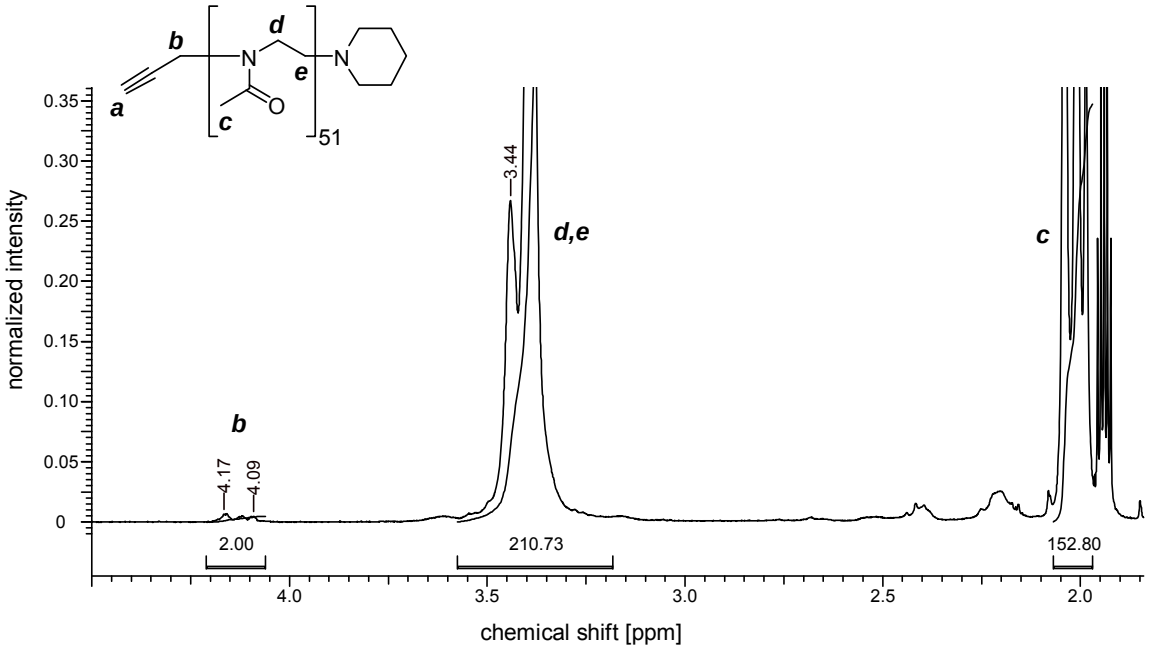

Figure 4–2: *^{1}H-NMR of alkyne functionalized P(MeOx) in CD_3CN with 50 repetition units and a molecular weight of about 4300 g·mol^{-1}.*

For the determination of M_n and *Đ,* of the synthesized alkyne-functionalized POx, SEC was used and showed narrow dispersity of *Đ*~1.15, indicating a living polymerization mechanism. Here it should be mentioned, that the initiation is also

possible with the cheaper propargyl benzenesulfonate. The measured *Đ* strongly depends on which SEC-solvent is used. In water it leads to broader molecular weight distributions (*Đ*~1.3, M_n = 2500 g·mol^{-1},**Figure 4–26** and experimental section **Figure 5–7**), which suggests a non-complete living polymerization mechanism with termination or the initiation step is not fast enough. Nevertheless, the SEC-elugram is quite symmetric with some tailing, indicating the existence of lower molecular weight fractions or column interactions. In DMF-SEC, the elugram of the same polymer shows again a shoulder towards smaller molecular weights but the dispersity is still *Đ* = 1.14 (M_n = 5400 g·mol^{-1}, experimental section **Figure 5–7**), indicating a living mechanism, which is contrary to the results in H_2O-SEC. The different molecular weights during SEC measurements comparing DMF and water as solvents can be explained by different coiling behavior in the used solvents. The polymer chains are more expanded in DMF and consequently show a higher molecular weight which was contrary to expectations as water is a very good solvent for POx. In summary, with SEC it was not possible to determine a result that is unambiguous concerning the mechanism of the polymerization.

Matrix-assisted laser desorption/ionization time of flight mass spectroscopy (MALDI ToF MS) was also used to characterize the synthesized polymers. MALDI ToF MS is especially suitable for the characterization of bigger molecules like polymers and proteins as only little fragmentation of the analyte occurs. The analyte is embedded in a matrix and is irradiated by a pulsed laser, which provokes the removal and desorption of the sample and matrix material. The matrix consists of smaller organic molecules, which absorb the wavelength of the used laser in particular. After ionization, the analyte can be characterized by e.g. a ToF mass spectrometer. **Figure 4–3** shows the MALDI ToF mass spectrum of alkyne functionalized P(MeOx). The most intensive signal is visible at m/z = 4040 which can be assigned to polymers with 46 repeating units of MeOx, associated with a proton. The value of DP is in accordance with the value expected from $[M]_0/[I]_0$ which was set to be 50. Additional signals can be found which are assignable to potassium associated polymers.

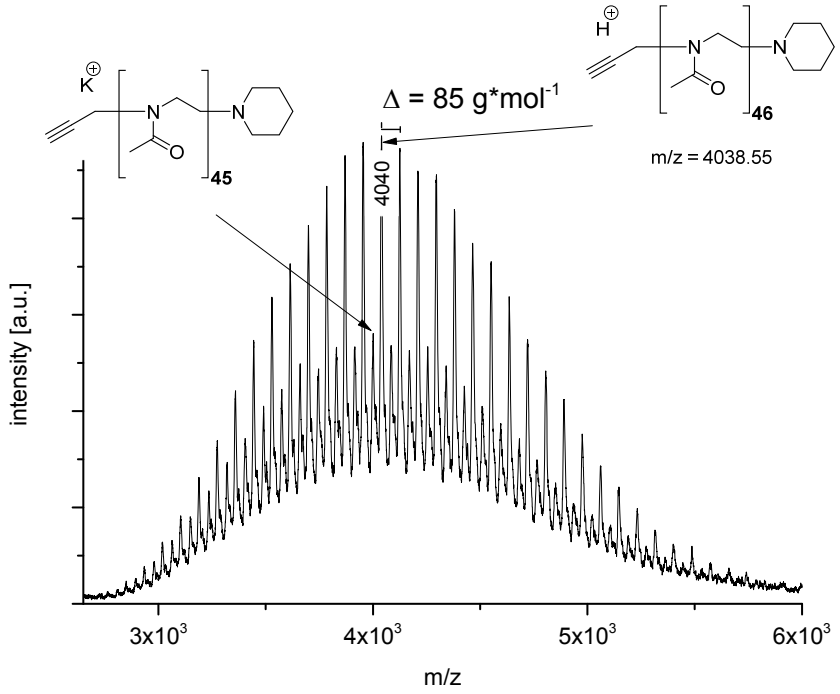

Figure 4–3: *MALDI ToF mass spectrum of alkyne functionalized P(MeOx) with narrow molecular weight distribution.*

4.1.3 Double-functionalized P(MeOx)

In addition to the partial functionalization of P(MeOx) with alkynes, polymers were terminated with piperidin-4-carboxylic acid ethyl ester to obtain hydrophilic polymers suitable for further reaction with amine-functionalized components. After ester cleavage a nucleophilic attack of amines towards P(MeOx) acid groups occurs.

The functionalization of POx with an additional alkyne group provided POx with further reactivity towards azides at the opposite α-terminus. The linking of P(MeOx) to any kind of amine and a second functionalization via azide–alkyne chemistry makes the formation of complex conjugates possible. **Scheme 4–2** shows the schematic overview of the synthesis.

The polymerization was initiated by the synthesized propargyl tosylate which was dried in vacuum before use. Acetonitrile was used as solvent and piperidin-4-carboxylic acid ethyl ester as termination reagent. After polymerization overnight the product was purified by precipitation into cold diethyl ether and dialysis against water. The corresponding ^{1}H-NMR (**Figure 4–4**) showed all expected signals.

The signals of the endgroups were only visible using deuterated acetonitrile during ^{1}H-NMR measurement. As internal reference the methylene group of the α-terminus at approximately δ = 4.16 ppm was used (H-***b***). By comparing the integral of this signal with the integrals of the signals at δ = 3.39 (H-***c*** and H-***d***) and 2.01 ppm (H-***e***) the calculation of DP is possible and shows the expected value (calculated degree of polymerization = DP_{calc} = 50; experimental degree of polymerization = DP_{exp} = 51). This value has to be treated with caution as the signal of the initiated alkyne function interferes with the ester group at the ω-terminus, as shown in **Figure 4–4**. Parts of the signal can be assigned to H-***f***. The corresponding signal of the neighbored methyl group is visible at δ = 1.20 ppm. The integrals of both signals were not as expected, as integrals of 2 and 3 were estimated. This result suggests the assumption of a partial ester-cleavage during dialysis or an incomplete termination with piperidin-4-carboxylic acid ethyl ester.

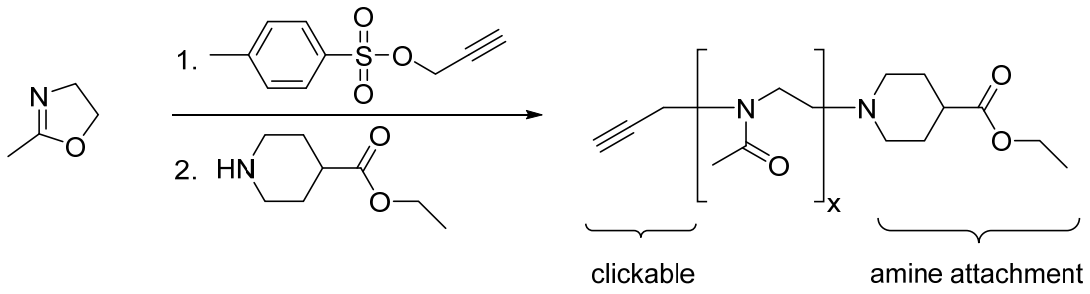

Scheme 4–2: *Schematical synthesis of clickable P(MeOx) for amine attachment.*

SEC measurements in water showed symmetric elugrams and narrow molecular weight distributions (*Đ* = 1.18, M_n = 3200 g·mol^{-1}). Nevertheless, the molecular weight calculated from ^{1}H-NMR (M_n = 4550 g·mol^{-1}) was higher than the measured value from SEC. This can be explained by the used PEG-standards for calibration, which has a different coiling behavior than POx in water.

The shown analytic data reflect the successful functionalization of (PMeOx) with alkyne-endgroups, beside the possibility of amine functionalization. This polymer class allows furthermore click chemistry with azide-functionalized components.

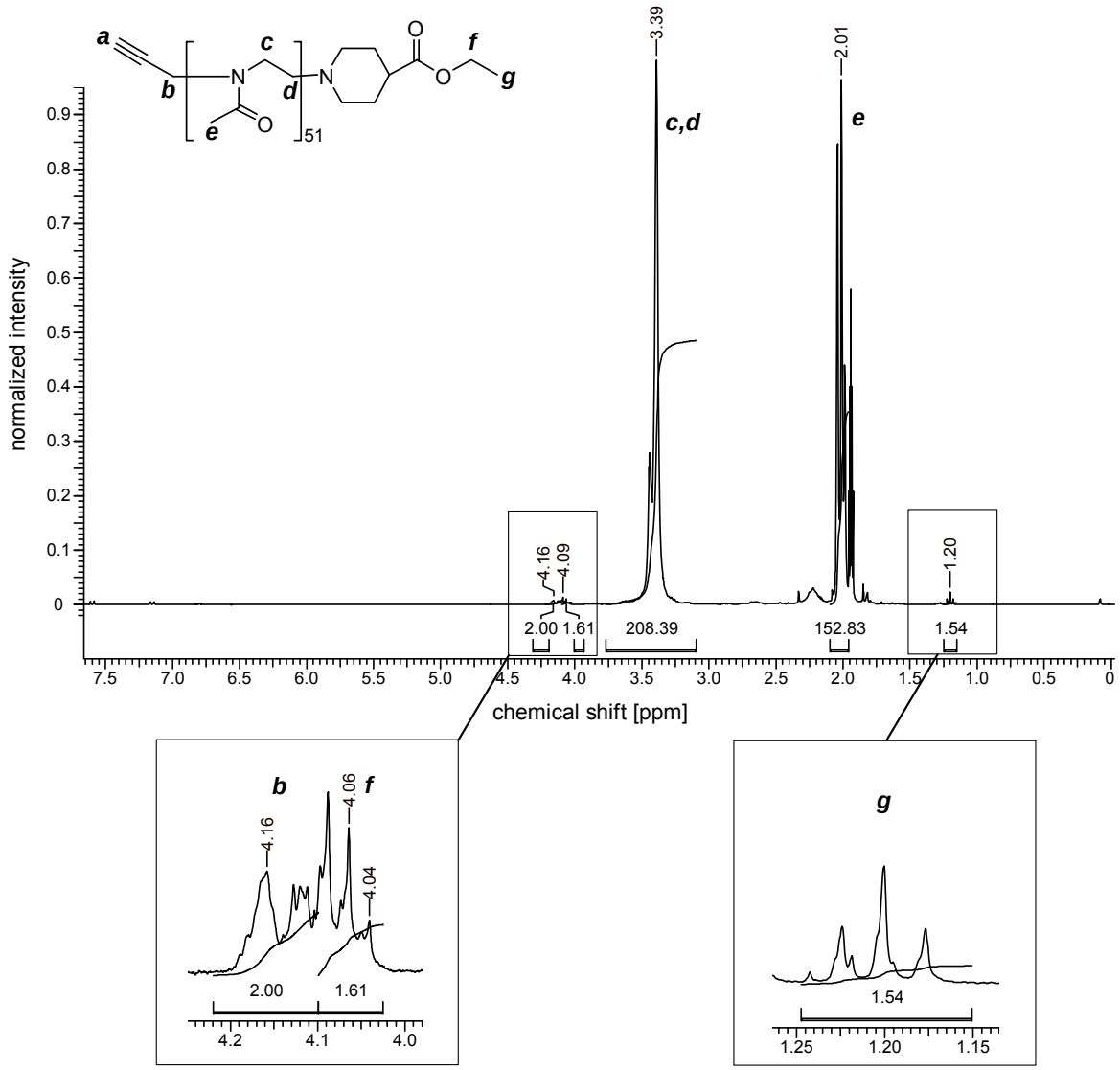

Figure 4–4: *^{1}H-NMR of alkyne- and ester-functionalized P(MeOx) in CD_3CN after purification. The signal at 4.09 ppm serves as intern reference for the calculation of repetition units and thus the molecular weight.*

4.1.4 Azide-functionalized P(MeOx)

4.1.4.1 Synthesis of 6-azidohexyl tosylate

For the synthesis of azide functionalized POx another initiator was prepared, which introduces an azide group at the *α*-terminus during initiation of the living cationic polymerization of 2-oxazolines.

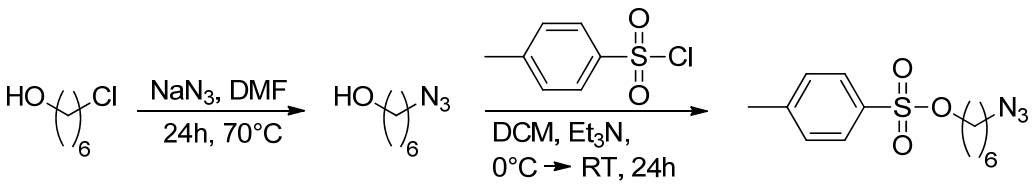

Scheme 4–3: *Scheme of the synthesis of azide initiator, 6-azidohexyl tosylate.*

The synthesis of the azide initiator was modified from a two stage synthesis of Kim *et al.*[186] 6-azido-1-hexanol was obtained by nucleophile substitution of 6-chloro-1-hexanol with sodium azide (**Scheme 4–3**). This was directly used without further purification for the synthesis of 6-azidohexyl tosylate (N_3-TOS) by addition of 4-toluenesulfonyl chloride and elimination of hydrochloric acid. The relatively long hexyl chain between azide and tosyl residue was chosen as linker between function and polymer backbone for subsequent reactions. After column chromatographically purification the successful synthesis with good yields of around 80% was confirmed by ^{1}H-NMR (experimental section, **Figure 5–1**) and IR-spectroscopy (**Figure 4–5** and experimental section **Figure 5–2**). The latter is perfectly suitable for azide-group verification as this has a characteristic vibration at approximately 2100 cm^{-1}. The ^{1}H-NMR spectrum confirms the successful synthesis of N_3-TOS, where only very small impurities (petrol ether) are visible. The aromatic unit is visible at δ = 7.78 and 7.37 ppm. The methylene group next to the tosylate group can be assigned to the signal at δ = 4.03 ppm (H-***d***), which was used as reference, and the integral was set to 2. At δ = 3.23 ppm (H-***i***), 1.66 – 1.55 ppm (H-***e*** and H-***f***) and at 1.34 ppm (H-***g*** and H-***h***) the other signals of the small aliphatic unit are visible. The signal at

δ = 2.46 ppm can be assigned to the methyl group of the toluene component. In all cases the integrals of the signals fit to the assigned protons.

4.1.4.2 Polymerization of MeOx with 6-azidohexyl tosylate

The first way to functionalize P(MeOx) with an azide was the polymerization of MeOx, initiated by N_3-TOS and terminated by piperidine. The cationic ring opening polymerization was successful and was characterized by ^{1}H-NMR (experimental section, **Figure 5–8**) and IR-spectroscopy (**Figure 4–5** and experimental section **Figure 5–9**). The IR spectrum shows the characteristic azide vibration at ~2100 cm^{-1} (**Figure 4–5**, red curve), demonstrating the successful initiation with N_3-TOS. Nevertheless, the result of the ^{1}H-NMR was ambiguous as a broad signal at δ = 3.01 ppm appeared which could not be assigned to the protons of the polymers' repetition units. As the azide is also known as a pseudo-halogen, this compound is adequate to start an additional polymerization which would explain the additional signal in the ^{1}H-NMR spectrum. Besides that, this signal does not match to the signals of the α-terminus as these signals should be visible at approximately δ = 1.5 ppm. In addition, both termini were not visible in the ^{1}H-NMR, as consequence no internal reference could be used for calculating the DP. Because of that, the result was doubtful and an alternative way to obtain azide-functionalized P(MeOx) was preferred.

4.1.4.3 Termination of P(MeOx) with NaN_3

NaN_3 was used as termination substance after the polymerization of MeOx with methyl tosylate (Me-TOS) as initiator according to literature.[187] NaN_3 is also able to react with the living polymerchain-end by nucleophilic attack. Here a longer reaction time of 48 h and a temperature of 50°C was needed.

Figure 4–5 shows the successful termination of P(MeOx) with an azide group as the characteristic N_3-vibration is visible at ~2100 cm^{-1} (blue curve). The ^{1}H-NMR spectrum (experimental section, chapter 5.2.7) shows all expected signals. By calculating the DP, the integral of the repeating units fit with the initiator to monomer ratio ($[I]_0/[M]_0$, 1:50) as the NMR spectrum shows ~54 repeat units.

MALDI ToF measurements showed a symmetric distribution with most intensive signal at m/z = 4399 (experimental section **Figure 5–12**). This mass can be assigned to polymers with 51 repetition units associated with a proton. The results are satisfactory as a pure polymer could be isolated providing the opportunity for click chemistry with an alkyne-functionalized component which is shown in chapter 4.2.1.

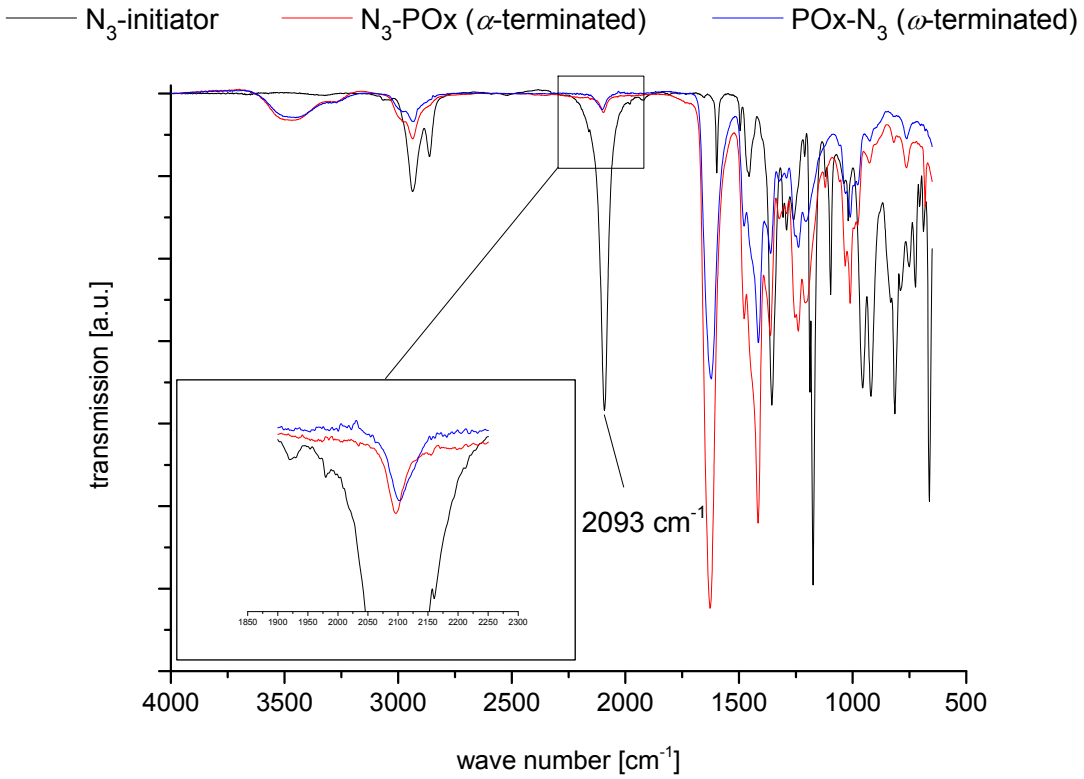

Figure 4–5: *FT-IR spectra of the azide initiator (N_3-TOS, black curve), azide functionalized P(MeOx) at the α-terminus (red curve) and azide functionalized P(MeOx) at the ω-terminus (blue curve). All three substances show the characteristic azide vibration at ~2100 cm^{-1}.*

4.1.5 Thiol–ene functionalizable POx

4.1.5.1 Synthesis of monomers

The cationic ring opening polymerization of 2-oxazolines was additionally used for the synthesis of statistical, hydrophilic copolymers for biochemical application. The idea was to use two types of monomers in a copolymerization to combine the functionality of allyl-compounds for further thiol–ene reaction and the hydrophilicity of MeOx to result in hydrophilic copolymers. *Iso*-propenyl-2-oxazoline is commercially available and bears olefin-function at the sidechain, but results in versatile products under cationic polymerization conditions as was previously described by Tomalia *et al*.[188]. Instead, MeOx was used in combination with ButenOx or DecenOx (**Figure 4–6**), whereby the latter are capable for further functionalization via thiol–ene chemistry. MeOx was used as main component as it is more hydrophilic than the often used EtOx and admits higher concentrations of ButenOx and DecenOx inside the polymer chains without losing hydrophilicity.

Figure 4–6: *Structural overview of the used monomers for multiple functionalization possibilities: commercially available 2-methyl-2-oxazoline (MeOx) synthesized 2-butenyl-oxazoline (ButenOx) and synthesized 2-decenyl-oxazoline (DecenOx).*

ButenOx was synthesized in three steps starting from 4-pentenoic acid which included an activation of the 4-pentenoic acid with EDC and NHS according to literature.[80] 2-chloroethyl-ammonium chloride was reacted with the activated acid in alkaline conditions followed by ring closure with methanolic KOH at 70°C to form ButenOx. Low pressure distillation (1 mbar, 65°C) resulted in the pure product with good yields of about 85% (relative to *N*-(2-chloroethyl)-4-pentenamide) which are comparable with values from literature.[80]

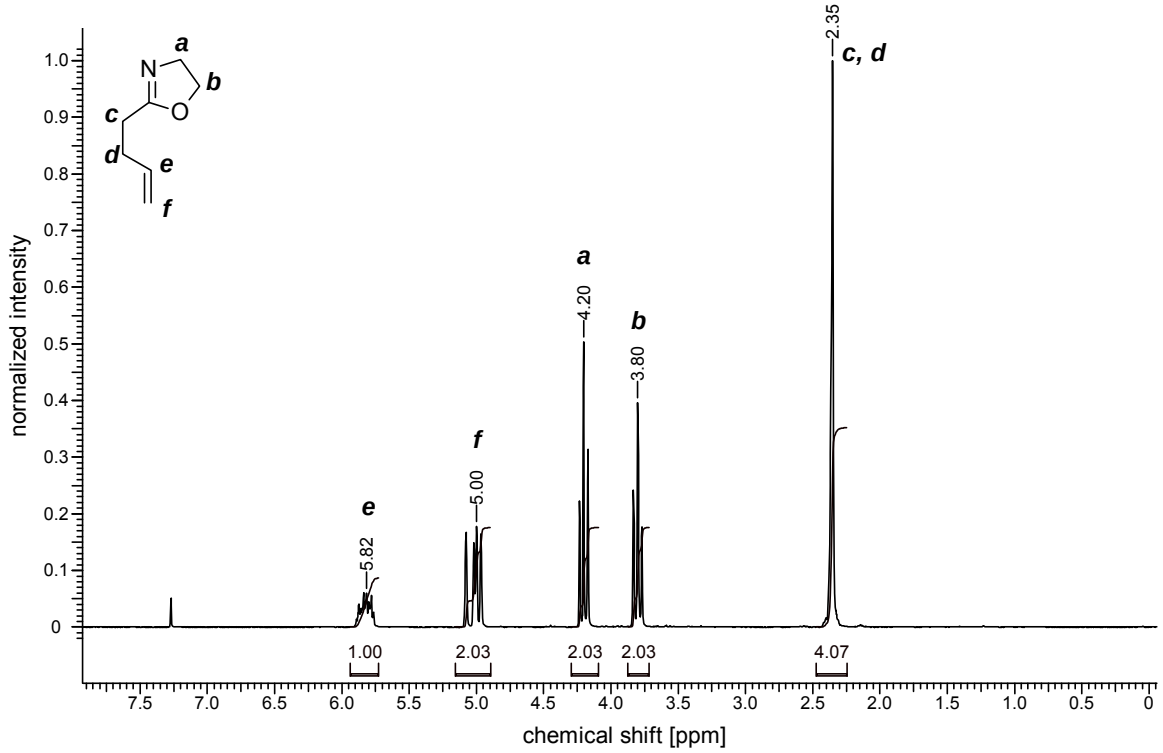

Figure 4–7: *^{1}H-NMR spectrum of 2-butenyl-2-oxazoline after purification via distillation.*

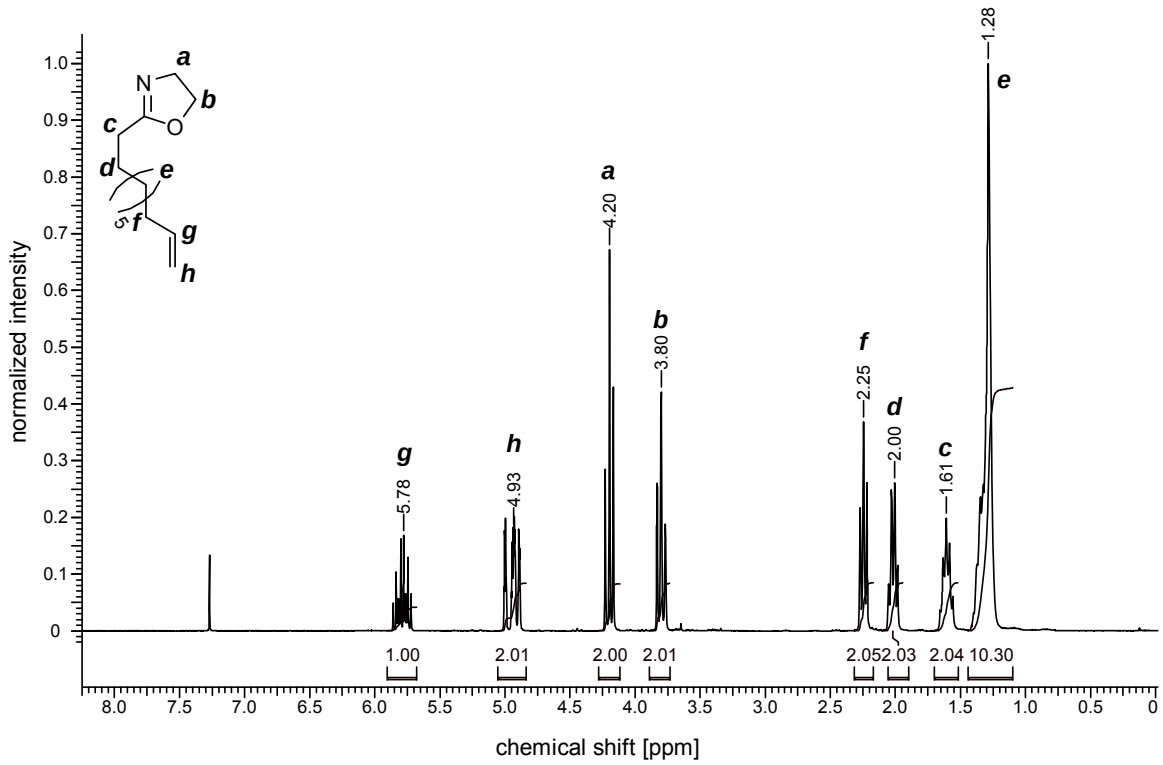

Figure 4–8: *^{1}H-NMR spectrum of 2-decenyl-2-oxazoline after purification.*

In **Figure 4–7,** the ^{1}H-NMR of ButenOx shows all expected signals at appropriate shifts. The signal at 2.35 ppm can be assigned to the two methylene groups between the double bond and the ring, the latter shows signals at δ = 3.80 and 4.20 ppm. Allyl-signals are visible at δ = 5.00 and 5.82 ppm.

DecenOx could successfully be prepared by a two step-synthesis in good yields (77%, relative to 10-undecenoyl chloride) also known from literature.[162] Started with the commercially available 10-undecenoyl chloride, the already activated acid reacted with CEAC chloride at 0°C in the presence of trimethylamine (Et_3N). The second step was identically carried out like the synthesis of ButenOx, by treatment with methanolic KOH at 70°C and purification by low pressure distillation ($1 \cdot 10^{-3}$ mbar, 65 – 75°C). **Figure 4–8** shows the ^{1}H-NMR of ButenOx. The signals at δ = 1.28, 1.62, 2.00 and 2.25 ppm can be assigned to the alkyl chain of eight methylene groups. The methylene group directly besides the ring causes a signal at δ = 1.61 ppm. Signals at δ = 3.80 and 4.20 ppm clarify the successful closure of the ring. The allyl endgroup results in signals at δ = 4.93 and 5.78 ppm. No further impurities are visible in both NMR-spectra of the monomers, which had to be extremely clean, as impurities would prevent the living character of the cationic ring opening mechanism.

4.1.5.2 Side-chain functionalized POx

Besides the functionalization at the termini of polymers, side-chain functionalization of polymers is a promising alternative. This technique allows multiple conjugations with further reagents. For implementation the use of different monomers is necessary. In Chapter 4.1.5.1, different monomers were introduced setting the basis of the side-chain functionalization. Multifunctional polymers in the range of 5 kDa were synthesized with a 5–10% amount of ButenOx or DecenOx. In all cases, Me-TOS served as initiator and dry acetonitrile as solvent with polymerization occuring at 75°C overnight. For the polymerization termination piperidine was used, as no further functionalization at the terminus was performed and the terminiation is extremely fast with piperidine[189]. After three times of precipitation into cold diethyl ether or dialysation of the polymer against distilled water (cut off, 1000 g·mol^{-1}) for two days, respectively, the pure polymer could be isolated. The following **Table 4–1**

gives an overview of the composition, molecular weights and dispersities of the synthesized polymers with molar fractions (x, theo = theoretical, determ = determined) and repeating units (n). All polymerizations resulted in narrow dispersities (*Đ* = 1.06 –1.20), nevertheless in all cases the molecular weight determined by SEC fall below the calculated ones. In addition, some SEC elugrams were broader than expected and tailing could be observed. This could be a hint of possible known side reactions (**Scheme 2–2,** chapter 2.3.2).[59,78]

Table 4–1: *Composition, molecular weights and dispersities of different polymers with molar fractions (x) and repeating units (n).*

polymer	x_{theo}	x_{determ}	n_{theo}	n_{determ}	M_n (NMR)[b]	M_n (SEC)[c]	M_w (SEC)[c]	*Đ*
				$p[(MeOx)_x–co–(ButenOx)_{1-x}]_n$				
I	0.95	0.95	47	44	3800	3550	3800	1,06
II	0.90	0.90	50	55	4900	4500	5300	1,17
				$p[(MeOx)_x–co–(DecenOx)_{1-x}]_n$				
III	0.95	0.95	47	44	4000	3550	3750	1,12
IV	0.90	0.90	50	55	5300	4800	5800	1,20

[a] The composition in the copolymer is identical with the composition in the feed; [b] Determined by ^{1}H NMR spectroscopy (300 MHz, $CDCl_3$ or D_2O); [c] Determined by SEC (DMF with LiCl) using PEG calibration.

Figure 4–9 shows a representative copolymer composition in the ^{1}H-NMR spectra of poly[$(MeOx)_{0.95}$–*co*–$(ButenOx)_{0.05}]_{48}$ (measured in D_2O). The signals at *δ* = 5.83 and 5.03 ppm are assigned to the allyl group of ButenOx. Methylene functions of MeOx and ButenOx are visible as broad signal at *δ* = 3.51 ppm. The signals at *δ* = 3.06 and 2.89 ppm can be assigned to the initiating methyl-group of Me-TOS and were used as internal reference to calculate the DP. The initiator signal was normalized to

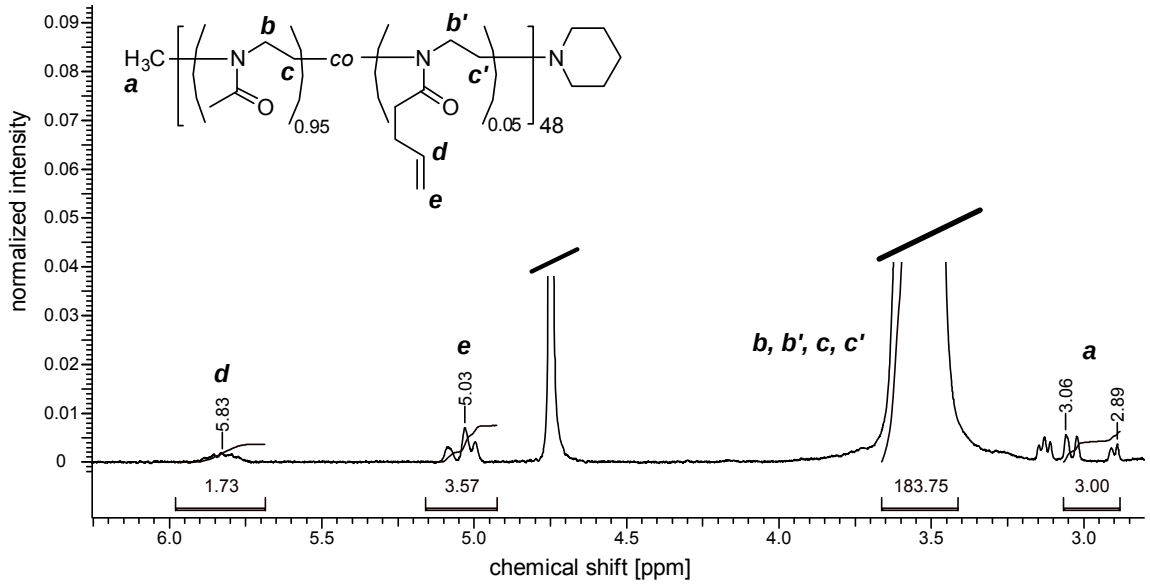

Figure 4–9: *Cut-out of ^{1}H-NMR spectra of Poly[(MeOx)$_{0.95}$-co-(ButenOx)$_{0.05}$]$_{48}$ bearing two double bonds per polymer chain or 5% of allyl containing substance in copolymer, respectively (measured in H_2O).*

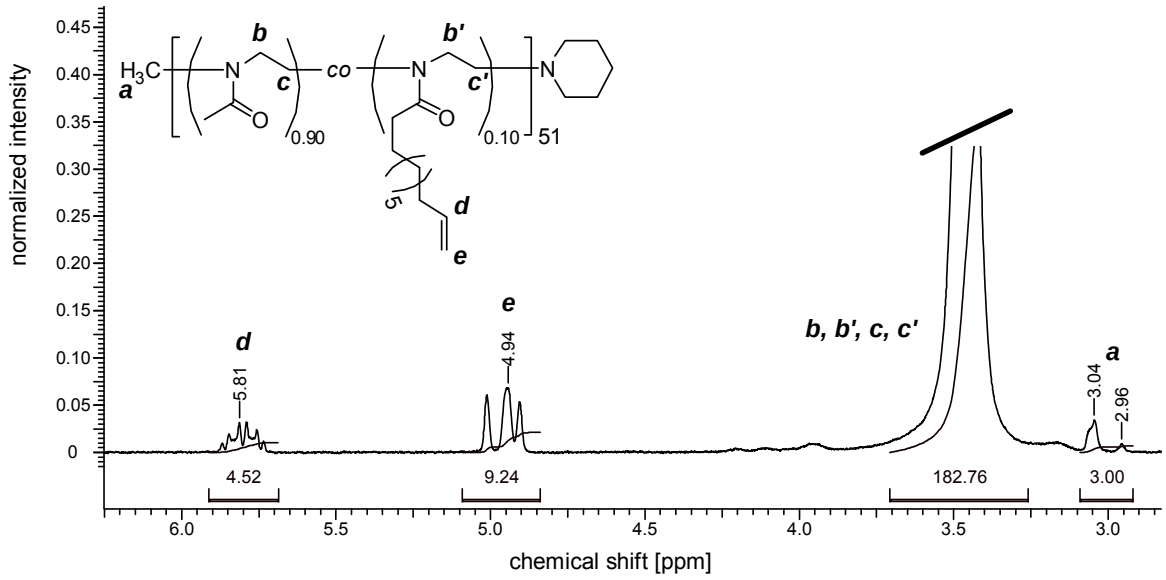

Figure 4–10: *Cut-out of ^{1}H-NMR spectra of Poly[(MeOx)$_{0.90}$-co-(DecenOx)$_{0.10}$]$_{51}$ bearing five double bonds per polymer chain or 10% of allyl containing substance in copolymer, respectively (measured in $CDCl_3$).*

3 protons. By integration of the allyl function at δ = 5.03 ppm and division with 2, the repetition units of the allyl component were calculated. The amount of MeOx repetition units was considered by subtracting the amount of allyl compound from the integral of the signal at δ = 3.51 ppm and dividing with 4. The initiator signal is not a single peak because of *syn*- and *anti*-conformers of the resulting polymer. The rotation around the amide function is possible and known in literature since 1996.[189] This effect is independent from the deuterated solvent used during ^{1}H-NMR measurement as shown in **Figure 4–10**. Here, the signal of the initiator is visible at δ = 3.04 and 2.96 ppm. Quite often the calculation of repeating units varied slightly, dependent on which deuterated solvent was used during NMR-measurement.

4.1.6 Cysteine-functionalization of poly(2-oxazolines)

Native chemical ligation, as one of the before mentioned chemoselective coupling reactions, is a promising method for subsequent functionalization of polymer chains. Polymers with cysteine or thioester residues qualify for chemoselective reactions with the right counter component.

The introduction of thiazolidine functionality equips polymers with protected cysteines. As mentioned previously, polymers bear multiple double bonds at the side-chain, thiol–ene reactions provide a promising method for numerous cysteine-functionalization of POx. Therefore, thiazolidine was functionalized with a thiol by the reaction of 3-formyl-2,2-dimethylthiazolidine-4-carboxylic acid (FTz4CA) with cysteamine which was already shown by Kuhlmann *et al* (**Scheme 4–4**).[190] The synthesis of FTz4CA is known in literature.[191-192] Cysteine hydrochloride was protected by an acetal group via refluxing in acetone and drying in vacuum. The resulting protected cysteine was additionally protected with an *N*-formyl-group to avoid a reaction of the amine with the carboxylic group in the following. The formyl-protection was performed by solving FTz4CA in a mixture of sodium formate and formic acid followed by the addition of acetic acid anhydride and stirring overnight. Recrystallization from EtOH/H_2O (1:1) resulted in the expected product and was confirmed by ^{1}H-NMR (**Figure 4–11**).

The formyl-protection group has the great advantage of being very small. Polymer-analog reactions close to the backbone of a polymer can be sterically demanding. In

this case, the small formyl-group has the best possibility of being cleaved under acidic conditions. Additionally, the deprotection in acidic milieu prevents the polymer from crosslinking, as the resulting cysteine residues are sensitive towards oxidation under neutral to basic conditions.

Thiol-functionalization of the protected cysteine was performed by activation of the carboxylic acid group via 1,1-carbonyldiimidazole (CDI) in chloroform. The use of CDI has one big advantage in contrast to other methods, like the activation via halides. It has a high driving force as CO_2 is formed during the reaction. As the activated ester is additionally reactive towards H_2O, all solvents and compounds had to be dry and oxygen free. The not presence of oxygen is important to obtain a monomeric product, as thiol functions have the propensity to form disulfide bridges which would result in dimers of mercapto-thiazolidine.

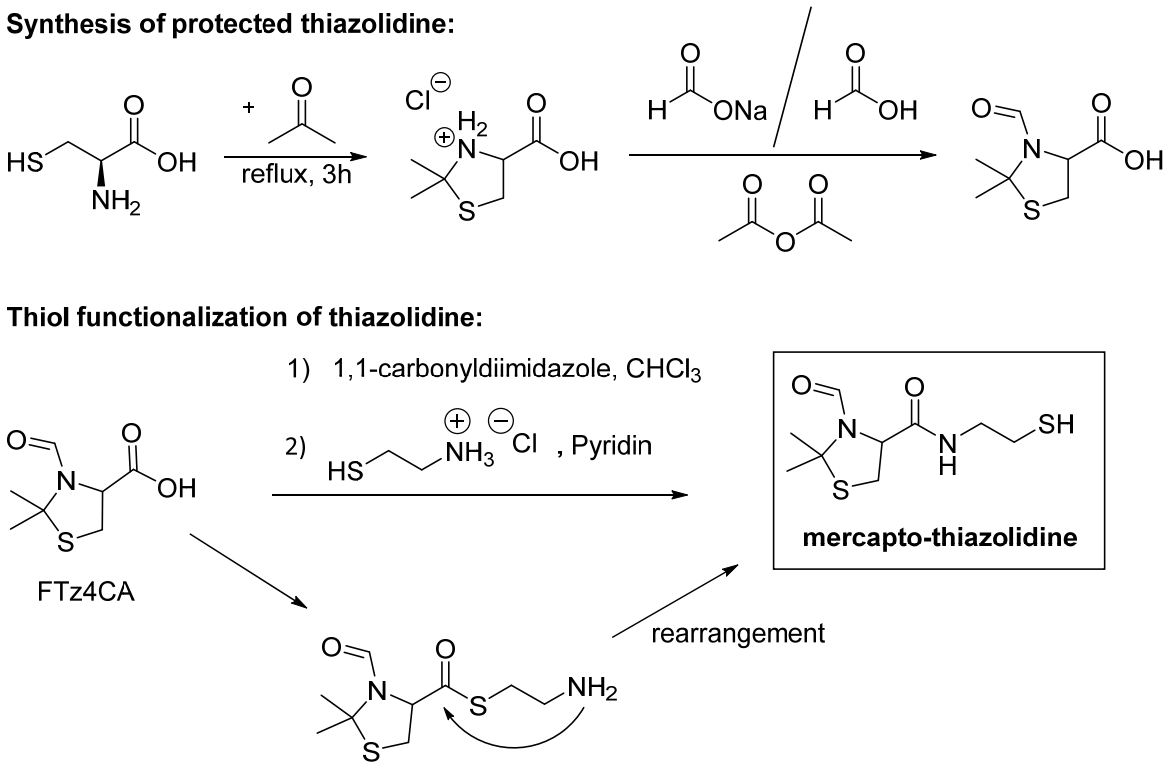

Scheme 4–4: *Synthesis of thiol functionalized thiazolidine.*

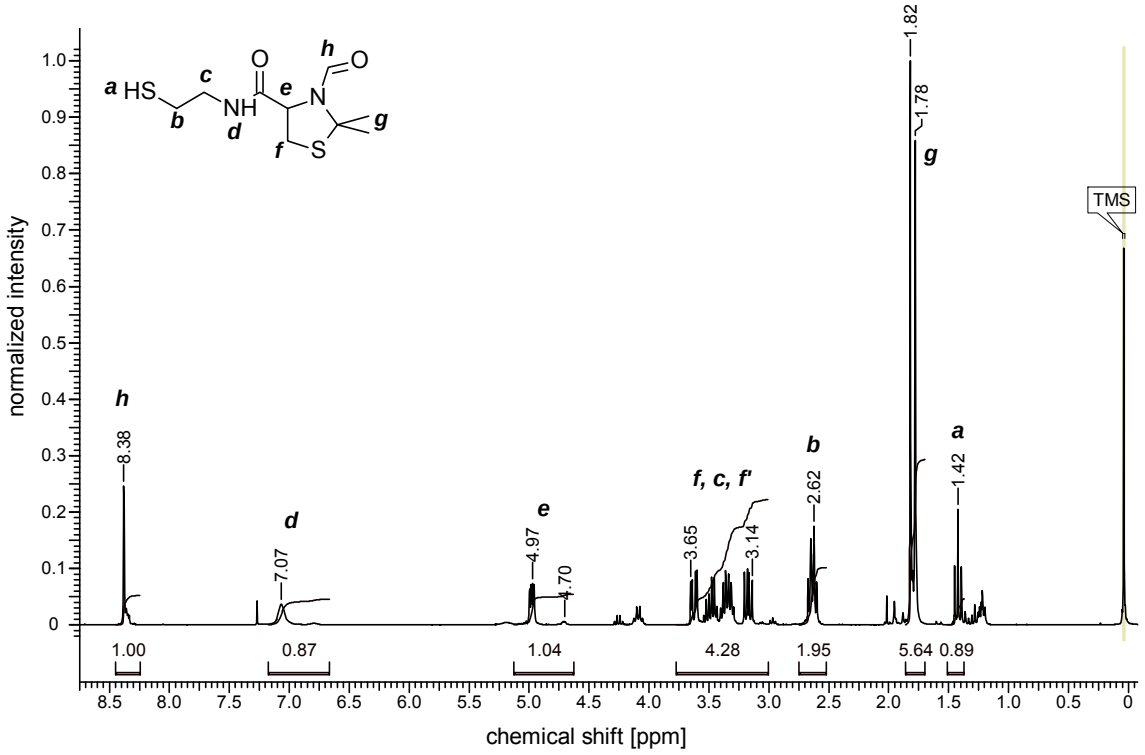

Figure 4–11: *^{1}H NMR spectrum of 3-formyl-N-(2-mercaptoethyl)-2,2-dimethylthiazolidine-4-carboxamide (mercaptothiazolidine) (in $CDCl_3$).*

FTz4CA was dispersed in chloroform. After activation with CDI the resulting active ester is completely soluble in chloroform and a solution of cysteamine hydrochloride (1 eq in respect to the carboxylic acid) in pyridine (for deprotonation) was added. The synthesis does not need any extensive purification, as the amine and thiol functionality of cysteamine undergoes the same rearrangement as in NCL, and consequently results in a stabile amide bond and a terminal thiol. Nevertheless the raw product was acidified and extracted with chloroform. After removal of the solvent and recrystallization from ethyl acetate, white needle-like crystals could be isolated.

Figure 4–11 shows the associated ^{1}H-NMR spectrum. The broad signal at δ = 8.38 ppm can be assigned to the protective formyl-group. The amide generates a split signal at δ = 7.07 – 6.61 ppm as well as the methine proton (H-***e***) at δ = 4.97 – 4.70 ppm caused by *cis* and *trans*-isomers of the formed product. Signals at δ = 3.65 and 3.14 ppm can be assigned to the CH_2 group of the thiazolidine-ring which enclose the signal of H-***c***. The methylene group next the terminal thiol

generates a signal at δ = 2.62 ppm. The protective acetal group can be observed at δ = 1.82 ppm – 1.78 ppm, whereas H-***a*** was determined to be at δ = 1.42 ppm.

Mercapto-thiazolidine was introduced into the polymers side-chains by thiol–ene reaction with 2,2-dimethoxyphenylacetophenone (DMPA) as radical source, UV-irradiation (λ = 365 nm) and 3 eq of mercapto-thiazolidine with respect to the allyl-groups in degassed methanol. After UV reaction and precipitation into cold diethyl ether the signals of the allyl function vanished, indicating a complete consumption of the UV reactive allyl groups. As an example the ^{1}H-NMR spectrum of a polymer based on MeOx and DecenOx functionalized with the synthesized cysteine protected ligand is shown in **Figure 4–12**. The signal of the initiator *δ* = 3.06 ppm) and the peak of the backbone (*δ* = 3.48 ppm) serve as references. The signals at *δ* = 1.81 – 1.85 ppm (doublet, acetal group of the protected cysteine), at *δ* = 2.51 and 2.65 ppm (protons next to sulfur atom), at *δ* = 4.74 and 5.01 ppm (methine proton next to the protected amine of the cysteine function), at *δ* = 7.03 ppm (amide proton of the side-chain) and at *δ* = 8.39 ppm (formyl group of the thiazolidine ring) can be assigned to the introduced thiazolidine. Additional information concerning the functionalization of poly[$(MeOx)_x$–*co*–$(ButenOx)_y]_z$ can be found in the experimental section in **Figure 5–17** – **Figure 5–19**.

SEC measurements in DMF (functionalization of poly[$(MeOx)_x$–*co*–$(ButenOx)_y]_z$ compare supporting information **Table 5–5** and **Table 5–6**; functionalization of poly[$(MeOx)_x$–*co*–$(DecenOx)_y]_z$ compare supporting information **Table 5–7** and **Table 5–8**) showed an increase of M_n along with a slight increase of dispersities, further supporting the successful coupling of the thiazolidine component. In all cases the molecular weights determined by SEC fall below the calculated ones. This deviation can be assigned to the PEG standards used for calibration of SEC and their different dependence of the hydrodynamic radius on the molecular weight compared to POx derivatives. However, also molecular interactions due to the introduced side-chains may contribute.

Under acidic conditions the *N*-formyl group can be cleaved and the resulting thiazolidine-ring subsequently equilibrates to cysteine and acetone in aqueous solution. Refluxing the polymer at 70°C for 5 d in 0.1 M HCl solution leaded to hydrolysis of the thiazolidine ring. Dialysis against H_2O produced oxidized polymers with gel-structures that were only soluble in reductive media. This suggests that the

H-exchange of amines and nearby thiols is very fast and leads to the formation of ammonium thiolates. They may rapidly build up disulfide bridges and generate gel-structures. However it remains unclear if the gels are solely covalently crosslinked as physical crosslinking is also possible (protonation of the amine and deprotonation of the thiol). In any case, dialysis against acetic acid (0.01 M) instead of water ensured permanently protonated thiols during work up and yielded stable products of cysteine functionalized POx (cys-POx, confirmed by ^{1}H-NMR, supporting information **Figure 5–19** and **Figure 5–23**) which could be lyophilized.

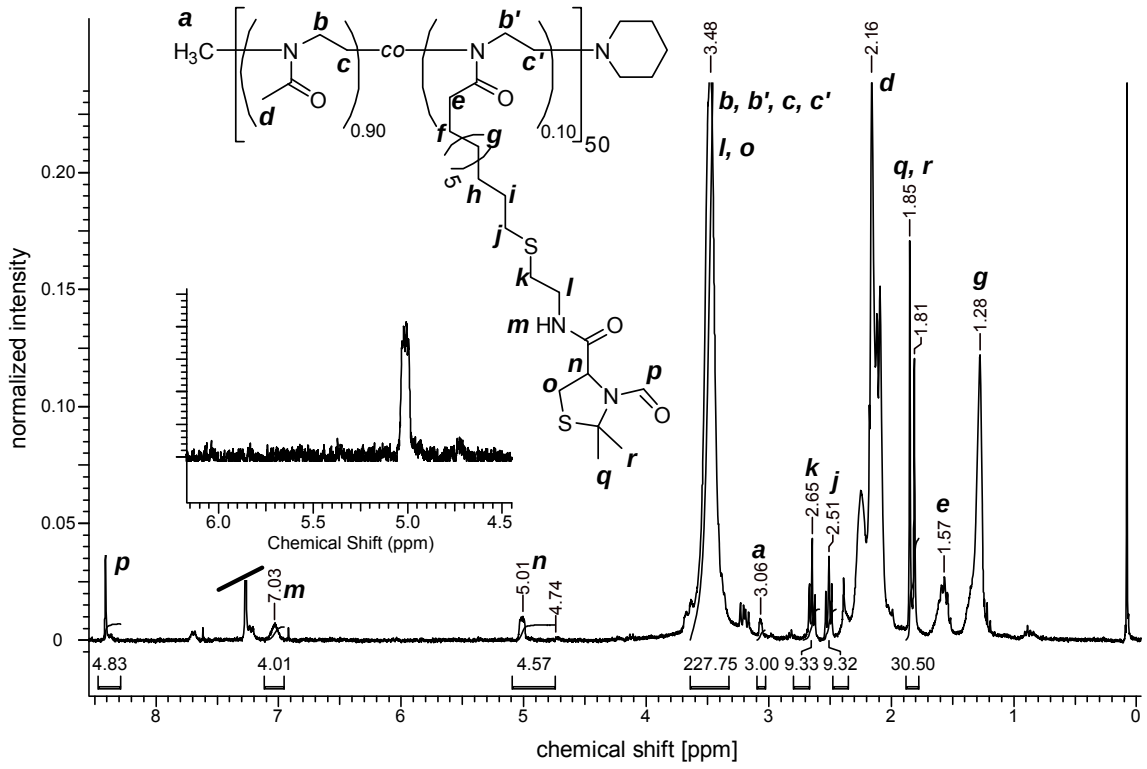

Figure 4–12: *^{1}H NMR spectra of thiazolidine functionalized Poly[(MeOx)$_{0.90}$-co-(DecenOx)$_{0.10}$]$_{51}$ (measured in CDCl$_3$).*

4.1.6.1 Quantification of cysteine functionality

Ellmans reagent is normally used for the quantification of thiol groups in chemical composition. As all cys-POx did not lead to a positive proof with Elmans reagent, alternatives were tested.

A trinitrobenzenesulfonic acid (TNBSA) assay was used under oxidative conditions to quantify cysteine functionality in POx. TNBSA is able to react with thiols and amines resulting in a trinitrophenyl component which can be quantified at a wavelength of 335 nm by UV-Vis spectroscopy.

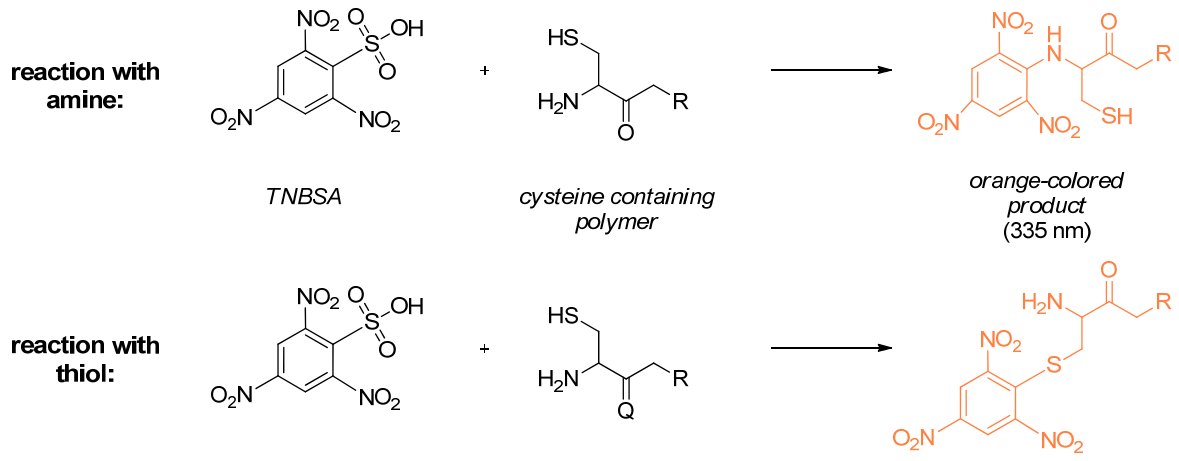

Scheme 4–5: *Possible reaction pathways of TNBSA with cysteine containing components.*

As thiols and amines are nucleophilic, both are able to attack the aromatic ring and the sulfonic acid group leaves the aromatic system easily (**Scheme 4–5**). In a former study, a calibration was performed with ethanolamine and mercaptoethanol with different concentrations. The absorbance in UV-Vis showed similar linear absorbance–concentration dependence for both substances which admits the conclusion, that the reaction is independent whether amines or thiols are used. In addition, the sterical demand of the reaction of vicinal thiols and amines were determined by comparing cysteine and cysteamine reactivity. It was clearly shown that both, steric- and charge-reasons influence the reactivity of the TNBSA assay. These results do not elucidate a clear answer because no double reaction of cysteine residues could be observed. For having only one reactive group in the quantification

of cysteines, it was tested if the assay could also be performed under oxidative conditions to suppress the influence of thiol residues. In order to determine the necessary oxidation time to remove all thiols in a solution, mercaptoethanol was treated with H_2O_2 and was compared to a solution containing only mercaptoethanol and a solution of ethanolamine hydrochloride with H_2O_2. It could be shown that after 1 h at 37°C the ethanolamine solution was not influenced by the hydrogen peroxide, whereas no absorbance could be measured in the case of mercaptoethanol in combination with H_2O_2. In summary, the quantification of cysteine functionality via single amine detection is possible after the oxidation of thiols.

For unambiguous quantification of the amines all thiol functions were oxidized prior to the quantification assay by treatment with hydrogen peroxide for 1 h at 37°C (~3 mM H_2O_2). While Ulbricht *et al.* showed that 5 mM H_2O_2 with Cu (II) solution has an influence on P(EtOx) (DP~50) after 8 h,[193] this should not influence the molecular weight in the present thesis. The concentration used here was much lower (~ 3 mM H_2O_2 without Cu (II)) and was shorter in treatement time (1 h), therefore no polymer destruction is considered. A concentration series of the polymer between 7.92 and 99.00 µmol·mL^{-1} (**Table 4–2**) yielded an average content of 5.0 ± 0.6 amines (cysteines) per polymer chain with a polymer bearing 5 cysteine functions calculated by ^{1}H-NMR spectroscopy.

Additionally a polymer bearing five cysteines at the side-chain having a molecular mass of about 10000 g·mol^{-1}, was analyzed by RAMAN spectroscopy in order to distinguish between thiols and oxidized species (**Figure 4–13**). However, detection limits of the method led to ambiguous results. The detection of any thiols in the region of ~2530-2610 cm^{-1} was not possible when measuring cys-POx. The measurement of pure cysteine·HCl and cystin by RAMAN spectroscopy underlined these results as the detection limit for thiol signals is very low (the thiol signal is weak in comparison with the signal of S–S-bridges, **Figure 4–14**). RAMAN measurements are unfortunately not suited for this analysis as the amount of thiols or S–S-bridges are very low in the synthesized polymers.

Table 4–2: *Results of the TNBSA assay in order to quantify the amount of cysteines attached to the POx backbone. In summary, 5.0 ± 0.6 cysteines per polymer chain were measured in a polymer bearing 5 cysteine functions calculated by NMR spectroscopy.*

	Polymer			Calibration	Ratio Calibration/Polymer
Entry	**µg·mL^{-1}**	**µmol·mL^{-1}**	**Abs. a.u.**	**NH_2 µmol**	**NH_2:Polymer**
1	0.59	0.00006	-0.010	-0.00421	-72.6
2	0.99	0.00010	0.004	-0.00099	-10.2
3	1.98	0.00019	0.006	-0.00053	-2.7
4	3.96	0.00039	0.011	0.00062	1.6
5	7.92	0.00078	0.026	0.00407	5.2
6	9.90	0.00097	0.026	0.00407	4.2
7	11.88	0.00117	0.032	0.00545	4.7
8	15.84	0.00155	0.044	0.00820	5.3
9	19.80	0.00194	0.056	0.01096	5.6
10	49.50	0.00486	0.104	0.02199	4.5
11	99.00	0.00972	0.253	0.05623	5.8
					5.0 ± 0.6

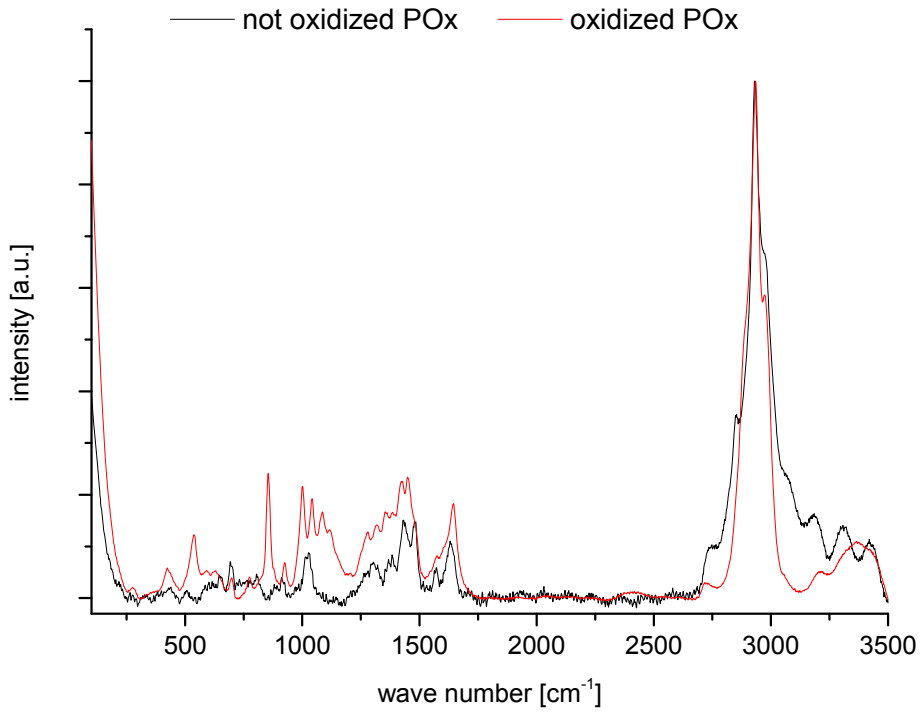

Figure 4–13: *RAMAN measurement of oxidized and non-oxidized POx with a molecular weight of about 10,000 g·mol^{-1} bearing five cysteine residues as polymer side-chains.*

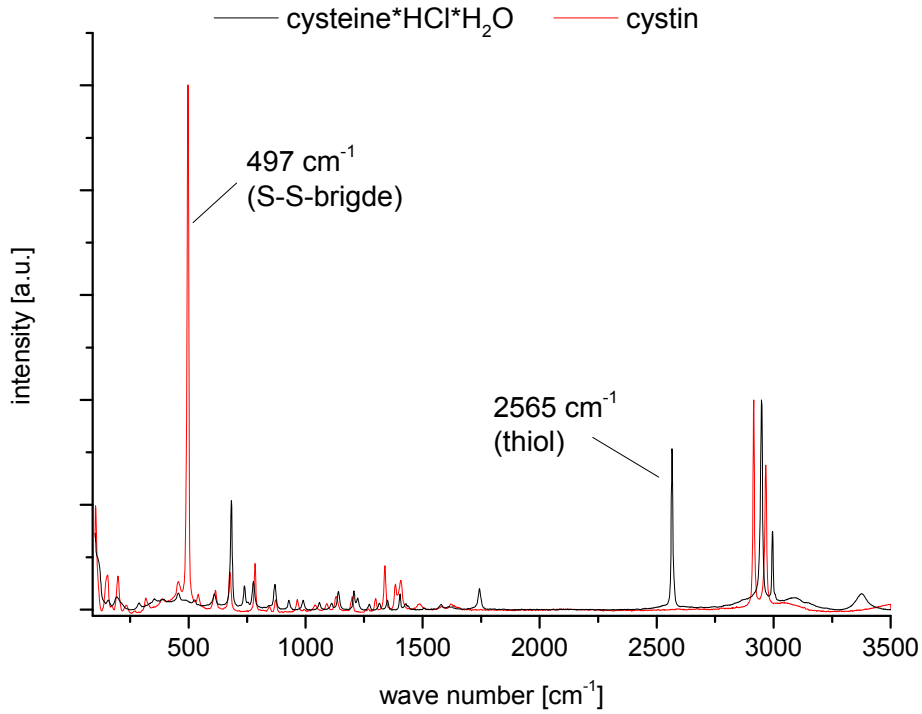

Figure 4–14: *Comparison of thiol signal of cystein and disulfide signal of cystin in RAMAN measurements.*

4.1.6.2 Cell toxicity tests

A number of tetrazolium dye-based assays such as MTT (3-(4,5-dimethylthiazol-2-yl)-2,5-diphenyltetrazolium bromide), XTT (2,3-bis-(2-methoxy-4-nitro-5-sulfophenyl)-2H-tetrazolium-5-carboxanilide) or WST (water soluble tetrazolium) are usually applied as standard methods to assess cell viability. In all these assays, reductive enzymes (reductases) generate a dye which can subsequently be measured colorimetrically and the intensity can be correlated with cell viability. Due to the reductive properties of the cysteine containing polymers, luminescence was measured, verifying the cytocompatibility of the polymers. The luminescence corresponds to ATP production, as a marker of cell viability with the "CellTiter-Glo® Luminescent Cell Viability Assay" (LCV-assay). Human fibroblasts were incubated with four functionalized polymers which varied in composition and cysteine moiety:

- P[$(MeOx)_{0.95}$–*co*–$(ButenOxCys)_{0.05}$]$_{44}$,
- P[$(MeOx)_{0.90}$–*co*–$(ButenOxCys)_{0.10}$]$_{55}$,
- P[$(MeOx)_{0.95}$–*co*–$(DecenOxCys)_{0.05}$]$_{54}$,
- P[$(MeOx)_{0.90}$–*co*–$(DecenOxCys)_{0.10}$]$_{57}$.

All samples with concentrations between 0.1 mg·mL^{-1} and 10.0 mg·mL^{-1} were analyzed concerning cell viability and cell number after 48 h incubation (**Figure 4–15** and **Figure 4–16**), whereby the bottom of tissue culture treated well plates served as reference. The shown values are the average of four samples per polymer with the corresponding standard deviation. Generally, the luminscence cell viability as well as the cell number showed that all polymers were cytocompatible up to concentrations of 1.0 mg·mL^{-1} independent of the different length of the side-chain, and also of the amount of the cysteine content. However at 10 mg·mL^{-1} the copolymer with 10% of cysteine functionalized ButenOx resulted in cell numbers smaller than 50% in respect to the polystyrene reference. This observation could not be detected in the measurements of luminescence.

Furthermore, luminescence and cell numbers of P[$(MeOx)_{0.95}$–*co*–$(ButenOxCys)_{0.05}$]$_{54}$, thus a polymer with only 5% of cysteine functionalized side-chains (in contrast to the one with 10%), caused a reduction down to 40% or 20% at 10 mg·mL^{-1}, respectively after 48 h treatment. There is no clear dependency on length of the hydrophobic side-chain linker or degree of functionalization of the

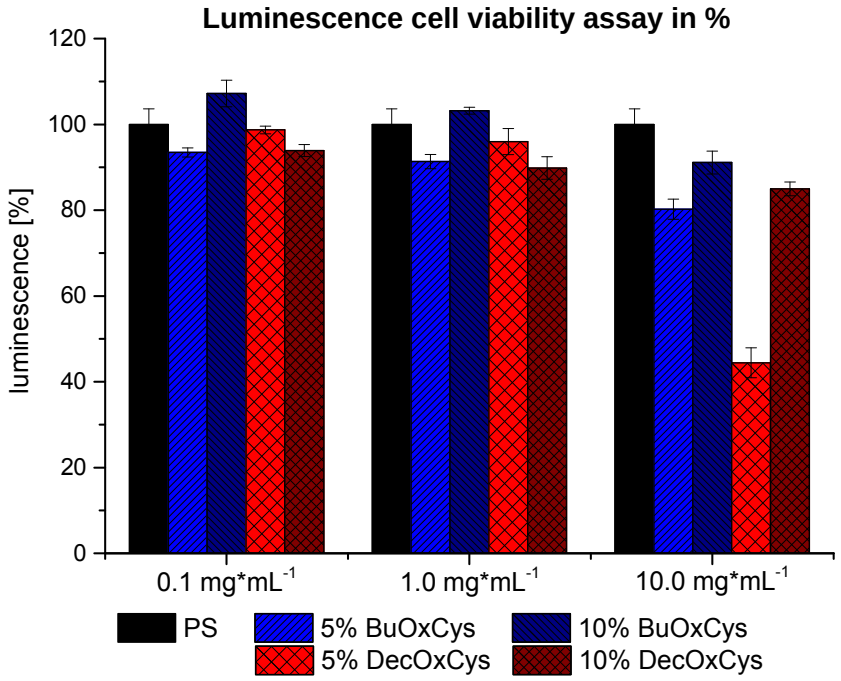

Figure 4–15: *CellTiter-Glo Luminescent Cell Viability Assay of $P[(MeOx)_{0.95}–co–(ButenOxCys)_{0.05}]_{44}$, $P[(MeOx)_{0.90}–co–(ButenOxCys)_{0.10}]_{55}$, $P[(MeOx)_{0.95}–co–(DecenOxCys)_{0.05}]_{54}$, and $P[(MeOx)_{0.90}–co–(DecenOxCys)_{0.10}]_{47}$ with concentrations of 0.1 mg·mL^{-1}, 1.0 mg·mL^{-1} and 10.0 mg·mL^{-1}.*

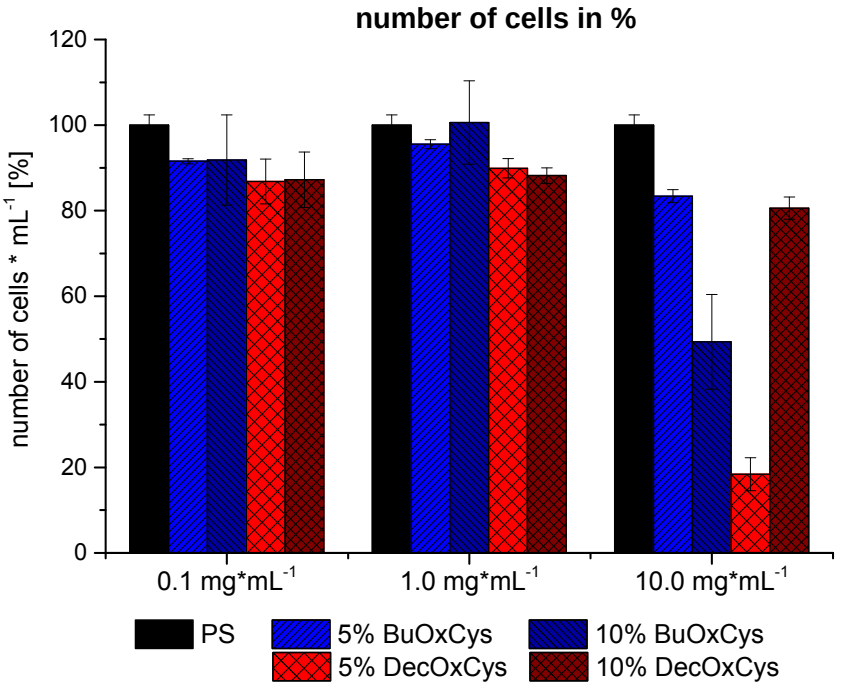

Figure 4–16: *Counted number of cells from CellTiter-Glo Luminescent Cell Viability Assay of $P[(MeOx)_{0.95}–co–(ButenOxCys)_{0.05}]_{44}$, $P[(MeOx)_{0.90}–co–(ButenOxCys)_{0.10}]_{55}$, $P[(MeOx)_{0.95}–co–(DecenOxCys)_{0.05}]_{54}$, and $P[(MeOx)_{0.90}–co–(DecenOxCys)_{0.10}]_{47}$ with concentrations of 0.1 mg·mL^{-1}, 1.0 mg·mL^{-1} and 10.0 mg·mL^{-1}.*

polymer, so that the partially negative influence on cell vitality and cell number of these polymers at high concentrations of 10 mg·mL^{-1} remains unclear or might be due to minor impurities during assay process or in the polymer itself. In chapter 4.3 the synthesis of nanogels with cys-POx is described. As pretests the self-assembly of cys-POx in millipore water was tested, resulting in particle or micelle formations beginning with concentrations ≥0.5 mg·mL^{-1} (observed by DLS and NTA). This may also influence the cell viability and number, respectively.
Yet in conclusion, no cytotoxicity concerning human fibroblasts was determined up to concentrations of 1.0 mg·mL^{-1}.

4.1.7 Reactive poly[(oligo ethylene glycol) acrylates]

Aside from the synthesis of multiple functionalized POx, the synthesis of reactive polyacrylates with hydrophilic ethylene oxide side-chains was completed using the RAFT process. The RAFT process allows the synthesis of highly precise polymer compositions in a living mechanism with narrow *Đ*. By giving these polymers chemoselective functionality towards cysteine or thioester compounds, an orthogonal and highly efficient bio-functionalization is possible.

4.1.7.1 Synthesis of active ester

PFPA was chosen as the active ester as it includes several advantages in contrast to other active esters like the frequently used NHS-ester. PFP is soluble in a wide range of solvents (e.g. chloroform and THF). The synthesis of acrylated-PFP is simple and after functionalization, the monomer is available for living radical polymerization techniques. Furthermore, it can be analyzed by ^{19}F-NMR measurements whereby an unambiguous signal assignment is possible.
PFPA was synthesized by nucleophilic attack of pentafluorophenol to acrylic acid chloride. The product could be isolated in good yield and quality after vacuum distillation. ^{1}H-NMR (experimental section **Figure 5–24**) shows characteristic allyl signals at δ = 6.76 – 6.70, 6.42 – 6.33 and 6.21 – 6.17 ppm. Additionally, **Figure 5–25**

(experimental section) shows the ^{19}F-NMR of PFPA where all expected signals are visible.

Besides the characterization of the monomer by ^{1}H- and ^{19}F-NMR, FT-IR spectroscopy (**Figure 4–19**) was used. PFPA bears a characteristic C-F vibration (experimental section **Figure 5–26**) which is visible at 992 cm^{-1}. Furthermore, an additional band of the activated ester is visible at 1515 cm^{-1} which is assignable to the carbon–carbon stretching vibrations of the aromatic ring. This signal serves for the interpretation of the amount of active ester in the polymer chains additionally to the ^{19}F-NMR signals.

4.1.7.2 Synthesis of hydrophilic active ester polymers

The synthesis of reactive P(OEGA) was previously completed by the copolymerization of two different monomers, OEGA and PFPA.[126] Both monomers bear acrylate groups thus they are easy to polymerize with living radical polymerization methods. OEGA and PFPA were polymerized using the RAFT process, where 2-cyano-2-propyl benzodithioate served as chain transfer agent (CTA) and AIBN as radical source. The monomers were dissolved in dry DMF and were combined with the CTA. After three pump–thaw-cycles the solution was heated to 80°C. The polymerization started as soon as AIBN was added and was stopped after 16h.

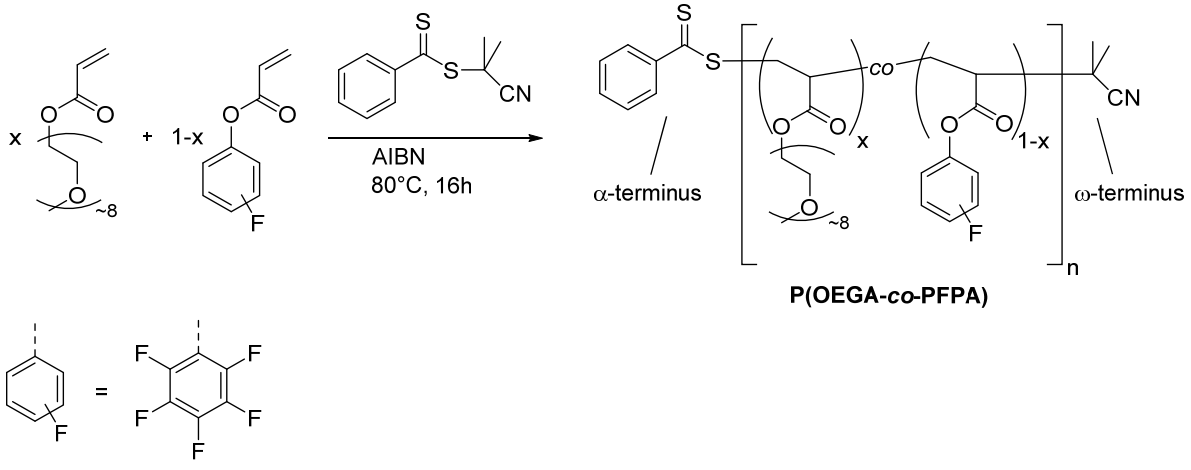

Scheme 4–6: *Schematic overview of the synthesis of hydrophilic hydrophilic active ester polymers.*

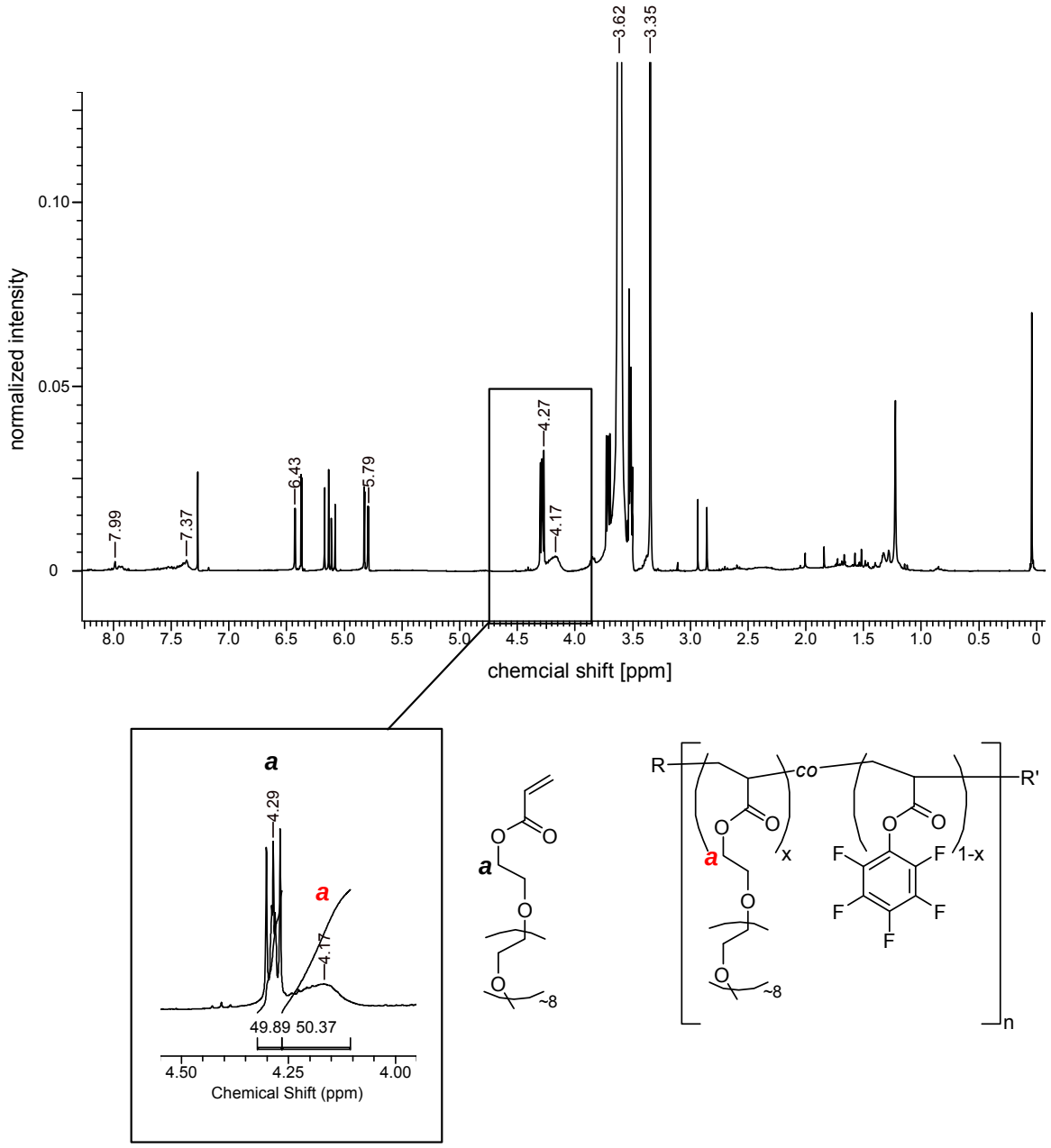

Figure 4–17: *Raw ^{1}H-NMR measurement of the copolymerization of OEGA and PFPA at the moment of polymerization termination by cooling to 0°C and exposure to air.*

For the calculation of the real polymer composition it is important to take an unpurified sample for ^{1}H- and ^{19}F-NMR measurements. The ^{1}H-NMR gives information about the conversion of OEGA. The signal at δ = 4.29 ppm can be assigned to the first repeating unit of ethylene glycol at the side-chain of the monomer (**Figure 4–17**). This signal changes into a broad signal at δ = 4.17 ppm. The combination of both signals was set to 100 for the percentage of conversion. By comparing the integrals of both signals, the actual amount of OEGA in the synthesized polymer could be calculated. For the calculation of the amount of PFPA present in the polymer chains ^{19}F-NMR (**Figure 4–18**) was required. Here, the monomer signals are assignable at δ = -162.75, -165.00, and -170.69 ppm. These shift to broad signals at δ = -152.04, -157.41, and -161.94 ppm and can clearly be distinguished as the polymer peaks. The integration-ratios between polymer and monomer signals gives more information about the conversion of PFPA.

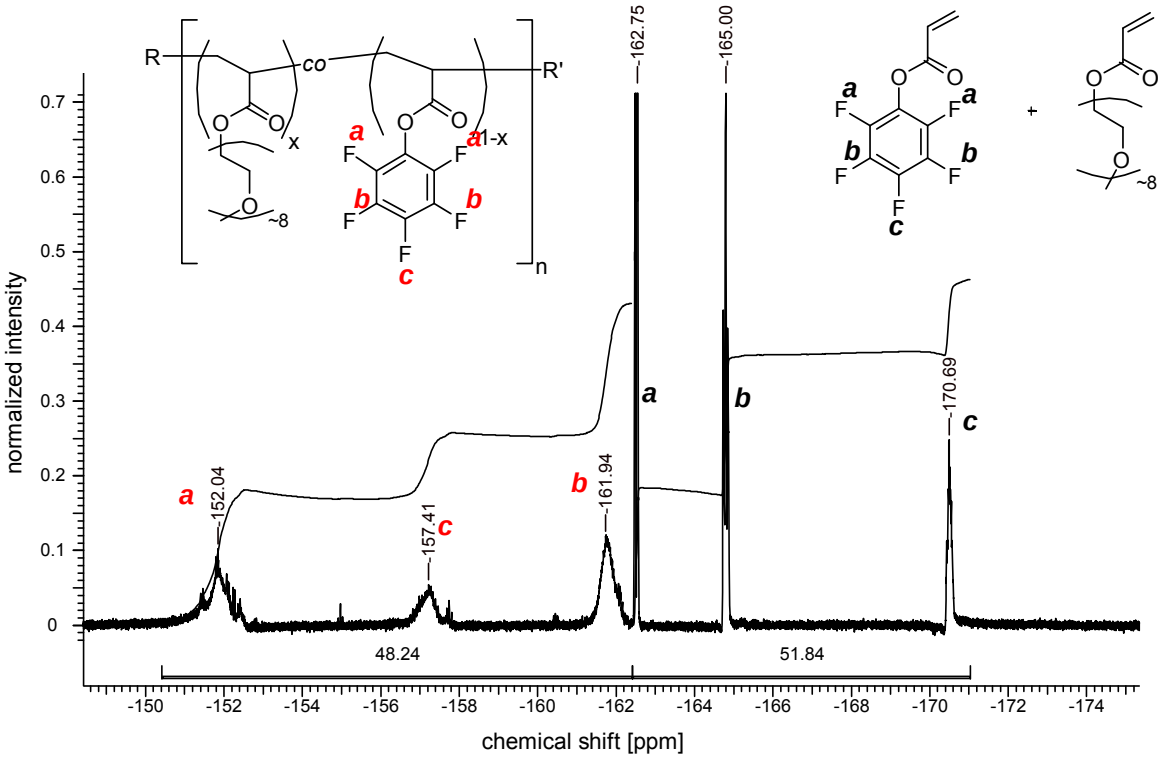

Figure 4–18: *Raw ^{19}F-NMR measurement of the copolymerization of OEGA and PFPA at the moment of polymerization termination by cooling to 0°C and exposure to air.*

Considering both calculations, the real polymer composition is assessable. As both NMR spectra (**Figure 4–17** and **Figure 4–18**) show that approximately 50% of both monomers reacted, the actual and target compositions are the same. After polymer purification, FT-IR spectroscopy can provide more information about the polymers' composition as the characteristic vibrations of the aromatic ring (1520 cm^{-1}) as well as the C–F-vibrations (997 cm^{-1}) are visible in the spectra of the polymers. **Figure 4–19** shows different amounts of active ester as part of the polymer and the FT-IR spectra reflects the amount of included PFPA very well, though a defined quantitative statement is not possible from that. The DP can be calculated from the ^{1}H-NMR after purification by using the aromatic unit at the terminus as internal reference with the signals at δ = 7.39 – 7.98 ppm set to 5 (**Figure 4–20**). Comparison of this integral with the integral of the first repeating unit of the OEG side-chain (δ = 4.20 ppm, H-***d***) or with the terminal methyl-group at the side-chain (δ = 3.38 ppm, H-***f***), the DP can be calculated and was found to be 8 and was exact the same as the desired DP as the molar ratio of $[M]_0$:$[I]_0$ was 8.

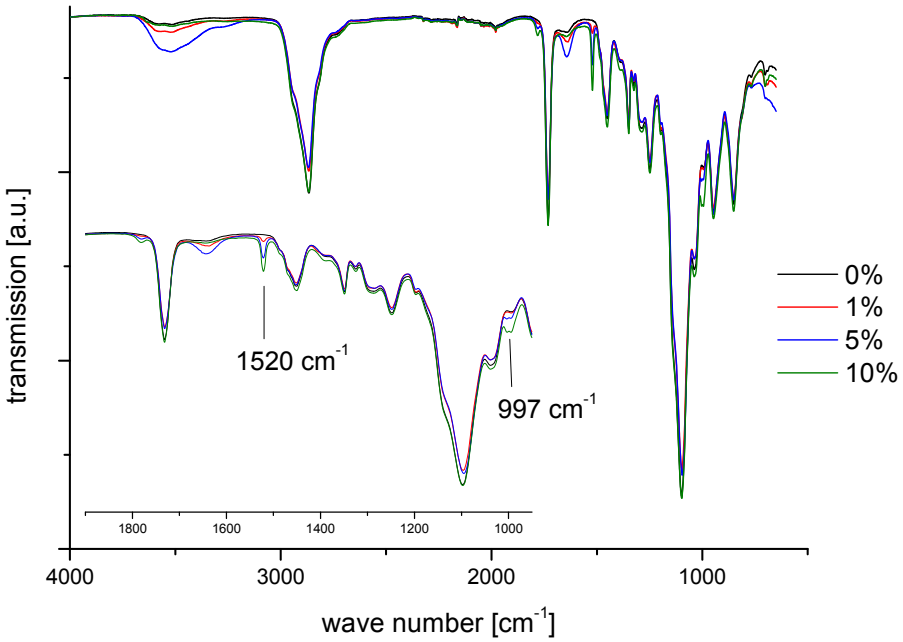

Figure 4–19: *FT-IR spectra of hydrophilic polymers with different amount of active ester side-chains (black: 0% active ester; red:1% active ester; blue: 5% active ester; green: 10% active ester.*

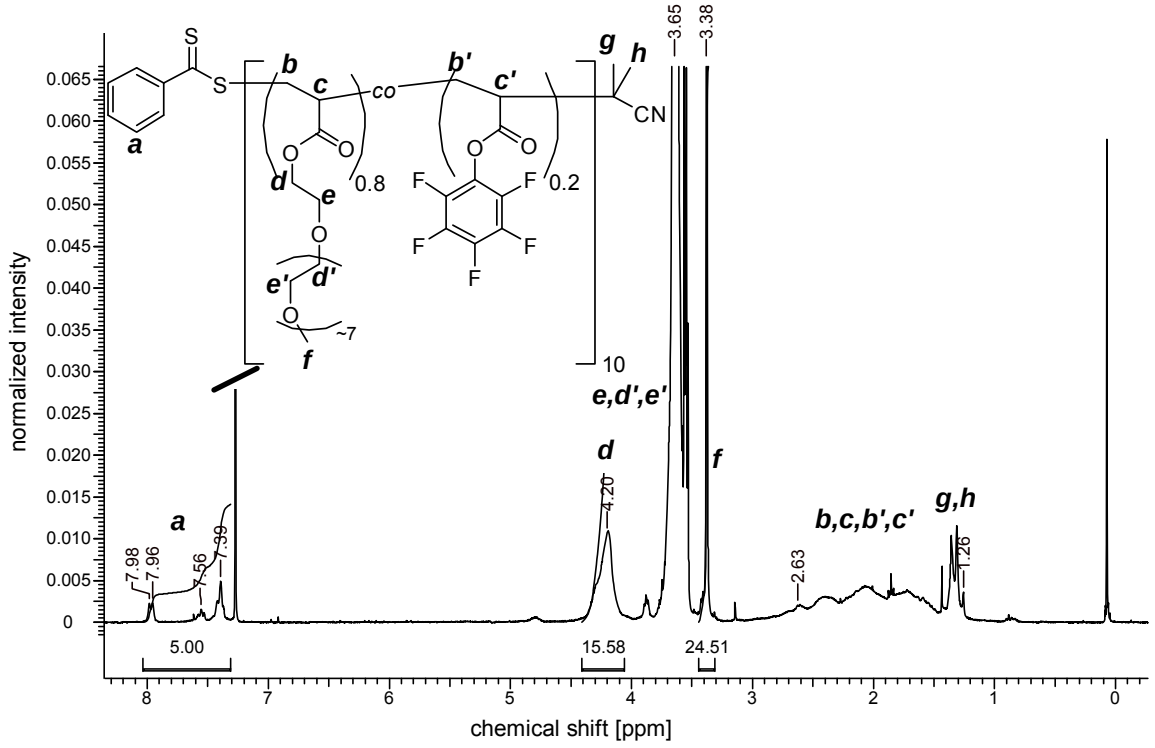

Figure 4–20: *^{1}H-NMR spectra of active ester P(OEGA) in $CDCl_3$ after the purification by precipitation into n-hexane:Et_2O = 1:1 (3 times). DP can be calculated by using the aromatic unit as intern reference.*

4.1.8 poly[oligo(ethylene glycol) acrylate]-functionalization for NCL

4.1.8.1 Cys-functionalization of reactive poly[oligo(ethylene glycol) acrylate]

Scheme 4–7 shows the synthesis of amine functionalized thiazolidine. The introduction of thiazolidine-functionality into the polymer side-chain was completed by polymer-analogue functionalization of the active ester with amine functionalized thiazolidine (ATHz).

FTz4CA was treated with an one-side protected diamine. The synthesis of FTz4CA was explained previously in detail in chapter 4.1.6.[191-192] For amine-functionalization, the carboxylic acid group was activated by CDI in chloroform. In the beginning the reagent was only dispersible in chloroform, but after activation the resulting active ester was soluble. The addition of *N*-boc-1,4-butanediamine lead to an intermediate followed by deprotection. After basic workup and extraction with chloroform the

product could be isolated in an approximate yield of 60%. The reaction conditions during the Boc-deprotection were performed so as to be as mild as possible and was completed by simply refluxing in water overnight.[194] Purification of the product was realized by extraction with chloroform and evaporation of the solvent. Taking the low yield of 60% into account, it could not be excluded that the conditions during deprotection may also partially deprotect the acetal and aldehyde protection-groups. If they were cleaved additionally, the solubility in water would be high, whereby the extraction with chloroform would not be possible anymore which can somehow explain the low yield.

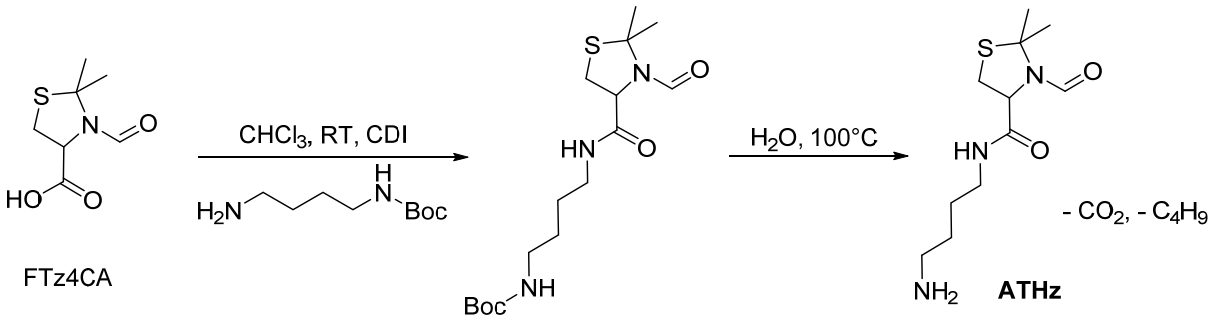

Scheme 4–7: Synthesis of amine functionalized thiazolidine (ATHz).

Figure 4–21 shows the associated ^{1}H-NMR including all expected signals. The formyl-protecting group generates a signal at δ = 8.38 ppm. The signal at δ = 6.97 ppm can be assigned to the proton of the secondary amine. The methine proton of the thiazolidine ring generates a signal in the range of δ = 5.01 – 4.67 ppm. Signals in the range of δ = 3.75 –3.12 ppm can be assigned to the methylene group next to the secondary amine and the methylene group in vicinity to the sulfur atom of the thiazolidine ring. The methylene group beside the terminal amine generates a triplet-signal at δ = 2.71 ppm. The signals at δ = 1.84 and 1.77 ppm can be assigned to the acetal-protecting group of the thiazolidine. The two methylene groups in the middle of the small alkyne chain generate a multiplet signal in the range of δ = 1.58 – 1.44 ppm. Even the proton signal of the terminal amine group is visible as a broad signal at δ = 1.24 ppm.

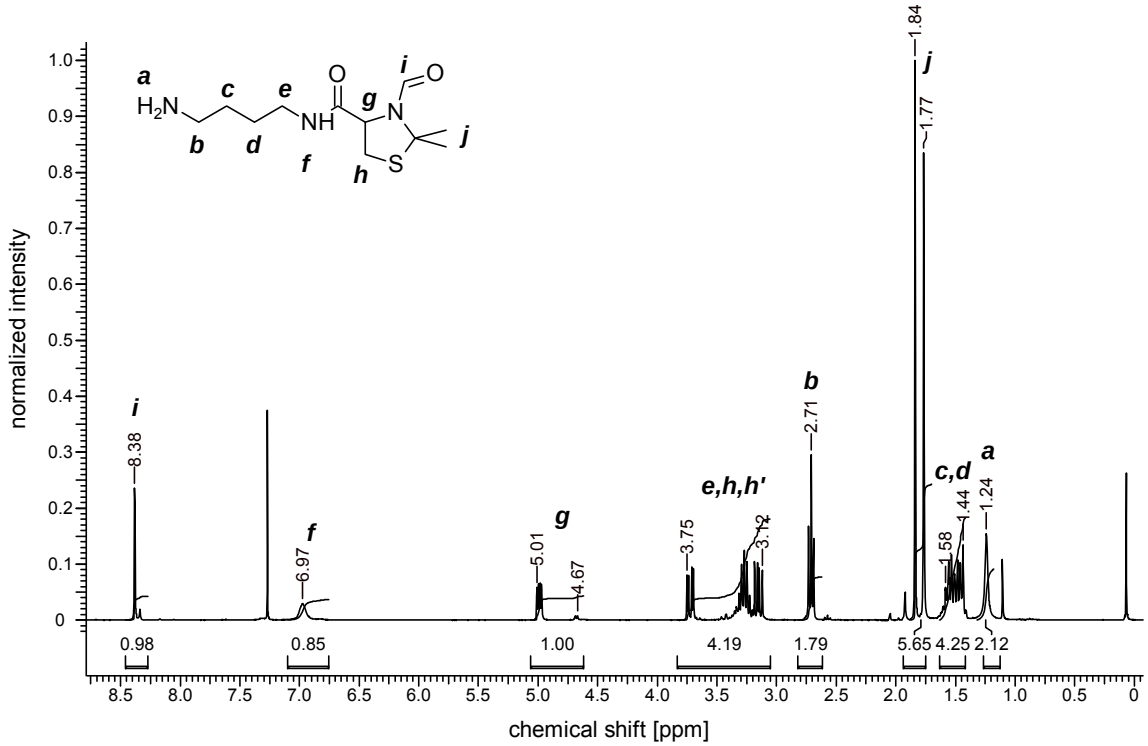

Figure 4–21: *^{1}H-NMR of amine-functionalized thiazolidine for cysteine-functionalization of P(OEGA) (measured in $CDCl_3$).*

For the cysteine-functionalization of P(OEGA) (**Scheme 4–8**), the reaction was performed in DMF as protic and polar solvents are beneficial for the nucleophilic attack of amines.[119] The addition of an amount of OEGA during the amine-functionalization is important, as aminolysis can result in thiols at the α-terminus of RAFT-polymers[195-196] that are able to react in situ with acrylates in nucleophilic thiol–ene reactions[144,197-199]. Without the addition of OEGA, the thiol end-group could form disulfide bridges by oxidation, resulting in bimodal polymer populations. Diazabicycloundecene (DBU) as non-nucleophilic base supports the aminolysis of the reactive polymer with ATHz. **Figure 5–32** (experimental section) shows the associated ^{19}F-NMR where the broad polymeric signals are not visible anymore at δ = -152.04, -157.41, and -161.94 ppm, but instead defined and narrow signals can be observed at δ = -169.44, -170.21, and -186.25 ppm which can be assigned to the redundant PFP unit. After purification of the polymer by precipitation into a mixture of cold diethylether and *n*-hexane (V/V, 1/1), no signals in ^{19}F-NMR were visible anymore.

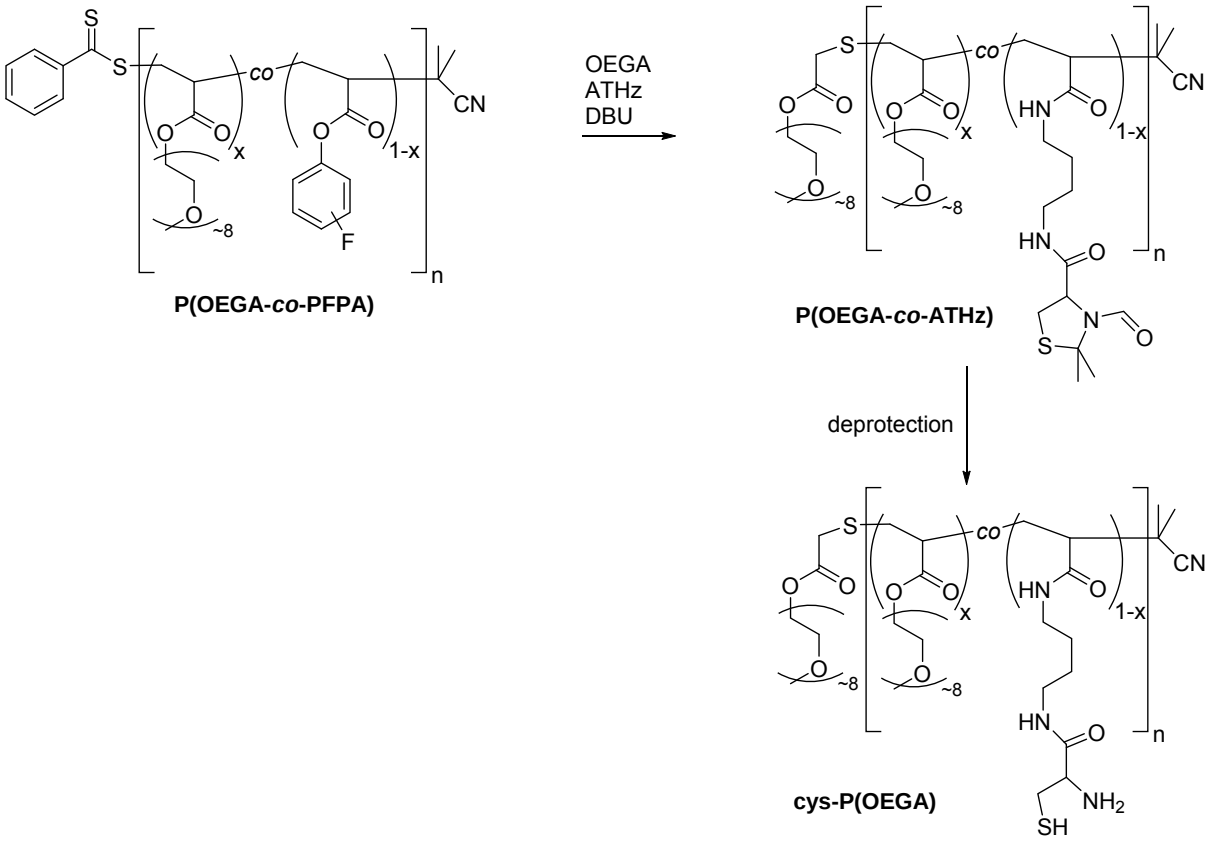

Scheme 4–8: *Synthesis of cys-P(OEGA).*

^{1}H-NMR measurement (**Figure 4–22**) supports the synthesis of the functional polymer, as the signals of the thiazolidine are visible at δ = 8.37 ppm (aldehyde protection group), 4.93 ppm (methine proton of the thiazolidine ring) and 1.52 ppm (acetal protection group). All other signals are difficult to assign, as they are overlaid with the polymeric protons. The integrals of a polymer bearing for example five active esters before functionalization apply perfectly.

Furthermore, **Figure 4–24** indicates the successful functionalization with amino-thiazoldines. It shows the FT-IR spectrum of the active ester polymer before and after functionalization with amino-thiazolidines, where the characteristic vibrations of C–F and aromatic C–C bonds almost completely disappeared after functionalization. In addition, the characteristic vibration of amides is visible at ~1650 cm^{-1}. The synthesis of cysteine-functionalized P(OEGA) could easily be completed by thiazolidine-deprotection by refluxing in 0.1 M HCl for 3 d. After dialysis against slightly acidified water and drying through lyophilization, cys-P(OEGA) could

be isolated. This was confirmed by ^{1}H-NMR measurements where the acetal and formyl protection-groups at δ = 8.37 ppm and 1.52 ppm were no longer visible (experimental section **Figure 5–34**).

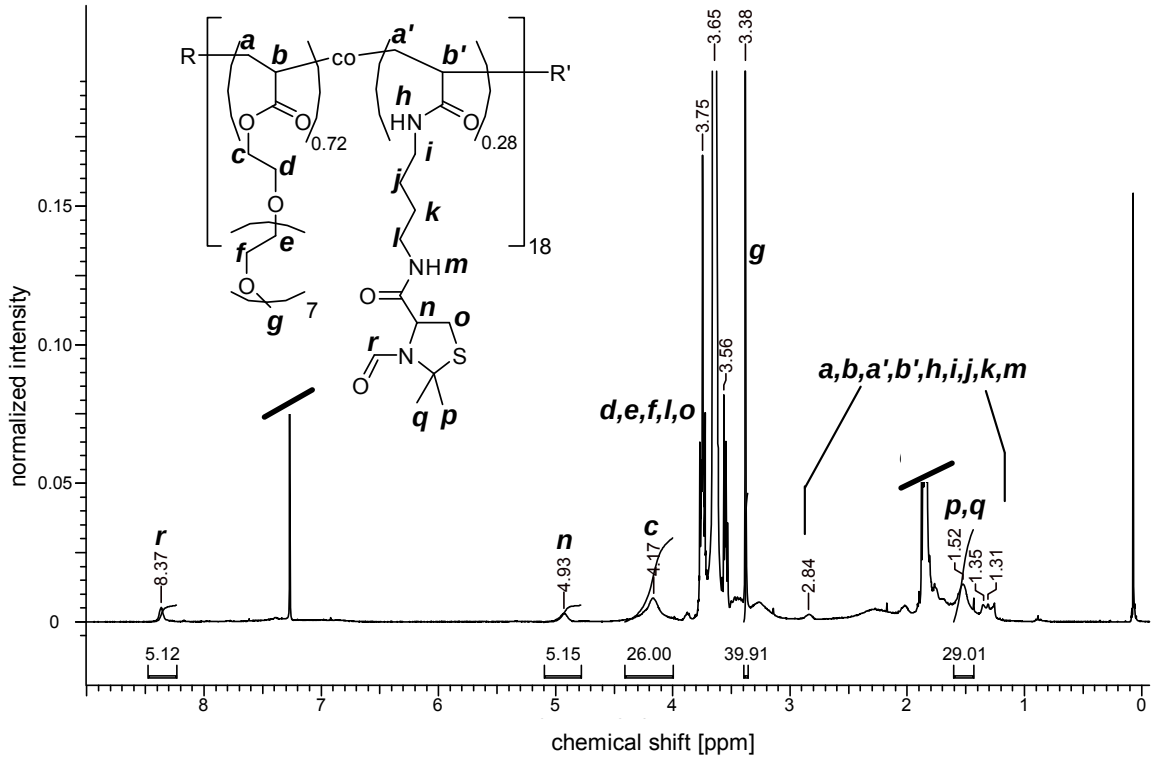

Figure 4–22: *^{1}H-NMR spectra of thiazolidine functionalized Poly[(OEGA)$_{0.72}$-co-(PFP)$_{0.28}$]$_{18}$ (measured in CDCl$_3$).*

4.1.8.2 Thioester-functionalization of reactive poly[oligo(ethylene glycol) acrylate]

Additionally, the reactive P(OEGA) was functionalized with a cyclic thioester for further NCL with a cysteine component (**Scheme 4–9**). The synthesis was performed in the same way as the amine-thiazolidine functionalization mentioned previously. DMF served as solvent and OEGA was added for the functionalization at the terminus of the polymer during aminolysis. As the cyclic thioester is not as nucleophilic as other primary amines, the reaction temperature had to be increased to 50°C. Additionally, the terminal functionalization with OEGA was only successfully

achieved for approximately 35% (calculated by ^{1}H-NMR) showing the less reactivity of the cyclic thioester. Nevertheless, no oxidation of possible thiol-groups at the termini occurred, as observed by a monomodal distribution in DMF-SEC.

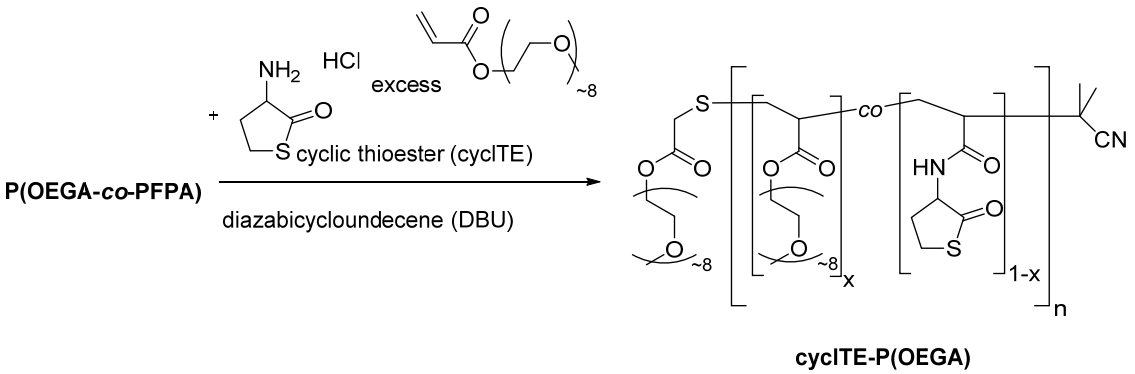

Scheme 4–9: *Schematic overview of the cyclic thioester-functionalization of P(OEGA-co-PFPA).*

In the ^{19}F-NMR (**Figure 4–23)** narrow signals can be observed at δ = -162.86, -165.76 and -172.47 ppm which can be assigned to the redundant PFP unit. The different chemical shifts of the resulting leaving group (in contrast to the signals after the reaction with amino-thiazolidine, or signals of pure PFP) can be explained by the nature of ^{19}F-NMR: The area of ^{19}F-chemical shifts is 100 times bigger than in ^{1}H-NMR spectroscopy. Thus, smallest changes of the chemical environment can be detected by this method and results in different chemical shifts of the same leaving group. An assumption that the redundant PFP could have reacted with the excess of unbound cyclic thioester has not been confirmed. Therefore a model reaction of PFP with the cyclic thioester has been accomplished in the same reaction conditions as in the polymer functionalization. Here, the signals in a ^{19}F-NMR didn't show a change in the chemical shifts of PFP.

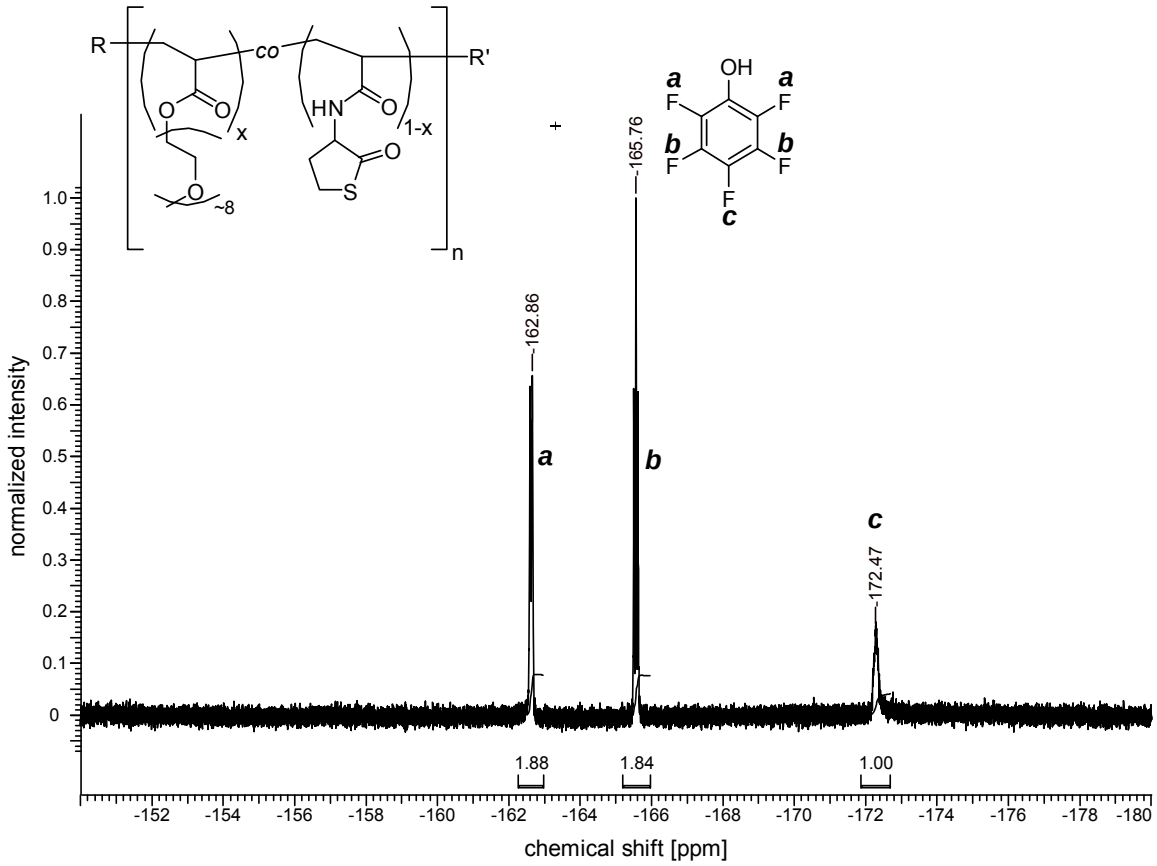

Figure 4–23: *Raw ^{19}F-NMR measurement of a polymer after functionalization with a cyclic thioester for further NCL. The characteristic broad signals at δ = -152.04, -157.41 and -161.94 ppm are not visible anymore. Furthermore new signals appear because of the redundant PFP unit.*

The ^{1}H-NMR spectrum of the functionalized polymer (experimental section **Figure 5–35**) is difficult to interpret as all signals of the bounded cyclic thioester are overlaid with the polymer signals. Nevertheless, a characteristic signal of the amide proton is visible at δ = 11.72 ppm.

Furthermore, the FT-IR spectrum of the active ester polymer after the functionalization with the cyclic thioester is shown in **Figure 4–24** and indicates again the successful functionalization. The characteristic vibrations of C–F and aromatic C–C bonds nearly disappeared after functionalization while on the other hand, the characteristic vibration of amides is visible at ~1650 cm^{-1}.

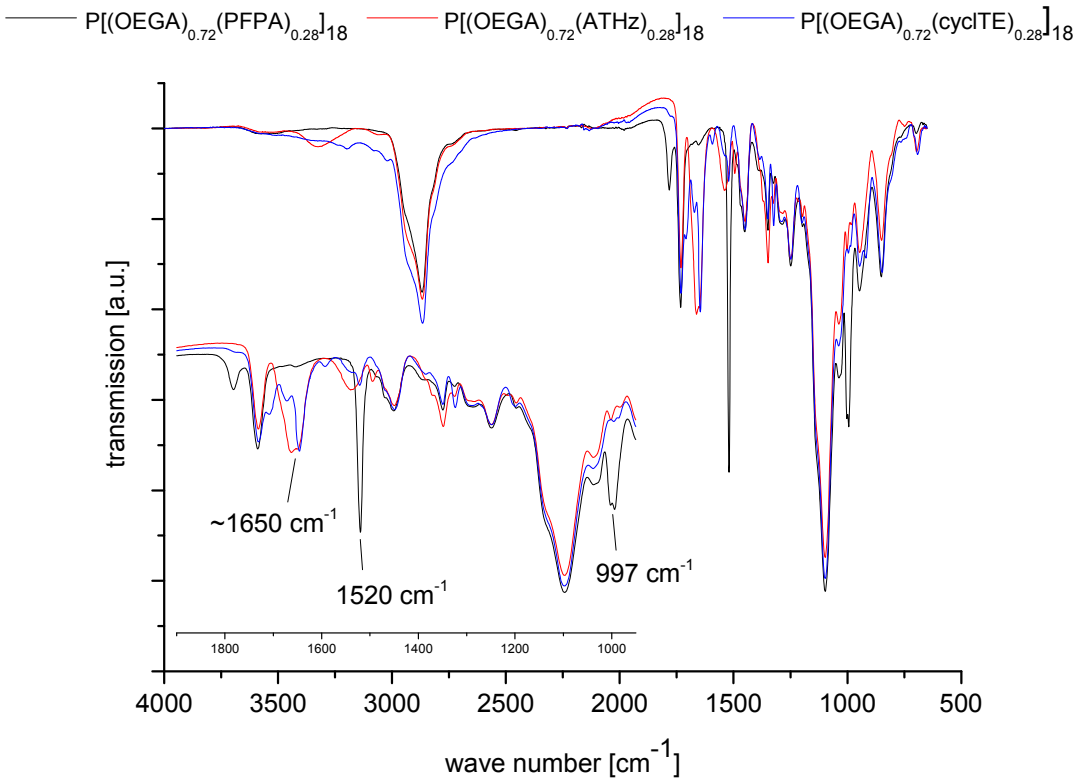

Figure 4–24: *FT-IR spectra of active P(OEGA) after the functionalization with amino–thiazolidine (red) or with cyclic thioester (blue).*

4.2 Coupling Reactions

4.2.1 Azide–alkyne chemistry with POx

In order to validate the successful synthesis of alkyne- and azide-functionalized POx, both polymers were used for azide–alkyne reaction with each other.

Therefore, the same molar amount of both polymers were combined and dissolved in millipore water. After the addition of $CuSO_4 \cdot 5\ H_2O$ as catalyst and sodium ascorbate as the reductive component for in situ production of Cu(I), the solution was stirred for 48 h. The pure product could be simply isolated by precipitation into cold diethyl ether.

The following **Figure 4–25** shows the ^{1}H-NMR spectrum of alkyne-functionalized P(MeOx) after the reaction with P(MeOx)–N_3. A shift of the methylene signal (H-***e***) from approximately δ = 4.10 ppm to 4.54 ppm indicates the successful coupling of azide- and alkyne-functionalized P(MeOx). In addition, the characteristic proton of the generated 1,2,3-triazole is visible at δ = 7.59 ppm (H-***d***). The number-average DP, can be calculated using the signal ascribed to the methylene protons of the repeat unit at δ = 3.39 ppm (H-***b***, H-***c***, H-***b'*** and H-***c'***) and the resonance of the terminal methyl-group at δ = 2.85 – 2.99 ppm (H-***a***). The integral increases to a value of 340 which corresponds to 85 repeating units.

The successful linking of two POx polymers is also underpinned by the results of SEC measurements (**Figure 4–26**). Here, the molecular weight distribution of azide- (black curve) and alkyne-functionalized P(MeOx) (red curve) measured by H_2O-SEC is shown, as well as the distribution after azide–alkyne chemistry. Alkyne-functionalized P(MeOx) has a broader distribution, as it was initiated by propargyl benzenesulfonate (as already stated in chapter 4.1.2). The fronting of the curve indicates the existence of lower molecular weight fractions (because of a not completely living mechanism of the polymerization) or column interactions. After the click reaction (blue curve), the distribution is obviously shifted to higher molecular weights. The small fronting of the blue curve might be attributed to not reacted polymer chains during the click-reaction.

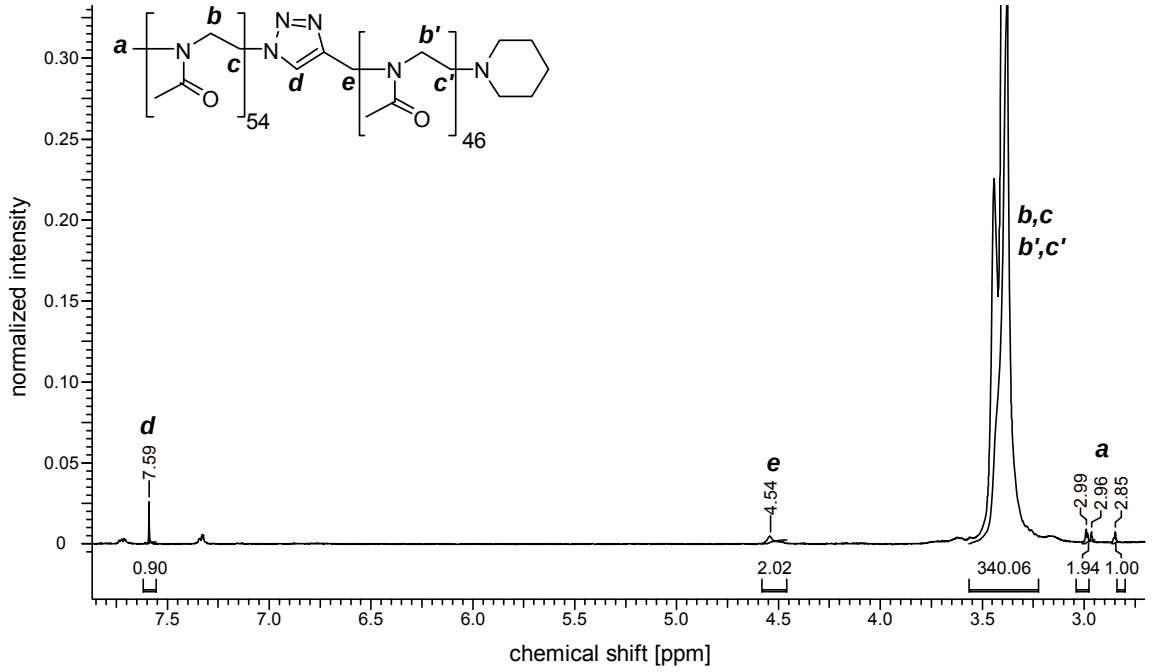

Figure 4–25: *^{1}H-NMR spectrum of P(MeOx) in CD_3CN after the click reaction of azide- and alkyne-functionalized P(MeOx). The characteristic peak of the generated 1,2,3-triazole is visible at 7.59 ppm.*

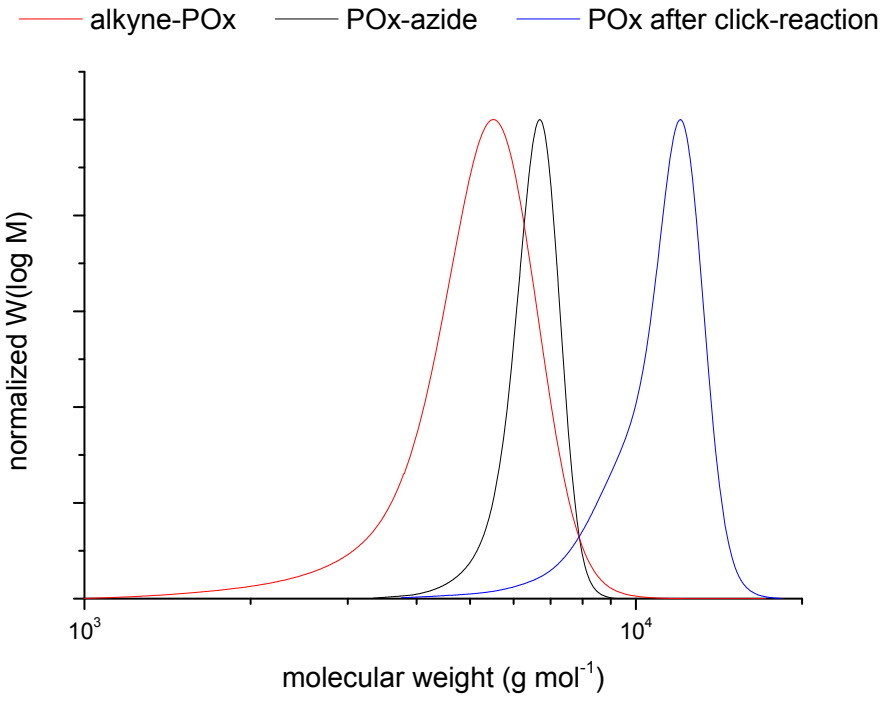

Figure 4–26: *Molecular weight distribution of azide- and alkyne-functionalized P(MeOx) measured by H_2O-SEC (black curve: POx-azide; red curve: alkyne-POx). After click reaction (blue curve) the distribution is clearly shifted to higher molecular weights.*

The molecular weight of all polymers determined by SEC falls below the calculated ones again. This can be explained by the calibration with PEG which has a different coiling behavior in water in contrast to POx. Nevertheless, the successful reaction of alkyne- and azide-functionalized POx can be seen in the SEC diagram.
In addition, FT-IR measurements with P(MeOx) after azide–alkyne reaction showed no characteristic azide-vibration at ~2100 cm^{-1} anymore, indicating the successful reaction between azide- and alkyne-functionalized POx (experimental section **Figure 5–39**).

4.2.2 Native chemical ligation with cysteine-functionalized POx

(*) In order to investigate the accessibility and chemical reactivity of the cysteine-functionalities, NCL was used for the formation of multiple polymer–peptide conjugates. Therefore, a polymer bearing five cysteine side-chains (calculated by ^{1}H-NMR) was employed and coupled to C-terminal thioester peptides with polymer:peptide ratio of 1:5. As the model peptide, a sequence of phenylalanine with glycine was used. This peptide was terminated with a benzimidazole derivate in order to form the reactive thioester *in situ* during NCL with the cysteine functionalized polymer. NCL was performed overnight at RT and at a pH of 7.0 under reductive conditions with 4-mercaptophenylacetic acid (MPAA) as aromatic NCL-catalyst (the thioester is formed *in situ*). HPLC was applied to remove salts and excess MPAA. Polymer containing fractions were collected and showed no unreacted peptide by UV/MS analysis.
Figure 4–27 shows the ^{1}H-NMR of polymer–peptide conjugates. The DP and functionalization was predetermined by the copolymerization of MeOx and DecenOx. The peak at δ = 2.0 ppm (which can be assigned to the methyl group of MeOx) was used as reference for the calculation of the attached peptide sequences. The integral of this signal was set to 150. After NCL, all predicted signals were visible in the ^{1}H-NMR spectrum. Besides the polymer signals, new signals associated with the attached peptide were evident at δ = 3.9 ppm (methylene group of glycine),

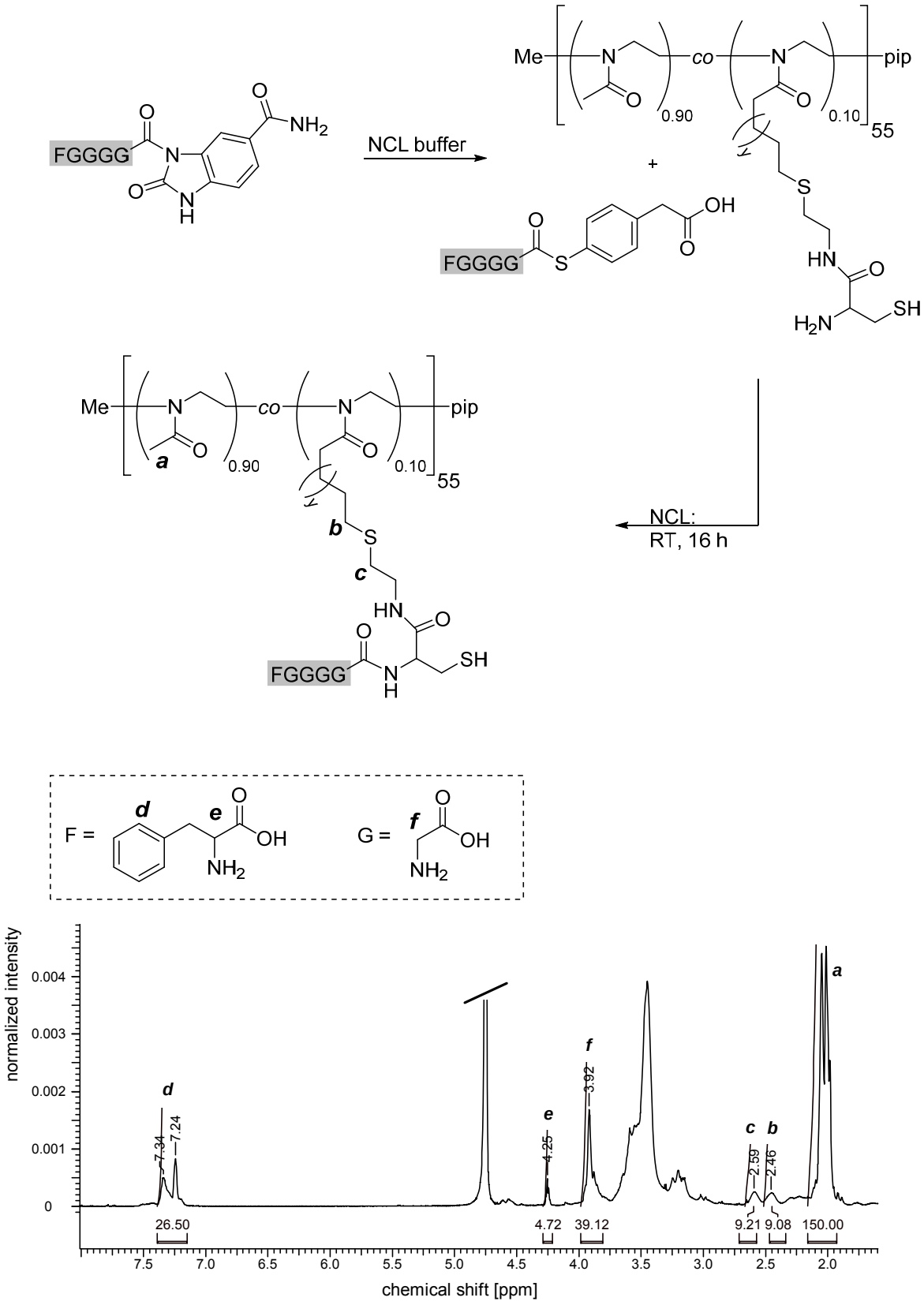

Figure 4–27: *^{1}H NMR of polymer–peptide conjugates bearing five peptides per polymer chain (in D_2O).*

δ = 4.2 ppm (methine group of phenylalanine), and δ = 7.2 – 7.3 ppm (aromatic unit of phenylalanine). The integrals of these signals further confirm the attachment of five peptides to the polymer.

MALDI ToF measurements of the polymer before and after NCL showed a broader signal after NCL as expected (experimental section **Figure 5**–41). Therefore, as expected, with this analytical method, a comprehensive result could not be achieved. While SEC and HPLC measurements did not yield unambiguous results as the elugrams after the reaction did not differentiate from elugrams before the reaction. The ^{1}H NMR spectroscopy characterization showed the attachment of small peptides to cys-POx.

As the chosen peptide is biologically irrelevant and has no further function, the reactivity of NCL with tau[390-410] sequence (Thz-EIVYKSPVVSGDTSPRHLSN, Thz: Thiazolidine protected cysteine, 2443 g·mol^{-1}) was additionally proved which is sterically demanding and known in the research area of Alzheimer's disease. A 5800 g·mol^{-1} polymer bearing six cysteine side-chains (calculated by NMR) was employed and coupled with the peptide in polymer:peptide ratios of 1:1, 1:3 and 1:6. NCL was performed in the same conditions as in the first experiment. HPLC was used to remove salts and excess MPAA. Polymer containing fractions were collected and showed no unreacted peptide by UV/MS analysis.

Again, the results of an analytic HPLC measurement were ambiguous, consequently MALDI ToF measurements were performed and are shown in **Figure 4–28** which demonstrates the successful formation of polymer–peptide conjugates. These experiments demonstrate the possibility of multiple NCL of C-terminal thioester peptides with cys-POx, although bearing in mind that MALDI ToF measurements are challenging even in the case of pure copolymers. During polymerization many different species of polymer chains are generated and each species has a different behavior in MALDI ToF. The functionalization and equipment of polymers with peptides enhances the severities that occur. For interpretation of the MALDI ToF spectra it is important that dispersity of the polymer, its functionalization with the thiazolidine, and the functionalization with peptides overlay. All calculated (expected) and observed masses can be found in the experimental section in **Table 5–15** – **Table 5–18**.

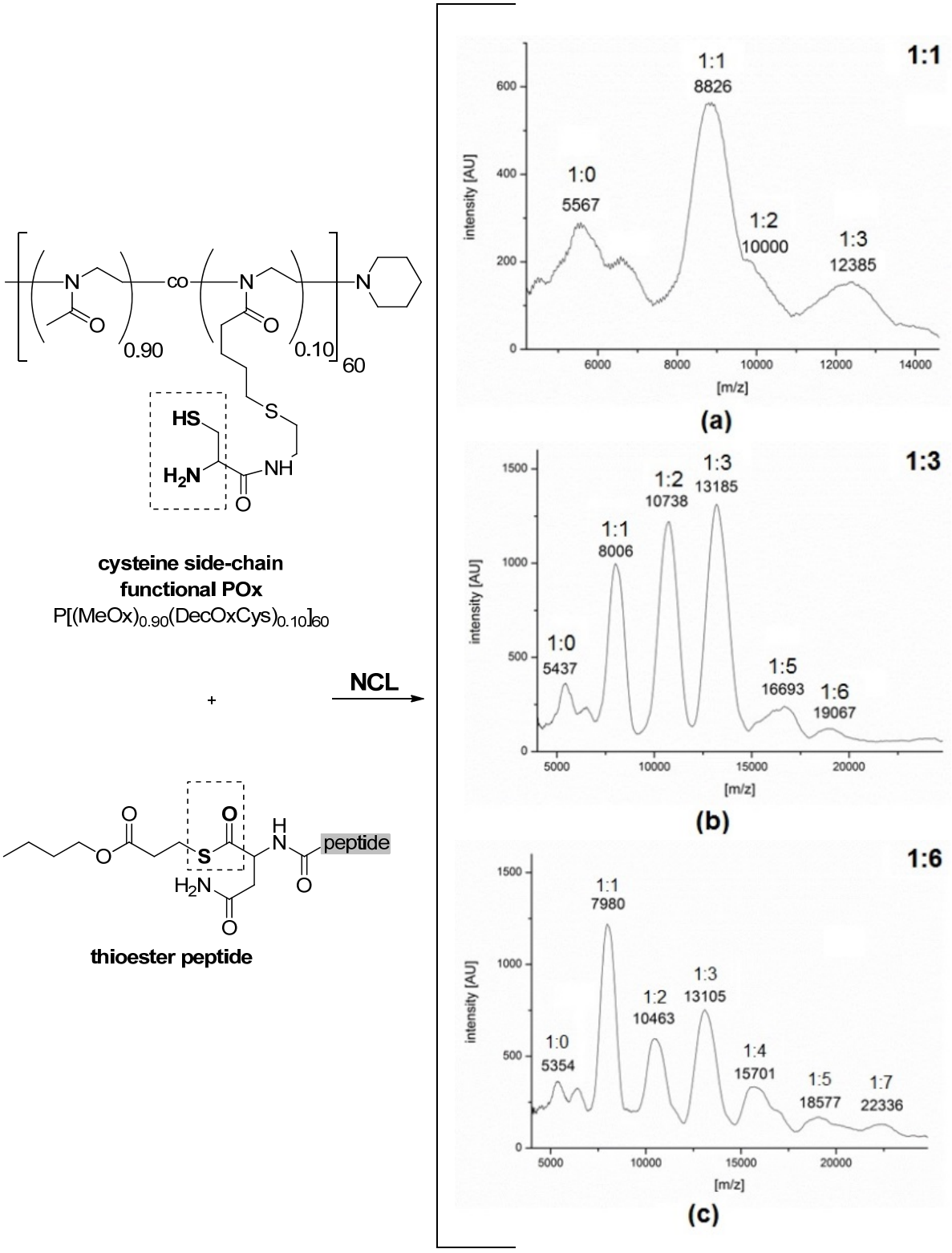

Figure 4–28: *MALDI ToF measurements of polymer–peptide conjugates with polymer:peptide feed ratios of 1:1, 1:3 and 1:6 with corresponding estimated maxima of the signals and the amount of peptides at each polymer. The molecular weight of the pure polymer was M_n = 5800 g·mol^{-1} as calculated by ^{1}H-NMR measurements.*

The signal at 5567 g·mol^{-1} in **Figure 4–28a** revealed uncoupled cys-POx. For a 1:1 molar ratio between polymer and peptide in the reaction mixture, the signal at 8826 g·mol^{-1} indicated the main species in this sample showing the conjugation of one cys-POx with one peptide. The signal for double conjugated peptide merely occurred as a shoulder of the main signal at molecular masses around 10000 g·mol^{-1}, and the weak signal at 12385 g·mol^{-1} was attributed to triple conjugation of peptides to the polymer. In the case of a polymer:peptide ratio of 1:3 (**Figure 4–28b**) signals at 8006 g·mol^{-1}, 10738 g·mol^{-1} and 13185 g·mol^{-1} could be assigned to conjugates of one polymer chain with 1, 2 and 3 peptides, respectively. However, the signals at 16693 g·mol^{-1} and 19067 g·mol^{-1} reveal that conjugation of one polymer with five or six peptides also occurred.

A possible signal around 15000 g·mol^{-1} which could be assigned to conjugates with four peptides cannot be assigned unambiguously. In order to provoke the formation of high conjugate numbers a six fold excess of peptide with respect to the polymer was also applied (**Figure 4–28c**). Almost all expected signals were obtained, with most intensive signals in the range of 1 – 3 peptides per polymer chain (7980 g·mol^{-1}, 10463 g·mol^{-1} and 13105 g·mol^{-1}). Despite the higher excess of peptide, higher signals are very broad and weak which could be a hint of steric hindrance caused by the relatively large peptide sequence. Nevertheless, maxima with shoulders are visible at 15701 g·mol^{-1}, 18577 g·mol^{-1} and 22336 g·mol^{-1} showing occurrence of higher conjugates. The broad signal distribution might be assumed to be the overlay of the different species.

4.2.3 NCL with thiolactone functionalized P(OEGA)

Additionally to the NCL of cys-POx with two different peptides, NCL was performed using P(OEGA) functionalized with a thiolactone group. A model reaction was performed to test the reactivity of the lactone with the addition of a pure cysteine. NCL was performed with $NaBH_4$ as reducing reagent overnight. The ^{1}H-NMR spectrum of the raw product shows the successful reaction between thiolactone and cysteine, whereby all reactant signals are no longer present (supporting information **Figure 5–46**).

(*) A thiolactone-functionalized P(OEGA) of M_n = 3600 g·mol^{-1} bearing five thioesters on the side-chain (predetermined by the copolymerization of OEGA and PFPA) was used for NCL with a CGGGF-model-peptide (**Figure 4–29**). To achieve multiple peptide conjugation to the polymer a molar ratio of 1:5 was used. Similarly, NCL of P(OEGA) was performed using the same POx-NCL conditions, specifically stirring overnight at RT at a pH of 7.2 under reductive conditions and 4-mercapto-phenylacetic acid (MPAA) as aromatic NCL-catalyst. HPLC was employed to remove salts and excess MPAA. Fractions containing the polymer were collected and no unreacted peptide was observed by UV/MS analysis.

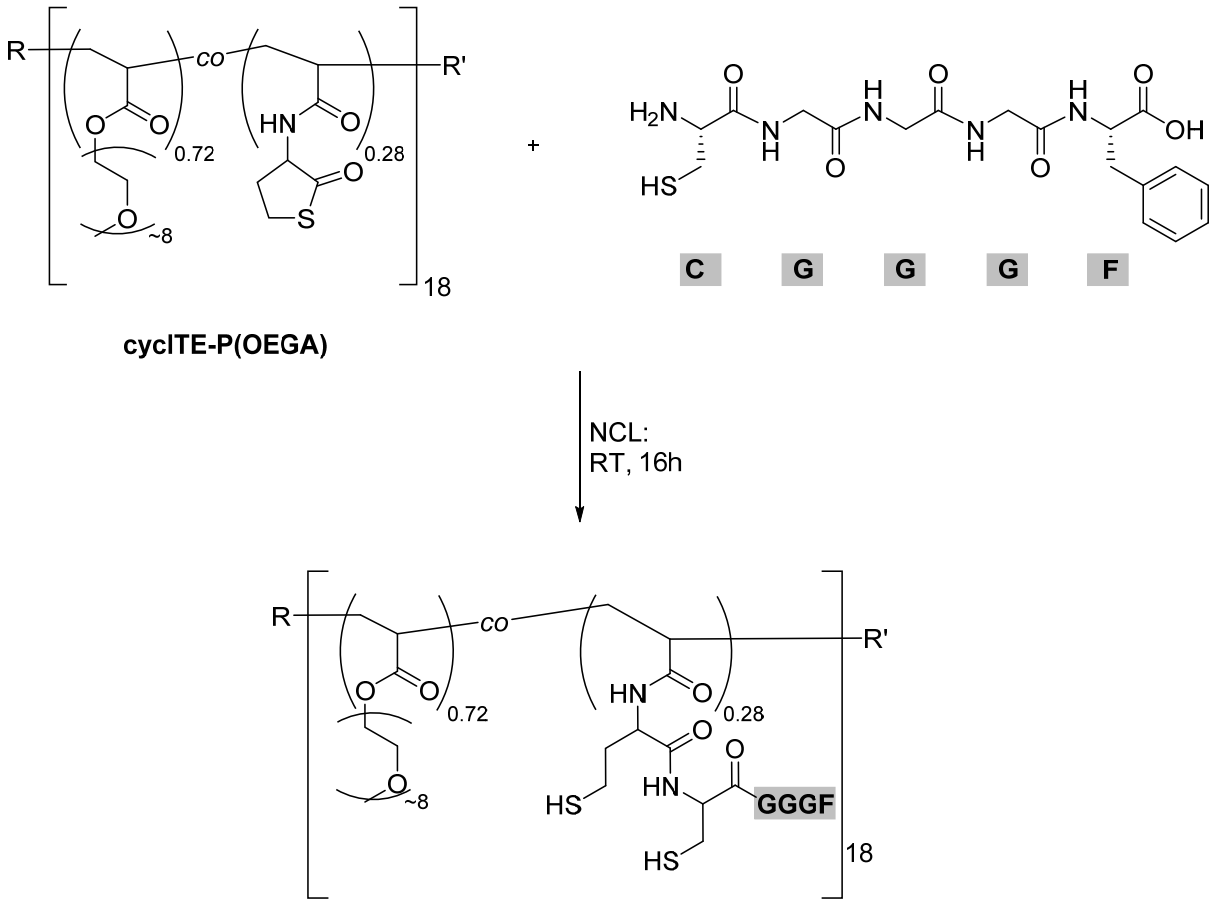

Figure 4–29: *NCL with thiolactone-functionalized P(OEGA) and a model peptide (CGGGF).*

Figure 4–30 shows the HPLC chromatogram of the thioester functionalized polymer recorded at 220 nm. Small impurities were detected between 15 – 25 min. The intense polymer peak is precisely visible after 9 min. As no aromatic units are in the molecular structure of the polymer, a chromatogram with a 272 nm laser lead to no absorbance and no signal was detected. After the NCL with CGGGGF-peptide, the HPLC chromatogram showed completely different results (**Figure 4–31**). Firstly, the retention time changes from 9 min to 26 min, which can be explained by the growing interaction of the conjugate with the column material and was evidence for the successful conjugation of the thioester-functionalized P(OEGA) with the peptide. Secondly, there is no peak visible at 9 min, a further indication that a complete conjugation between polymer and peptide was achieved. Moreover, an adsorption is detectable at 272 nm which can only be caused by the bonding of the polymer with the peptide that contains aromatic units through the presence of phenylalanine. A further quantification of the conjugation by ^{1}H-NMR could not be performed as the yield of the conjugate after HPLC was unfortunately too small (< 2 mg). Nevertheless, the HPLC-results show that the NCL of the cyclic-thioester-functionalized P(OEGA) with the model-peptide was successful.

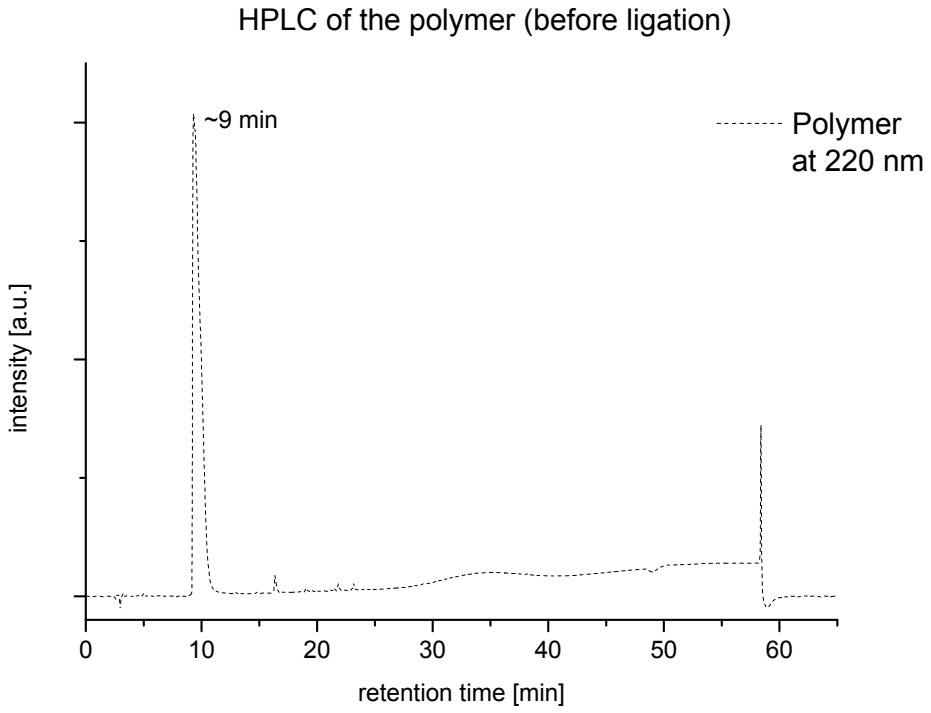

Figure 4–30: *HPLC chromatogram of P[(cyclTE)$_{0.28}$-P(OEGA)$_{0.72}$]$_{18}$ before Native Chemical Ligation.*

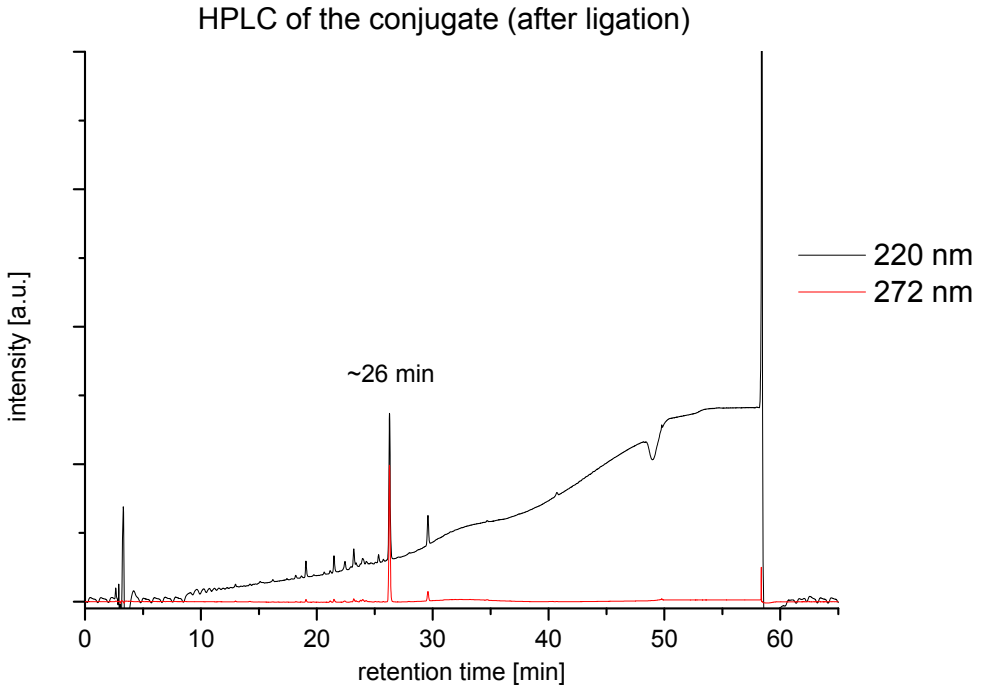

Figure 4–31: *HPLC chromatograms of conjugates consisting of P[(cyclTE)$_{0.28}$-P(OEGA)$_{0.72}$]$_{18}$ functionalized with five FGGGC-model peptides.*

4.3 Nanogels with cysteine-functionalized POx

4.3.1 Synthesis of Nanogels with cysteine-functionalized POx

Besides the chemoselective functionalization of POx with peptides, POx has also been used for the preparation of drug delivery systems.

By IUPAC, "nanogels are defined […] as particles of gel of any shape with an equivalent diameter of approximately 1 to 100 nm."[200] "Structures prepared in this work will also be called nanogels despite their size exceeding 100 nm, as many authors do in the current literature."[201] Before the synthesis of cys-POx-nanogels, the self-assembly was examined in order to see the behavior of the polymer in water. It is known that block copolymers form micelle structures in water (above the critical micelle concentration, CMC), if they consist of a hydrophilic and a hydrophobic block like surfactants. As cys-POx bears a hydrophilic backbone and hydrophobic side-chains (between the backbone and the cysteine function), therefore self-assembly is conceivable.

Two different polymers were tested regarding the self-assembly in water. The polymers contained 4% allyl- or cysteine-functionality in the structure, respectively and had a molecular weight of approximately 6000 – 6800 g·mol^{-1}. The polymers were dissolved in millipore water with concentrations between 5.0 and 0.1 mg·mL^{-1} and were measured directly in DLS and NTA, after stirring. Particle or micelle formation could be observed in DLS as well as in NTA, with concentrations ≥0.5 mg·mL^{-1} with an average diameter of ~150 nm (experimental section **Table 5–19**). This result indicates micelle formation occurs in aqueous environment due to the molecular structure of the polymer. The hydrophobic side-chains minimize their interaction with the water phase, consequently promoting micelle formation. The potential spontaneous oxidation of the cysteines' thiol groups, which would promote disulfide bridge crosslinks and a subsequent gel like structure, would also result in particle formation detectable by NTA and DLS.

For the synthesis of nanogels, a polymer was used bearing six cysteine residues per polymer chain. For PEG, it is known that renal clearance is possible if the molecular weight is <30.000 g·mol^{-1}.[4,202] POx possesses the same behavior like PEG,[65] hence, a polymer with approximately 6800 g·mol^{-1} was used for the preparation of nanogels.

The cysteine residue at the side-chain of the polymer allows for chemical crosslinking with the functional thiol group. After oxidation for example with H_2O_2, disulfide bridges are formed, providing a redox-sensitive network of polymer chains. The study shows not only the possibility of nanogel synthesis with cysteine-functionalized polymers, but also features the multiple-modal reactivity of the cysteines' thiol functionality.
The following **Figure 4–33** shows an overview of the synthesis of cys-POx nanogels via IME. The oil phase consisted of *n*-hexane in which Span 80 and Tween 80 (3:1) were dissolved. These surfactants stabilized the interface between oil and water whereby the water phase included the polymer. After ultrasonication, the IME is formed and the polymer is contained in the stabilized water drops. After crosslinking with H_2O_2, several washing steps and dialysis against millipore water were completed. The nanogels were collected as part of the aqueous dispersion.

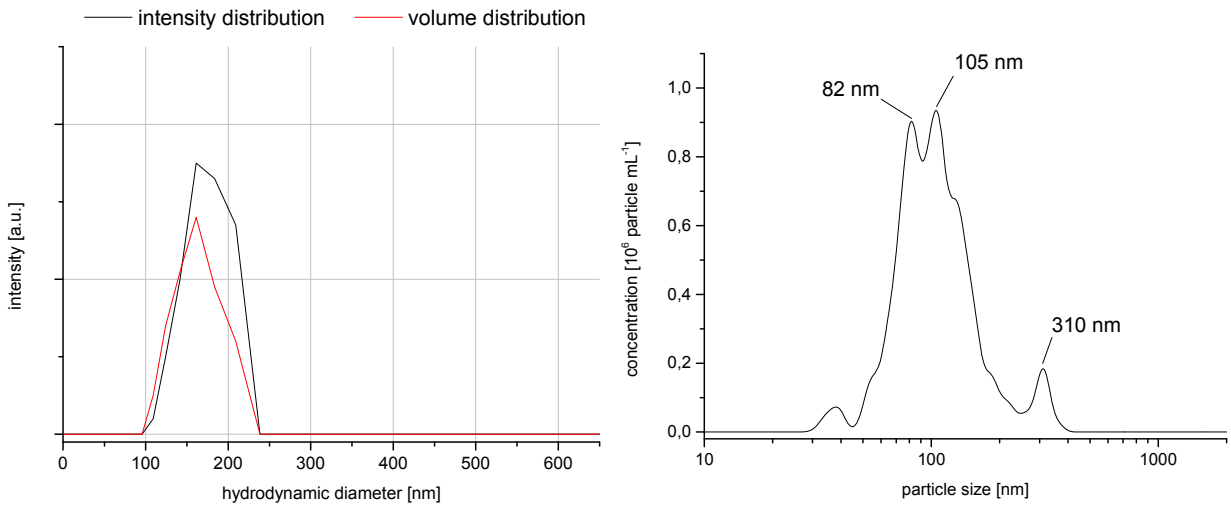

Figure 4–32: *DLS (left) and NTA (right) measurements of cysteine-functionalized POx nanoparticles at 100-fold dilution in millipore water.*

DLS and NTA measurements confirmed nanoparticle formation up to a dilution of 100-fold in water (**Figure 4–32**). The dilution is important to mention as self-assembly could be observed at concentrations of ≥0.5 $mg \cdot mL^{-1}$. 100-fold dilution in water means a concentration of $8 \cdot 10^{-3}$ $mg \cdot mL^{-1}$ particles in water. At higher dilution values ($8 \cdot 10^{-4}$ $mg \cdot mL^{-1}$), only NTA could observe nanoparticles.

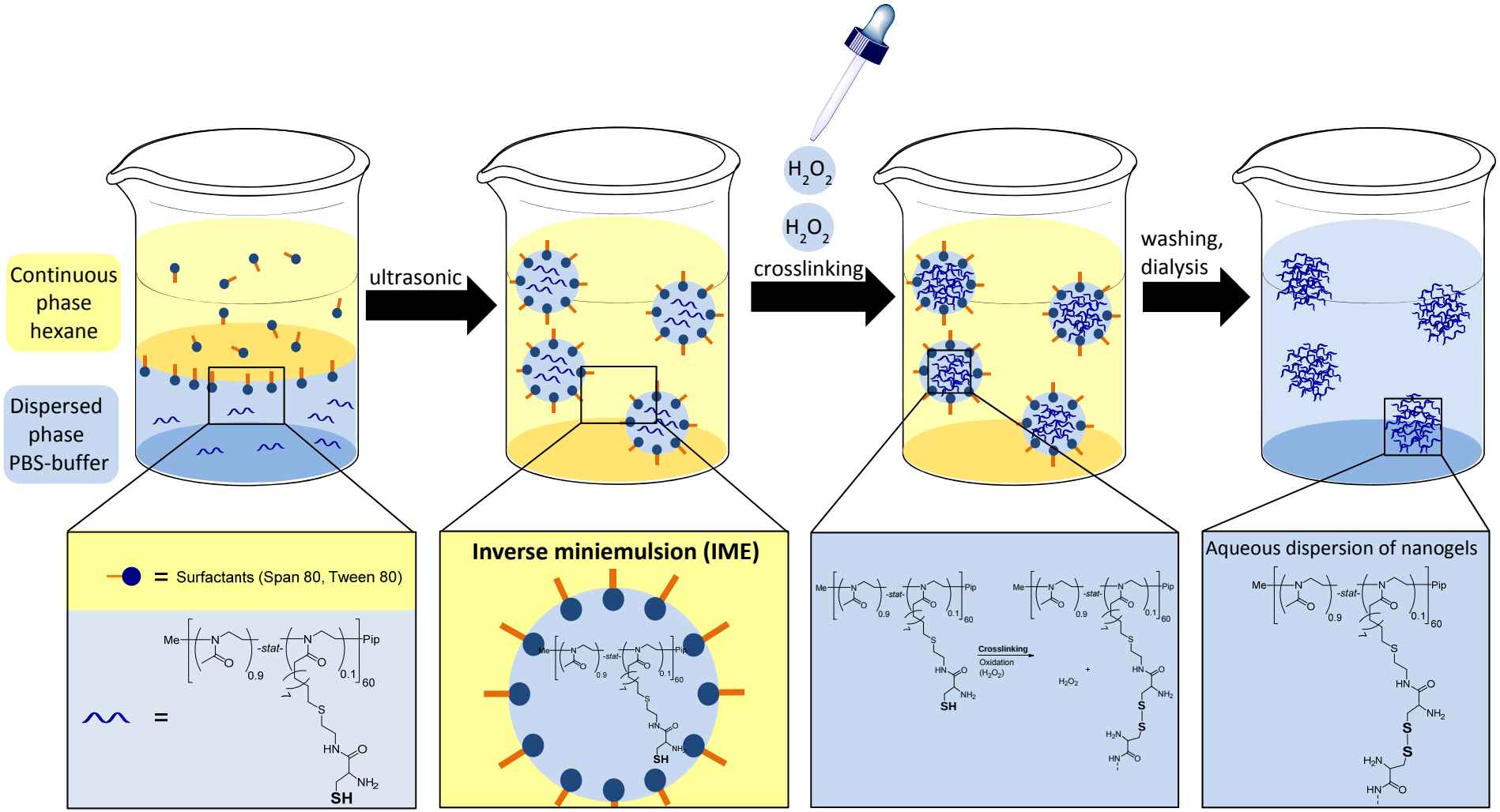

Figure 4–33: *Overview of the preparation of nanogels via inverse miniemulsion (IME).*

Nevertheless, the concentration of the particle solution is so low that micelle formation could be ruled out. The intensity- and volume-distribution of particles at 100-fold dilution are shown in **Figure 4–32** (left). The hydrodynamic diameter was determined to be 100 – 250 nm.

It is important to say that this value was the same regardless of the mode of the DLS used (intensity- or volume-distribution). This means that no “free polymer chains” are in the solution as this would lead to a signal at smaller diameters. The NTA results confirmed these results as shown also in **Figure 4–32** (right). Here, the particle size distribution was in the range of the value determined by DLS.

In addition, the particle solutions were analyzed by cryo-SEM (**Figure 4–34A**), performed by Vladimir Stepanenko, at the Institute for Organic Chemistry under the supervision of Prof. Frank Würthner of the University of Würzburg. The first thought was that only water crystals were visible though the particles are too far away from each other. Nonetheless, a high magnification would destroy water crystals as consequence of the high charging that occurs which could not be detected in the present work. Therefore, particles in the range of 130 – 210 nm could be observed, using different magnifications and images for the determination of the diameter. Furthermore, particles could be confirmed by AFM measurements, as shown in **Figure 4–34B**.

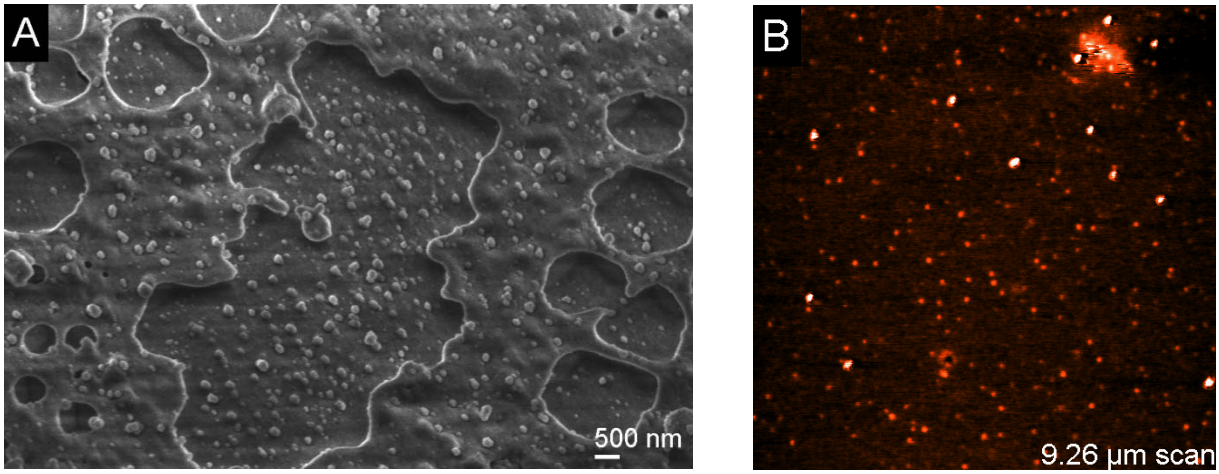

Figure 4–34: *Nanogels consisting of cysteine-functionalized POx. A: Cryo-SEM image of nanogels; B: AFM, 9.26 µm scan, topography image.*

Chapter 5

Experimental section

5.1 Chemicals

Reagents and solvents were, unless stated otherwise, commercially available as reagent grade and did not require further purification. All Fmoc-protected amino acids were purchased from IRIS BioTech or Novabiochem. Acetic acid (p.a., VWR), acetic acid anhydride (>98%, VWR), acetone (99.5%, Sigma-Aldrich), 1,1-carbonyldiimidazole (CDI, reagent grade, Sigma-Aldrich), 2-chloroethylamine hydrochloride (99%, Sigma-Aldrich), chloroform (>99%, VWR), cysteamine hydrochloride (AppliChem), Dawson Dbz NovaSyn TGR resin (Novabiochem), diethyl ether (Staub & Co, Nürnberg, Germany), 2,2-dimethoxy-2-phenyl acetophenone (DMPA, 99%, Sigma-Aldrich), N-(3-dimethylaminopropyl)-N'-ethylcarbodiimide hydrochloride (EDC, purum, ≥98 %, Sigma-Aldrich), N,N-diisopropylethylamine (Fisher Scientific), ethyl acetate (>99.5 %, Merck, Darmstadt, Germany), formic acid (≥98 %, Sigma-Aldrich), guanidine hydrochloride (Acros Organics), hydrochloride acid (HCl, 32%, Merck), hydroxybenzotriazole (IRIS Biotech GmbH), *N*-hydroxysuccinimide (NHS, 98%, Sigma-Aldrich), magnesium sulfate (p.a., Merck), 4-mercaptophenylacetic acid (Sigma-Aldrich), methanol (p.a., VWR), methyl *p*-toluenesulfonate (purum, ≥97.0%, Sigma-Aldrich), *p*-nitrophenylchloroformate (Sigma-Aldrich), 4-pentenoic acid (>98.0%, Sigma-Aldrich), piperidine (99.5%, Sigma-Aldrich), potassium hydroxide (Bernd Kraft), pyridine (≥99.8%, anhydrous, Sigma-Aldrich), sodium formate (>99.0%, Sigma-Aldrich), sodium chloride (≥99.8%, Sigma-Aldrich), sodium hydrogen phosphate (Sigma-Aldrich), sodium hydroxide (≥98%, Sigma-Aldrich), *N,N,N',N'*-tetramethyl-*O*-(1*H*-benzotriazol-1-yl)uronium hexafluorophosphate (IRIS Biotech GmbH), *N*,*N*,*N'*,*N'*-tetramethyl-*O*-(6-chloro-1*H*-benzotriazol-1-yl)uronium hexafluorophosphate (GL Biochem LTD), triethylamine (Et_3N, ≥99%, Sigma-Aldrich) trifluoroacetic acid (99%, ReagentPlus, Sigma-Aldrich), triisopropylsilane (Sigma-Aldrich) *tris*(2-carboxyethyl)phosphine (TCI) and 10-undecenoxyl chloride (97%, Sigma-Aldrich) were used as received. Acetonitrile (99.9%, Sigma-Aldrich) and 2-methyl-2-oxazoline (MeOx, Sigma-Aldrich) were dried over CaH_2 and distilled before use. Dichloromethane (DCM, ≥99.5%, VWR) was dried over $CaCl_2$ and filtered before use.

5.2 Synthesis of functional polymers

5.2.1 Synthesis of alkyne tosylate

A mixture of THF (20 mL) with sodium hydroxide (2.5 M, 20 mL) was prepared and cooled to 0°C. Propargyl alcohol (2.06 g, 36.8 mmol, 1.1 eq) together with benzyltrimethyl ammonium chloride (0.84 g, 3.7 mmol, 0.1 eq) was slowly added to the solution and stirred for ½ h. Tosyl chloride (6.37 g, 33.4 mmol, 1.0 eq) was solved in THF (20 mL) and was slowly added. After stirring for 1 h at 0°C the aqueous phase was removed, the organic phase was dissolved with ethyl acetate and washed with water and brine. After drying in vacuum the pure product could be isolated.

^{1}H-NMR spectrum is visible in **Figure 4–1**.

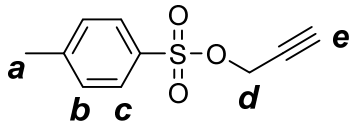

^{1}H NMR ($CDCl_3$, ppm): *δ*/ppm = 7.81 – 7.79 (br-d, 2H, H-***c***), 7.36 – 7.34 (br-d, 2H, H-***b***), 4.68 (br-d, 2H, H-***d***), 2.49 (tr, 1H, H-***e***), 2.44 (br-s, 3H, H-***a***).

5.2.2 Synthesis of azide tosylate

Azide tosylate was synthesized according to a synthesis of *Kim et al.*[186]

Sodium azide (1.79 g, 27.6 mmol, 2.0 eq) was dissolved in DMF and heated to 70°C. After stirring with 6-bromo-1-hexanol (2.50 g, 13.8 mmol, 1.0 eq) overnight at 70°C the solution was diluted with distilled water (50 mL), dried with $MgSO_4$ and was concentrated.

6-Azido-1-hexanol (2.68 g, 18.7 mmol, 1.0 eq) was solved in DCM (7 mL), followed by the addition of Et_3N (2.08 g, 20.6 mmol, 1.1 eq) and cooling to 0°C. Tosyl chloride (3.92 g, 20.6 mmol, 1.1 eq) was slowly added. The solution was stirred for 3h and allowed to warm up to room temperature. After washing with distilled water, the organic phase was dried with $MgSO_4$ filtered and concentrated. After column chromatography (petrol ether:ethyl acetate, 5:1) and solvent evaporation, the product could be isolated.

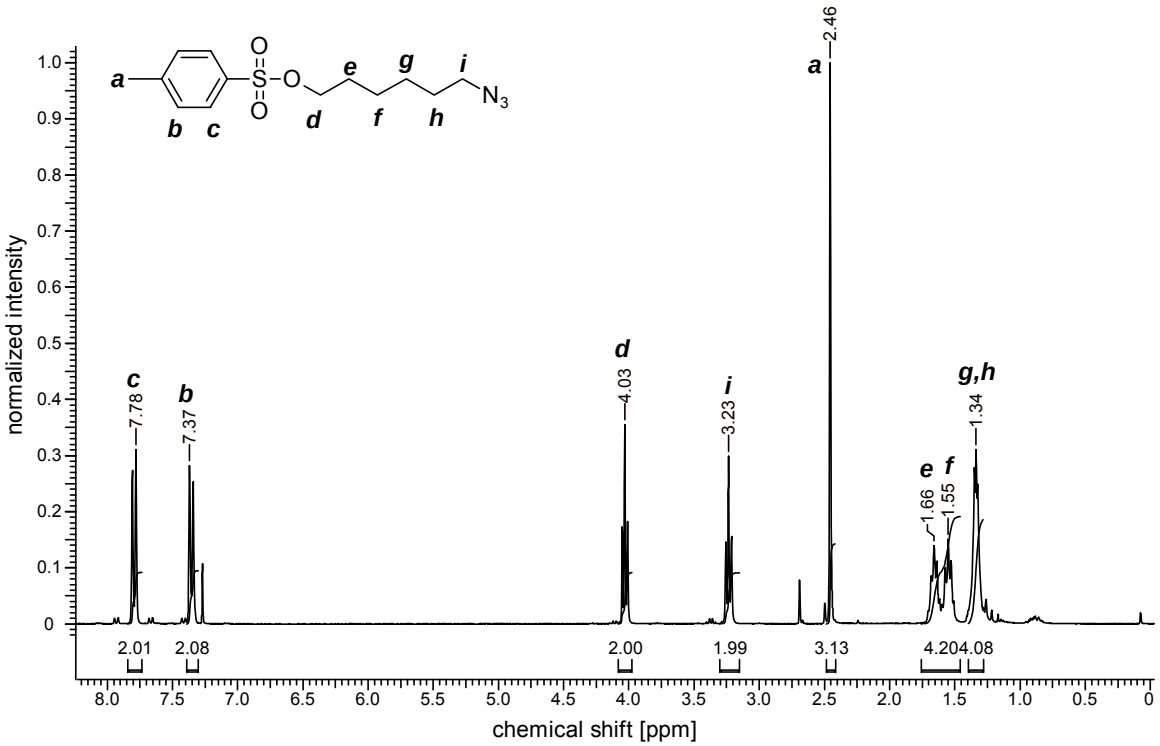

Figure 5–1: *^{1}H-NMR of 6-azidohexyl tosylate in $CDCl_3$ after purification.*

^{1}H-NMR ($CDCl_3$, ppm): *δ*/ppm = 7.81 – 7.79 (br-d, 2H, H-***c***), 7.36 – 7.34 (br-d, 2H, H-***b***), 4.68 (br-d, 2H, H-***d***), 2.49 (tr, 1H, H-***e***), 2.44 (br-s, 3H, H-***a***).

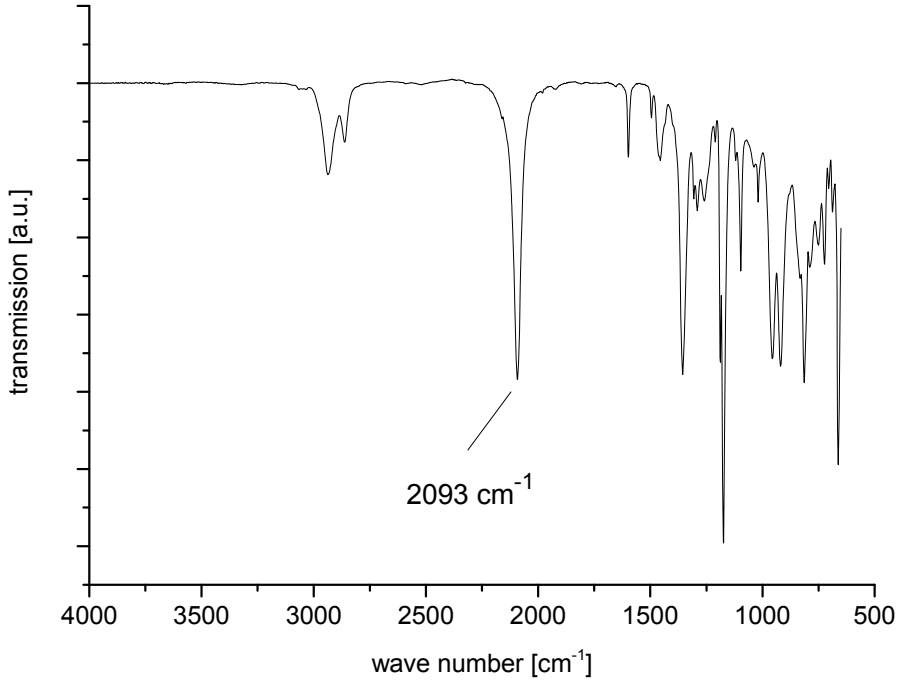

Figure 5–2: *FT-IR spectrum of azide-tosylate with the characteristic azide vibration at 2093 cm^{-1}.*

5.2.3 Polymerization of MeOx with propargyl tosylate

Alkyne *p*-toluenesulfonate (0.17 g, 0.3 mmol, 1.0 eq) was dried in vacuum before use. MeOx (2.41 g, 28.3 mmol, 35.0 eq) was weight in a flask in argon atmosphere. The monomer and the initiator were dissolved in dry acetonitrile and heated to 70°C in two separated flasks. After combining both solutions the polymerization was carried out overnight. Piperidine (0.20 g, 2.4 mmol, 3.0 eq) was added and at the next day the solution was precipitated three times into icecold diethyl ether (solvent: $CHCl_3$/MeOH, V/V, 1/1). Sometimes, the precipitate was received in water, after dialysis (MWCO: 1000 g·mol^{-1}) and lyophilization the white product could be isolated.

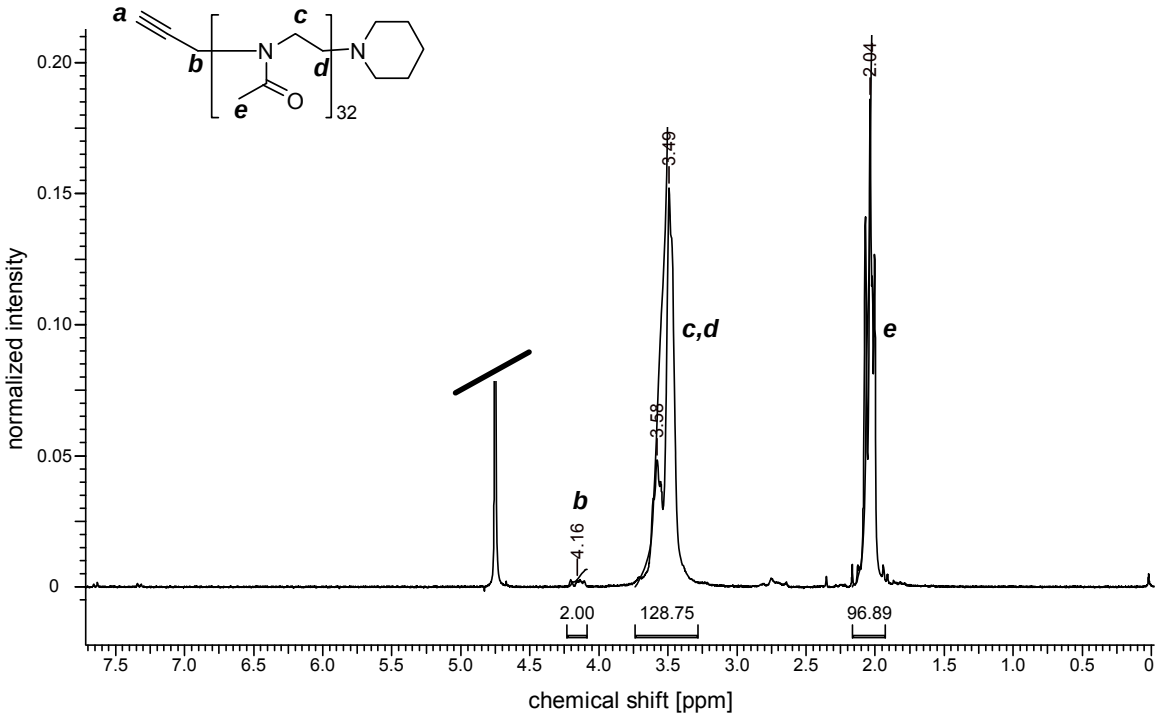

Figure 5–3: *^{1}H-NMR of alkyne functionalized POx in with DP = 32.*

^{1}H-NMR (D_2O, ppm): *δ*/ppm = 4.11 (2H, H-***b***), 3.58 – 3.49 (2H, H-***c***; 2H, H-***d***), 2.04 (3H, H-***e***).

Table 5–1: *SEC-measurements of alkyne functionalized P(MeOx) with propargyl tosylate as initiator.*

H_2O-SEC, 1 mL·min^{-1}, PEG-Standard, universal, MALVERN	
M_n	3400 g·mol^{-1}
M_w	3900 g·mol^{-1}
Đ	1.15
modality	monomodal

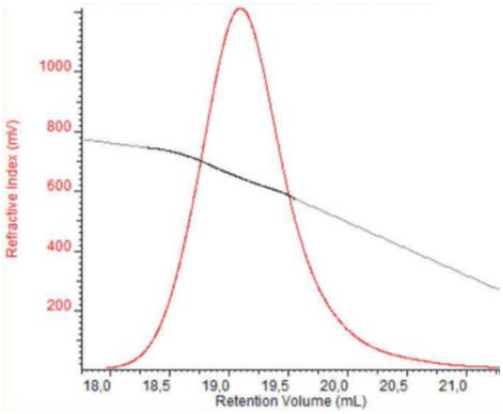

Figure 5–4: *SEC-elugram of alkyne functionalized P(MeOx) measured in water with propargyl tosylate as initiator.*

5.2.4 Synthesis of double-functionalized P(MeOx)

Alkyne *p*-toluenesulfonate (0.10 g, 0.5 mmol, 1.0 eq) was dried in vacuum before use. MeOx (2.11 g, 24.7 mmol, 50.0 eq) was weight in a flask in argon atmosphere. The monomer and the initiator were dissolved in dry acetonitrile and heated to 70°C in two separated flasks. After combining both solutions the polymerization was carried out overnight. Piperidin-4-carboxylic acid ethyl ester (0.23 g, 1.5 mmol, 3.0 eq) was added and at the next day the solution was precipitated into icecold diethyl ether. The precipitate was received in water, after dialysis (MWCO: 1000 g·mol^{-1}) and lyophilization the white product could be isolated.

^{1}H-NMR spectrum is visible in **Figure 4–4**.

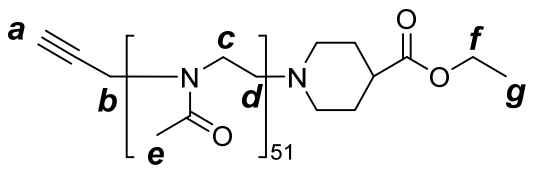

^{1}H NMR (CD_3CN, ppm): δ/ppm = 4.09 (2H, H-***b***), 3.44 – 3.39 (2H, H-***c***; 2H, H-***d***), 2.01 (3H, H-***e***).

Table 5–2: *SEC-measurements of alkyne functionalized P(MeOx) for amine attachment.*

H_2O-SEC, 1 mL·min^{-1}, PEG-Standard, universal, MALVERN	
M_n	3200 g·mol^{-1}
M_w	3800 g·mol^{-1}
Đ	1.18
modality	monomodal

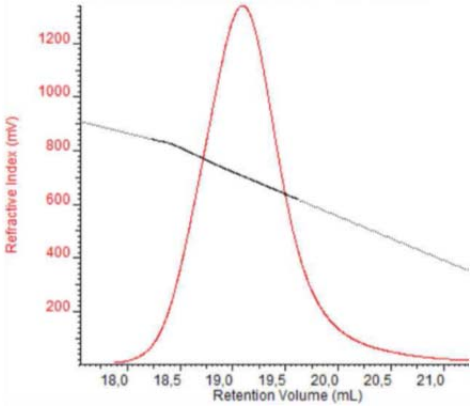

Figure 5–5: *SEC-elugram of alkyne functionalized P(MeOx) measured in water with propargyl tosylate as initiator.*

5.2.5 Polymerization of MeOx with propargyl benzenesulfonate

Propargyl benzenesulfonate (0.06 g, 0.3 mmol, 1.0 eq) was freshly destilled over CaH_2 before use. MeOx (1.35 g, 15.9 mmol, 50.0 eq) was weight in a flask in argon atmosphere. The monomer and the initiator were dissolved in dry acetonitrile and heated to 70°C in two separated flasks. After combining both solutions the polymerization was carried out overnight. Piperidine (0.08 g, 0.9 mmol, 3.0 eq) was added and at the next day the solution was cooled to room temperature and an amount of K_2CO_3 (0.15 g) was added. The solution was additionally stirred overnight. The polymer was precipitated three times into icecold diethyl ether (solvent: $CHCl_3$/MeOH, V/V, 1/1). After drying by lyophilization the white product could be isolated.

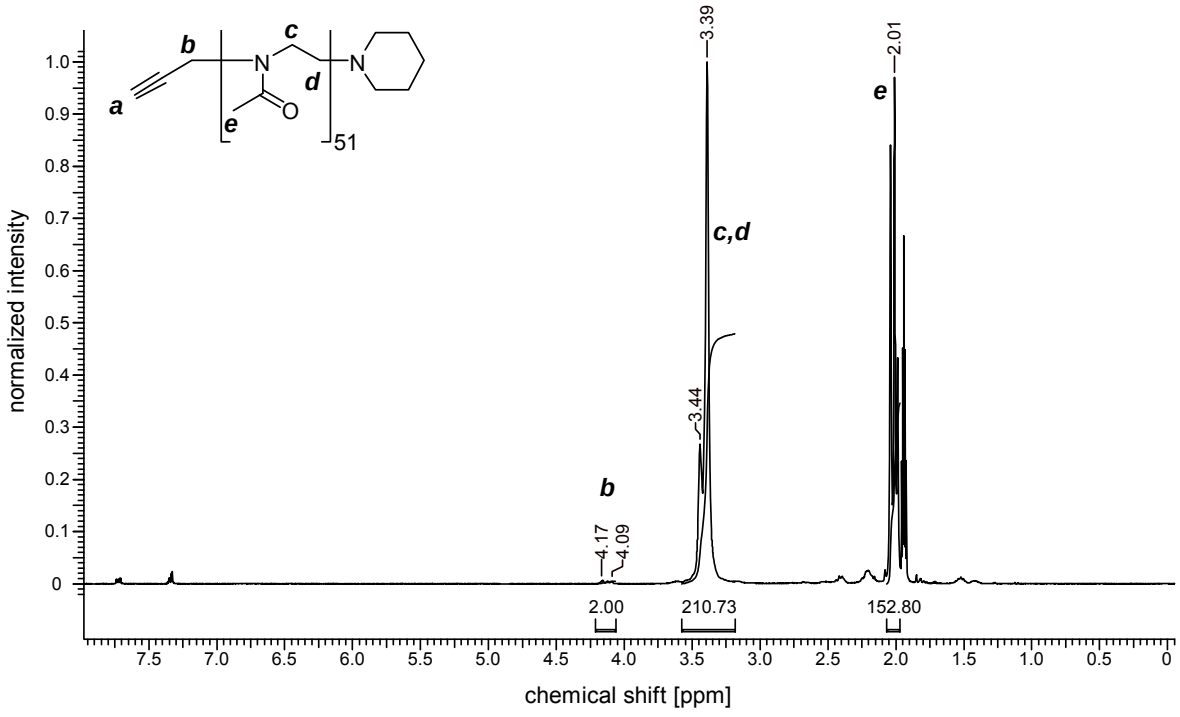

Figure 5–6: *^{1}H-NMR of alkyne functionalized POx with propargyl benzenesulfonate as inititor.*

^{1}H-NMR (CD_3CN, ppm): *δ*/ppm = 4.11 (2H, H-***b***), 3.44 – 3.39 (2H, H-***c***; 2H, H-***d***), 2.01 (3H, H-***e***).

Table 5–3: *SEC-measurements of alkyne functionalized P(MeOx) with propargyl benzenesulfonate as initiator.*

1 mL·min^{-1}, PEG-Standard, conventional	**H_2O-SEC [g·mol^{-1}]**	**DMF-SEC [g·mol^{-1}]**
M_n	2500	5400
M_w	3300	6100
Đ	1.32	1.14
modality	monomodal	monomodal

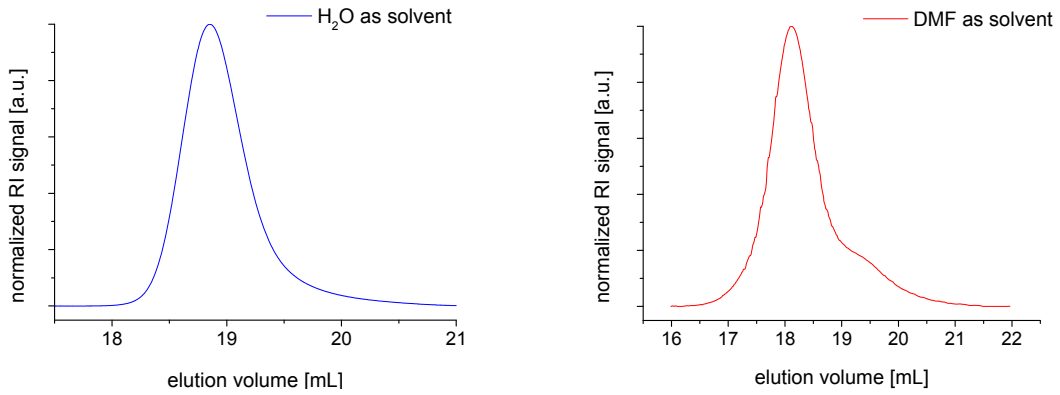

Figure 5–7: *SEC-elugrams of alkyne functionalized P(MeOx) with propargyl benzenesulfonate as initiator (left: measured in water; right: measured in DMF).*

MALDI ToF mass spectrum of alkyne functionalized P(MeOx) with propargyl benzenesulfonate is visible in **Figure 4–3**.

5.2.6 Synthesis of azide-functionalized P(MeOx) at the α-terminus (N_3-POx)

Azide tosylate (0.11 g, 0.4 mmol, 1.0 eq) was dried 5 h in vacuum before use. In a second, dry flask, MeOx (1.76 g, 20.7 mmol, 58.0 eq) was added in dry argon atmosphere. The monomer and the initiator were dissolved in dry acetonitrile (each 10 mL) and heated to 70°C in two separated flasks. After combining both solutions the polymerization was carried out for 3 d. The solution was cooled to room temperature, Piperidine (0.09 g, 1.1 mmol, 3.0 eq) was added and after 1 d the solution was precipitated into icecold diethyl ether two times (solvent: $CHCl_3$/MeOH, V/V, 1/1). The precipitate was received in water and after lyophilization the white product could be isolated. As the product was not clean (signal at δ = 3.01 ppm) the polymer was additionally precipitated for three times into icecold diethyl ether, but the impurity could not be removed.

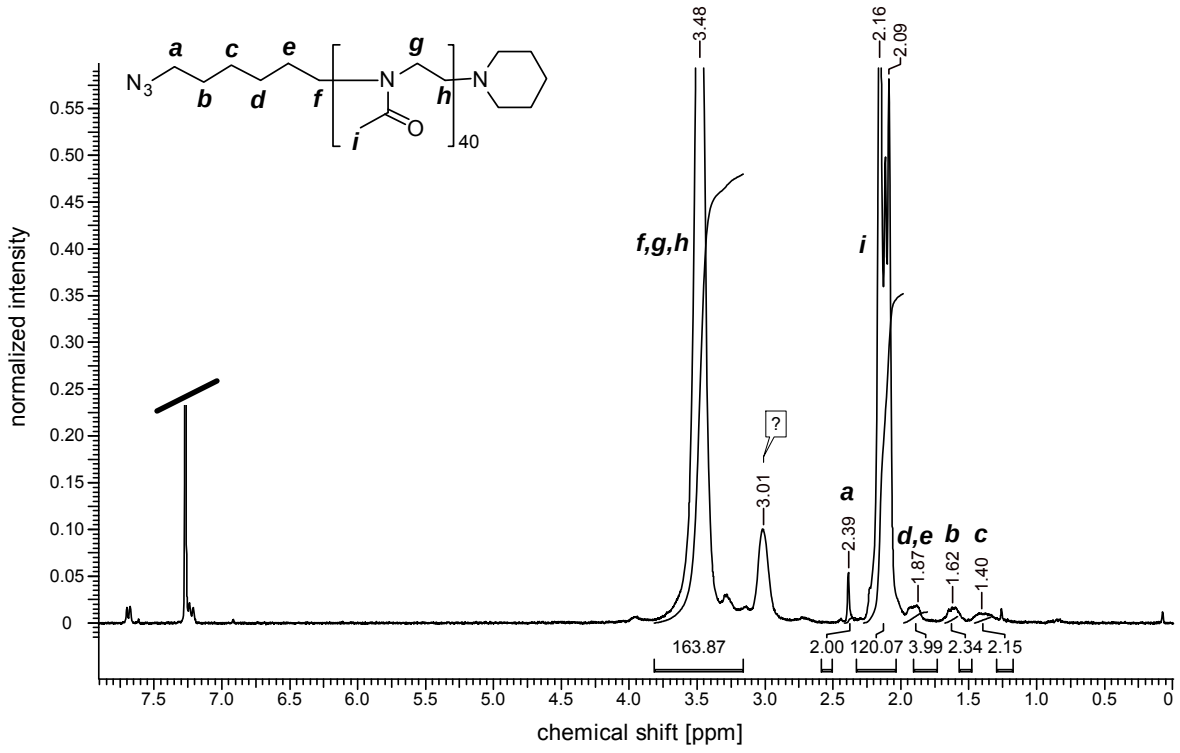

Figure 5–8: *^{1}H-NMR of azide functionalized P(MeOx) at the α-terminus measured in $CDCl_3$.*

^{1}H-NMR ($CDCl_3$, ppm): *δ*/ppm = 3.48 (2H, H-***f***; 2H, H-***g***; 2H, H-***h***), 2.39 (2H, H-***a***), 2.16 (3H, H-***i***), 1.87 (2H, H-***d,*** 2H, H-***e***), 1.62 (2H, H-***b)***, 1.40 (2H, H-***c***).

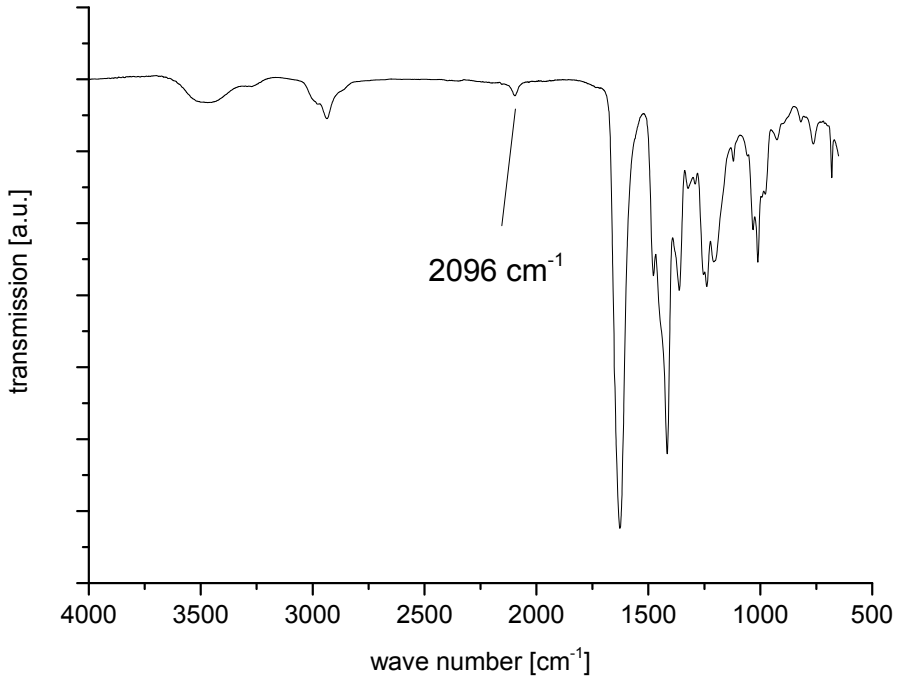

Figure 5–9: *FT-IR spectrum of azide functionalized P(MeOx) with the characteristic azide vibration at ~2100 cm^{-1}.*

5.2.7 Termination of P(MeOx) with sodium azide (P(MeOx)-N_3)

Methyl *p*-toluenesulfonate (0.11 g, 0.6 mmol, 1.0 eq) was dried 1 h in vacuum before use. MeOx (2.40 g, 28.2 mmol, 50.0 eq) was weight into a flask in argon atmosphere. The monomer and the initiator were dissolved in dry acetonitrile (each 10 mL) and heated to 70°C in two separated flasks. After combining both solutions the polymerization was carried out overnight. Sodium azide (0.16 g, 2.8 mmol, 5 eq) was added and stirred at 70°C for 3 d. The polymer was precipitated into icecold diethyl ether for three times (solvent: $CHCl_3$/MeOH, V/V, 1/1). The precipitate was received in water, after dialysis (MWCO: 1000 g·mol^{-1}) for one day and lyophilization, the white product could be isolated.

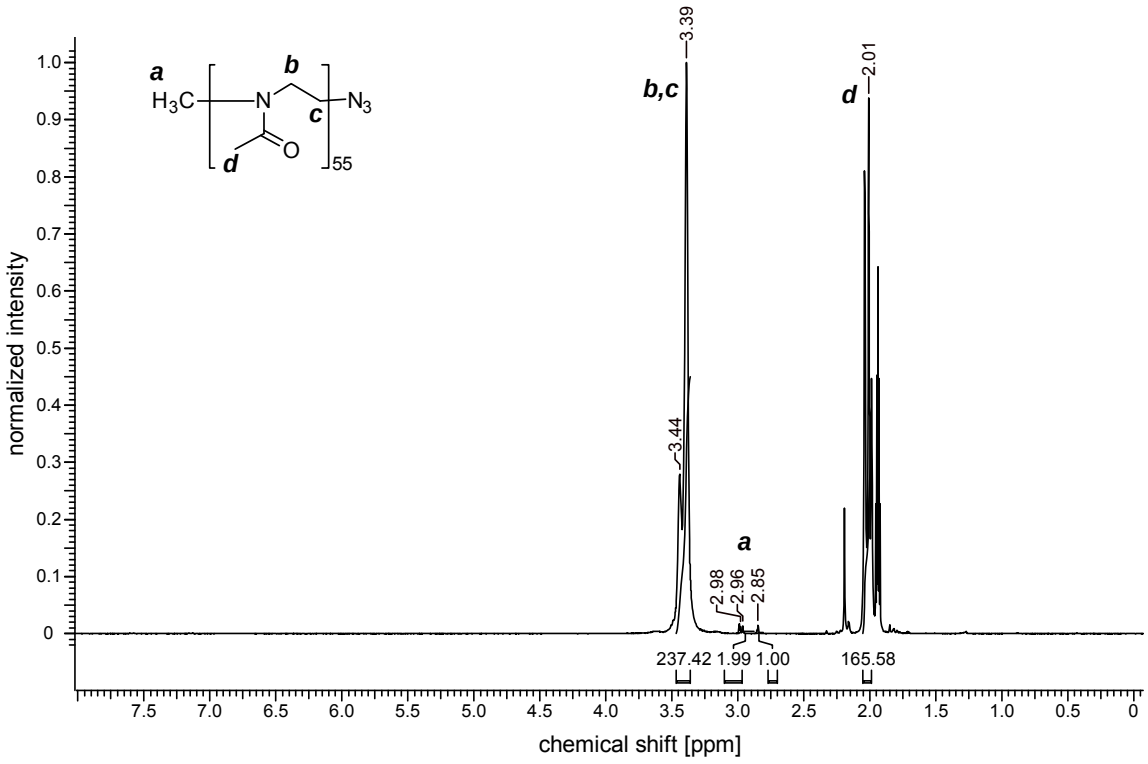

Figure 5–10: *Azide functionalized P(MeOx) by termination with NaN_3.*

^{1}H-NMR (CD_3CN, ppm): *δ*/ppm = 3.44 – 3.39 (2H, H-***b****;* 2H, H-***c***), 2.98 – 2.96 + 2.85 (3H, H-***a***), 2.01 (3H, H-***d***).

Table 5–4: *SEC-measurements of the resulting P(MeOx)-N_3.*

1 mL·min^{-1}, PEG-Standard, conventional	**H_2O-SEC [g·mol^{-1}]**	**DMF-SEC [g·mol^{-1}]**
M_n	3300	3300
M_w	4000	3700
Đ	1.21	1.12
modality	monomodal	monomodal

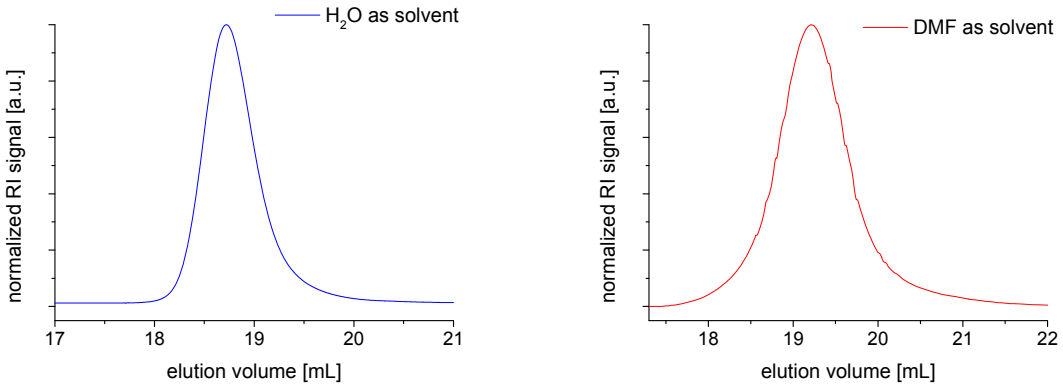

Figure 5–11: *SEC-elugrams of azide terminated P(MeOx) (left: measured in water; right: measured in DMF).*

The FT-IR spectrum of P(MeOx)-N_3 with the characteristic azide vibration at ~2100 cm^{-1} is visible in **Figure 4–5**.

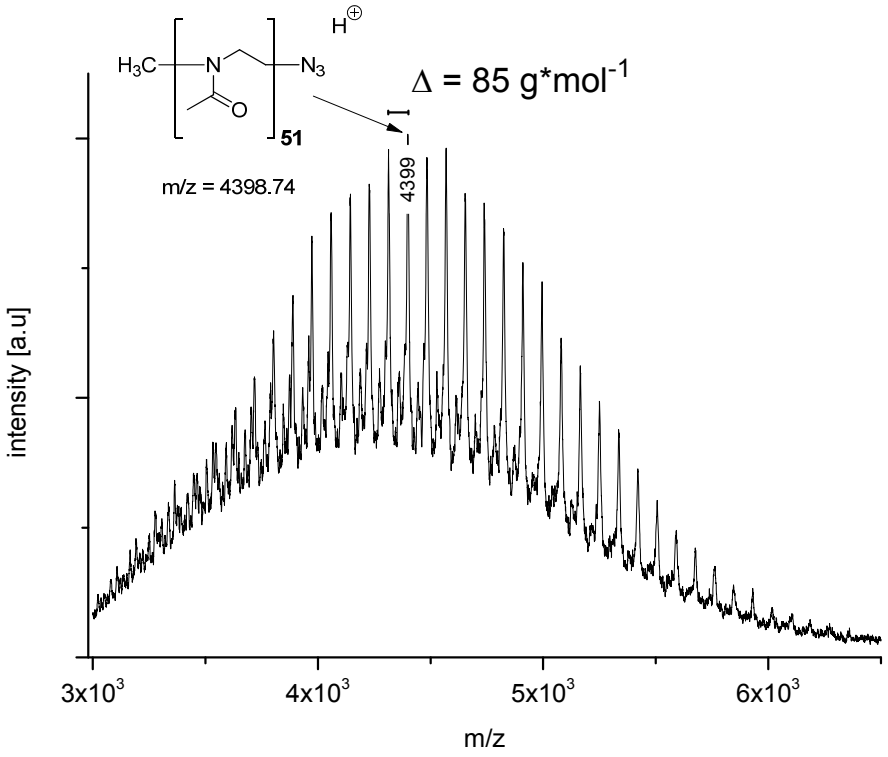

Figure 5–12: *MALDI ToF mass spectrum of azide functionalized P(MeOx) with narrow molecular weight distribution.*

5.2.8 Synthesis of 2,2-Dimethylthiazolidine-4-carboxylic acid

2,2-Dimethylthiazolidine-4-carboxylic acid was synthesized according to Woodward *et al*.[192]

Cysteine hydrochloride (14 g, 88.8 mmol) was dispersed in acetone (280 mL) and refluxed for 3 h at 75°C. After cooling to room temperature it was filtered and the solid mass was dried in vacuum.

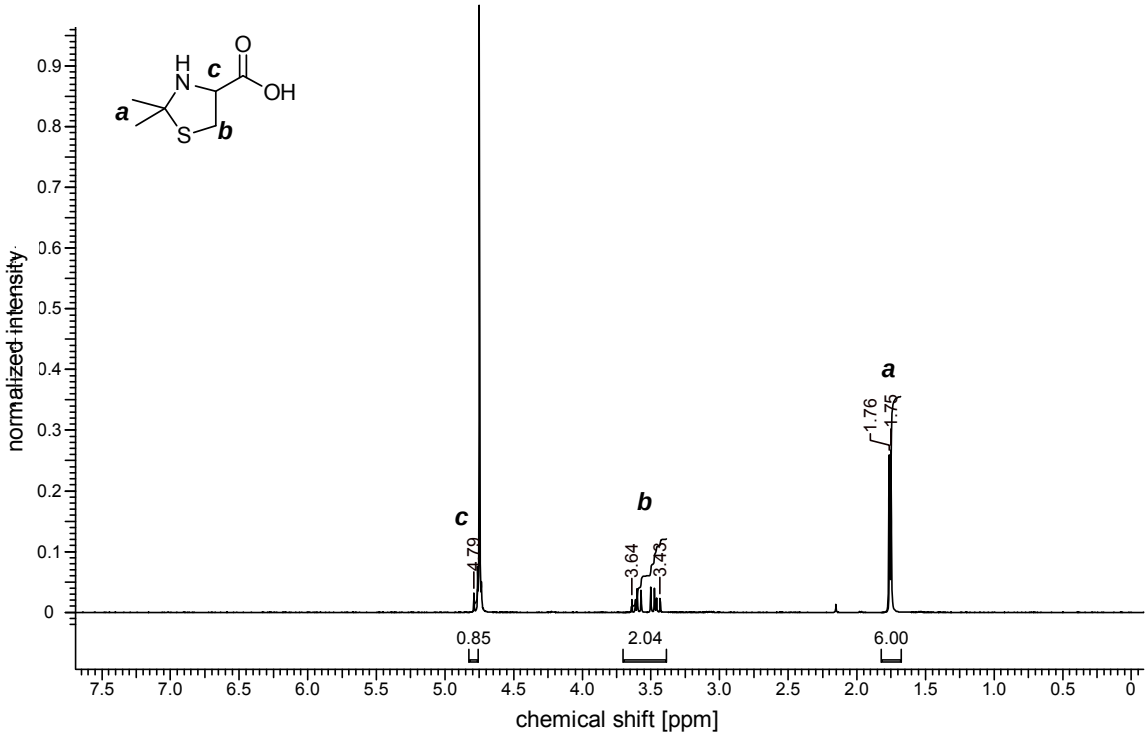

Figure 5–13: *^{1}H-NMR of 2,2-Dimethylthiazolidine-4-carboxylic acid.*

^{1}H-NMR (D_2O, ppm): *δ*/ppm = 4.79 (s, 1H, H-***c***), 3.64 – 3.43 (m, 2H, H-***b***), 1.76 – 1.75 (d, 6H, H-***a***).

5.2.9 Synthesis of 2,2-Dimethylthiazolidin-3-(N-formyl)-4-carboxylic acid

2,2-Dimethylthiazolidin-3-(N-formyl)-4-carboxylic acid (FTz4CA) was prepared according to Kuhlmann *et al*.[190]

Sodium formate (1.032 g, 15.2 mmol, 1.0 eq) was solved in formic acid (22.0 mL) and cooled to 0°C. 2,2-Dimethylthiazolidine-4-carboxylic acid (3.0 g, 15.2 mmol, 1.0 eq) was added and stirred until the solid was dissolved. After the addition of acetic anhydride (dropwise in 1 h, 7.747 g, 75.9 mmol, 5.0 eq) the solution was stirred overnight. Ice cold water (25 mL) was added the precipitated white solid was filtered and washed with ice cold water. The solid was dried in vacuum and was recrystallized from methanol/water to yield the clean product of FTz4CA.

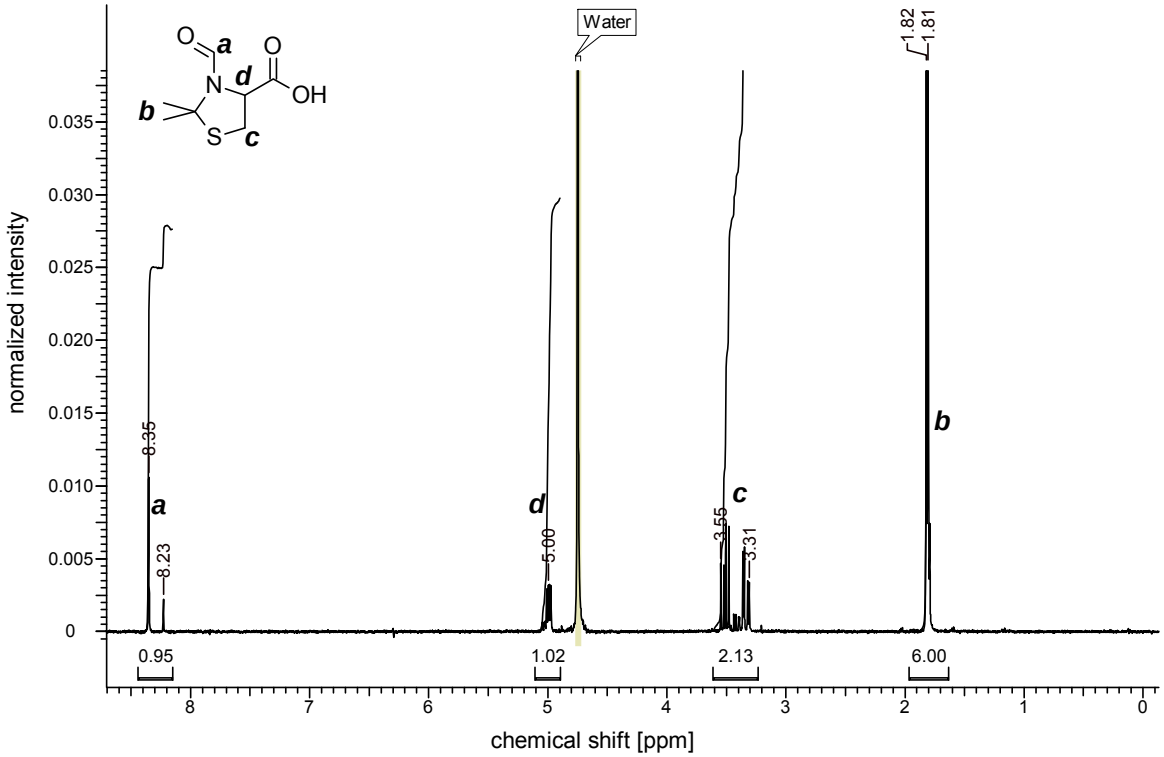

Figure 5–14: *2,2-Dimethylthiazolidin-3-(N-formyl)-4-carboxylic acid (FTz4CA).*

^{1}H-NMR (D_2O, ppm): *δ*/ppm = 8.31 – 8.19 (2s, 1H, H-***a***), 4.96 (dd/dq, 1H, H-***c***), 3.51 – 3.27 (m, 2H, H-***d***), 1.77 (s, 6H, H-***b***).

5.2.10 Synthesis of mercapto-thiazolidine

Mercapto-thiazolidine was prepared according to Kuhlmann *et al.*[190] using chloroform instead of DMF as solvent.

FTz4CA (1.336 g, 7.06 mmol, 1.0 eq) was dispersed in chloroform and argon was bubbled through the solution. After the addition of *N'N*-carbonyldiimidazol (CDI, 1.374 g, 8.47 mmol, 1.2 eq) in 20 min the turbid solution was stirred for 1 ½ h at room temperature under argon atmosphere (the solution get limpid). In a second flask, cysteamine hydrochloride (0.963 g, 8.47 mmol, 1.2 eq) was dissolved in pyridine (5 mL) under argon and was added to the solution of the activated FTz4CA. After 2 h, the solvents were removed by condensation and aqueous HCl (0.1M, ~100 mL) was added (till the pH is acidic). The aqueous phase was extracted with chloroform (3 x 40 mL), dried with $MgSO_4$ and filtered. The solvent was removed, the product was recrystallized from ethyl acetate and dried in high vacuum.

^{1}H-NMR spectrum is visible in **Figure 4–11**.

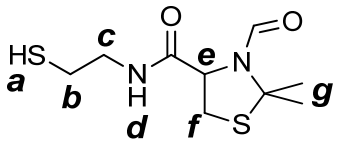

^{1}H-NMR ($CDCl_3$, ppm): *δ*/ppm = 8.38 (s, 1H, H-***h***) 7.07 (br-s, 1H, H-***d***), 4.97/4.70 (m, 1H, H-***e***), 3.65 – 3.14 (4H, H-***c***, H-***f***, H-***f'***), 2.62 (m, 2H, H-***b***), 1.82 – 1.78 (6H, H-***g***), 1.42 (1H, H-***a***).

5.2.11 Side-chain cysteine-functionalization of POx

5.2.11.1 Synthesis of 2-butenyl-2-oxazoline (ButenOx)

The synthesis of ButenOx was prepared according to *Gress et al*.[80]

A solution of N-(3-dimethylaminopropyl)-n'-ethylcarbodiimide·hydrochloride (EDC·HCl, 25.4 g, 132 mmol, 1.2 eq) with *n*-hydroxysuccinimide (20.332 g, 177 mmol, 1.6 eq) in DCM (500 mL) was produced. Pentenoic acid (11.055 g, 110 mmol, 1.0 eq) was added and stirred overnight. The solvent was evaporated and the product was dissolved in Et_2O/H_2O (V/V, 7/2, 225 mL/65 mL). The organic phase was washed with water (5x 20 mL). After drying with $MgSO_4$ and solvent removal the pure product could be isolated. *N*-succinimidyl-4-pentanate (16.130 g, 81.8 mmol, 1.0 eq) was dissolved in DCM and cooled to 0°C. In a second flask a solution of chloroethylamine·HCl (18.814 g, 164 mmol, 2.0 eq) in water (150 mL) was prepared and cooled to 0°C. After the addition of NaOH (6.544 g, 164 mmol, 2.0 eq) the mixture was slowly dropped into the DCM solution. It was stirred overnight at room temperature. The organic phase was washed with H_2O (5x 50 mL), dried over $MgSO_4$ and filtered. After evaporation of the solvent the product could be isolated. *N*-(2-chloroethyl)-4-pentenamide (10.208 g, 63.2 mmol, 1.0 eq) was dried for 1 h in vacuum ($1 \cdot 10^{-3}$ mbar) and dissolved in dry methanol (30 mL). A solution of KOH (3.544 g, 63.2 mmol, 1.0 eq) in dry methanol (30 mL) was prepared and was added dropwise into the *N*-(2-chloroethyl)-4-pentenamide solution. The turbid solution was refluxed overnight by 80°C. The solvent was evaporated and the crude product was cleaned by distillation (1 mbar, 65°C).

^{1}H-NMR spectrum is visible in **Figure 4–7**.

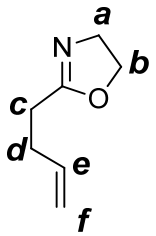

^{1}H-NMR (300 MHz, $CDCl_3$): *δ*/ppm = 5.82 (m, 1H, H-***e***), 5.00 (m, 2H, H-***f***), 4.20 (tr, 2H, H-***b***), 3.80 (tr, 2H, H-***a***), 2.35 (br-s, 4H, H-***c***, H-***d***).

5.2.11.2 Copolymerization of MeOx and ButenOx

The synthesis of the copolymer was prepared according to *Gress et al.*[80]

Methyl *p*-toluenesulfonate was dried 1 h in vacuum before use. MeOx and ButenOx were weight into a flask in argon atmosphere. Depending of the desired molecular composition of the copolymer the ratio of MeOx and ButenOx varied. The monomer mixture and the initiator were dissolved in dry acetonitrile and heated to 70°C in two separated flasks. After combining both solutions the polymerization was carried out overnight. Piperidine (3 eq in relation to the initiator) was added and at the next day the solution was precipitated into icecold diethyl ether (solvent: $CHCl_3$/MeOH, V/V, 1/1). The precipitate was received in water, after dialysis (MWCO: 1 kDa or 3.5 kDa) and lyophilization, the white product could be isolated.

As an example a NMR-spectrum is shown with about two double bonds per polymer chain and 42 repetition units of MeOx.

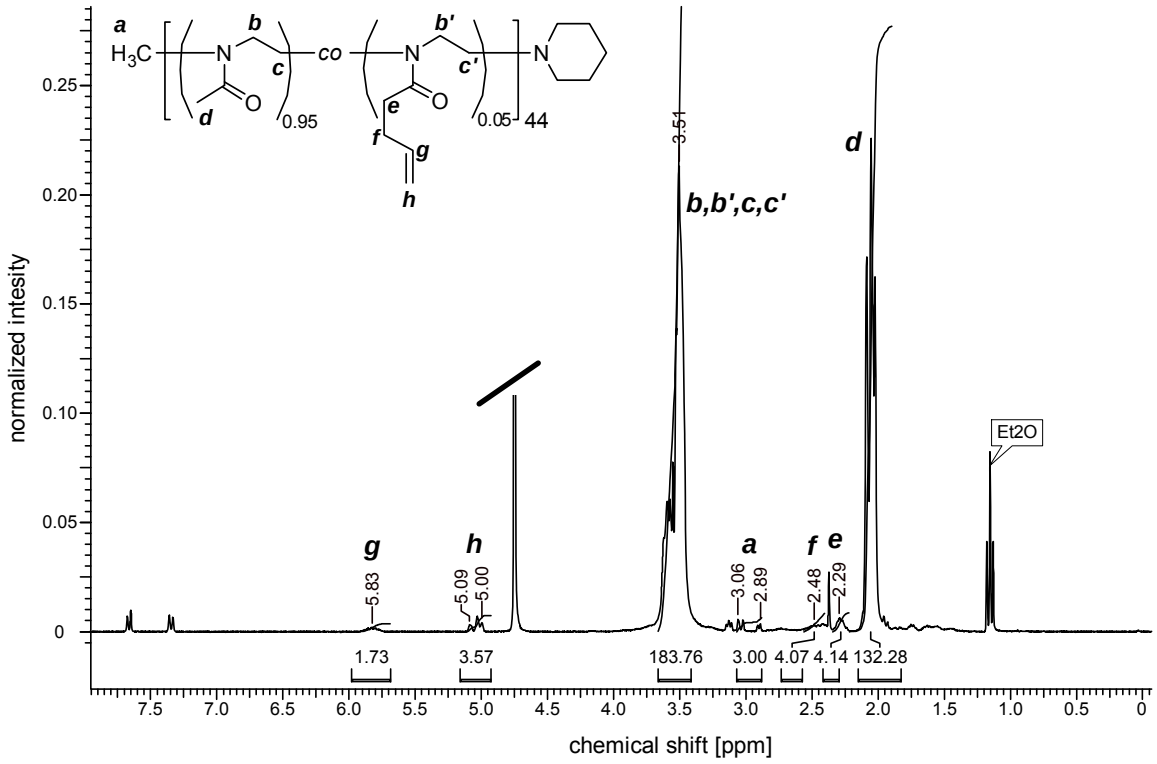

Figure 5–15: *the copolymer consisting of repeated MeOx and ButenOx monomer units.*

^{1}H-NMR (300 MHz, $CDCl_3$): δ/ppm = 5.84 (1H, H-***g***), 5.03 (2H, H-***h***), 3.46 (2H, H-***b***; 2H, H-***c***; 2H, H-***b'***; 2H, H-***c'***), 3.04 – 2.95 (3H, H-***a***), 2.47 (2H, H-***e***), 2.37 (2H, H-***f***), 2.14 (3H, H-***d***).

Table 5–5: *SEC-measurements of P[(MeOx)$_x$-co-(ButenOx)$_{1-x}$]$_n$.*

DMF-SEC, 1 mL·min^{-1}, PEG-Standard					
Polymer No.	**feed MeOx/ButenOx**	**copolymer MeOx/ButenOx**	**$M_{n(NMR)}$ [g·mol^{-1}]**	**$M_{n(SEC)}$ [g·mol^{-1}]**	***Đ***
I	45/2	60/2	3550	3800	1.06
II	45/2	42/2	3750	3350	1.15
III	45/5	50/5	4900	3250	1.26
IV	110/5	120/5	10850	7750	1.05

As examples the elugrams of sample no. **II** and **IV** are shown:

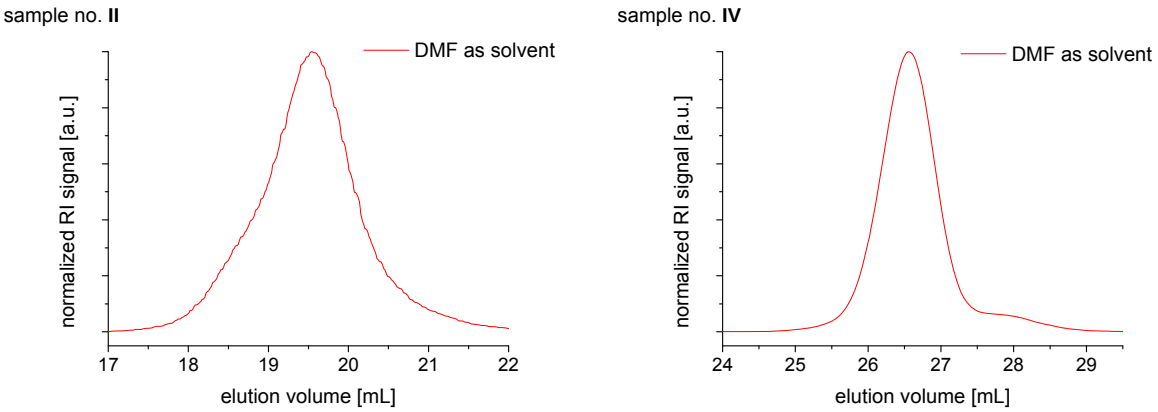

Figure 5–16: *SEC-elugrams of P[(MeOx)$_x$-co-(ButenOx)$_{1-x}$]$_n$ measured in DMF.*

5.2.11.3 Polymer-analogue thiol–ene reaction with mercapto-thiazolidine and P[(MeOx)$_x$-co-(ButenOx)$_{1-x}$]$_n$

For the polymer functionalization the use of 3 eq mercapto-thiazolidine related to every allyl-group was necessary. The polymer was solved in methanol and argon was guided through the solution for 15 min. After the addition of mercapto-thiazolidine, DMPA (0.5 eq) was added as UV reactive radical starter. After 30 min of exposure with UV-light the reaction was complete. Precipitation into cold diethyl ether three times (solvent: $CHCl_3$/MeOH, V/V, 1/1) and drying in vacuum revealed the product in good quality.

As an example, a NMR-spectrum is shown with about two mercapto-thiazolidines per polymer chain and 48 repetition units of MeOx.

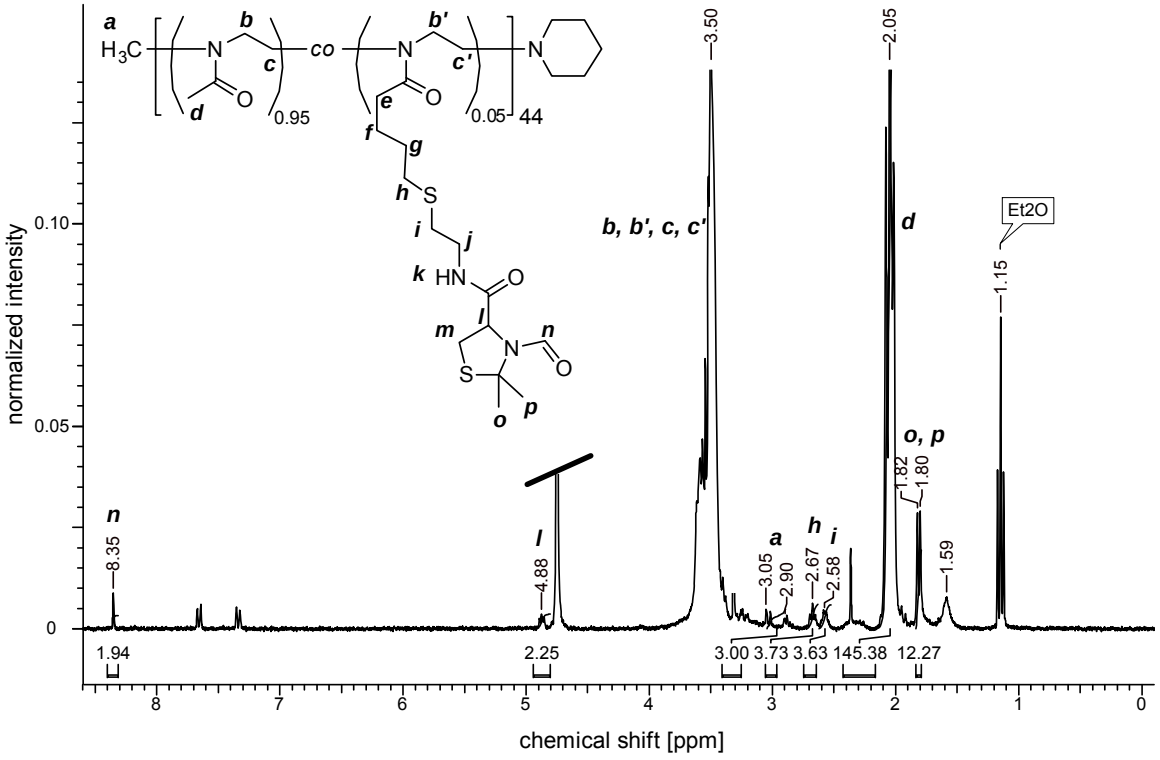

Figure 5–17: *P[(MeOx)$_{0.95}$-co-(ButenOx)$_{0.05}$]$_{44}$ after the functionalization with mecapto-thiazolidine via thiol-ene chemistry.*

^{1}H-NMR (300 MHz, D_2O): δ/ppm = 8.35 (1H, H-***n***), 4.88 (1H, H-***l***), 3.69 – 3.14 (2H, H-***b***; 2H, H-***c***; 2H, H-***b'***; 2H, H-***c'***; 2H, H-***f***; 2H, H-***j***), 3.05 – 2.90 (3H, H-***a***), 2.67 (2H, H-***h***), 2.58 (2H, H-***i***), 2.05 (3H, H-), 1.82 – 1.80 (2xCH_3, H-**o**, H-***p***), 1.59 (2H, H-***e***).

Table 5–6: *SEC-measurements of $P[(MeOx)_x\text{-}co\text{-}(ButenOx)_{1-x}]_n$ after the thiol–ene click reaction with mercapto-thiazolidine.*

DMF-SEC, 1 mL·min^{-1}, PEG-Standard					
Functionalized Polymer No.	**Copolymer MeOx/ButenOx**	**$M_{n(NMR)}$ [g·mol^{-1}]**	**$M_{n(SEC)}$ [g·mol^{-1}]**	**$M_{w(SEC)}$ [g·mol^{-1}]**	***Đ***
I (functionalization of polymer no. III, Table 5–5)	50/5	6100	3650	4650	1.28
II (functionalization of polymer no. III, Table 5–5)	50/5	6100	3900	4900	1.27

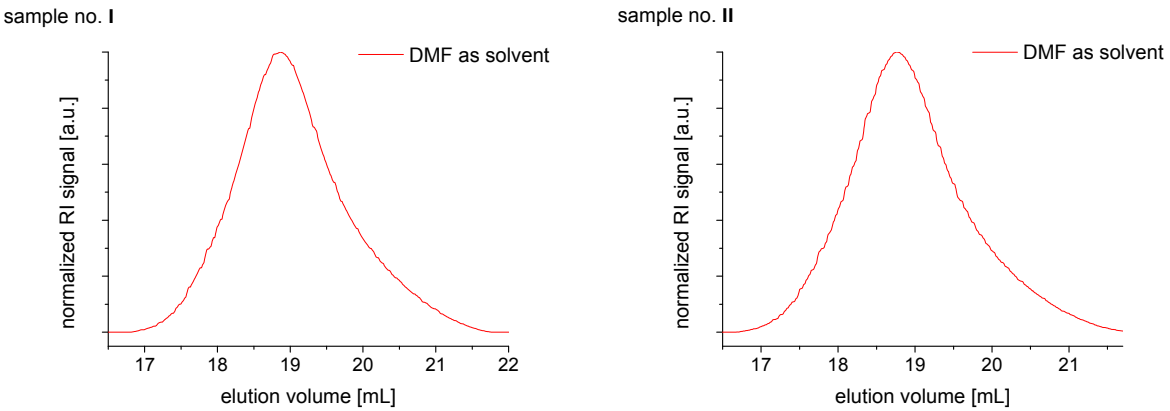

Figure 5–18: *SEC-elugrams of thiazolidine functionalized $P[(MeOx)_x\text{-}co\text{-}(ButenOx)_{1-x}]_n$ measured in DMF.*

5.2.11.4 Hydrolysis of thiazolidine side-chains

The deprotection of the thiazolidine ring took place in 0.1 M HCl at 70°C for 5 d. After dialysis against diluted acetic acid (0.01 M) and lyophilisation the functionalized polymer was complete.

As an example a NMR-spectrum is shown with about two cysteine residues per polymer chain and 40 repetition units of MeOx.

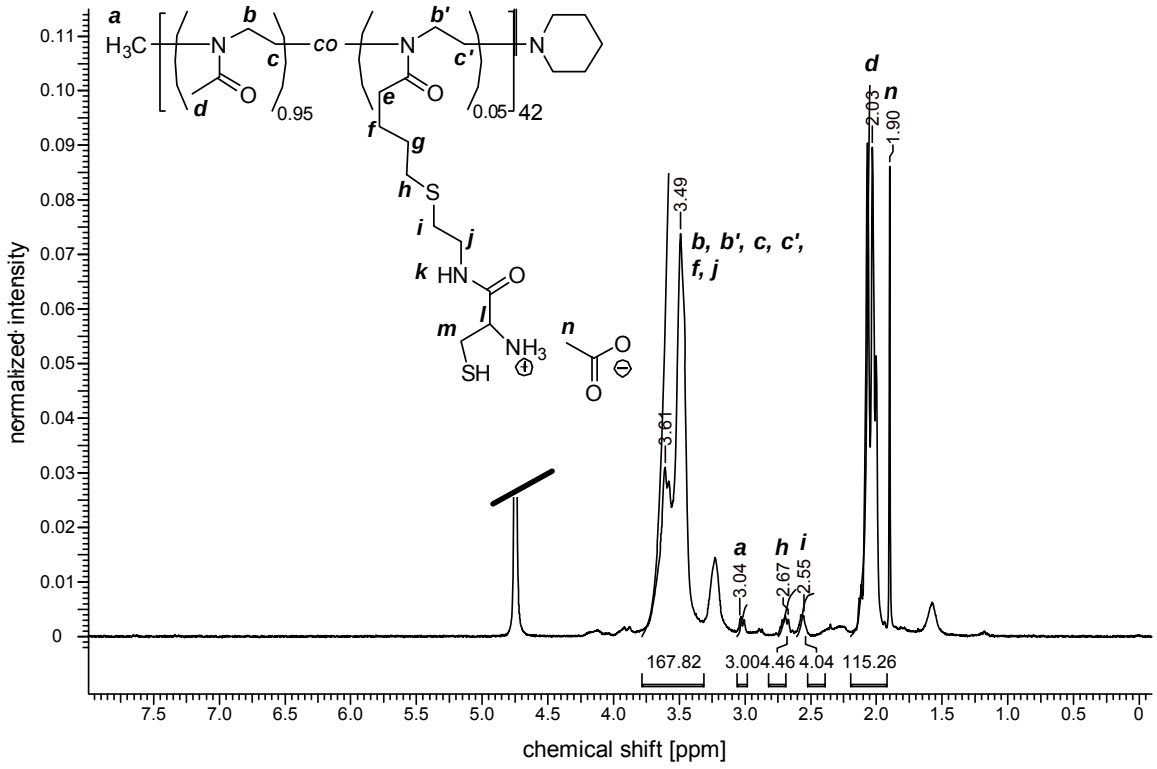

Figure 5–19: *P[(MeOx)$_{0.95}$-co-(ButenOx)$_{0.05}$]$_{42}$.*

^{1}H-NMR (300 MHz, D_2O): δ/ppm = 3.92 – 3.14 (2H, H-***b***; 2H, H-***c***; 2H, H-***b'***; 2H, H-***c'***; 2H, H-***f***; 2H, H-***j***), 3.03 – 2.87 (3H, H-***a***), 2.67 (2H, H-***h***), 2.55 (2H, H-***i***), 2.07 (3H, H-***d***), 1.89 (3H, acetate, H-***n***) 1.58 (2H, H-***e***).

5.2.11.5 Synthesis of 2-decenyl-2-oxazoline (DecenOx)

The synthesis of the DecenOx was prepared according to Kempe *et al.*[162]
2-chloroethylammonium chloride (7.49 g, 65.1 mmol, 1.0 eq) was dissolved in dry DCM and was added to 10-undecenoyl chloride (13.20 g, 65.1 mmol, 1.0 eq) under argon atmosphere. The solution was stirred for 1 ½ h. After cooling to 0°C, Et_3N (15.15 g, 150 mmol, 2.3 eq) was added dropwise. The solution was stirred for 30 min at 0°C and afterwards stirred at room temperature overnight. Water (100 mL) was added and extracted with DCM (3 x 35 mL). After washing of the organic phase with water and brine the solution was dried with $MgSO_4$. The solvent was removed and the product was dried in vacuum ($1 \cdot 10^{-3}$ mbar).
For ring closure *N*-(2-chloroethyl)-undec-10-enamide) (11.79 g, 48 mmol, 1.0 eq) was dissolved in dry methanol (25 mL). Methanolic KOH (2.69 g, 48 mmol, 1.0 eq KOH in 10 mL methanol) was added and stirred the solution for 48 h by 80°C. The suspension was filtered into a separating funnel and diluted with distilled water (80 mL). After extraction with Et_2O (3 x 50 mL) the organic phase was washed with water and brine and was dried with $MgSO_4$. The solvent was removed and after distillation ($1 \cdot 10^{-3}$ mbar, up to 130°C) the product could be isolated as colorless liquid.

^{1}H-NMR spectrum is visible in **Figure 4–8**.

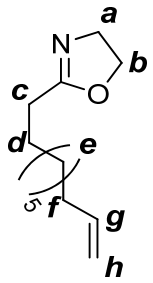

^{1}H-NMR (300 MHz, $CDCl_3$): *δ*/ppm = 5.78 (m, 1H, H-***g***), 4.98 – 4.88 (m, 2H, H-***h***), 4.20 (tr, 2H, H-***b***), 3.80 (tr, 2H, H-***a***), 2.25 (br-tr, 2H, H-***f***), 2.00 (br-quar, 2H, H-***d***), 1.61 (m, 2H, H-***c***), 1.28 (br, 10H, (br, 5x 2H, H-***e***).

5.2.11.6 Synthesis of P[(MeOx)$_x$-*co*-(DecenOx)$_{1-x}$]$_n$

The synthesis of the copolymer was prepared according to *Dargaville et al.*[83]

To a hot solution of methyl *p*-toluenesulfonate in dry acetonitrile (70°C) was added a mixture of MeOx and DecenOx under dry argon atmosphere. Depending of the desired molecular composition of the copolymer the ratio of MeOx and DecenOx varied. The mixture was stirred for 48 h at 70°C under argon atmosphere. For endcapping of the polymer piperidine (3 eq) was added and was additionally stirred overnight. The reaction mixture was precipitated into cold diethylether (solvent: $CHCl_3$/MeOH, V/V, 1/1), was dissolved in water, and was submitted to dialysis against water (MWCO: 1 kDa or 3.5 kDa).

As an example a NMR-spectrum is shown with about five double bonds per polymer chain and 45 repetition units of MeOx.

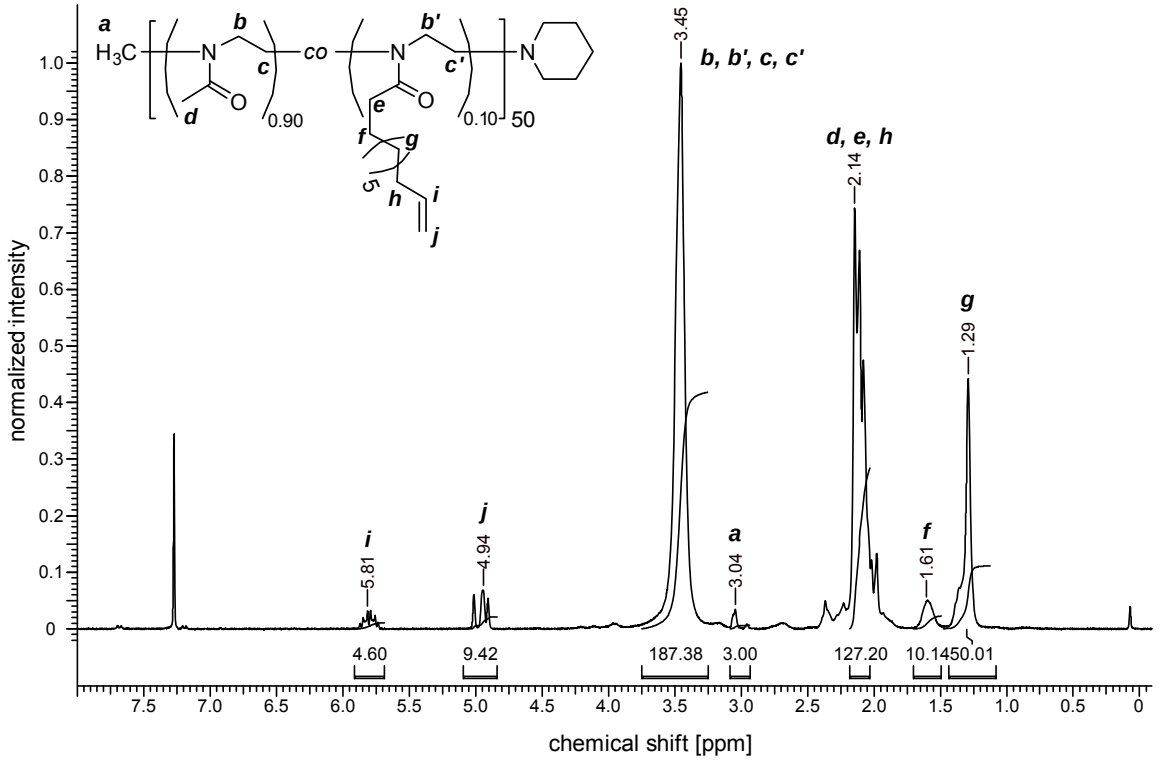

Figure 5–20: *the copolymer consisting of repeating MeOx and DecenOx monomer units.*

^{1}H-NMR (300 MHz, $CDCl_3$): δ/ppm = 5.81 (1H, H-***i***), 4.94 (2H, H-***j***), 3.45 (2H, H-***b***; 2H, H-***c***; 2H, H-***b'***; 2H, H-***c'***), 3.04 – 2.95 (3H, H-***a***), 2.37 – 1.98 (3H, H-***d***; 2H, H-***e***; 2H, H-***h***), 1.61 (2H, H-***f***), 1.29 (5x CH_2, H-***g***).

Table 5–7: *SEC-measurements of P[(MeOx)$_x$-co-(DecenOx)$_{1-x}$]$_n$.*

DMF-SEC, 1 mL·min^{-1}, PEG-Standard					
Polymer No.	**feed MeOx/DecenOx**	**copolymer MeOx/DecenOx**	**$M_{n(NMR)}$ [g·mol^{-1}]**	**$M_{n(SEC)}$ [g·mol^{-1}]**	***Đ***
I	45/2	64/2	5950	4000	1.04
II	45/2	52/2	4750	3450	1.10
III	45/5	42/5	4600	3350	1.12
IV	45/5	40/3	4000	5000	1.17 (bimodal)
V	45/5	50/5	5300	4800	1.20
VI	110/5	110/5	10400	8300	1.21

As examples, the elugrams of sample no. **II** and **VI** are shown:

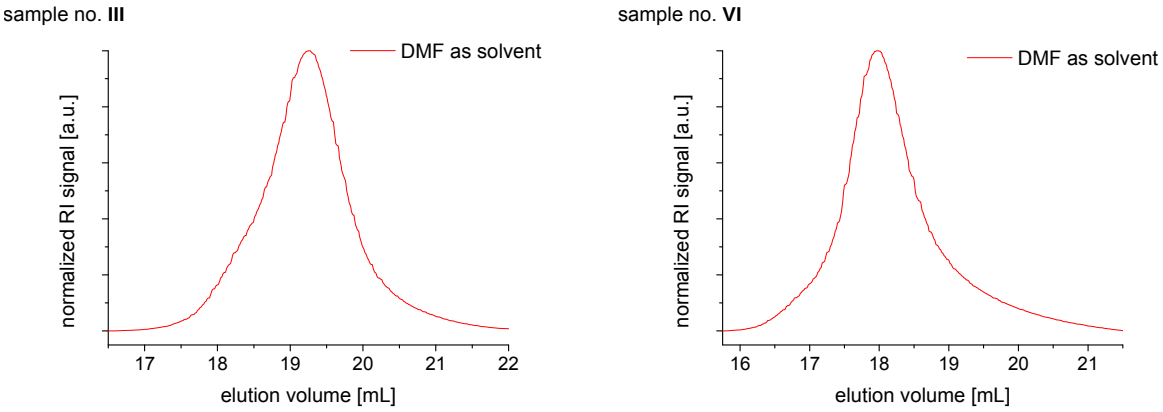

Figure 5–21: *SEC-elugrams of P[(MeOx)$_x$-co-(DecenOx)$_{1-x}$]$_n$ measured in DMF.*

5.2.11.7 Polymer-analogue thiol–ene reaction with mercapto-thiazolidine and P[(MeOx)$_x$-co-(DecenOx)$_{1-x}$]$_n$

For the polymer functionalization with thiazolidine the use of 3 eq thiols related to every allyl is necessary. The polymer was dissolved in methanol and argon was guided through the solution for 15 min. After the addition of mercapto-thiazolidine, DMPA (0.5 eq) was added as UV reactive radical starter. After 30 min of exposure with UV-light the reaction was complete. Precipitation into cold diethyl ether three times (solvent: $CHCl_3$/MeOH, V/V, 1/1) and drying in vacuum revealed the product in good quality.

^{1}H-NMR spectrum is visible in **Figure 4–12**.

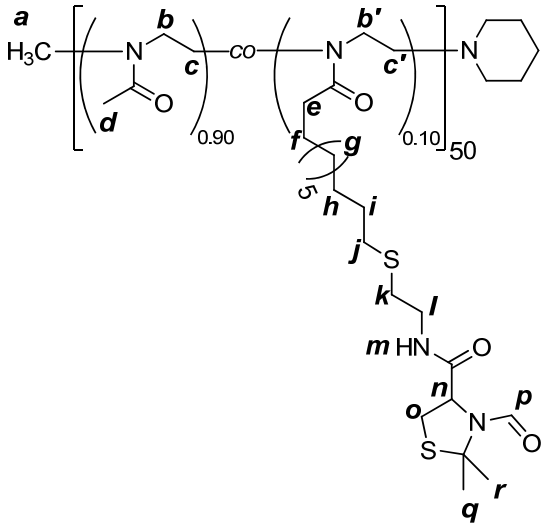

^{1}H-NMR (300 MHz, $CDCl_3$): *δ*/ppm = 8.39 (1H, H-***p***), 7.01 (1H, H-***m***), 4.98 – 4.70 (1H, H-***n***), 3.69 – 3.14 (2H, H-***b***; 2H, H-***c***; 2H, H-***b'***; 2H, H-***c'***; 2H, H-***k***; 2H, H-***o***), 3.03 – 2.94 (3H, H-***a***), 2.62 (2H, H-***j***), 2.49 (2H, H-***k***), 2.13 (3H, H-***d***), 1.83 – 1.79 (2x CH_3, H-***q***, H-***r***), 1.54 (2H, H-***e***), 1.25 (2H, H-***g***).

Table 5–8: *SEC-measurements of P[(MeOx)$_x$-co-(DecenOx)$_{1-x}$]$_n$ after the functionalization with mercapt-thiazolidine.*

DMF-SEC, 1 mL·min^{-1}, PEG-Standard					
Functionalized Polymer No.	**Copolymer MeOx/DecenOx**	**$M_{n(NMR)}$ [g·mol^{-1}]**	**$M_{n(SEC)}$ [g·mol^{-1}]**	**$M_{w(SEC)}$ [g·mol^{-1}]**	***Đ***
I (functionalization of polymer no. III, Table 5–7)	42/5	5800	4050	4800	1.19
II (functionalization of polymer no. V, Table 5–7)	50/5	6500	5900	7400	1.24
III (functionalization of polymer no. VI, Table 5–7)	110/5	11500	10000	11900	1.19

As examples the elugrams of sample no. **I** and **III** are shown:

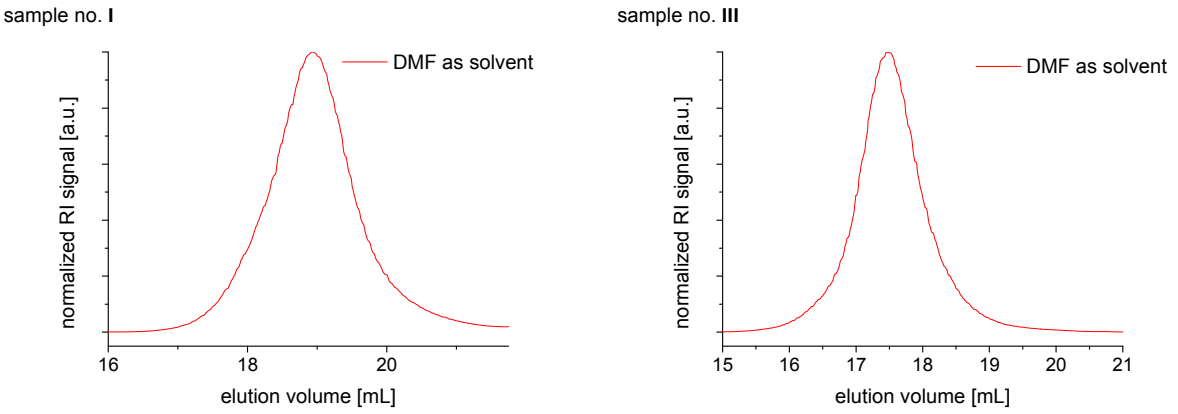

Figure 5–22: *SEC-elugrams of thiazolidine functionalized P[(MeOx)$_x$-co-(DecenOx)$_{1-x}$]$_n$ measured in DMF.*

5.2.11.8 Hydrolysis of thiazolidine side-chains

The deprotection of the thiazolidine ring took place in 0.1 M HCl at 70°C for 5 d. After dialysis against diluted acetic acid (0.01 M) and lyophilisation the functionalized polymer was complete.

As an example a NMR-spectrum is shown with about five cysteine residues per polymer chain and 45 repetition units of MeOx.

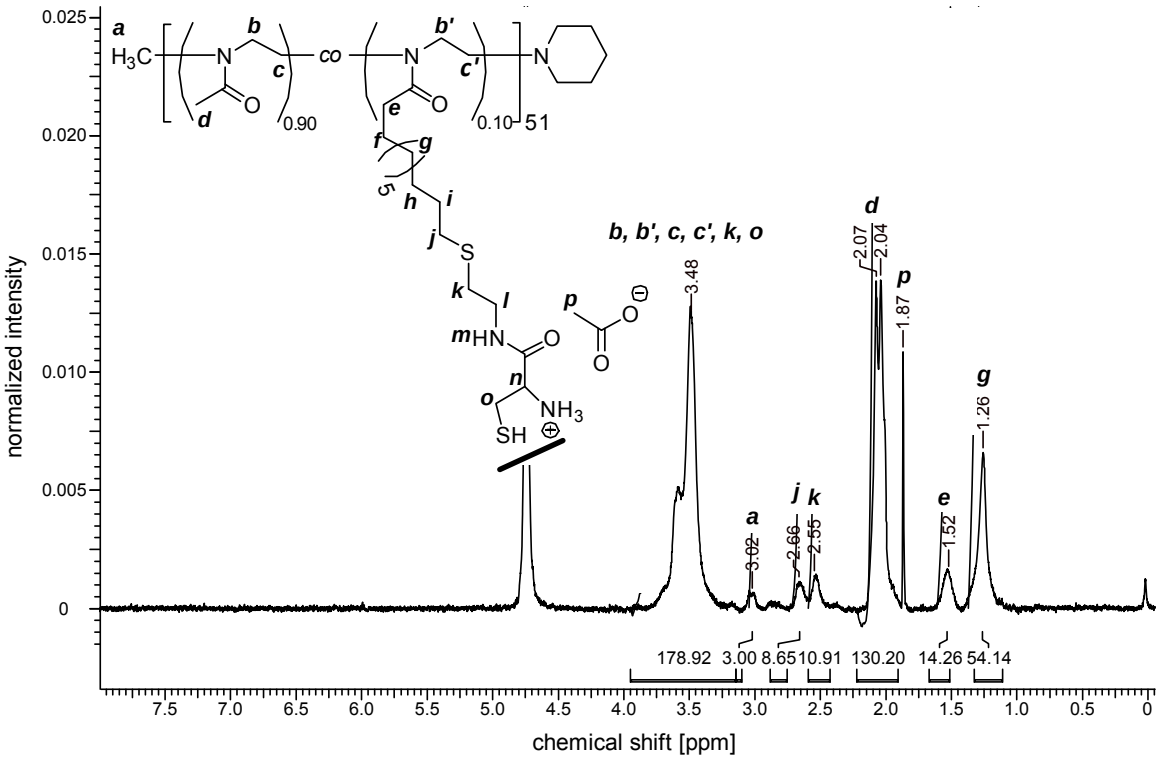

Figure 5–23: *P[(MeOx)$_{0.90}$-co-(DecenOx)$_{0.10}$]$_{51}$.*

^{1}H-NMR (300 MHz, $CDCl_3$): *δ*/ppm = 3.92 – 3.14 (2H, H-***b***; 2H, H-***c***; 2H, H-***b'***; 2H, H-***c'***; 2H, H-***k***; 2H, H-***o***), 3.03 – 2.88 (3H, H-***a***), 2.65 (2H, H-***j***), 2.53 (2H, H-***k***), 2.06 – 2.02 (3H, H-***d***), 1.52 (2H, H-***e***), 1.24 (2H, H-***g***).

5.2.12 Synthesis of pentafluorophenyl acrylate (PFPA)

Pentafluorophenol (3.0 g, 16.3 mmol, 1.0 eq) was dissolved in diethyl ether (30 mL) and cooled to 0°C. After the addition of Et_3N (1.98 g, 19.6 mmol, 1.2 eq), acrylic acid chloride (1.77 g, 19.6 mmol, 1.2 eq) was added dropwise. The mixture was allowed to warm up to room temperature and was stirred overnight. The resulting precipitate was filtered off and was washed with ethyl ether. The solvent was evaporated and a small amount of cresol was added to the liquid. After vacuum distillation (30 mbar, 101°C) the clean product could be isolated.

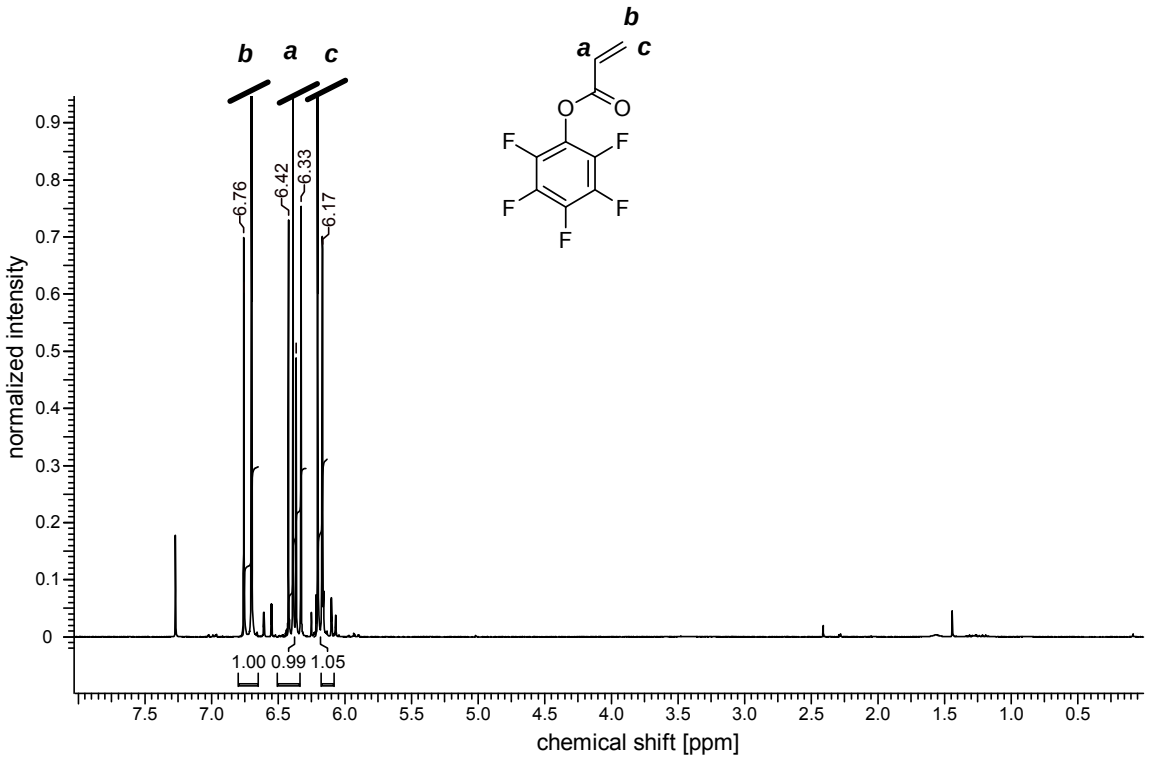

Figure 5–24: *^{1}H-NMR spectrum of pentafluorophenyl acrylate.*

^{1}H-NMR ($CDCl_3$, ppm): *δ*/ppm = 6.76 – 6.70 (d, 1H, H-***b***), 6.42 – 6.33 (qu, 1H, H-***a***), 6.21 – 6.17 (d, 1H, H-***c***).

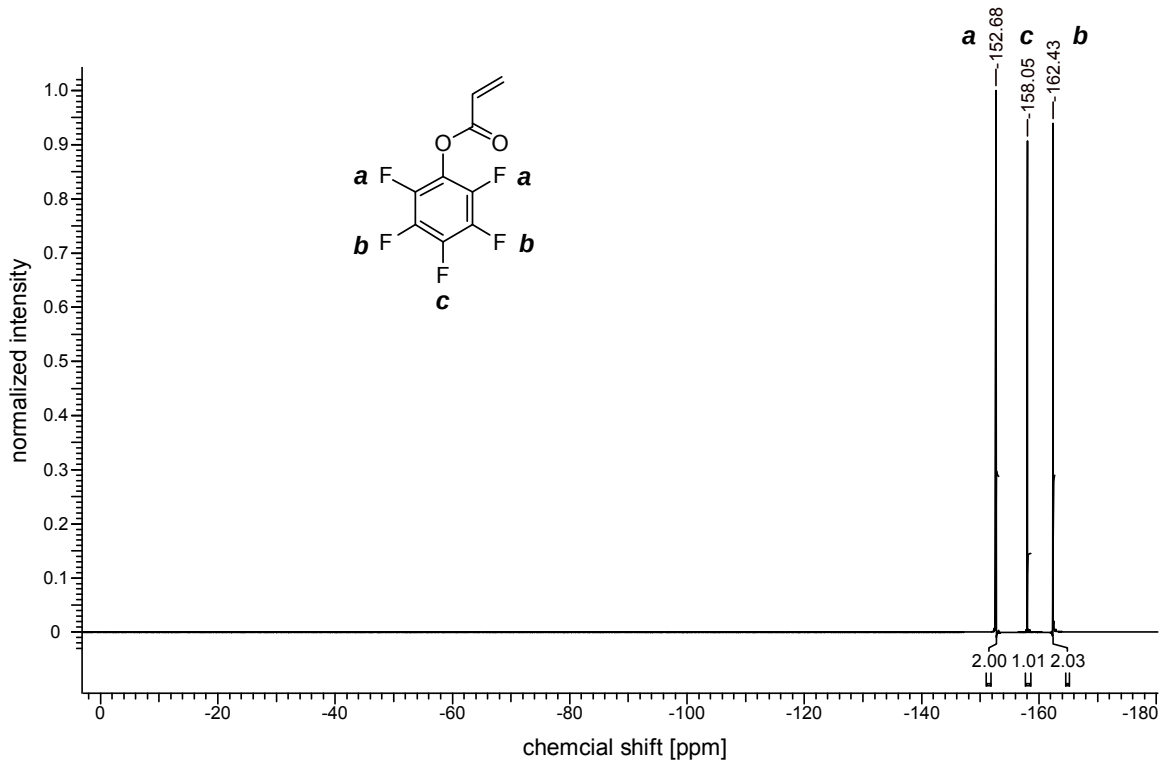

Figure 5–25: *^{19}F-NMR spectrum of pentafluorophenyl acrylate.*

^{19}F-NMR ($CDCl_3$, ppm): *δ*/ppm = -152.68 (2F, F-***a***), -158.05 (1F, F-***c***), -162.43 (2F, F-***b***).

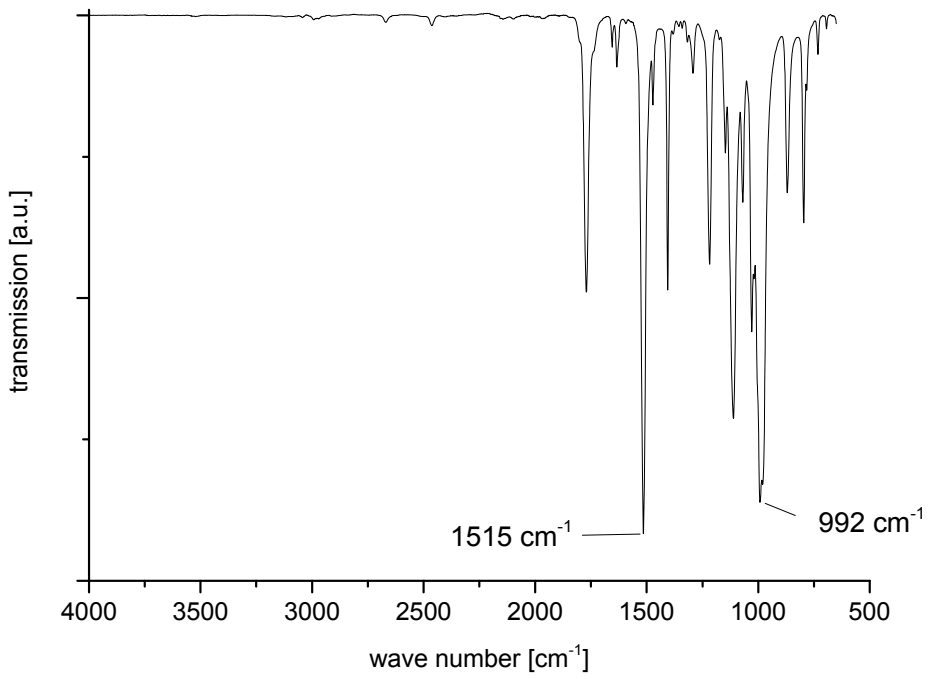

Figure 5–26: *FT-IR spectrum of pentafluorophenyl acrylate.*

5.2.13 Synthesis of *N*-boc-protected amino-thiazolidine

FTz4CA (1.00 g, 2.28 mmol, 1.0 eq) was dispersed in chloroform (11 mL) and argon was bubbled through the solution. After the addition of *N'N*-carbonyldiimidazol (CDI, 0.857 g, 5.28 mmol, 1.0 eq), the turbid solution was stirred for 1 h at room temperature under argon atmosphere (the solution get limpid). *N*-boc-1,4-butanediamine (0.995 g, 5.28 mmol, 1 eq) was slowly added and the solution was stirred overnight. The solvent was removed in vacuum and distilled water (20 mL) was added. After extraction with chloroform and evaporation of the solvent, the raw product could be isolated. Purification by recrystallization from ethyl acetate and drying in vacuum led to the white product.

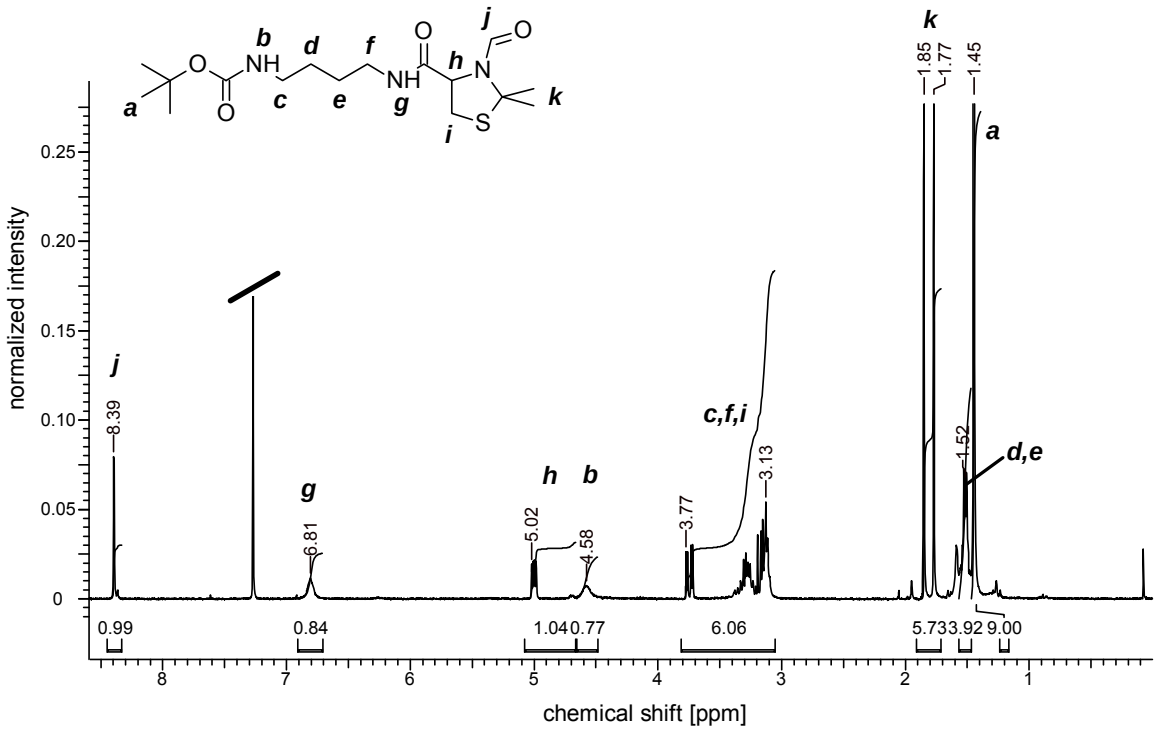

Figure 5–27: *^{1}H-NMR of BOC-protected amino-thiazolidine.*

^{1}H-NMR ($CDCl_3$, ppm): *δ*/ppm = 8.39 (s, 1H, H-***j***) 6.81 (br-s, 1H, H-***g***), 5.02/4.71 (m, 1H, H-***h***), 4.58 (br-s, 1H, H-***b***) 3.77 – 3.13 (m, 6H, H-***c***, H-***f,*** H-***i***), 1.85 – 1.77 (6H, H-***k***), 1.52 (br, 4H, H-***d,*** H-***e***), 1.45 (s, 9H, H-***a***).

5.2.14 Synthesis of amino-thiazolidine (ATHz)

N-boc-protected ATHz (0.359 g, 1.00 mmol, 1.0 eq) was refluxed in millipore water (20 mL) for 24 h. The solvent was removed and the raw product was deprotonated by the addition of sodium hydroxide (0.1M, 15 mL). The aqueous phase was extracted with chloroform (5 x 5 mL), dried with $MgSO_4$ and filtered. The product could be isolated by evaporation of the solvent and drying in vacuum.

^{1}H-NMR spectrum is visible in **Figure 4–21**.

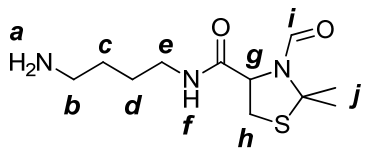

^{1}H-NMR ($CDCl_3$, ppm): *δ*/ppm = 8.38 (s, 1H, H-***i***) 6.97 (br-s, 1H, H-***f***), 5.01/4.67 (m, 1H, H-***g***), 3.75 – 3.12 (m, 4H, H-***e***, H-***h***), 2.71 (tr, 2H, H-***b***), 1.84 – 1.77 (6H, H-***j***), 1.58 – 1.44 (m, 2H, H-***c,*** 2H, H-***d***), 1.24 (br, 2H, H-***a***).

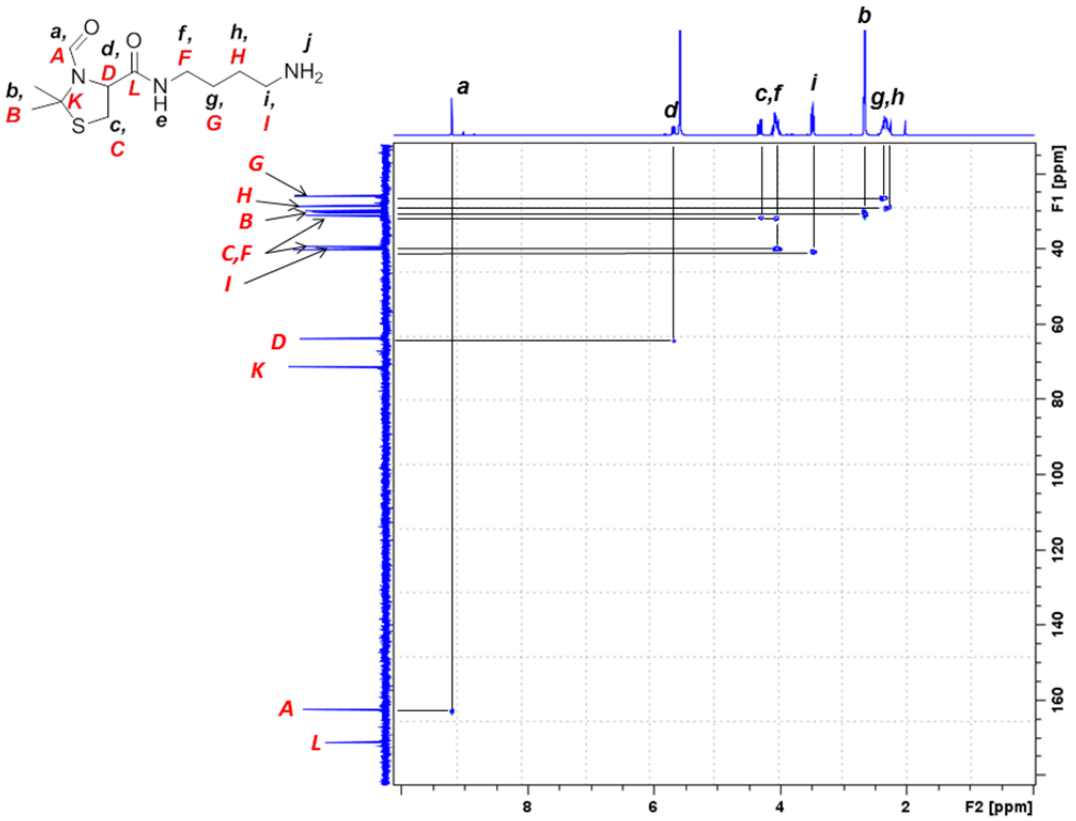

Figure 5–28: *HSQC-NMR of amino-thiazolidine. All signals could be assigned to the corresponding groups.*

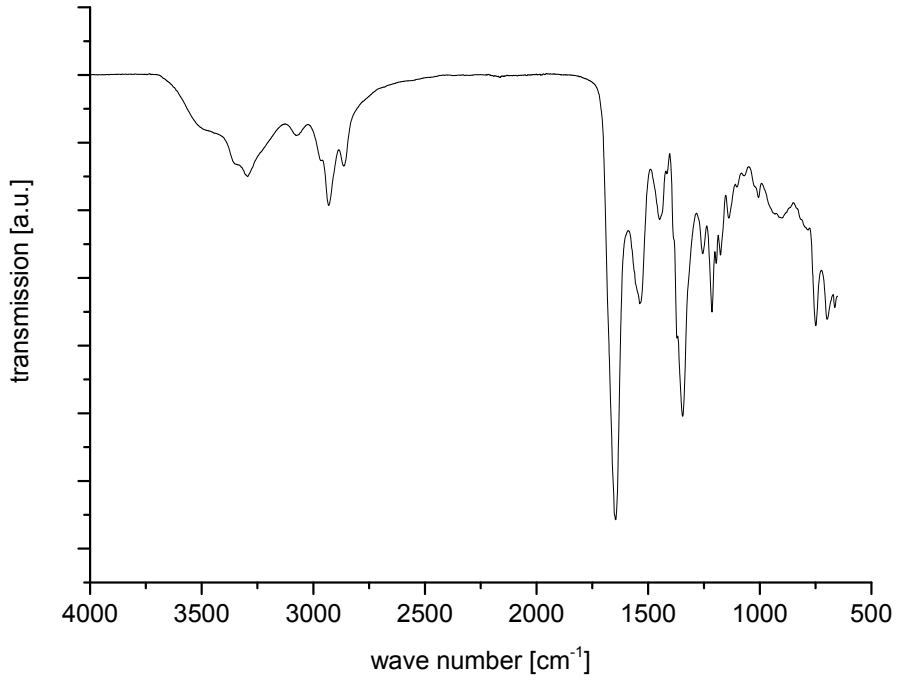

Figure 5–29: *FT-IR spectrum of amino-thiazolidine.*

5.2.15 Synthesis of active ester P(OEGA)

Depending of the desired molecular composition of the copolymer the ratio of 2-cyano-2-propyl benzodithioate (chain transfer agent, CTA), OEGA, PFPA, and AIBN varied.

E.g. CTA (0.066 g, 0.3 mmol, 1.0 eq) was dried in vacuum for 1 h. OEGA (1.145 g, 2.39 mmol, 8.0 eq), PFPA (0.142 g, 0.6 mmol, 2.0 eq) were added and solved in DMF (5 mL). Three *freeze-pump-thaw cycles* were performed, meaning that the solution was frozen with liquid N_2 and the flask was evacuated for 15 min ($1 \cdot 10^{-3}$ mbar). Afterwards, the flask was warmed to RT and was flushed with Ar. This cycle was performed three times. In the following the solution was heated to 80°C and AIBN (0.024 g, 0.15 mmol, 0.5 eq) was added. The polymerization was terminated by aerating and cooling to 0°C after 16 h. A raw-sample was extracted from the solution for the determination of the polymer composition. The solvent was removed with vacuum and an external cooling trap, and the residue was dissolved in THF and was precipitated into Et_2O/*n*-hexane, V/V, 1/1 (3 times, each 40 mL of precipitant) and was centrifuged. The precipitate was dissolved in THF and was dried under reduced pressure.

^{1}H-NMR spectrum is visible in **Figure 4–20**.

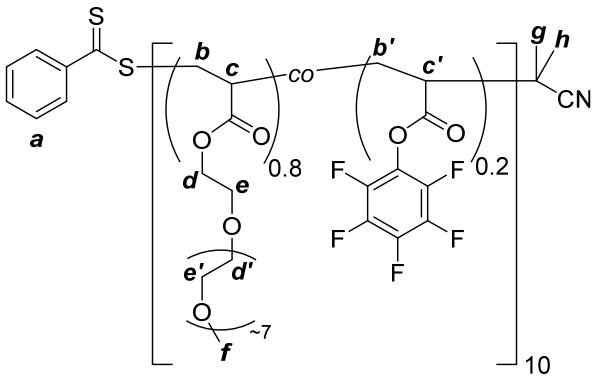

^{1}H-NMR ($CDCl_3$, ppm): *δ*/ppm = 7.98 – 7.39 (m, 5H, H-***a***), 4.20 (br s, 2H, H-***d***), 3.65 (br, 2H, H-***e;*** 2H, H-***d';*** 2H, H-***e'***), 3.38 (br s, 3H, H-***f***), 2.63 – 1.26 (m, 2H, H-***b;*** 2H, H-***c;*** 2H, H-***b';*** 2H, H-***c';*** 2H, H-***g;*** 2H, H-***h***).

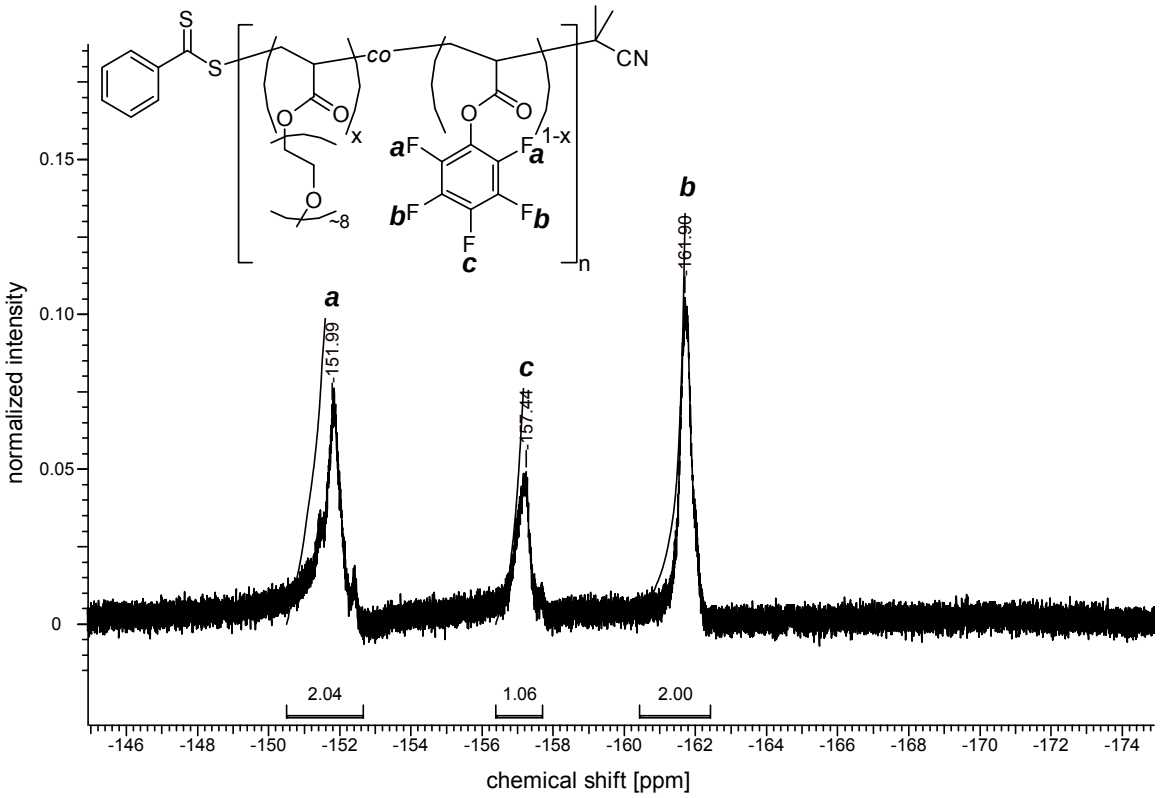

Figure 5–30: *^{19}F-NMR of active ester P(OEGA) after purification.*

^{19}F-NMR ($CDCl_3$, ppm): *δ*/ppm = -151.99 (2F, F-***a***), -157.44 (1F, F-***c***), -161.00 (2F, F-***b***).

Table 5–9: *SEC-measurement of the copolymer P[(OEGA)$_{0.72}$-co-(PFP)$_{0.28}$]$_{18}$.*

DMF-SEC, 1 mL·min^{-1}, PEG-Standard	
M_n	3600 g·mol^{-1}
M_w	4300 g·mol^{-1}
Đ	1.20
Modality	monomodal

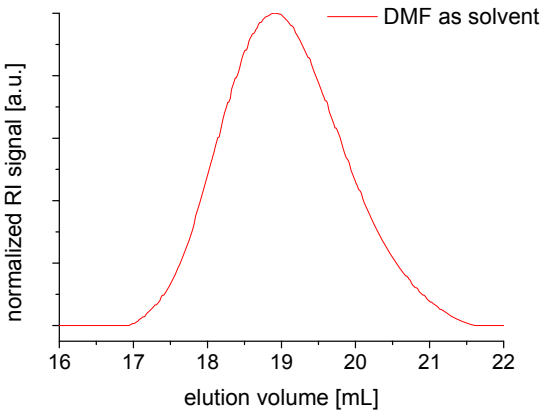

Figure 5–31: *SEC-elugram of active ester P(OEGA) measured in DMF.*

5.2.16 Side-chain functionalization of active ester P(OEGA) for NCL

5.2.16.1 Synthesis of thiazolidine functionalized P(OEGA)

The active ester polymer (0.150 g, 0.03 mmol) bearing 20% PFP (0.006 mmol) was dissolved in a solution of DMF (2 mL) containing ATHz (0.017 g, 0.06 mmol, 10 eq in relation to PFP), DBU (0.017 g, 0.06 mmol, 10 eq in relation to PFP), and OEGA (0.078 g, 0.16 mmol, 5 eq in relation to the polymer). After 24h the solvent was removed with high vacuum and an external cooling trap, and the residue was dissolved in THF and was precipitated into Et_2O/*n*-hexane, V/V, 1/1 (3 times, each 40 mL of precipitant) and was centrifuged. The precipitate was dissolved in THF and was dried under reduced pressure. Sometimes the polymer was additionally dialyzed against water for 3 d (exchange of water every day 3 times). Then, the viscous polymer could be isolated after lyophilization.

^{1}H-NMR spectrum is visible in **Figure 4–22**.

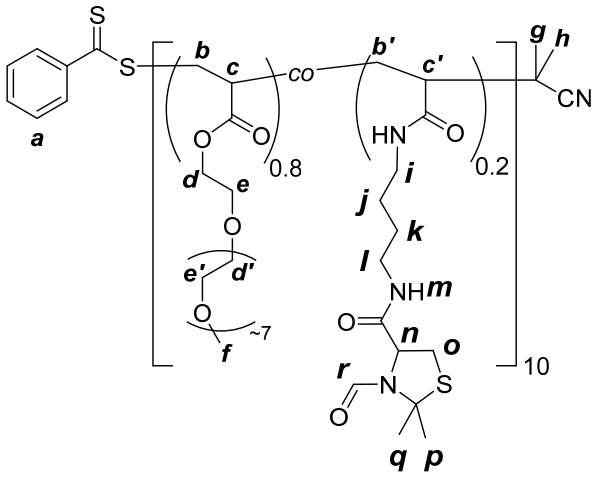

^{1}H-NMR (300 MHz, $CDCl_3$): *δ*/ppm = 8.37 (1H, H-***r***), 4.93 (1H, H-***n***), 4.17 (2H, H-***c***), 3.75 – 3.56 (2H, H-***d***; 2H, H-***e***; 2H, H-***f***; 2H, H-***l***; 2H, H-***o***), 3.38 (3H, H-***g***), 2.84 – 1.31 (2H, H-***a;*** 2H, H-***b;*** 2H, H-***a';*** 2H, H-***b';*** 2H, H-***h;*** 2H, H-***i;*** 2H, H-***j;*** 2H, H-***k;*** 2H, H-***m;***), 1.52 (2xCH_3, H-**p**, H-***q***).

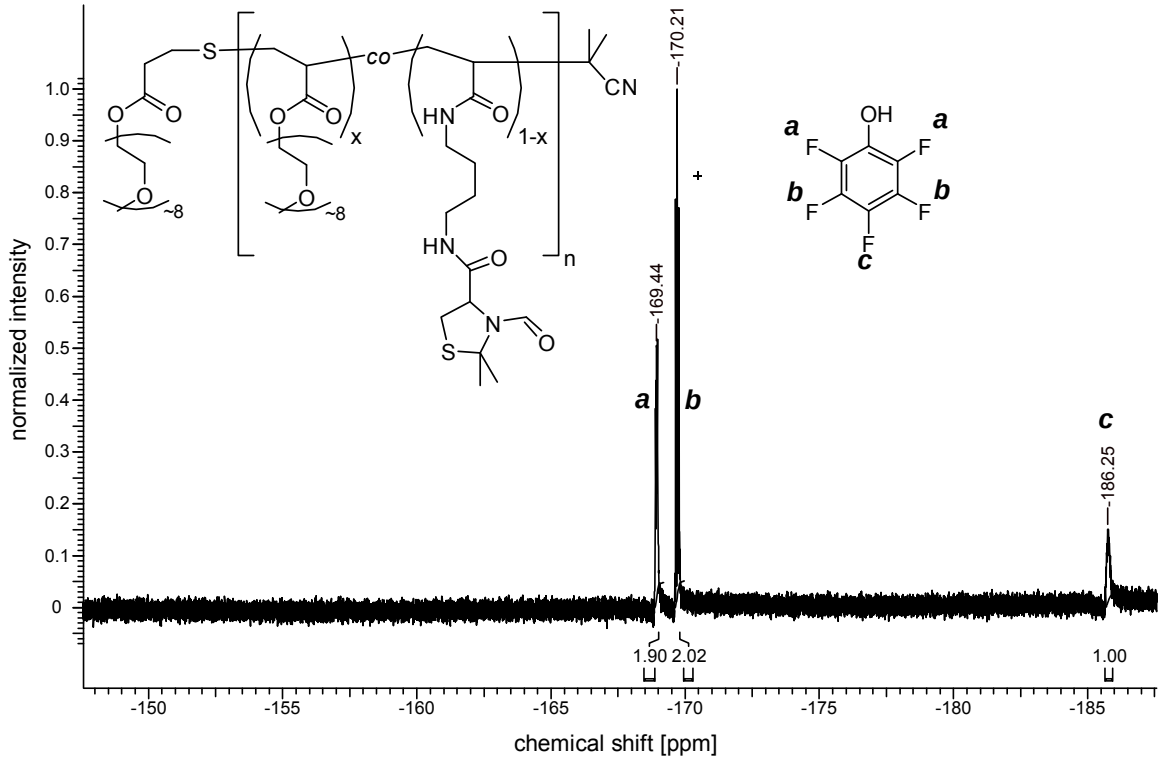

Figure 5–32: *Raw ^{19}F-NMR measurement of the thiazolidine functionalized polymer for further NCL. The characteristic broad signals at δ = -152.04, -157.41 and -161.94 ppm are not visible anymore. Furthermore new signals appear because of the redundant PFP unit.*

Raw ^{19}F-NMR ($CDCl_3$, ppm): *δ*/ppm = -169.44 (2F, F-***a***), -170.21 (2F, F-***b***), -186.25 (1F, F-***c***).

Table 5–10: *SEC-measurement of the copolymer P[(OEGA)$_{0.72}$-co-(PFP)$_{0.28}$]$_{18}$.*

DMF-SEC, 1 mL·min^{-1}, PEG-Standard	
M_n	4400 g·mol^{-1}
M_w	5300 g·mol^{-1}
Đ	1.21
Modality	monomodal

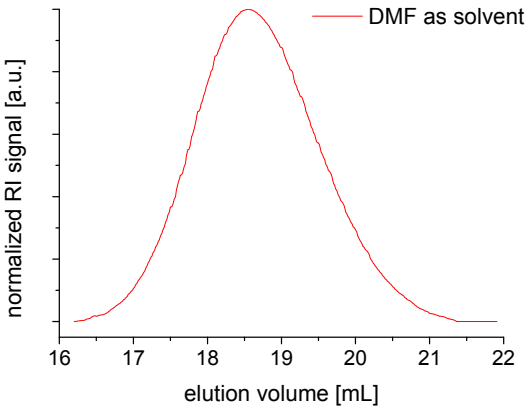

Figure 5–33: *SEC-elugram of thiazolidine functionalized P(OEGA) measured in DMF.*

5.2.16.2 Synthesis of cysteine-functionalized P(OEGA)

The deprotection of the thiazolidine ring took place in 0.1 M HCl at 70°C for 5 d. After dialysis against diluted acetic acid (0.01 M) and lyophilisation the functionalization of the polymer was complete.

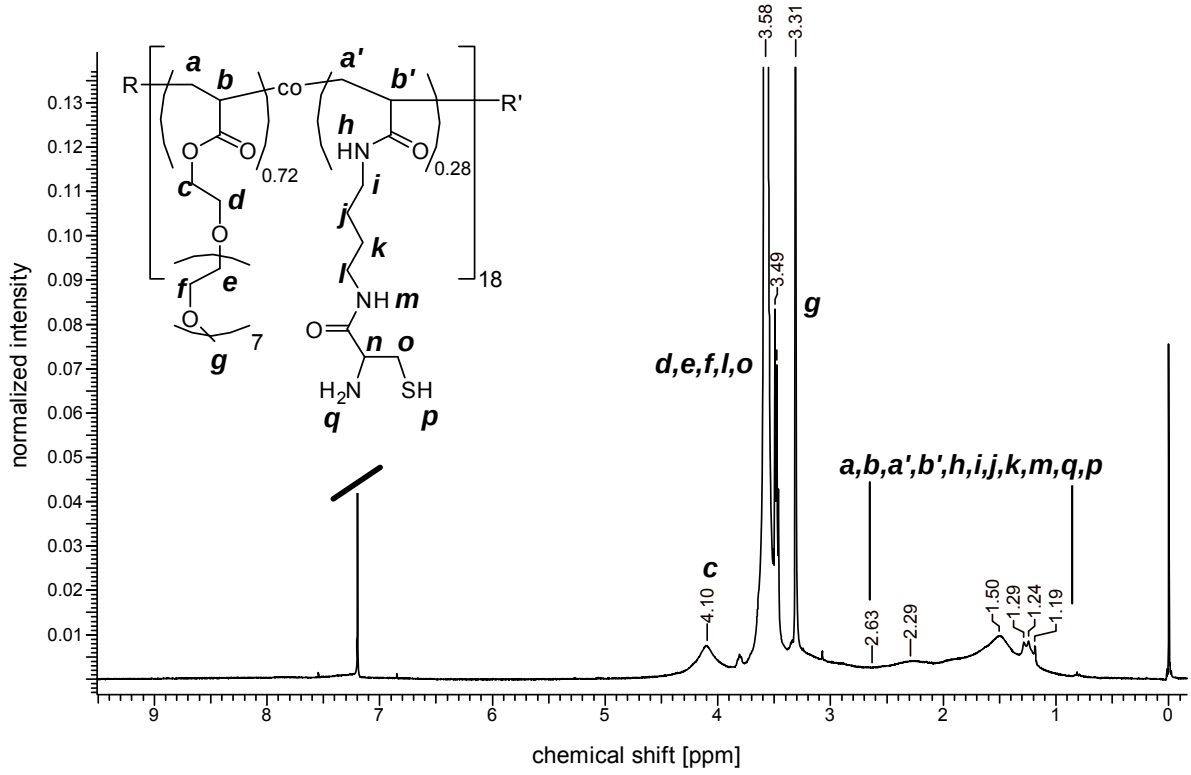

Figure 5–34: *^{1}H-NMR spectrum of cysteine-functionalized P(OEGA).*

^{1}H-NMR (300 MHz, $CDCl_3$): *δ*/ppm = 4.10 (2H, H-***c***), 3.58 – 3.49 (2H, H-***d***; 2H, H-***e***; 2H, H-***f***; 2H, H-***l***; 2H, H-***o***), 3.31 (3H, H-***g***), 2.63 – 1.19 (2H, H-***a;*** 2H, H-***b;*** 2H, H-***a';*** 2H, H-***b';*** 2H, H-***h;*** 2H, H-***i;*** 2H, H-***j;*** 2H, H-***k;*** 2H, H-***m;*** 1H, H-**p**; 2H, H-***q***).

5.2.16.3 Synthesis of thioester functionalized P(OEGA)

The active ester polymer (0.250 g, 0.05 mmol) bearing 20% PFP (0.01 mmol) was dissolved in a solution of DMF (2 mL) containing the DL-homocysteine thiolactone hydrochloride (cyclic thioester, 0.017 g, 0.11 mmol, 10 eq in relation to PFP), DBU (.0.020 g, 0.13 mmol, 12 eq in relation to PFP), and OEGA (0.132 g, 0.27 mmol, 5 eq in relation to the polymer). After 24h an amount of water was added and the solution was dialyzed against water for 3 d (exchange of water every day 3 times). The viscous polymer could be isolated after lyophilization.

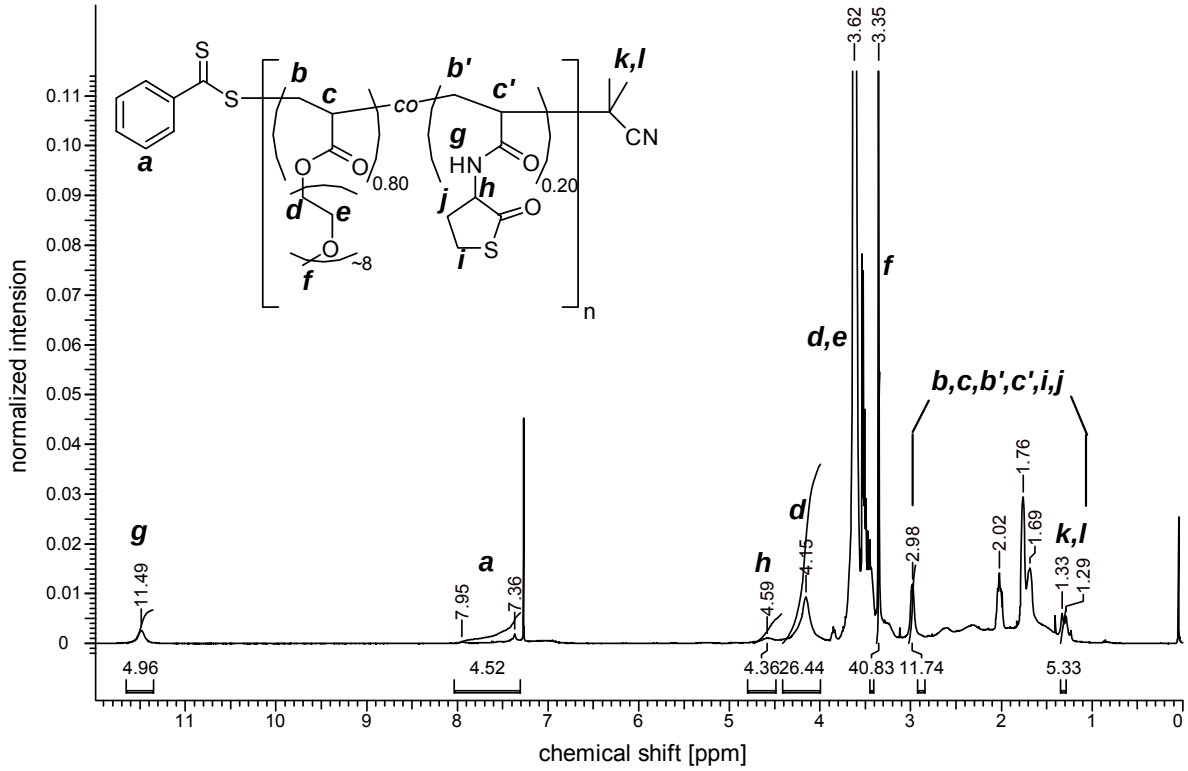

Figure 5–35: *^{1}H-NMR spectra of cyclic thioester functionalized Poly[(OEGA)$_{0.72}$-co-(PFP)$_{0.28}$]$_{18}$ (measured in CDCl$_3$).*

^{1}H-NMR (300 MHz, CDCl$_3$): δ/ppm = 11.49 (1H, H-***g***), 7.95 – 7.36 (5H, H-***a***), 4.59 (1H, H-***h***), 4.15 (2H, H-***d***) 3.62 (2H, H-***d***; 2H, H-***e***), 3.35 (3H, H-***f***), 2.98 – 1.29 (2H, H-***b;*** 2H, H-***c;*** 2H, H-***b';*** 2H, H-***c';*** 2H, H-***j;*** 2H, H-***i***), 1.33 (2xCH$_3$, H-***k***, H-***l***).

^{19}F-NMR spectrum is visible in **Figure 4**–23.

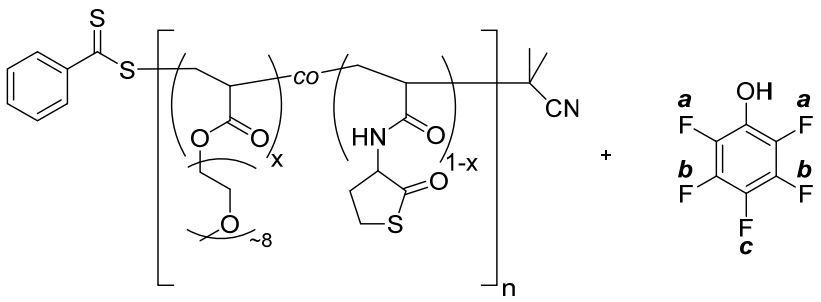

Raw ^{19}F-NMR ($CDCl_3$, ppm): *δ*/ppm = -162.86 (2F, F-***a***), -165.76 (2F, F-***b***), -172.47 (1F, F-***c***).

Table 5–11: *SEC-measurement of the copolymer P[(OEGA)$_{0.72}$-co-(PFP)$_{0.28}$]$_{18}$.*

DMF-SEC, 1 mL·min^{-1}, PEG-Standard	
M_n	3900 g·mol^{-1}
M_w	4700 g·mol^{-1}
Đ	1.22
Modality	monomodal

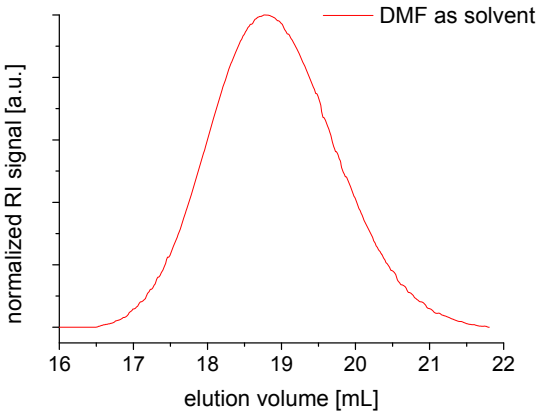

Figure 5–36: *SEC-elugram of thioester functionalized P(OEGA) measured in DMF.*

5.3 Quantification of cysteine-functionalized POx (TNBSA)

Two stock solution were prepared consisting of the polymer (10 mg) and the calibration compound (10 mg) in 0.1M $NaHCO_3$ (1 mL) and of H_2O_2 (10 mg) in 0.1M $NaHCO_3$ (1 mL). 50 µL of each stock solution were combined with 0.1M $NaHCO_3$ (4.950 mL) to yield a new stock solution with a concentration of 99 $\mu g \cdot mL^{-1}$ which was stored 1 h at 37°C before a concentration series was prepared. This series ranged from 99.0 – 0.59 $\mu g \cdot mL^{-1}$ with sample volumes of 500 µL. $NaHCO_3$ (500 µL, 0.1M) without H_2O_2 was used as blank solution. A TNBSA solution (250 µL, 0.085 µmol TNBSA, 0.01% in 0.1M $NaHCO_3$) was added and the samples were stored for 2 h at 37°C whereby, depending on the concentration, some samples turned yellow. Afterwards, the samples were diluted with 10% SDS solution (250 µL) and 1M HCl (125 µL). The produced CO_2 (while reaction) was removed by shaking. UV-Vis measurements were performed in cuvettes at 335 nm with each sample (1 mL). As the thiols were oxidized before the TNBSA assay, the could not influence the analysis anymore. The amount of cysteines per polymer chain could be calculated by the realtion between amine concentration and polymer concentration.
Hydrogen peroxide did not influence the calibration with ethanolamine. In addition we tested the influence of hydrogen peroxide on thiol components and could see full consumption of thiols during the incubation of 1 h with 37°C.[190]

5.4 CellTiter-Glo®Luminescent – Cell Viability Assay

Cell Culture Materials. Human fibroblasts (isolated from foreskin) were cultured in Dulbecco's Modified Eagle Medium (DMEM, Life Technologies) contained 10% fetal bovine serum (FBS) in the presence of 100 units·mL^{-1} penicillin and 0.1 mg·mL^{-1} streptomycin.

Biocompatibility test. Biocompatibility tests were measured utilizing the CellTiter-Glo Luminescent Cell Viability Assay (Technical Bulletin, Promega Corporation, Madison, WI, USA). When added to cells, the assay reagent produces luminescence in the presence of ATP from viable cells. Human fibroblasts in cell medium were plated in 24-well plates at a density of 50000 cells per well and incubated for 24 h at standard cell culture conditions (37°C, 5% CO_2). 4 polymers were tested with different concentrations (10.0 mg·mL^{-1}, 1.0 mg·mL^{-1}, and 0.1 mg·mL^{-1}) and compositions (P[$(MeOx)_{0.95}$–*co*–$(ButenOxCys)_{0.05}]_{44}$, P[$(MeOx)_{0.95}$–*co*–$(DecenOxCys)_{0.05}]_{54}$, P[$(MeOx)_{0.90}$–*co*–$(ButenOxCys)_{0.10}]_{55}$, and P[$(MeOx)_{0.90}$–*co*–$(DecenOxCys)_{0.10}]_{57}$). Test samples were solubilized in medium to the desired treatment concentration and cells were treated with 100 µL of each solution.

For the luminescent tests the overlap was remoted, 110 µL of medium and 110 µL of the assay reagent were added to each well and cell lysis was induced on an orbital shaker for 2 min. Plates were incubated at room temperature for 10 min to stabilize the luminescence signal and results were read on an Elisa Reader Spectrafluor Plus (Tecan, Deutschland GmbH, Crailsheim). All plates had control wells containing medium without cells to obtain a value for background luminescence and we used Polystyrene as a control substance.

5.5 Coupling reactions

5.5.1 Azide–alkyne click chemistry with POx

Sodium ascorbate (0.040 g, $2.14 \cdot 10^{-5}$ mmol, 1.0 eq) was dissolved in millipore water (1 mL). In a second Eppendorf cap $CuSO_4 \cdot 5\ H_2O$ (0.005 g, $2.14 \cdot 10^{-5}$ mmol, 1.0 eq) was also dissolved in millipore water (1 mL). Azide functionalized POx (POx-N_3, 0.100 g, $2.14 \cdot 10^{-5}$ mmol, 1.0 eq) was combined with alkyne functionalized POx (0.093 g, $2.14 \cdot 10^{-5}$ mmol, 1.0 eq) and was dissolved in millipore water (1 mL). Argon was passed through the solution and after the adding of sodium ascorbate- and copper sulfate-solution (each 10 µL), the flask was closed with no effort to exclude oxygen and stirred for 48h at RT. The solvent was removed and the polymer was precipitated into cold diethyl ether (solvent: $CHCl_3$/MeOH, V/V, 1/1). The polymer was dried in vacuum.

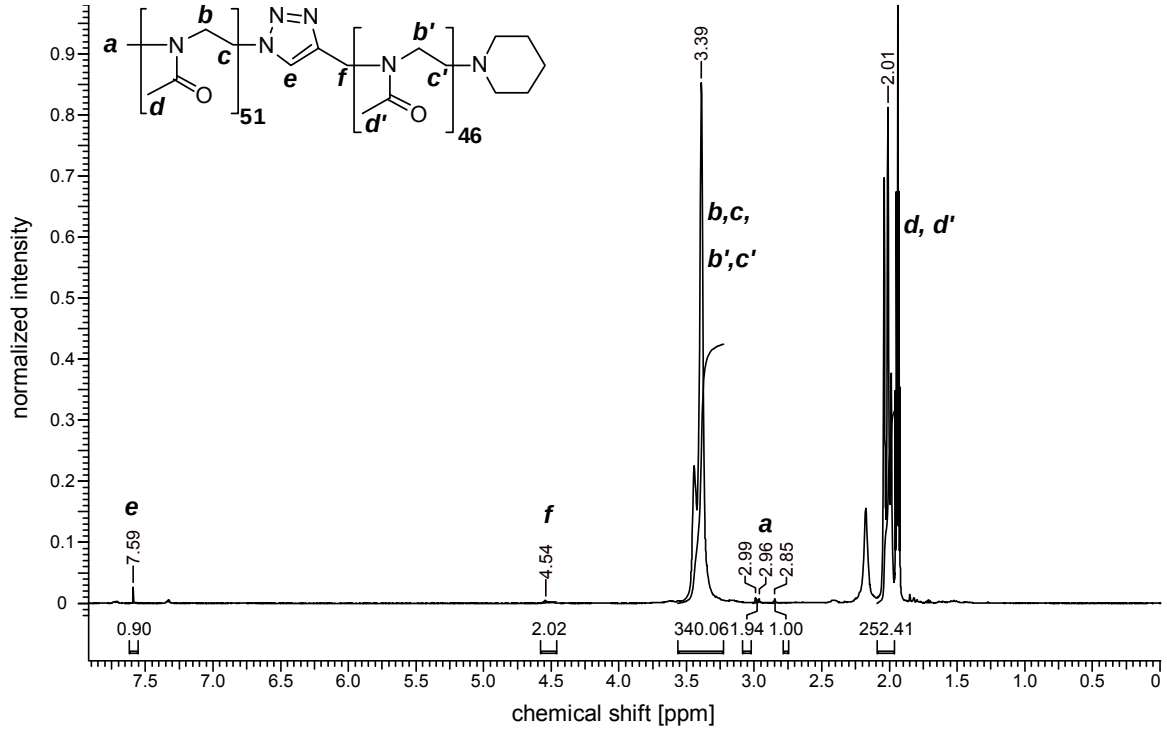

Figure 5–37: *^{1}H-NMR after the click reaction of alkyne- and azide-functionalized P(MeOx).*

^{1}H-NMR (CD_3CN, ppm): *δ*/ppm = 7.59 (1H, H-***e***), 3.39 (2H, H-***b;*** 2H, H-***c,*** 2H, H-***b';*** 2H, H-***c'***), 2.99 – 2.96 + 2.85 (3H, H-***a***), 2.01 (3H, H-***d,*** 3H, H-***d***).

Table 5–12: *SEC-measurements of the P(MeOx) after azide–alkine click reaction.*

1 mL·min^{-1}, PEG-Standard, conventional	H_2O-SEC [g·mol^{-1}]	DMF-SEC [g·mol^{-1}]
M_n	4700	4900
M_w	6800	5800
Đ	1.43	1.20
modality	monomodal	bimodal

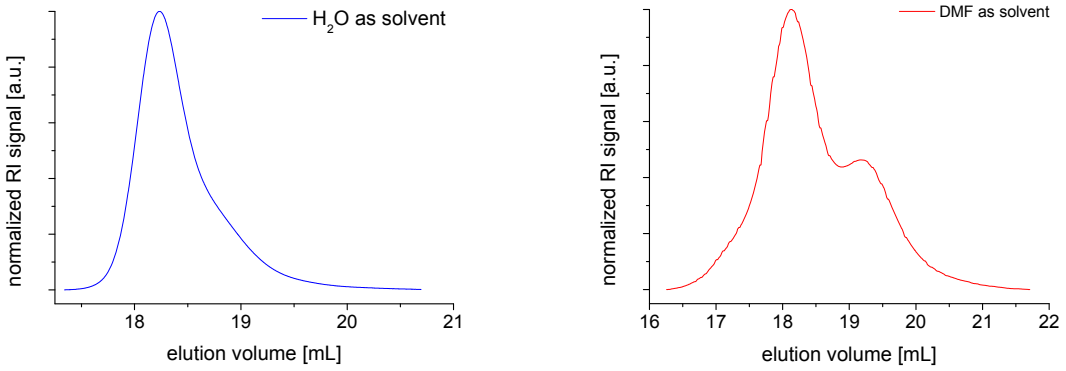

Figure 5–38: *SEC-elugrams of POx after azide–alkyne chemistry (left: measured in water; righ: measured in DMF).*

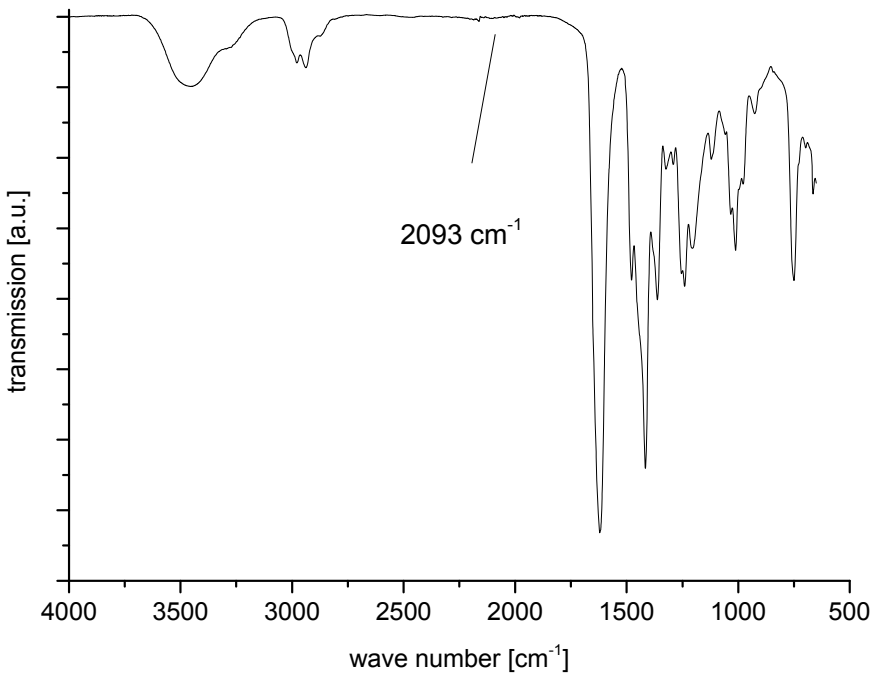

Figure 5–39: *FT-IR spectra of P(MeOx) after azide–alkyne click-reaction. The characteristic azide-vibration at ~2100 cm^{-1} is not visible anymore, indicating the successful click reaction.*

5.5.2 Native chemical ligation of cys-POx

5.5.2.1 NCL with model peptide 1

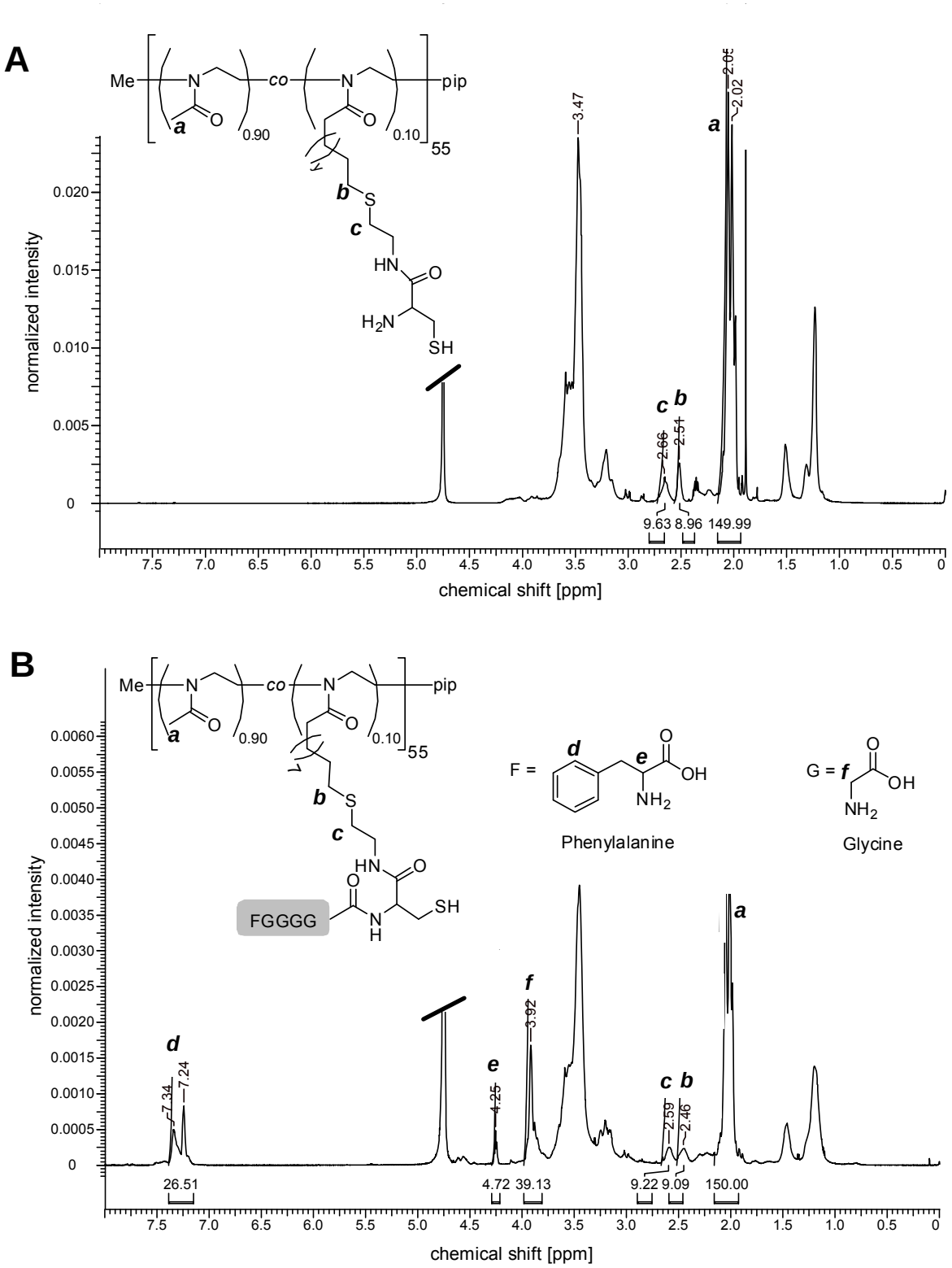

Figure 5–40: *^{1}H-NMR of cys-POx and of thioesterification of C-terminally activated peptide **1** upon dissolving in MPAA containing ligation buffer, followed by NCL to the polymer.*

(*) The native chemical ligation between peptide **1** (2.24 mg, 4.1 µmol, 5 eq) and cysteine-functionalized POx (poly[$(MeOx)_{50}$-*co*-$(DecenOx)_5$], 5 mg, 0.8 µmol, 1 eq) was carried out in ligation buffer (6M Gn·HCl, 100 mM NaH_2PO_4, 50 mM TCEP, 200 mM, pH 7.0) for 4 h. The reaction volume was 170 µL, which corresponds to a concentration of peptide **1** of 5 mM, while the concentration of the polymer was 1 mM. Then, an additional portion of peptide **1** (1.1 mg, 2.0 µmol, 2.5 eq) was added to the ligation mixture and the reaction was allowed to proceed overnight. The final mixed ratio between peptide (M_n as non-thioester = 393.16 g·mol^{-1}) and polymer (M_n = 6150 g·mol^{-1}) was 7.5:1. The reaction was quenched by the addition of H_2O containing 0.1% TFA to a total volume of 2 mL and subsequently submitted to HPLC (JASCO) on a C18 column.

The polymer was analyzed by MALDI ToF and ^{1}H-NMR spectrometry before and after functionalization.

Table 5–13: *Calculated masses of polymer functionalized with peptide **1**.*

polymer:peptide [molar ratio]	$[M+H]^+$ calculated $[g \cdot mol^{-1}]$
1:0	6150
1:1	6525
1:2	6900
1:3	7275
1:4	7650
1:5	8025

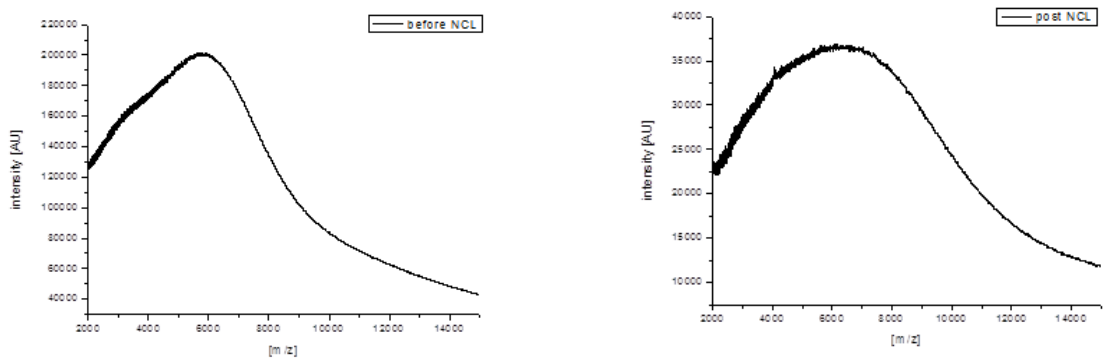

Figure 5–41: *MALDI TOF spectrum of POx polymer in super 2,5-dihydroxybenzoic acid (SDHB) matrix, before (left, estimated by NMR, m/z: 6150 $[M+H]^+$) and after (right, 5x functionalized, calcd. m/z: 8025 $[M+H]^+$) native chemical ligation.*

5.5.2.2 NCL with peptide 2 (tau[390-410] sequence)

(*) Cys-POx was dissolved in filtered and degased ligation buffer (6M Gn·HCl, 200 mM NaH_2PO_4, 200 mM 4-mercaptophenylacetic acid (MPAA), 10 mM *tris*(2-carboxyethyl)phosphine (TCEP)). The pH was readjusted to 7.2 by the addition of NaOH or HCl and the mixture was added to peptide **2** to give a final concentration of 4 mM with respect to the peptide. The reactions were left overnight at RT before they were quenched by the addition of H_2O containing 0.1% TFA to a total volume of 2 mL and subsequently submitted to HPLC (JASCO) on a C18 column.
The mixed ratios between peptide (M_w = 2443 g·mol^{-1}) and polymer (M_w = 5800 g·mol^{-1}) were 1:1, 3:1 and 6:1.

Table 5–14: *Ratios and used amounts of peptide in comparison to the cysteine-functionalized polyoxazoline.*

polymer:peptide [molar ratio]	Polymer [nmol]	Peptide [nmol]
1:1	345	345
1:3	172	517
1:6	172	1030

HPLC was applied to remove salts and excess MPAA. Polymer containing fractions were collected and showed no unreacted peptide by UV/MS. HPLC was performed on a Nucleodur C18 column with a gradient of MeCN (0.1% TFA)/H_2O (0.1% TFA) of 5-95% in 40 min.

All MALDI ToF measurements showed peptide peaks in the range of m/z <4000.

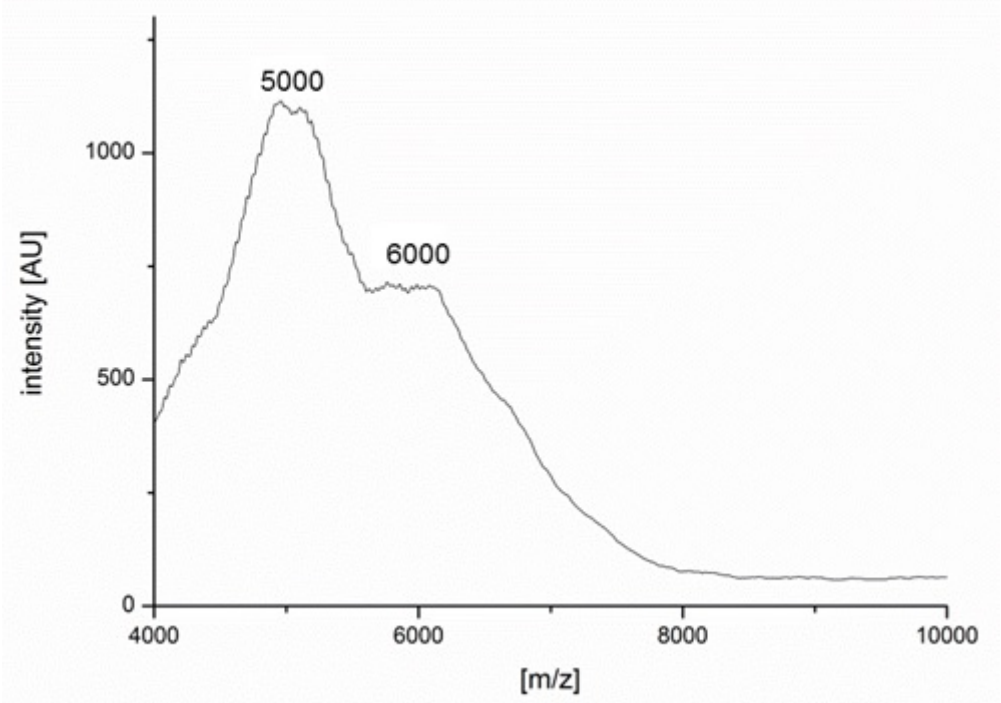

Figure 5–42: *MALDI ToF spectrum of POx polymer in SDHB matrix with m/z = 5000-6000 Da $[M+H]^+$ (calcd. by NMR, m/z: 5800).*

Table 5–15: *Calculated and observed masses of polymer.*

polymer:peptide [molar ratio]	$[M+H]^+$ calculated [$g \cdot mol^{-1}$]	$[M+H]^+$ observed [$g \cdot mol^{-1}$]
1:0	5800	5000
		6000

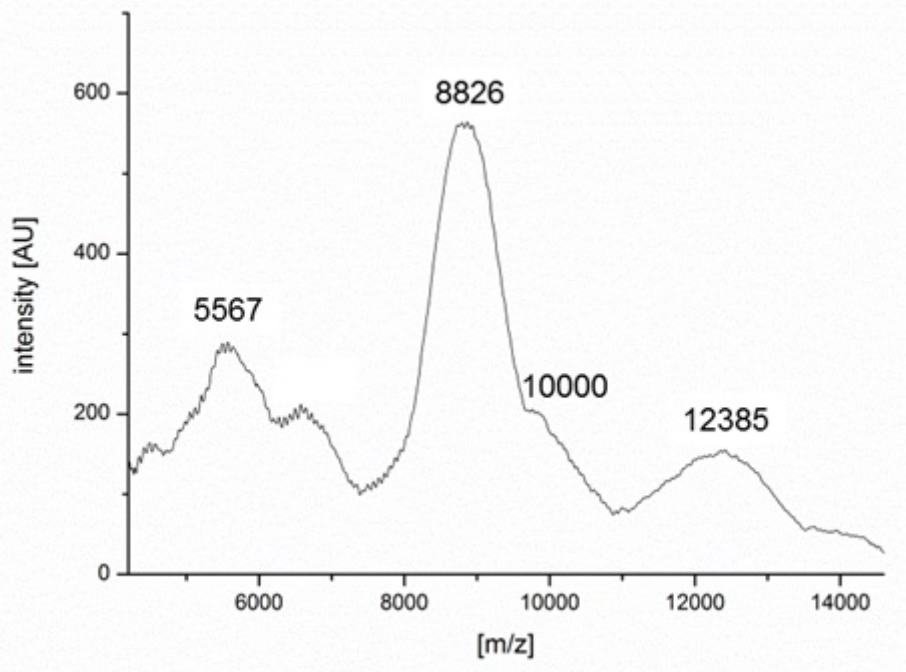

Figure 5–43: *MALDI ToF spectrum of ligation reaction between polymer and peptide **2** in a 1:1 ratio.*

Table 5–16: *Calculated and observed masses of 1:1 polymer functionalized with peptide **2**.*

polymer:peptide [molar ratio]	$[M+H]^+$ calculated [$g \cdot mol^{-1}$]	$[M+H]^+$ observed [$g \cdot mol^{-1}$]
1:0	5800	5567
1:1	8082	8826
1:2	10364	10000
1:3	12646	12385

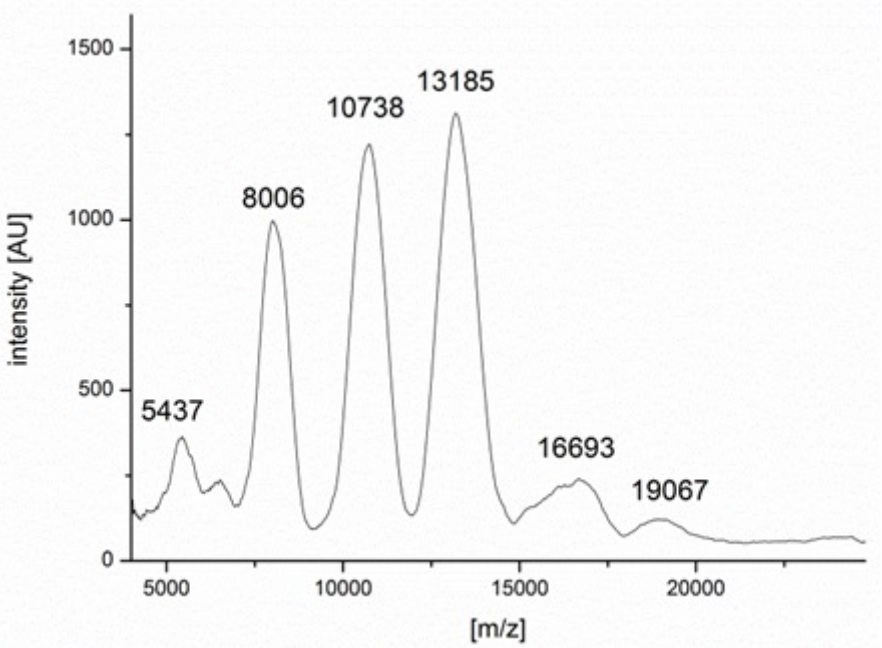

Figure 5–44: *MALDI ToF spectrum of ligation reaction between polymer and peptide **2** in a 1:3 ratio.*

Table 5–17: *Calculated and observed masses of 1:3 polymer functionalized with peptide **2**.*

polymer:peptide [molar ratio]	$[M+H]^+$ calculated [$g \cdot mol^{-1}$]	$[M+H]^+$ observed [$g \cdot mol^{-1}$]
1:0	5800	5437
1:1	8082	8006
1:2	10364	10738
1:3	12646	13185
1:4	14928	---
1:5	17210	16693
1:6	19492	19067

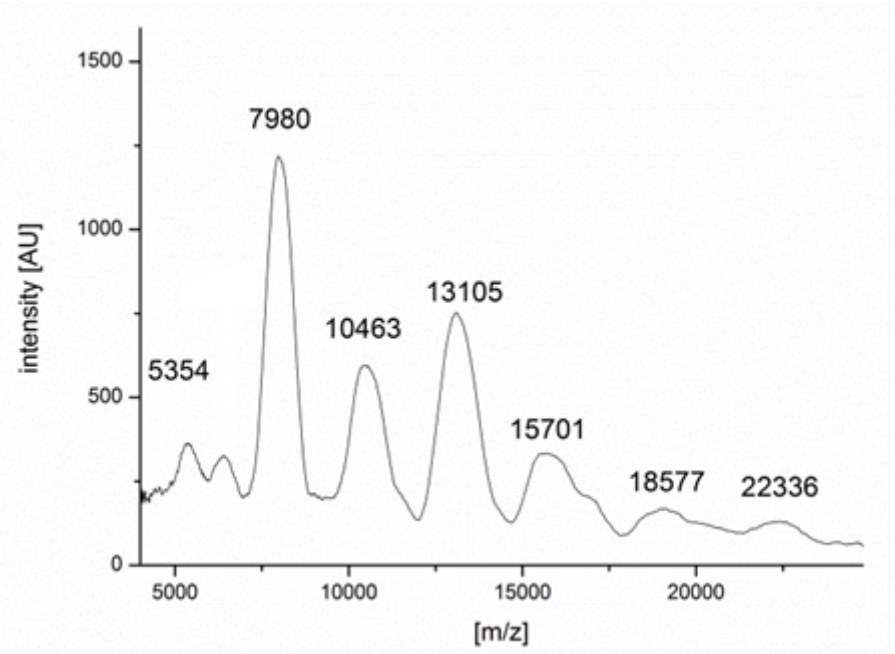

Figure 5–45: *MALDI ToF spectrum of ligation reaction between polymer and peptide **2** in a 1:6 ratio.*

Table 5–18: *Calculated and observed masses of 1:6 polymer functionalized with peptide **2**.*

polymer:peptide [molar ratio]	$[M+H]^+$ calculated [$g \cdot mol^{-1}$]	$[M+H]^+$ observed [$g \cdot mol^{-1}$]
1:0	5800	5424
1:1	8082	7980
1:2	10364	10463
1:3	12646	13105
1:4	14928	15701
1:5	17210	---
1:6	19492	18577
1:7	21774	22336

5.5.3 NCL with functional P(OEGA)s

5.5.3.1 Pretrial of NCL with thiolactone hydrochloride and cysteine hydrochloride

Cysteine hydrochloride (0.057 g, 0.33 mmol) was dissolved in dry methanol under argon atmosphere. $NaBH_4$ (0.025 g, 0.66 mmol) was added whereby gas development could be observed. The thiolactone was added (0.050 g, 0.33 mmol) and the solution was stirred overnight. A sample was extracted, dried under reduced pressure and was used for NMR measurements.

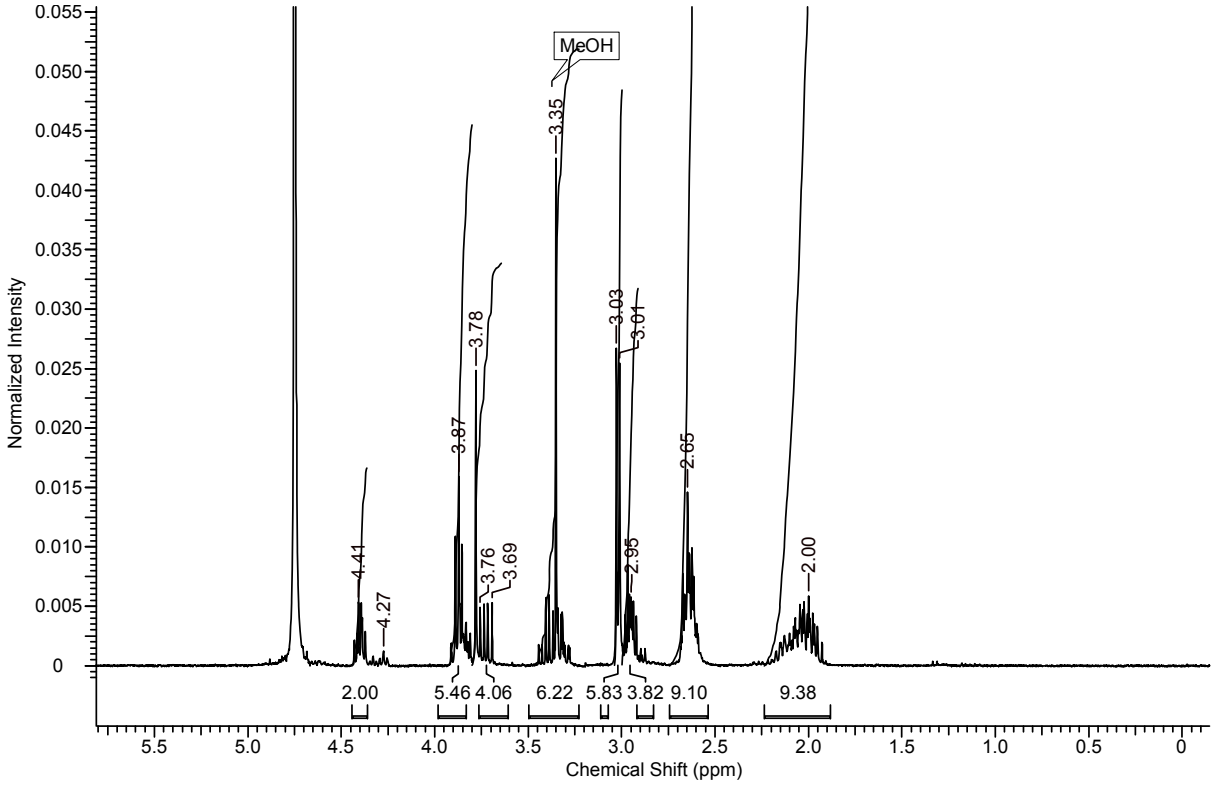

Figure 5–46: *^{1}H-NMR spectra of the pretrial of NCL with thiolactone- and cysteine hydrochloride (measured in D_2O).*

5.5.3.2 NCL of multiple thioester-functionalized P(OEGA) with cysteine-functionalized model peptide (FGGGC)

(*) Thiolactone functionalized P(OEGA) (M_n = 3600 g·mol^{-}1, 5 mg, 0.75 µmol) bearing five thioesters on the side-chain and a CGGGF-model-peptide (1.65 mg, 3.70 µmol) were dissolved in 150 µL ligation buffer (6 M Gn.HCl, 100 mM NaH_2PO_4, 50 mM TCEP.HCl, 200 mM MPAA) and the pH was adjusted to 6.9. The ligation was shaken at 25 °C for 4 hrs, then more peptide **1** (0.8 mg, 1.85 µmol) was added. The ligation was shaken at 25 °C overnight. It was then diluted to a total volume of 2 mL with ddH_2O and the reaction was subsequently purified by semi-preparative HPLC.

HPLC chromatograms are visible in **Figure 4–30** and **Figure 4–31**.

5.6 Nanogels with cysteine-functionalized POx

5.6.1 Self-assembly of cys-POx in millipore water

Two different polymers bearing 4% allyl or cysteine functionality in the structure, respectively, and a molecular weight of approximately 6000 or 6500 g·mol^{-1}, were dissolved in millipore water with concentrations between 5.0 and 0.1 mg·mL^{-1} and was measured directly in DLS and NTA after stirring. The first measured size in DLS is always the intensity distribution and the second value the volume distribution. If only one value is given, both were the same. The different values in NTA show the peaks of the whole distribution.

Table 5–19: *DLS and NTA measurements of self-assembled poly[(methyl-oxazoline)-co-(decenyl-oxazoline)] and cysteine-functionalized poly[(methyl-oxazoline)-co-(decenyl-oxazoline)] with different concentrations in aqueous solution.*

	5.0 [mg·mL^{-1}]		**2.0 [mg·mL^{-1}]**		**1.0 [mg·mL^{-1}]**		**0.5 [mg·mL^{-1}]**		**0.1 [mg·mL^{-1}]**	
	DLS [nm]	NTA [nm]	DLS [nm]	NTA [nm]	DLS [nm]	NTA [nm]	DLS [nm]	NTA [nm]	DLS [nm]	NTA [nm]
P[(MeOx)$_{0.9}$-*co*-(DecenOx)$_{0.1}$]$_{60}$	7 247	101 236 350	n.d.	n.d.	2 250	107 195	100	89 140 245	2	n.d.
P[(MeOx)$_{0.9}$-*co*-(cysDecenOx)$_{0.1}$]$_{60}$	n.d.	n.d.	180	n.d.	160	130 175	130	97 205	9	n.d.

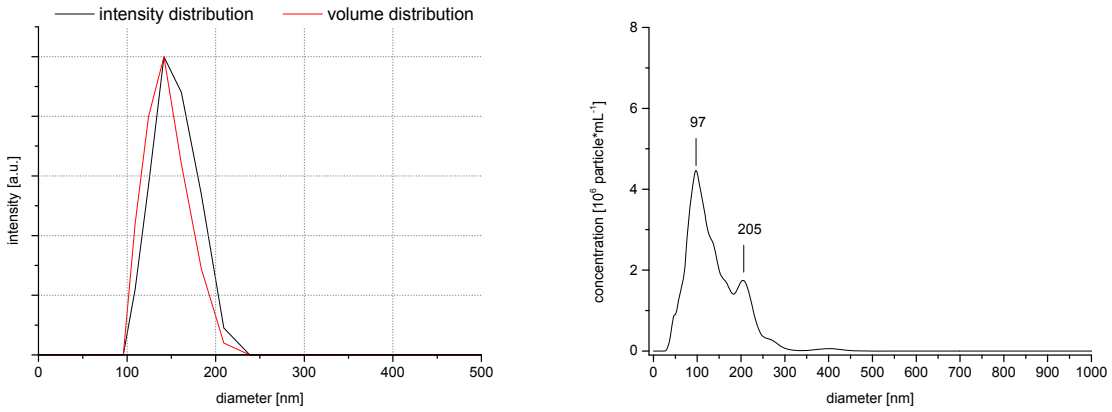

Figure 5–47: *DLS (left) and NTA (right) measurement of cysteine-functionalized, self-assembled poly[(methyl-oxazoline)-co-(decenyl-oxazoline)] particles in aqueous solution (concentration: 0.5 mg·mL^{-1}).*

5.6.2 Inverse mini-emulsion with cys-POx

Surfactant (76.9 mg of 3:1 weight ratio of Span 80 and Tween 80) dissolved in *n*-hexane (2.5 mL) was used as organic phase. The aqueous phase consisted of cys-POx (six cysteine residues per polymer chain, 6800 g·mol^{-1}, 25 mg, 4.47·10^{-3} mmol), dissolved in 250 µL of phosphate buffer (pH = 6). The organic and aqueous phases were combined by vortex. The icecold emulsion was ultrasonicated for 60 s (with an amplitude of 10%, 0.4 s pulse, 0.6 s pause). Glass vials of 18 mm in diameter were used for the nanogel synthesis. The horn immersed to the middle of the phase boundary during ultrasonication. Crosslinking was initiated by subsequent addition of H_2O_2 (30 µL, 0.1M) followed by a further sonication for 60 sec. After stirring for 20 min the reaction was quenched by the addition of 2-hydroxy acrylate (30 µL, 0.25 M solution in water) at pH = 7.4 and was additionally stirred for 20 min. Separation of the nanogels was achieved by centrifugation at 12000 rpm for 10 min followed by decantation of the supernatant. Nanogels present in the aqueous layer were carefully washed with *n*-hexane (2 x 500 µL) and THF (1 x 500 µL) in order to remove the surfactants and unreacted polymer. The remaining organic phase was removed by evaporation and rests of it by dialysis against distilled water (cut off: 10000 g·mol^{-1}). Purified nanogels were stored in millipore water at 4°C for further use.

DLS and NTA measurements are visible in **Figure 4–32**.

Figure 4–34 shows cryo-SEM and AFM measurements of cys-POx nanogels.

Chapter 6

Summary / Zusammenfassung

6.1 Summary

The **aim of this study** was to synthesize hydrophilic polymers that can extend the range of hydrophilic coatings and chemoselective functionalization of materials.

As hydrophilic polymers, **chemoselective poly(oxazolines) (POx) and poly[(oligo ethylene glycol) acrylates]** were synthesized. First, an initiator was produced for the preparation of poly(oxazoline) polymers capable of participating in click chemistry reactions which allows the functionalization of the polymer at the *α*-terminus. The successful synthesis was confirmed by ^{1}H-NMR spectroscopy. The initiator was subsequently used for the polymerization of hydrophilic 2-methyl-2-oxazoline (MeOx), whereby chemoselective, alkyne-functionalized polymers could be prepared for the Cu-catalyzed azide–alkyne cycloaddition. The desired molecular weight could be achieved through the living, ring-opening cationic polymerization and was confirmed by ^{1}H-NMR, SEC and MALDI-ToF measurements. Polymers were terminated with piperidine if no further functionalization was needed, or with an ester derivate for enabling amine attachment in a subsequent step. In addition, polymers were functionalized by termination with NaN_3 in order to provide the counterpart to the azide–alkyne reaction. Here, IR spectroscopy was suitable for the azide-detection. The coupling of the two polymers with each other showed the reactivity and could be confirmed by SEC, ^{1}H-NMR and IR spectroscopy.

The composition of **cysteine functionalized POx** was completed by thiol–ene chemistry. For this, a copolymer was synthesized with allyl side chains. Since the commercially available *iso*-2-propyl-2-oxazoline is not available for the cationic polymerization, 2-butenyl- and 2-decenyl-2-oxazoline (ButenOx and DecenOx) were first prepared in several steps. The synthesis of both copolymers, based on MeOx could be confirmed by ^{1}H-NMR as well as with SEC, whereby narrow distributions with dispersities of 1.06 could be achieved. The cysteine functionalization of the copolymers was enabled by the creation of a thiazolidine component which could be synthesized by acetal- and formyl-protection of cysteine and subsequent functionalization with a thiol. The component enabled the reaction of the polymer with a protected cysteine derivative by the thiol–ene reaction which was started by the addition of dimethoxyphenylacetophenone and was catalyzed by irradiation with UV light. Both copolymers, with a shorter hydrophobic sidechain, due to the use of

ButenOx during the polymerization, as well as polymers with longer hydrophobic sidechains (copolymers with DecenOx) could be functionalized by thiol–ene chemistry. ^{1}H-NMR spectroscopic analysis showed the complete disappearance of the allyl function and hence a quantitative reaction with the thiazolidine derivate. After deprotection by an acidic workup the desired, cysteine functionalized polymer could be isolated. **Quantification of cysteine-functions** was ensured by a modified TNBSA assay, whereby the thiols were first oxidized in order to confirm an independent measurement of amine functions. Both, the TNBSA assay as well as the NMR measurement showed a polymer with five cysteines and thus the desired number of cysteine residues.

In addition, the cytotoxicity of functionalized polymers with different compositions was tested by a **luminescent cell viability assay** (LCVA). Both, the amount of cysteine-functions (5–10%) inside the copolymers as well as the length of the hydrophobic side-chain were varied. All polymers did not show cytotoxicity up to concentrations of 10 mg·mL^{-1}. The cell activity and cell numbers only decreased below 50% and 20% respectively, when copolymers with 5% cysteine and longer sidechains were measured, which was attributed to a contamination of the sample itself. The cooperation partner performed **Native Chemical Ligation (NCL)** with various model peptides and purified the products by HPLC. In order to ensure the attachment of the highest amount of peptides to the polymer, a sterically non-demanding peptide was synthesized, consisting of an aromatic amino acid and four glycine units. The aromatic unit was used for the quantification of the polymer–peptide-conjugate in the ^{1}H-NMR spectroscopy. A polymer having five cysteine side-chains has been fully implemented by NCL to a conjugate of one polymer with five peptides. A sterically more demanding peptide was additionally used and MALDI-ToF measurements confirmed the successful conjugation.

Furthermore the cysteine-functionalized polymer was used for the synthesis of **nanogels**. Here, the thiol of the cysteine-function was oxidized in an inverse mini-emulsion by H_2O_2, resulting in nanogels (~500 nm) which could be confirmed by SEM, AFM, DLS and NTA measurements. Thus, these polymers are also conceivable for the use as a drug delivery system. Besides POx, **oligo (ethylene glycol)acrylates (OEGA)** were polymerized; by copolymerization with the reactive pentafluorophenyl acrylate (PFPA) reactive and amphiphilic polymers were obtained.

The synthesis of PFPA could be confirmed spectroscopically by ^{1}H-, ^{19}F-NMR, and by FT-IR. Copolymers were synthesized by RAFT polymerization with narrow dispersities and the desired molecular weights could be achieved. The functionalization with an amine functionalized thiazolidine led to a hydrophilic cysteine-functionalized polymer after acidic deprotection. Apart from this polymer, a **thioester-functionalization** was successfully performed by reaction of the active polymer with a cyclic amine-functionalized thioester. During NCL, this component does not release a toxic by-product (such as the resulting thiol) and thus features a very high potential to replace former thioester in this chemoselective coupling.

In the future the synthesis of such hydrophilic and functional polymers will expand the spectrum of producible biomaterials with permanent hydrophilic coatings and simultaneous orthogonal functionalization.

6.2 Zusammenfassung

Ziel dieser Arbeit war die Synthese von hydrophilen Polymeren, die das Spektrum für hydrophile Beschichtungen und chemoselektive Funktionalisierung von Materialien erweitern.

Als hydrophile Polymere wurden chemoselektive Poly(oxazoline) (POx) und Poly(oligoethylenglykol)acrylate synthetisiert. **Für die Darstellung von „klickfähigen" Poly(oxazolinen)** wurde zunächst ein Initiator synthetisiert, welcher eine Funktionalisierung des Polymers am *α*-Terminus ermöglicht. Die erfolgreiche Darstellung wurde mittels ^{1}H-NMR Spektroskopie bewiesen. Der Initiator wurde darauffolgend für die Polymerisation von hydrophilem 2-Methyl-2-oxazoline (MeOx) eingesetzt, wodurch chemoselektive, Alkin-funktionalisierte Polymere für die kupferkatalysierte Azid–Alkin-Cycloaddition dargestellt werden konnten. Die gewünschten Molmassen konnten jederzeit durch die lebende, ringöffnende kationische Polymerisation erreicht werden und durch ^{1}H-NMR sowie GPC- und MALDI-Messungen bewiesen werden. Die Terminierung der Polymere erfolgte durch Abbruch mit Piperidin, wenn keine weitere Funktionalisierung erwünscht war, oder durch Abbruch mit einem Ester-Derivat um die Anbindung mit Aminen zu ermöglichen. Außerdem wurden Polymere durch die Terminierung mit NaN_3 funktionalisiert, um das Pendant zur Azid–Alkin-Cycloaddition liefern zu können. Die IR-Spektroskopie eignete sich hierbei für die Azid-Detektion. Die Kopplung beider Polymere miteinander, zum Nachweis der Reaktivität, konnte durch die GPC, ^{1}H-NMR und IR-Spektroskopie bestätigt werden.

Die Darstellung von Cystein-funktionalisierten POx konnte durch Thiol–en Chemie realisiert werden. Dazu wurde zunächst ein Copolymer mit Allylseitenketten synthetisiert. Da das kommerziell erhältliche iso-Propyloxazoline nicht für die kationische Polymerisation zur Verfügung steht, wurden zunächst Butenyl- und Decenyloxazolin (ButenOx und DecenOx) über mehrere Stufen synthetisiert. Die Darstellung des Copolymers, basierend auf MeOx, konnte sowohl mit ^{1}H-NMR als auch mit der GPC bestätigt werden. Enge Verteilungen bis zu einer Disperistät von 1.06 wurden erreicht. Die Cysteinfunktionalisierung der Copolymere wurde durch die Synthese eines Thiazolidinbausteins ermöglicht. Dieser konnte durch Acetal- und Formylschützung von Cystein und anschließender Funktionalisierung mit einem Thiol

dargestellt werden. Der Baustein ermöglichte die Umsetzung des Polymers mit dem geschützten Cysteinderivat durch die Thiol–en Reaktion. Diese wurde durch Zugabe von Dimethoxyphenylacetophenon gestartet und durch Bestrahlung mit UV-Licht katalysiert. Sowohl Copolymere mit einer kürzeren hydrophoben Seitenkette, bedingt durch den Einsatz von ButenOx während der Polymerisation, als auch Polymere mit längeren hydrophoben Seitenketten (Copolymere mit DecenOx) konnten mittels Thiol–en Chemie funktionalisiert werden. ^{1}H-NMR spektroskopische Analysen zeigten das komplette Verschwinden der Doppelbindung und somit eine quantitative Umsetzung mit dem Thiazolidinderivat. Nach Entschützung durch saure Aufarbeitung konnte das gewünschte, Cystein-funktionalisierte Polymer isoliert werden. Die Quantifizierung der Cysteinfunktionen wurde durch einen modifizierten TNBSA assay gewährleistet, wobei die Thiole des Cysteins zunächst oxidiert wurden, damit diese keinen Einfluss auf die Messung haben konnten. Sowohl der TNBSA assay als auch die NMR-spektroskopische Messmethode zeigte bei einem Polymer mit fünf Cysteinseitenketten die gewünschte Anzahl von Cysteinresten.

Außerdem wurden die funktionalisierten Polymere mit unterschiedlichen Zusammensetzungen auf **Zelltoxizität** geprüft. Sowohl der Anteil an Cysteinfunktionen (5-10%) als auch die Länge der hydrophoben Seitenkette wurden variiert. Alle Polymere waren bis zu einer Konzentration von 1 mg·mL^{-1} nicht toxisch. Die Zellaktivität und Zellzahl sank nur beim Copolymer mit 5% Cystein und langer Seitenkette unter einen Wert von 50% bzw. 20%, was auf eine Verunreinigung der Probe zurückgeführt wurde. Der Kooperationspartner führte die **Native Chemische Ligation (NCL)** mit verschiedenen Modellpeptiden durch und reinigte die Produkte mittels HPLC. Um das Anbinden von möglichst vielen Peptiden an das Polymer zu gewährleisten, wurden sterisch unanspruchsvolle Peptide synthetisiert, die aus einer aromatischen Aminosäure und vier Glycineinheiten bestanden. Der Aromat konnte in der ^{1}H-NMR Spektroskopie für die Quantifizierung der Polymer–Peptid-Konjugate genutzt werden. Ein Polymer mit fünf Cysteinseitenketten wurde vollständig mittels NCL zu einem Konjugat aus einem Polymer mit fünf Peptiden umgesetzt. Ein sterisch anspruchsvolleres Peptid wurde im Nachhinein verwendet, wobei MALDI-ToF Messungen die Konjugation bestätigten. Das cysteinfunktionaliserte Polymer wurde außerdem für die Nanogelsynthese verwendet. Hierbei wurde das Thiol der Cysteinfunktion mittels H_2O_2 in einer inversen Miniemulsion oxidiert, woraus

Nanogele resultierten, die mittels REM, AFM, DLS und NTA bestätigt werden konnten. Somit sind diese Polymere auch für die Anwendung als Drug Delivery System denkbar.

Neben den Poly(oxazolinen) wurden (Oligoehtylenglykol)acrylate polymerisiert und durch Copolymerisation mit Pentafluorophenylacrylat reaktive, amphiphile Polymere erhalten. Die Darstellung von Pentafluorophenylacrylat konnte durch ^{1}H- und ^{19}F-NMR als auch durch FT-IR spektroskopisch bestätigt werden. Copolymere wurden mittels RAFT Polymerisation mit engen Dispersitäten und den gewünschten Molmassen synthetisiert. Die Funktionalisierung mit einem aminfunktionalisierten Thiazolidin führte nach saurer Entschützung zu einem hydrophilen cysteinfunktionalisierten Polymer. Neben dieser Komponente konnte eine Thioesterfunktionalisierung durch Reaktion mit einem cyclischen aminfunktionalisierten Thiolacton erfolgreich durchgeführt werden. Dieser setzt bei der NCL keine toxischen Nebenprodukte (wie das entstehende Thiol) frei und hat somit ein hohes Potential, frühere Thioester in dieser chemoselektiven Kopplung, gerade im Bezug auf Biomaterialien zu ersetzen.

Die Synthesen der hydrophilen, funktionalen Polymere sind Vorarbeiten für hydrophile Polymere die das Spektrum für permanente hydrophile Beschichtungen bei gleichzeitiger orthogonalen Funktionalisierung von Biomaterialien in Zukunft erweitern.

Literature

1 Williams, D. F. "Consensus and definitions in biomaterials" in *Advances in biomaterials*; Vol. 8; de Putter, C., de Lange, K., de Groot, K., Lee, A. J. C., Eds.; Elsevier Science Publishers B.V.: Amsterdam, 1988, p. 11.

2 Wintermantel, E.; Ha, S.-W. *Medizintechnik - Life Science Engineering*; 5 ed.; Springer-Verlag: Berlin, Heidelberg, 2009.

3 Williams, D. F.: "On the nature of biomaterials." *Biomaterials* **2009**, *30*, 5897.

4 Dingels, C.; Schömer, M.; Frey, H.: "Die vielen Gesichter des Poly(ethylenglykol)s." *Chemie in unserer Zeit* **2011**, *45*, 338.

5 Götz, H.; Beginn, U.; Bartelink, C. F.; Grünbauer, H. J. M.; Möller, M.: "Preparation of Isophorone Diisocyanate Terminated Star Polyethers." *Macromolecular Materials and Engineering* **2002**, *287*, 223.

6 Knop, K.; Hoogenboom, R.; Fischer, D.; Schubert, U. S.: "Poly(ethylene glycol) in Drug Delivery: Pros and Cons as Well as Potential Alternatives." *Angewandte Chemie International Edition* **2010**, *49*, 6288.

7 Lutz, J.-F.: "Polymerization of oligo(ethylene glycol) (meth)acrylates: Toward new generations of smart biocompatible materials." *Journal of Polymer Science Part A: Polymer Chemistry* **2008**, *46*, 3459.

8 Luxenhofer, R.; Han, Y.; Schulz, A.; Tong, J.; He, Z.; Kabanov, A. V.; Jordan, R.: "Poly(2-oxazoline)s as Polymer Therapeutics." *Macromolecular Rapid Communications* **2012**, *33*, 1613.

9 Fraser, J. R. E.; Laurent, T. C.; Laurent, U. B. G.: "Hyaluronan: its nature, distribution, functions and turnover." *Journal of Internal Medicine* **1997**, *242*, 27.

10 Burdick, J. A.; Prestwich, G. D.: "Hyaluronic Acid Hydrogels for Biomedical Applications." *Advanced Materials* **2011**, *23*, H41.

11 Ramshaw, J. A. M.; Werkmeister, J. A.; Peters, D. E. "Collagen as a biomaterial" in *Current perspectives on implantable devices*; D.F., W., Ed.; Jai Press Ltd: London, 1990, p. 151.

12 Dang, V.-L.; Dang, M.-H. "Chitin and its derivates" in *The polymeric materials encyclopedia synthesis, properties and applications*; J.C., S., Ed.; CRC Press: Boca Raton, 1995, p.

13 Grey, E. G.: "Fibrin as a haemostatic in cerebral surgery." *Surgery, Gynecology and Obstetrics* **1915**, *21*, 452.

14 Shu, X. Z.; Ghosh, K.; Liu, Y.; Palumbo, F. S.; Luo, Y.; Clark, R. A.; Prestwich, G. D.: "Attachment and spreading of fibroblasts on an RGD peptide–modified injectable hyaluronan hydrogel." *Journal of Biomedical Materials Research Part A* **2004**, *68A*, 365.

15 Rutjes, A. W. S.; Jüni, P.; da Costa, B. R.; Trelle, S.; Nüesch, E.; Reichenbach, S.: "Viscosupplementation for Osteoarthritis of the KneeA Systematic Review and Meta-analysis." *Annals of Internal Medicine* **2012**, *157*, 180.

16 Franck, A.; Biederbick, K. *Kunststoff-Kompendium*; Vogel Fachbuch: Werkstoffkunde: Würzburg, 1990.

17 Jones, D. W. "Materials for fixed and removable prosthodontics" in *Materials Science and Technology*; Vol. 14; Cahn, R. W., Haasen, P., Kramer, E. J., Eds.; VCH-Verlag: Weinheim, 1992, p. 429.
18 Williams, D. F. "Materials for ophthalmology" in *Materials Science and Technology*; Vol. 14; Cahn, R. W., Haasen, P., Kramer, E. J., Eds.; VCH-Verlag: Weinheim, 1992, p. 415.
19 Lidgren, L.; Bodelind, B.; Moller, J.: "Bone cement improved by vacuum mixing and chilling." *Acta Orthopaedica Scandinavica* **1987**, *58*, 27.
20 Williams, D. F. "Polytetrafluorethylene" in *Concise encyclopedia of medical and dental materials*; Williams, D. F., Ed.; Pergamon Press: Oxford, 1990, p. 299.
21 Iordanskii, A. L.; T.E., R.; Zaikov, G. E. *Interaction of polymers in bioactive and corrosive media*; VSP BV: Utrecht, The Netherlands, 1994.
22 de Koning, G. J. M. "Prospects of bacterial poly[(R)-3-hydroxyalkanoates]", 1993.
23 Sun, H.; Mei, L.; Song, C.; Cui, X.; Wang, P.: "The in vivo degradation, absorption and excretion of PCL-based implant." *Biomaterials* **2006**, *27*, 1735.
24 Miner, M. R.; Berzins, D. W.; Bahcall, J. K.: "A Comparison of Thermal Properties Between Gutta-Percha and a Synthetic Polymer Based Root Canal Filling Material (Resilon)." *Journal of Endodontics* **2006**, *32*, 683.
25 Jones, D. S.; Djokic, J.; McCoy, C. P.; Gorman, S. P.: "Poly(ε-caprolactone) and poly(ε-caprolactone)-polyvinylpyrrolidone-iodine blends as ureteral biomaterials: characterisation of mechanical and surface properties, degradation and resistance to encrustation in vitro." *Biomaterials* **2002**, *23*, 4449.
26 Middleton, J. C.; Tipton, A. J.: "Synthetic biodegradable polymers as orthopedic devices." *Biomaterials* **2000**, *21*, 2335.
27 Woodruff, M. A.; Hutmacher, D. W.: "The return of a forgotten polymer—Polycaprolactone in the 21st century." *Progress in Polymer Science* **2010**, *35*, 1217.
28 Langer, R.: "New methods of drug delivery." *Science* **1990**, *249*, 1527.
29 Langer, R.; Cima, L. G.; Tamada, J. A.; Wintermantel, E.: "Future directions in biomaterials." *Biomaterials* **1990**, *11*, 738.
30 Mathiowitz, E.; Amato, C.; Dor, P.; Langer, R.: "Polyanhydride microspheres: 3. Morphology and characterization of systems made by solvent removal." *Polymer* **1990**, *31*, 547.
31 Benagiano, G.; Gabelnick, H. L.: "Biodegradable systems for the sustained release of fertility-regulating agents." *Journal of Steroid Biochemistry* **1979**, *11*, 449.
32 Frisch, E. E. "Polysiloxanes" in *Concise encyclopedia of medical and dental materials*; Williams, D. F., Ed.; Pergamon Press: Oxford, 1990, p. 289.
33 Szycher, M.: "Biostability of Polyurethane Elastomers: A Critical Review." *Journal of Biomaterials Applications* **1988**, *3*, 297.
34 Zhang, Z.; King, M. W.; Guidoin, R.; Therrien, M.; Pezolet, M.; Adnot, A.; Ukpabi, P.; Vantal, M. H.: "Morphological, physical and chemical evaluation of the Vascugraft arterial prosthesis: comparison of a novel polyurethane device with other microporous structures." *Biomaterials* **1994**, *15*, 483.
35 Planck, H. *Kunststoffe und Elastomere in der Medizin*; Verlag W. Kohlhammer: Stuttgart, 1993.

36 Chu, C. C. "Polyesters and polyamides " in *Concise encyclopedia of medical and dental materials*; Williams, D. F., Ed.; Pergamon Press: Oxford, 1990, p. 261.

37 Wening, J. V.; Marquardt, H.; Katzer, A.; Jungbluth, K. H.; Marquardt, H.: "Cytotoxicity and mutagenicity of Kevlar®: an in vitro evaluation." *Biomaterials* **1995**, *16*, 337.

38 D'Adriano, M. D.; Latour, R. A.; Kennedy, J. M.; Schutte, H. D.; Freidman, R. J. "Long term shear strength durability of carbon fiber reinforced PEEK composite in physiological saline" in *The 20th annual meeting of the society for biomaterials* Boston, MA, USA, 1994, p. 184.

39 Zhang, G.; Latour, R. A.; Kennedy, J. M.; Schutte, H. D.; R.J., F. "Long term compressive strength durability of carbon fiber reinforced PEEK composite in physiological saline" in *The 20th annual meeting of the society for biomaterials* Boston, MA, USA, 1994, p. 160.

40 Wichterle, O. "Hydrogels" in *Encyclopedia of polymer science and technology*; Mark, H. F., Gaylord, N. G., Eds.; Interscience: New York, 1971, p. 273.

41 Lantos, P. R.: "Plastics in Medical Applications." *Journal of Biomaterials Applications* **1987**, *2*, 358.

42 Deiters, A.; Cropp, T. A.; Summerer, D.; Mukherji, M.; Schultz, P. G.: "Site-specific PEGylation of proteins containing unnatural amino acids." *Bioorganic & Medicinal Chemistry Letters* **2004**, *14*, 5743.

43 Mantovani, G.; Lecolley, F. o.; Tao, L.; Haddleton, D. M.; Clerx, J.; Cornelissen, J. J. L. M.; Velonia, K.: "Design and Synthesis of N-Maleimido-Functionalized Hydrophilic Polymers via Copper-Mediated Living Radical Polymerization: A Suitable Alternative to PEGylation Chemistry." *Journal of the American Chemical Society* **2005**, *127*, 2966.

44 Hamidi, M.; Azadi, A.; Rafiei, P.: "Pharmacokinetic Consequences of Pegylation." *Drug Delivery* **2006**, *13*, 399.

45 Zarafshani, Z.; Obata, T.; Lutz, J.-F.: "Smart PEGylation of Trypsin." *Biomacromolecules* **2010**, *11*, 2130.

46 Nischan, N.; Hackenberger, C. P. R.: "Site-specific PEGylation of Proteins: Recent Developments." *Journal of Organic Chemistry* **2014**, *79*, 10727.

47 Szwarc, M.: ""Living" Polymers." *Nature* **1956**, *178*, 1168.

48 Flory, P. J.: "Molecular Size Distribution in Ethylene Oxide Polymers." *Journal of the American Chemical Society* **1940**, *62*, 1561.

49 Moad, G.; Rizzardo, E.; Thang, S. H.: "Living Radical Polymerization by the RAFT Process." *Australian Journal of Chemistry* **2005**, *58*, 379.

50 Stepto, R. F. T.: "Dispersity in polymer science (IUPAC Recommendation 2009)." *Polymer International* **2010**, *59*, 23.

51 Strobl, G. *The Physics of Polymers*; Springer: Berlin Heidelberg New York, 2006.

52 Garay, R. P.; Labaune, J. P.: "Immunogenicity of Polyethylene Glycol (PEG)." *The Open Conference Proceedings Journal* **2011**, *2*, 104.

53 Tagami, T.; Nakamura, K.; Shimizu, T.; Yamazaki, N.; Ishida, T.; Kiwada, H.: "CpG motifs in pDNA-sequences increase anti-PEG IgM production induced by PEG-coated pDNA-lipoplexes." *Journal of Controlled Release* **2010**, *142*, 160.

54 Schellekens, H.; Hennink, W. E.; Brinks, V.: "The Immunogenicity of Polyethylene Glycol: Facts and Fiction." *Pharmaceutical Research* **2013**, *30*, 1729.

55 Barz, M.; Luxenhofer, R.; Zentel, R.; Vicent, M. J.: "Overcoming the PEG-addiction: well-defined alternatives to PEG, from structure-property relationships to better defined therapeutics." *Polymer Chemistry* **2011**, *2*, 1900.

56 Viegas, T. X.; Bentley, M. D.; Harris, J. M.; Fang, Z.; Yoon, K.; Dizman, B.; Weimer, R.; Mero, A.; Pasut, G.; Veronese, F. M.: "Polyoxazoline: Chemistry, Properties, and Applications in Drug Delivery." *Bioconjugate Chemistry* **2011**, *22*, 976.

57 Kagiya, T.; Narisawa, S.; Maeda, T.; Fukui, K.: "Ring-opening polymerization of 2-substituted 2-oxazolines." *Journal of Polymer Science Part B: Polymer Letters* **1966**, *4*, 441.

58 Bassiri, T. G.; Levy, A.; Litt, M.: "Polymerization of cyclic imino ethers. I. Oxazolines." *Journal of Polymer Science Part B: Polymer Letters* **1967**, *5*, 871.

59 Levy, A.; Litt, M.: "Polymerization of cyclic iminoethers. V. 1,3-oxazolines with hydroxy-, acetoxy-, and carboxymethyl-alkyl groups in the 2 position and their polymers." *Journal of Polymer Science Part A-1: Polymer Chemistry* **1968**, *6*, 1883.

60 Goddard, P.; Hutchinson, L. E.; Brown, J.; Brookman, L. J.: "Soluble polymeric carriers for drug delivery. Part 2. Preparation and in vivo behaviour of N-acylethylenimine copolymers." *Journal of Controlled Release* **1989**, *10*, 5.

61 Manzenrieder, F.; Luxenhofer, R.; Retzlaff, M.; Jordan, R.; Finn, M. G.: "Stabilization of Virus-like Particles with Poly(2-oxazoline)s." *Angewandte Chemie International Edition* **2011**, *50*, 2601.

62 Mero, A.; Pasut, G.; Via, L. D.; Fijten, M. W. M.; Schubert, U. S.; Hoogenboom, R.; Veronese, F. M.: "Synthesis and characterization of poly(2-ethyl 2-oxazoline)-conjugates with proteins and drugs: Suitable alternatives to PEG-conjugates?" *Journal of Controlled Release* **2008**, *125*, 87.

63 Tong, J.; Luxenhofer, R.; Yi, X.; Jordan, R.; Kabanov, A. V.: "Protein Modification with Amphiphilic Block Copoly(2-oxazoline)s as a New Platform for Enhanced Cellular Delivery." *Molecular Pharmaceutics* **2010**, *7*, 984.

64 Volet, G.; Chanthavong, V.; Wintgens, V.; Amiel, C.: "Synthesis of Monoalkyl End-Capped Poly(2-methyl-2-oxazoline) and Its Micelle Formation in Aqueous Solution." *Macromolecules* **2005**, *38*, 5190.

65 Gaertner, F. C.; Luxenhofer, R.; Blechert, B.; Jordan, R.; Essler, M.: "Synthesis, biodistribution and excretion of radiolabeled poly(2-alkyl-2-oxazoline)s." *Journal of Controlled Release* **2007**, *119*, 291.

66 Woodle, M. C.; Engbers, C. M.; Zalipsky, S.: "New Amphipatic Polymer-Lipid Conjugates Forming Long-Circulating Reticuloendothelial System-Evading Liposomes." *Bioconjugate Chemistry* **1994**, *5*, 493.

67 Bauer, M.; Lautenschlaeger, C.; Kempe, K.; Tauhardt, L.; Schubert, U. S.; Fischer, D.: "Poly(2-ethyl-2-oxazoline) as Alternative for the Stealth Polymer Poly(ethylene glycol): Comparison of in vitro Cytotoxicity and Hemocompatibility." *Macromolecular Bioscience* **2012**, *12*, 986.

68 Luxenhofer, R.; Sahay, G.; Schulz, A.; Alakhova, D.; Bronich, T. K.; Jordan, R.; Kabanov, A. V.: "Structure-property relationship in cytotoxicity and cell

uptake of poly(2-oxazoline) amphiphiles." *Journal of Controlled Release* **2011**, *153*, 73.
69 Hoogenboom, R.: "Poly(2-oxazoline)s: A Polymer Class with Numerous Potential Applications." *Angewandte Chemie International Edition* **2009**, *48*, 7978.
70 Sedlacek, O.; Monnery, B. D.; Filippov, S. K.; Hoogenboom, R.; Hruby, M.: "Poly(2-Oxazoline)s – Are They More Advantageous for Biomedical Applications Than Other Polymers?" *Macromolecular Rapid Communications* **2012**, *33*, 1648.
71 Gabriel, S.; Eschenbach, G.: "Ueber Dibromdiäthylamin." *Berichte der deutschen chemischen Gesellschaft* **1897**, *30*, 809.
72 McManus, H. A.; Guiry, P. J.: "Recent Developments in the Application of Oxazoline-Containing Ligands in Asymmetric Catalysis." *Chemical Reviews* **2004**, *104*, 4151.
73 Meyers, A. I.; Mihelich, E. D.: "The Synthetic Utility of 2-Oxazolines." *Angewandte Chemie International Edition* **1976**, *15*, 270.
74 Aoi, K.; Okada, M.: "Polymerization of oxazolines." *Progress in Polymer Science* **1996**, *21*, 151.
75 Adams, N.; Schubert, U. S.: "Poly(2-oxazolines) in biological and biomedical application contexts." *Advanced Drug Delivery Reviews* **2007**, *59*, 1504.
76 Kobayashi, S.: "Ethylenimine polymers." *Progress in Polymer Science* **1990**, *15*, 751.
77 Kobayashi, S.; Uyama, H.: "Polymerization of cyclic imino ethers: From its discovery to the present state of the art." *Journal of Polymer Science Part A: Polymer Chemistry* **2002**, *40*, 192.
78 Litt, M.; Levy, A.; Herz, J.: "Polymerization of Cyclic Imino Ethers. X. Kinetics, Chain Transfer, and Repolymerization." *Journal of Macromolecular Science, Chemistry* **1975**, *9*, 703.
79 Hoogenboom, R.; Paulus, R. M.; Fijten, M. W. M.; Schubert, U. S.: "Concentration effects in the cationic ring-opening polymerization of 2-ethyl-2-oxazoline in N,N-dimethylacetamide." *Journal of Polymer Science Part A: Polymer Chemistry* **2005**, *43*, 1487.
80 Gress, A.; Völkel, A.; Schlaad, H.: "Thio-Click Modification of Poly[2-(3-butenyl)-2-oxazoline]." *Macromolecules* **2007**, *40*, 7928.
81 Kedracki, D.; Chekini, M.; Maroni, P.; Schlaad, H.; Nardin, C.: "Synthesis and Self-Assembly of a DNA Molecular Brush." *Biomacromolecules* **2014**, *15*, 3375.
82 Kedracki, D.; Maroni, P.; Schlaad, H.; Vebert-Nardin, C.: "Polymer–Aptamer Hybrid Emulsion Templating Yields Bioresponsive Nanocapsules." *Advanced Functional Materials* **2014**, *24*, 1133.
83 Dargaville, T. R.; Forster, R.; Farrugia, B. L.; Kempe, K.; Voorhaar, L.; Schubert, U. S.; Hoogenboom, R.: "Poly(2-oxazoline) Hydrogel Monoliths via Thiol-ene Coupling." *Macromolecular Rapid Communications* **2012**, *33*, 1695.
84 Wiesbrock, F.; Hoogenboom, R.; Leenen, M. A. M.; Meier, M. A. R.; Schubert, U. S.: "Investigation of the Living Cationic Ring-Opening Polymerization of 2-Methyl-, 2-Ethyl-, 2-Nonyl-, and 2-Phenyl-2-oxazoline in a Single-Mode Microwave Reactor†." *Macromolecules* **2005**, *38*, 5025.

85 Lava, K.; Verbraeken, B.; Hoogenboom, R.: "Poly(2-oxazoline)s and click chemistry: A versatile toolbox toward multi-functional polymers." *European Polymer Journal* **2015**, *65*, 98.
86 Cesana, S.; Kurek, A.; Baur, M. A.; Auernheimer, J.; Nuyken, O.: "Polymer-Bound Thiol Groups on Poly(2-oxazoline)s." *Macromolecular Rapid Communications* **2007**, *28*, 608.
87 Durek, T.; Becker, C. F. W.: "Protein semi-synthesis: New proteins for functional and structural studies." *Biomolecular Engineering* **2005**, *22*, 153.
88 Lahiri, S.; Brehs, M.; Olschewski, D.; Becker, C. F. W.: "Total Chemical Synthesis of an Integral Membrane Enzyme: Diacylglycerol Kinase from Escherichia coli." *Angewandte Chemie International Edition* **2011**, *50*, 3988.
89 Hu, B.-H.; Su, J.; Messersmith, P. B.: "Hydrogels Cross-Linked by Native Chemical Ligation." *Biomacromolecules* **2009**, *10*, 2194.
90 Luxenhofer, R. "Novel functional poly(2-oxazoline)s as potential carriers for biomedical application", Technische Universität München, 2007.
91 Luxenhofer, R.; Jordan, R.: "Click Chemistry with Poly(2-oxazoline)s." *Macromolecules* **2006**, *39*, 3509.
92 Taubmann, C.; Luxenhofer, R.; Cesana, S.; Jordan, R.: "First Aldehyde-Functionalized Poly(2-oxazoline)s for Chemoselective Ligation." *Macromolecular Bioscience* **2005**, *5*, 603.
93 Satoh, T.; Ihara, R.; Kawato, D.; Nishikawa, N.; Suemasa, D.; Kondo, Y.; Fuchise, K.; Sakai, R.; Kakuchi, T.: "Precise Synthesis of Clickable Poly(n-hexyl isocyanate)." *Macromolecules* **2012**, *45*, 3677.
94 Kempe, K.; Hoogenboom, R.; Jaeger, M.; Schubert, U. S.: "Three-Fold Metal-Free Efficient ("Click") Reactions onto a Multifunctional Poly(2-oxazoline) Designer Scaffold." *Macromolecules* **2011**, *44*, 6424.
95 Buruaga, L.; Gonzalez, A.; Iruin, J.: "Electrospinning of poly (2-ethyl-2-oxazoline)." *Journal of Materials Science* **2009**, *44*, 3186.
96 Hochleitner, G.; Hümmer, J. F.; Luxenhofer, R.; Groll, J.: "High definition fibrous poly(2-ethyl-2-oxazoline) scaffolds through melt electrospinning writing." *Polymer* **2014**, *55*, 5017.
97 http://serinatherapeutics.com/news/#press.
98 Lutz, J.-F.; Andrieu, J.; Üzgün, S.; Rudolph, C.; Agarwal, S.: "Biocompatible, Thermoresponsive, and Biodegradable: Simple Preparation of "All-in-One" Biorelevant Polymers." *Macromolecules* **2007**, *40*, 8540.
99 Chua, G. B. H.; Roth, P. J.; Duong, H. T. T.; Davis, T. P.; Lowe, A. B.: "Synthesis and Thermoresponsive Solution Properties of Poly[oligo(ethylene glycol) (meth)acrylamide]s: Biocompatible PEG Analogues." *Macromolecules* **2012**, *45*, 1362.
100 Neugebauer, D.: "Graft copolymers with poly(ethylene oxide) segments." *Polymer International* **2007**, *56*, 1469.
101 Han, S.; Hagiwara, M.; Ishizone, T.: "Synthesis of Thermally Sensitive Water-Soluble Polymethacrylates by Living Anionic Polymerizations of Oligo(ethylene glycol) Methyl Ether Methacrylates." *Macromolecules* **2003**, *36*, 8312.
102 Lutz, J.-F.; Hoth, A.: "Preparation of Ideal PEG Analogues with a Tunable Thermosensitivity by Controlled Radical Copolymerization of 2-(2-Methoxyethoxy)ethyl Methacrylate and Oligo(ethylene glycol) Methacrylate." *Macromolecules* **2006**, *39*, 893.

103 Vancoillie, G.; Frank, D.; Hoogenboom, R.: "Thermoresponsive poly(oligo ethylene glycol acrylates)." *Progress in Polymer Science* **2014**, *39*, 1074.

104 Hawker, C. J.; Bosman, A. W.; Harth, E.: "New Polymer Synthesis by Nitroxide Mediated Living Radical Polymerizations." *Chemical Reviews* **2001**, *101*, 3661.

105 Moad, G.; Rizzardo, E.: "Alkoxyamine-Initiated Living Radical Polymerization: Factors Affecting Alkoxyamine Homolysis Rates." *Macromolecules* **1995**, *28*, 8722.

106 Sciannamea, V.; Jérôme, R.; Detrembleur, C.: "In-Situ Nitroxide-Mediated Radical Polymerization (NMP) Processes: Their Understanding and Optimization." *Chemical Reviews* **2008**, *108*, 1104.

107 Tebben, L.; Studer, A.: "Nitroxide: Anwendungen in der Synthese und in der Polymerchemie." *Angewandte Chemie* **2011**, *123*, 5138.

108 Rizzardo, E.; Solomon, D. H.: "On the Origins of Nitroxide Mediated Polymerization (NMP) and Reversible Addition–Fragmentation Chain Transfer (RAFT)*." *Australian Journal of Chemistry* **2012**, *65*, 945.

109 Le, T. P.; Moad, G.; Rizzardo, E.; Thang, S. H.: "Polymerization with living characteristics." *US7714075 B1*, **2010**.

110 Chiefari, J.; Chong, Y. K.; Ercole, F.; Krstina, J.; Jeffery, J.; Le, T. P. T.; Mayadunne, R. T. A.; Meijs, G. F.; Moad, C. L.; Moad, G.; Rizzardo, E.; Thang, S. H.: "Living Free-Radical Polymerization by Reversible Addition−Fragmentation Chain Transfer: The RAFT Process." *Macromolecules* **1998**, *31*, 5559.

111 Keddie, D. J.; Moad, G.; Rizzardo, E.; Thang, S. H.: "RAFT Agent Design and Synthesis." *Macromolecules* **2012**, *45*, 5321.

112 Bodanszky, M. *Principles of Peptide Synthesis*; Springer-Verlag: Berlin, Heidelberg, 1993.

113 Wieland, T.; Schäfer, W.; Bokelmann, E.: "Über Peptidsynthesen V. Über eine bequeme Darstellungsweise von Acylthiophenolen und ihre Verwendung zu Amid- und Peptid-Synthesen." *Justus Liebigs Annalen der Chemie* **1951**, *573*, 99.

114 Wieland, T.; Bokelmann, E.; Bauer, L.; Lang, H. U.; Lau, H.: "Über Peptidsynthesen. 8. Mitteilung Bildung von S-haltigen Peptiden durch intramolekulare Wanderung von Aminoacylresten." *Justus Liebigs Annalen der Chemie* **1953**, *583*, 129.

115 Gais, H.-J.: "Synthese von Thiol- und Selenolestern aus Carbonsäuren und Thiolen bzw. Selenolen." *Angewandte Chemie* **1977**, *89*, 251.

116 Pollak, A.; Blumenfeld, H.; Wax, M.; Baughn, R. L.; Whitesides, G. M.: "Enzyme immobilization by condensation copolymerization into crosslinked polyacrylamide gels." *Journal of the American Chemical Society* **1980**, *102*, 6324.

117 Das, A.; Theato, P.: "Activated Ester Containing Polymers: Opportunities and Challenges for the Design of Functional Macromolecules." *Chemical Reviews* **2016**, *116*, 1434.

118 Kisfaludy, L.; Löw, M.; Nyéki, O.; Szirtes, T.; Schőn, I.: "Die Verwendung von Pentafluorphenylestern bei Peptidsynthesen." *Justus Liebigs Annalen der Chemie* **1973**, *1973*, 1421.

119 Beija, M.; Li, Y.; Lowe, A. B.; Davis, T. P.; Boyer, C.: "Factors influencing the synthesis and the post-modification of PEGylated pentafluorophenyl acrylate containing copolymers." *European Polymer Journal* **2013**, *49*, 3060.

120 Jones, M. W.; Gibson, M. I.; Mantovani, G.; Haddleton, D. M.: "Tunable thermo-responsive polymer-protein conjugates via a combination of nucleophilic thiol-ene "click" and SET-LRP." *Polymer Chemistry* **2011**, *2*, 572.

121 Gelbrich, T.; Reinartz, M.; Schmidt, A. M.: "Active Ester Functional Single Core Magnetic Nanostructures as a Versatile Immobilization Matrix for Effective Bioseparation and Catalysis." *Biomacromolecules* **2010**, *11*, 635.

122 Liu, G. Y.; Qiu, Q.; An, Z. S.: "Development of thermosensitive copolymers of poly(2-methoxyethyl acrylate-co-poly(ethylene glycol) methyl ether acrylate) and their nanogels synthesized by RAFT dispersion polymerization in water." *Polymer Chemistry* **2012**, *3*, 504.

123 Micic, M.; Suljovrujic, E.: "Network parameters and biocompatibility of p(2-hydroxyethyl methacrylate/itaconic acid/oligo(ethylene glycol) acrylate) dual-responsive hydrogels." *European Polymer Journal* **2013**, *49*, 3223.

124 Negru, I.; Teodorescu, M.; Stanescu, P. O.; Draghici, C.; Lungu, A.; Sarbu, A.: "Thermogelation Properties of ABA Triblock Copolymers of Poly(Ethylene Glycol) (B) and Copolyacrylates of Oligo(Ethylene Glycol)s (A) in Aqueous Solution." *Soft Materials* **2013**, *11*, 149.

125 Hou, L.; Ma, K.; An, Z. S.; Wu, P. Y.: "Exploring the Volume Phase Transition Behavior of POEGA- and PNIPAM-Based Core-Shell Nanogels from Infrared-Spectral Insights." *Macromolecules* **2014**, *47*, 1144.

126 Steinhauer, W.; Keul, H.; Möller, M.: "Synthesis of reversible and irreversible cross-linked (M)PEG-(meth)acrylate based functional copolymers." *Polymer Chemistry* **2011**, *2*, 1803.

127 Viswanathan, P.; Themistou, E.; Ngamkham, K.; Reilly, G. C.; Armes, S. P.; Battaglia, G.: "Controlling Surface Topology and Functionality of Electrospun Fibers on the Nanoscale using Amphiphilic Block Copolymers To Direct Mesenchymal Progenitor Cell Adhesion." *Biomacromolecules* **2014**, *16*, 66.

128 Gentsch, R.; Pippig, F.; Nilles, K.; Theato, P.; Kikkeri, R.; Maglinao, M.; Lepenies, B.; Seeberger, P. H.; Börner, H. G.: "Modular Approach toward Bioactive Fiber Meshes Carrying Oligosaccharides." *Macromolecules* **2010**, *43*, 9239.

129 Kolb, H. C.; Finn, M. G.; Sharpless, K. B.: "Click-Chemie: diverse chemische Funktionalität mit einer Handvoll guter Reaktionen." *Angewandte Chemie* **2001**, *113*, 2056.

130 Rostovtsev, V. V.; Green, L. G.; Fokin, V. V.; Sharpless, K. B.: "A Stepwise Huisgen Cycloaddition Process: Copper(I)-Catalyzed Regioselective “Ligation” of Azides and Terminal Alkynes." *Angewandte Chemie International Edition* **2002**, *41*, 2596.

131 Tornøe, C. W.; Christensen, C.; Meldal, M.: "Peptidotriazoles on Solid Phase: [1,2,3]-Triazoles by Regiospecific Copper(I)-Catalyzed 1,3-Dipolar Cycloadditions of Terminal Alkynes to Azides." *Journal of Organic Chemistry* **2002**, *67*, 3057.

132 Link, A. J.; Tirrell, D. A.: "Cell Surface Labeling of Escherichia coli via Copper(I)-Catalyzed [3+2] Cycloaddition." *Journal of the American Chemical Society* **2003**, *125*, 11164.

133 Agard, N. J.; Prescher, J. A.; Bertozzi, C. R.: "A Strain-Promoted [3 + 2] Azide−Alkyne Cycloaddition for Covalent Modification of Biomolecules in Living Systems." *Journal of the American Chemical Society* **2004**, *126*, 15046.

134 Prescher, J. A.; Bertozzi, C. R.: "Chemistry in living systems." *Nat Chem Biol* **2005**, *1*, 13.

135 El-Sagheer, A. H.; Brown, T.: "Click chemistry with DNA." *Chemical Society Reviews* **2010**, *39*, 1388.

136 Gramlich, P. M. E.; Warncke, S.; Gierlich, J.; Carell, T.: "Click–Click–Click: Single to Triple Modification of DNA." *Angewandte Chemie International Edition* **2008**, *47*, 3442.

137 Huisgen, R.: "1.3-Dipolare Cycloadditionen Rückschau und Ausblick." *Angewandte Chemie* **1963**, *75*, 604.

138 Spiteri, C.; Moses, J. E.: "Kupferkatalysierte Azid-Alkin-Cycloadditionen: regioselektive Synthese von 1,4,5-trisubstituierten 1,2,3-Triazolen." *Angewandte Chemie* **2010**, *122*, 33.

139 Becer, C.; Hoogenboom, R.; Schubert, U.: "Klick-Chemie jenseits von metallkatalysierten Cycloadditionen." *Angewandte Chemie* **2009**, *121*, 4998.

140 Lutz, J. F.: "Kupferfreie Azid-Alkin-Cycloadditionen: Erkenntnisse und Perspektiven." *Angewandte Chemie* **2008**, *120*, 2212.

141 Stevens, M. P. *Polymer Chemistry: An introduction*; Oxford University Press: Oxford, New York, 1999.

142 Posner, T.: "Beiträge zur Kenntniss der ungesättigten Verbindungen. II. Ueber die Addition von Mercaptanen an ungesättigte Kohlenwasserstoffe." *Berichte der deutschen chemischen Gesellschaft* **1905**, *38*, 646.

143 Kade, M. J.; Burke, D. J.; Hawker, C. J.: "The power of thiol-ene chemistry." *Journal of Polymer Science Part A: Polymer Chemistry* **2010**, *48*, 743.

144 Lowe, A. B.: "Thiol-ene "click" reactions and recent applications in polymer and materials synthesis." *Polymer Chemistry* **2010**, *1*, 17.

145 Nair, D. P.; Podgórski, M.; Chatani, S.; Gong, T.; Xi, W.; Fenoli, C. R.; Bowman, C. N.: "The Thiol-Michael Addition Click Reaction: A Powerful and Widely Used Tool in Materials Chemistry." *Chemistry of Materials* **2014**, *26*, 724.

146 Hoyle, C. E.; Bowman, C. N.: "Thiol–Ene Click Chemistry." *Angewandte Chemie International Edition* **2010**, *49*, 1540.

147 Dawson, P.; Muir, T.; Clark-Lewis, I.; Kent, S.: "Synthesis of proteins by native chemical ligation." *Science* **1994**, *266*, 776.

148 van Baal, I.; Malda, H.; Synowsky, S. A.; van Dongen, J. L. J.; Hackeng, T. M.; Merkx, M.; Meijer, E. W.: "Multivalent Peptide and Protein Dendrimers Using Native Chemical Ligation." *Angewandte Chemie International Edition* **2005**, *44*, 5052.

149 Boere, K. W. M.; Soliman, B. G.; Rijkers, D. T. S.; Hennink, W. E.; Vermonden, T.: "Thermoresponsive Injectable Hydrogels Cross-Linked by Native Chemical Ligation." *Macromolecules* **2014**, *47*, 2430.

150 Bang, D.; Pentelute, B. L.; Kent, S. B. H.: "Kinetically Controlled Ligation for the Convergent Chemical Synthesis of Proteins." *Angewandte Chemie International Edition* **2006**, *45*, 3985.

151 Johnson, E. C. B.; Kent, S. B. H.: "Insights into the Mechanism and Catalysis of the Native Chemical Ligation Reaction." *Journal of the American Chemical Society* **2006**, *128*, 6640.

152 Hackenberger, C. P. R.; Schwarzer, D.: "Chemoselektive Ligations- und Modifikationsstrategien für Peptide und Proteine." *Angewandte Chemie* **2008**, *120*, 10182.
153 Markey, L.; Giordani, S.; Scanlan, E. M.: "Native Chemical Ligation,Thiol–Ene Click: A Methodology for the Synthesis of Functionalized Peptides." *Journal of Organic Chemistry* **2013**, *78*, 4270.
154 Hackeng, T. M.; Griffin, J. H.; Dawson, P. E.: "Protein synthesis by native chemical ligation: Expanded scope by using straightforward methodology." *Proceedings of the National Academy of Sciences of the United States of America* **1999**, *96*, 10068.
155 Dawson, P. E.; Churchill, M. J.; Ghadiri, M. R.; Kent, S. B. H.: "Modulation of Reactivity in Native Chemical Ligation through the Use of Thiol Additives." *Journal of the American Chemical Society* **1997**, *119*, 4325.
156 Messersmith, P. B.; Su, J.; Hu, B. H.: "Catalyst and byproduct-free native chemical ligation using cyclic thioester precursors." *9012594*, **2011**.
157 Ringsdorf, H.: "Structure and Properties of pharmacologically active Polymers." *J. Polym. Sci. Polym. Symp.* **1975**, *51*, 135.
158 Oh, J. K.; Drumright, R.; Siegwart, D. J.; Matyjaszewski, K.: "The development of microgels/nanogels for drug delivery applications." *Progress in Polymer Science* **2008**, *33*, 448.
159 Ferrari, M.: "Cancer nanotechnology: opportunities and challenges." *Nature Reviews: Cancer* **2005**, *5*, 161.
160 Farrugia, B. L.; Kempe, K.; Schubert, U. S.; Hoogenboom, R.; Dargaville, T. R.: "Poly(2-oxazoline) Hydrogels for Controlled Fibroblast Attachment." *Biomacromolecules* **2013**, *14*, 2724.
161 Kempe, K.; Ng, S. L.; Noi, K. F.; Müllner, M.; Gunawan, S. T.; Caruso, F.: "Clickable Poly(2-oxazoline) Architectures for the Fabrication of Low-Fouling Polymer Capsules." *ACS Macro Letters* **2013**, *2*, 1069.
162 Kempe, K.; Vollrath, A.; Schaefer, H. W.; Poehlmann, T. G.; Biskup, C.; Hoogenboom, R.; Hornig, S.; Schubert, U. S.: "Multifunctional Poly(2-oxazoline) Nanoparticles for Biological Applications." *Macromolecular Rapid Communications* **2010**, *31*, 1869.
163 Chujo, Y.; Sada, K.; Saegusa, T.: "Reversible gelation of polyoxazoline by means of Diels-Alder reaction." *Macromolecules* **1990**, *23*, 2636.
164 Hartlieb, M.; Pretzel, D.; Englert, C.; Hentschel, M.; Kempe, K.; Gottschaldt, M.; Schubert, U. S.: "Matrix Supported Poly(2-oxazoline)-Based Hydrogels for DNA Catch and Release." *Biomacromolecules* **2014**, *15*, 1970.
165 McAllister, K.; Sazani, P.; Adam, M.; Cho, M. J.; Rubinstein, M.; Samulski, R. J.; DeSimone, J. M.: "Polymeric Nanogels Produced via Inverse Microemulsion Polymerization as Potential Gene and Antisense Delivery Agents." *Journal of the American Chemical Society* **2002**, *124*, 15198.
166 Landfester, K.; Willert, M.; Antonietti, M.: "Preparation of Polymer Particles in Nonaqueous Direct and Inverse Miniemulsions." *Macromolecules* **2000**, *33*, 2370.
167 Meng, F.; Hennink, W. E.; Zhong, Z.: "Reduction-sensitive polymers and bioconjugates for biomedical applications." *Biomaterials* **2009**, *30*, 2180.
168 Saito, G.; Swanson, J. A.; Lee, K.-D.: "Drug delivery strategy utilizing conjugation via reversible disulfide linkages: role and site of cellular reducing activities." *Advanced Drug Delivery Reviews* **2003**, *55*, 199.

169 Singh, S.; Topuz, F.; Hahn, K.; Albrecht, K.; Groll, J.: "Einbau aktiver Proteine und lebender Zellen in redoxsensitive Hydrogele und Nanogele durch enzymatische Vernetzung." *Angewandte Chemie* **2013**, *125*, 3074.
170 Singh, S.; Zilkowski, I.; Ewald, A.; Maurell-Lopez, T.; Albrecht, K.; Möller, M.; Groll, J.: "Mild Oxidation of Thiofunctional Polymers to Cytocompatible and Stimuli-Sensitive Hydrogels and Nanogels." *Macromolecular Bioscience* **2013**, *13*, 470.
171 Groll, J.; Singh, S.; Albrecht, K.; Möller, M.: "Biocompatible and degradable nanogels via oxidation reactions of synthetic thiomers in inverse miniemulsion." *Journal of Polymer Science Part A: Polymer Chemistry* **2009**, *47*, 5543.
172 Chujo, Y.; Sada, K.; Naka, A.; Nomura, R.; Saegusa, T.: "Synthesis and redox gelation of disulfide-modified polyoxazoline." *Macromolecules* **1993**, *26*, 883.
173 Binnig, G.; Quate, C. F.; Gerber, C.: "Atomic Force Microscope." *Physical Review Letters* **1986**, *56*, 930.
174 Giessibl, F. J.: "Advances in atomic force microscopy." *Reviews of Modern Physics* **2003**, *75*, 949.
175 Jalili, N.; Laxminarayana, K.: "A review of atomic force microscopy imaging systems: application to molecular metrology and biological sciences." *Mechatronics* **2004**, *14*, 907.
176 Pecora, R. *Dynamic Light Scattering - Applications of Photon Correlaltion Spectroscopy*: Plenum Press, New York, 1985.
177 Schmitz, K. S. "CHAPTER 1 - Introduction" in *Introduction to Dynamic Light Scattering by Macromolecules*; Academic Press: Oxford, 1990, p. 1.
178 Lorber, B.; Fischer, F.; Bailly, M.; Roy, H.; Kern, D.: "Protein analysis by dynamic light scattering: Methods and techniques for students." *Biochemistry and Molecular Biology Education* **2012**, *40*, 372.
179 Montaudo, G.; Samperi, F.; Montaudo, M. S.: "Characterization of synthetic polymers by MALDI-MS." *Progress in Polymer Science* **2006**, *31*, 277.
180 Macha, S. F.; Limbach, P. A.: "Matrix-assisted laser desorption/ionization (MALDI) mass spectrometry of polymers." *Current Opinion in Solid State and Materials Science* **2002**, *6*, 213.
181 Carr, B.; Wright, M. *Nanoparticle Tracking Analysis - A Review of Applications and Usage 2010-2012*; NanoSight Ltd, 2013.
182 Wider, G.: "Structure determination of biological macromolecules in solution using nuclear magnetic resonance spectroscopy." *Biotechniques* **2000**, *29*, 1278.
183 Hendra, P. J.; Stratton, P. M.: "Laser-Raman spectroscopy." *Chemical Reviews* **1969**, *69*, 325.
184 Isaacman, M. J.; Barron, K. A.; Theogarajan, L. S.: "Clickable amphiphilic triblock copolymers." *Journal of Polymer Science Part A: Polymer Chemistry* **2012**, *50*, 2319.
185 Fijten, M. W. M.; Haensch, C.; van Lankvelt, B. M.; Hoogenboom, R.; Schubert, U. S.: "Clickable Poly(2-Oxazoline)s as Versatile Building Blocks." *Macromolecular Chemistry and Physics* **2008**, *209*, 1887.
186 Kim, E. Y. L.; Gronewold, C.; Chatterjee, A.; von der Lieth, C.-W.; Kliem, C.; Schmauser, B.; Wiessler, M.; Frei, E.: "Oligosaccharide Mimics Containing Galactose and Fucose Specifically Label Tumour Cell Surfaces and Inhibit Cell Adhesion to Fibronectin." *ChemBioChem* **2005**, *6*, 422.

187 Volet, G.; Lav, T.-X.; Babinot, J.; Amiel, C.: "Click-Chemistry: An Alternative Way to Functionalize Poly(2-methyl-2-oxazoline)." *Macromolecular Chemistry and Physics* **2011**, *212*, 118.
188 Tomalia, D. A.; Thill, B. P.; Fazio, M. J.: "Ionic Oligomerization and Polymerization of 2-Alkenyl-2-oxazolines." *Polym J* **1980**, *12*, 661.
189 Nuyken, O.; Maier, G.; Groß, A.; Fischer, H.: "Systematic investigations on the reactivity of oxazolinium salts." *Macromolecular Chemistry and Physics* **1996**, *197*, 83.
190 Kuhlmann, M.; Reimann, O.; Hackenberger, C. P. R.; Groll, J.: "Cysteine-Functional Polymers via Thiol-ene Conjugation." *Macromolecular Rapid Communications* **2015**, *36*, 472.
191 Sheehan, J. C.; Yang, D.-D. H.: "A New Synthesis of Cysteinyl Peptides1." *Journal of the American Chemical Society* **1958**, *80*, 1158.
192 Woodward, G. E.; Schroeder, E. F.: "The Reaction of Cysteine with Acetone. A Note on the Titration of Cysteine by the Acetone—Hydrochloric Acid Method of Linderstr˘om-Lang." *Journal of the American Chemical Society* **1937**, *59*, 1690.
193 Ulbricht, J.; Jordan, R.; Luxenhofer, R.: "On the biodegradability of polyethylene glycol, polypeptoids and poly(2-oxazoline)s." *Biomaterials* **2014**, *35*, 4848.
194 Wang, J.; Liang, Y.-L.; Qu, J.: "Boiling water-catalyzed neutral and selective N-Boc deprotection." *Chemical Communications* **2009**, 5144.
195 Kato, S.; Ishida, M.: "Acyclic Dithiocarboxylic Acid Esters - Reactions and Syntheses." *Sulfur reports* **1988**, *8*, 155.
196 Mayadunne, R. T. A.; Rizzardo, E.; Chiefari, J.; Krstina, J.; Moad, G.; Postma, A.; Thang, S. H.: "Living Polymers by the Use of Trithiocarbonates as Reversible Addition Fragmentation Chain Transfer (RAFT) Agents: ABA Triblock Copolymers by Radical Polymerization in Two Steps." *Macromolecules* **2000**, *33*, 243.
197 Boyer, C.; Granville, A.; Davis, T. P.; Bulmus, V.: "Modification of RAFT-polymers via thiol-ene reactions: A general route to functional polymers and new architectures." *Journal of Polymer Science Part A: Polymer Chemistry* **2009**, *47*, 3773.
198 Hoyle, C. E.; Lowe, A. B.; Bowman, C. N.: "Thiol-click chemistry: a multifaceted toolbox for small molecule and polymer synthesis." *Chemical Society Reviews* **2010**, *39*, 1355.
199 Qiu, X.-P.; Winnik, F. M.: "Facile and Efficient One-Pot Transformation of RAFT Polymer End Groups via a Mild Aminolysis/Michael Addition Sequence." *Macromolecular Rapid Communications* **2006**, *27*, 1648.
200 Alemán, J.; Chadwick, a. V.; He, J.; Hess, M.; Horie, K.; Jones, R. G.; Kratochvíl, P.; Meisel, I.; Mita, I.; Moad, G.; Penczek, S.; Stepto, R. F. T.: "Definitions of Terms Relating to the Structure and Processing of Sols, Gels, Networks, and Inorganic-Organic Hybrid Materials." *Pure and Applied Chemistry* **2007**, *79*, 1801.
201 Legros, C.; De Pauw-Gillet, M.-C.; Tam, K. C.; Lecommmandoux, S.; Taton, D.: "pH and redox responsive hydrogels and nanogels made from poly(2-ethyl-2-oxazoline)." *Polymer Chemistry* **2013**, *4*, 4801.

202 Yamaoka, T.; Tabata, Y.; Ikada, Y.: "Distribution and tissue uptake of poly(ethylene glycol) with different molecular weights after intravenous administration to mice." *Journal of Pharmaceutical Sciences* **1994**, *83*, 601.

Danksagung

Zu guter Letzt möchte ich mich ganz herzlich bei allen bedanken, die zum Gelingen der vorliegenden Arbeit beigetragen haben.

Großer Dank gebührt in erster Linie Prof. Dr. Jürgen Groll, der mir überhaupt erst die Möglichkeit zur Durchführung dieser Doktorarbeit gegeben hat. Vielen Dank für das interessante Thema der Arbeit, die Unterstützung in schwierigen Zeiten und das immer offene Ohr und die Hilfsbereitschaft bei Problemstellungen. Mit ihm von Aachen nach Würzburg gezogen zu sein hat mich gelernt wie es ist von ganz vorne anzufangen, auch wenn die ersten 2 Jahre im Arbeitskreis von Prof. Dr. Frank Würthner, dafür gebührt auch Ihm großer Dank, eine organisatorische Herausforderung darstellten.

Des Weiteren möchte ich mich ganz herzlich bei allen Mitarbeitern der Arbeitskreise von Prof. Dr. Frank Würthner und Prof. Dr. Bernd Engels bedanken – ohne euch wäre der Beginn der Arbeit unmöglich gewesen. Danke, dass ich jedes publizierte Paper und jeden Geburtstag mitfeiern durfte, und danke für die gute Laune und die schöne Zeit auf diversen Weinfesten Würzburgs. Danke Jana Gershberg und Eva Kirchner für den Support bei diversen ^{19}F-NMR-Messungen. Danke Vladimir Stepanenko für die Messungen am REM. Besonderer Dank geht an Matthias Stolte und Florian Beuerle, die mich nicht nur am Anfang, sondern durch die ganze Zeit der Doktorarbeit bei Kaffee, Wein und Bier begleitet haben – es war mir eine Ehre!

Ganz herzlich bedanken möchte ich mich natürlich beim gesamten Arbeitskreis der FMZ! Ich denke, dass eine Doktorarbeit nur mit kollegialem Miteinander funktionieren kann und da würde ich sagen ist das FMZ Meister! Danke für das mehr als angenehme „Betriebsklima“ und die individuelle Hilfe die jeder Einzelne einbringt, besonderer Dank hierbei an Jörg Tessmar, Harald Hümpfer und Anton Hoffmann. Danke Simone Werner, Maria Aniolek und Andrea Ewald bei der Unterstützung der Zellversuche. Danke Claus Moseke und Judith Friedlein für diverse REM Bilder. Danke Isabell Biermann für die Unterstützung bei Fragen bezüglich anorganischem

Chemie Labor, Müllentsorgung und Büro-Schnick-Schnack. Besonderer Dank an meine ehemaligen und heutigen Bürokollegen Matthias Kuhlmann, Martina Kessler, Eva Esser, Jodie Haigh, Moataz Bellah Youssef und Andrej Hrynevich für die Unterstützung in fachlicher Hinsicht aber auch für die Unterhaltungen zwischendurch!

Thanks Jodie!!! You are the best!!! Thank you for all your support during writing, proofreading and office dancing!

Danke auch an Robert Luxenhofer für die Durchsicht der Arbeit und die Unterstützung während der gesamten Zeit.

Danke Matthias Kuhlmann, Ilona Zilkowski, Steffi Hauck und Tomasz Jüngst – für ALLES!

Vielen Dank an meine Familie und Freunde! Ihr habt mich immer motiviert, unterstützt und mir mit Rat und Tat zur Seite gestanden.
Danke Julia, dass du mir immer hilfst den Kopf über Wasser zu halten. Danke für deine Unterstützung, deine Geduld, deine Einfühlsamkeit, deinen Humor und deine liebenswerte Art. Danke, dass du so bist wie du bist!!!